ISSN 0257 - 3660

ACTA MINERALOGICA PAKISTANICA

Volume 3

1987

NATIONAL CENTRE OF EXCELLENCE IN MINERALOGY
(UNIVERSITY OF BALUCHISTAN), QUETTA, PAKISTAN

ACTA MINERALOGICA PAKISTANICA

VOLUME 3-1987

CHIEF EDITOR : ZULFIQAR AHMED

REFEREES FOR 1987

ZULFIQAR AHMED, QUETTA, PAKISTAN.
KHAWAJA AZAM ALI, ISLAMABAD, PAKISTAN.
AFTAB AHMAD BUTT, LAHORE, PAKISTAN.
JOHN COSGROVE, LONDON, UK.
RHYS G. DAVIES, SURREY, UK.
ANTHONY HALL, LONDON, UK.
R.A. HOWIE, LONDON, UK.
D.R.C. KEMPE, LONDON, UK.
SHERJIL AHMAD KHAN, LAHORE, PAKISTAN.
GEORGE R. McCORMICK, IOWA, USA.
JAMES W. McDOUGALL, VIRGINIA, USA.
DUANE M. MOORE, ILLINOIS, USA.
SALLY RADFORD, LONDON, UK.

ISSN-0257-3660

PRICE

PAKISTANI RUPEES 70.00 OR U.S. $ 10.00 OR U.K. £ 6.00

(includes surface mail postage and handling charges)

Published in December each year.
Printed at KASHMIR OFFSET PRESS, QUETTA, PAKISTAN.

ACTA MINERALOGICA PAKISTANICA VOLUME 3, 1987.

CONTENTS

ON THE COVER

Field photographs showing two views of the Pahoehoe lava outcrops located in the volcanic sequence of the Bela ophiolite, Pakistan. The pahoehoe lavas generally result from subaerial eruption of lava and provide food for thought when found in the otherwise submarine erupted and mostly pillowed ophiolitic basalts like this occurrence.

(Located and photographed by Zulfiqar Ahmed).

MAP OF PAKISTAN SHOWING LOCATIONS OF AREAS DEALT WITH IN THE PAPERS OF THIS ISSUE.

Roman numerals correspond to the serial number of each artical in the table of contents.

Major cities are shown by solid circles.

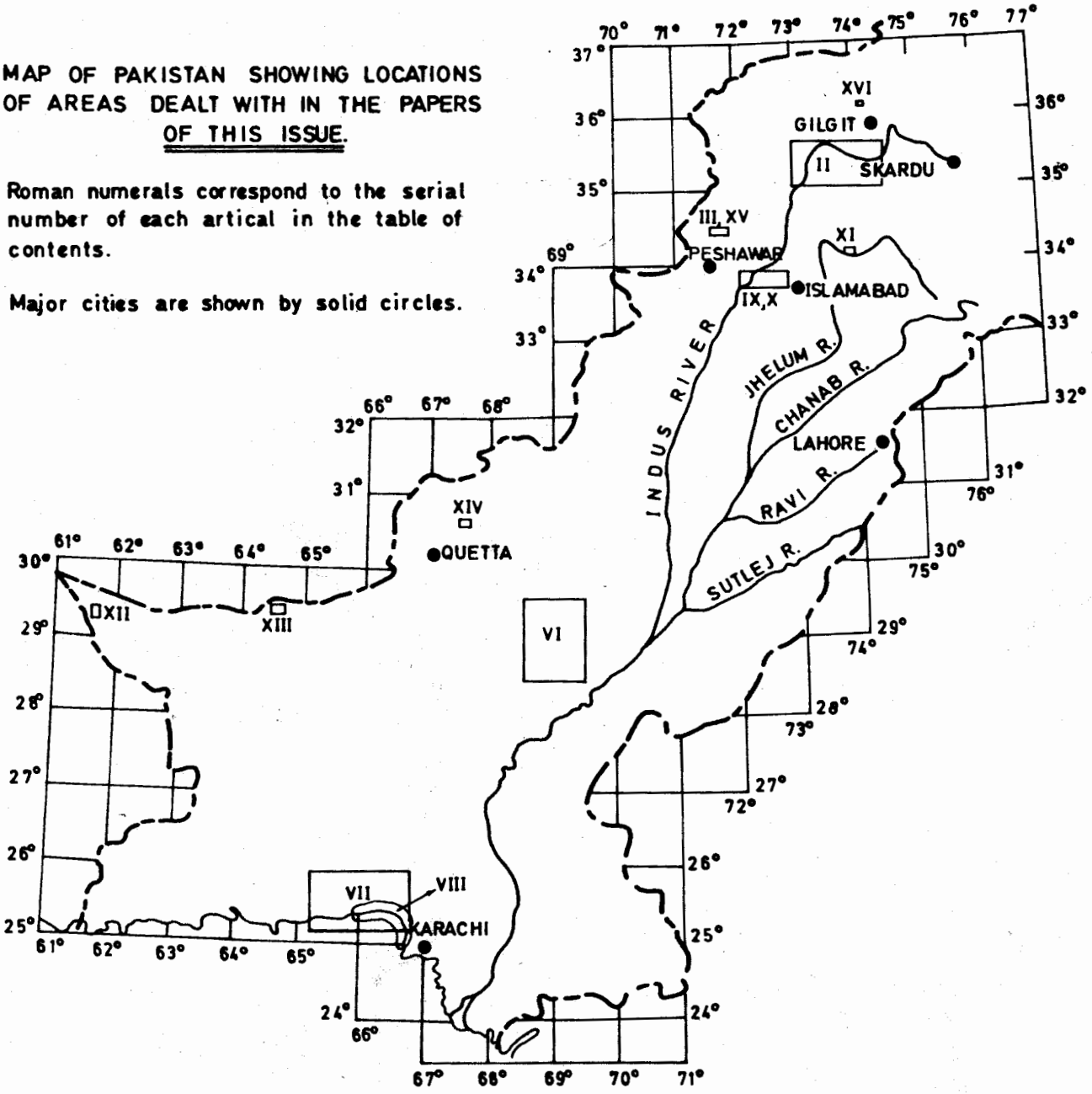

Blank Page

ACTA MINERALOGICA PAKISTANICA
VOLUME 3 (1987) pp. 5 - 25

SOME GARNETS, EPIDOTES, BIOTITIC MICAS,AND FELDSPARS FROM THE SOUTHERN PART OF KOHISTAN, NW PAKISTAN.

M. QASIM JAN[1] & R.A. HOWIE[2]

1. **National Centre of Excellence in Geology, University of Peshawar, Pakistan.**
2. **Department of Geology, Royal Holloway & Bedford New College (University of London), Egham Hill, Egham, Surrey TW20 OEX, U.K.**

ABSTRACT: Partial or complete analyses of 52 minerals (with trace elements for 22) from amphibolitic rocks, mafic granulites and quartz diorites are presented. Garnet development in the amphibolite belt is sporadic and controlled by bulk chemistry, especially low Mg/Fe, but in Lilauni area of the amphibolite belt and in the garnet granulites of Jijal, abundant garnet has developed in response to high pressures.The amphibolite facies garnets are distinctly richer in almandine+ spessartine and poorer in pyrope and grossular components as compared to the high-pressure granulites. The epidote is mostly monoclinic with Ps content ranging from 0 to 32 mole %. Epidote composition is controlled by the Fe^{3+}/Al ratios of the environment and by fO_2 but other factors might also exert some influence. No obvious difference is seen in the epidote compositions from the amphibolites and Jijal granulites.

The biotites in granulites generally have higher Ti, and lower Mn, Al and Na than those in amphibolites and diorites which are considered to have equilibrated at lower temperatures than the granulites. Four of the biotites are altered to varying extent and show a loss in K (and Si) and gain in H_2O^+ and,to a lesser extent, in Ca. The feldspar analyses in some cases have excess Si and Al over Ca and alkalis. The plagioclase in a calc-silicate rock within the amphibolite terrain is albitic, its abnormally low An content reflecting the peculiar bulk chemical and mineralogical composition of this rock.

INTRODUCTION

Regional Petrology

The ~36000 km² Kohistan tectonic zone (northern Pakistan), bounded by the Main Karakoram Thrust (MKT) in the north and Main Mantle Thrust (MMT) in the south, is comprised of a variety of volcanic, plutonic and minor sedimentary rocks of Cretaceous-Tertiary age. The MKT and MMT are major shear (suture) zones with associated middle Mesozoic ophiolites/melanges–near Shyok, Chalt, Ishkoman and Drosh along the MKT, and Dras, Jijal, Shangla-Mingora along the MMT. The Shangla and Dras melanges have local occurrences of high-P-low-T blueschists, whereas the Jijal complex has undergone a high-P granulite facies metamorphism. The MKT and MMT extend eastwards across Ladakh and join into the Indus-Zangbo suture zone in SW Tibet, and westwards in Afghanistan, the two megashears are terminated by the extension of the Chaman transform fault.

To the N of the MKT occur rocks of the Karakoram plate whilst to the S of MMT are those of the Indo-Pakistan plate. The area between the two is split into Kohistan and Deosai-Ladakh due to the recent rise (Zeitler *et al.*, 1982) and, possibly, northwards push of the N-S elongated Nanga Parbat-Haramosh dome. Lithologies in Ladakh and Kohistan, respectively to the E and W of Nanga Parbat, have many similarities. However, because of a faster rate of uplift and consequent rapid erosion, the Kohistan region exposes higher grade metamorphic rocks of deeper level and only local sediments of the Tertiary "cover" as compared to Ladakh.

Recent investigations (Tahirkheli *et al.*, 1979; Bard *et al.*, 1980; Klootwijk *et al.*, 1979; Coward *et al.*, 1982,1986; Jan and Asif, 1981, 1983; Andrews-Speed and Brookfield, 1982; Bard, 1983a,b; Virdi, 1981;Searle *et al.*, 1987) suggest that the Kohistan-Ladakh region represents a Cretaceous island-arc that became an Andean-type margin in the late Cretaceous. Voluminous outpouring of island-arc stage (Late Jurassic-Cretaceous) volcanic rocks are seen in Dras, Chalt and their metamorphosed equivalents (amphibolites) in southern Kohistan. Cretaceous sedimentary rocks are interbedded with and overlie these rocks both in Ladakh and Kohistan. An early mafic (calc-alkaline) magmatism (~125 m.y. ago according to Bard, 1983, but possibly a little older) resulted in plutono-metamorphic complexes of Chilas, Jijal-Patan and Kargil. Honegger *et al.* (1982) and Coward *et al.* (1986) suggest that these complexes may represent cumulates in the magma chambers of the volcanic rocks. The Chilas complex, consisting principally of norithic rocks with subordinate troctolites, pyroxenites, anorthosites, peridotites and dunite (Khan *et al.*, in press), extends for 300 x up to 40 km between the Trans-Himalayan "granitic" and southern amphibolite belts of Kohistan (Fig. 1). Following these, the volcanic rocks were intruded by subduction-related calc-alkaline diorites, tonalite, granodiorite and minor granites between 100 and 55 m.y. ago (Jan and Asif, 1983).

The Kohistan-Ladakh island arc was welded to the Karakoram plate during the Late Cretaceous (Petterson and Windley, 1985) whence it became an Andean-type margin. This was followed by calc-alkaline intrusions and andesite-dacite-rhyolite-ignimbrite volcanics in the Eocene (Kalam-Dir area) and early Oligocene (Shyok; Sharma and Gupta, 1983). Post-dating these volcanics are the voluminous young silicic plutons and late basic to intermediate minor dykes of the Trans-Himalayan plutonic belt some of which, at least, owe their origin to crustal anatexis.

Metamorphism

The Kohistan region has experienced a complex interplay of continental collision and deformation, magmatism and metamorphism, orgeny and uplift. Petrographic details of this region have been presented by Tahirkheli and Jan (1979) and structure and metamorphism discussed by Coward *et al.*, (1982a, b, 1986) and Bard (1983a, b). Coward *et al.* noted that the region underwent at least two phases of isoclinal folding and was tilted during the Himalayan collision so that the structures are now subvertical. The grade of metamorphism increases from greenschist- to pyroxene-granulite facies towards the Chilas complex. In the southern (Kamila) amphibolites and pyroxene granulites (i.e. the Chilas complex), the mineral assemblages post-date an early phase of intense deformation associated with the isoclinal folding of the Chilas complex and thickening of the whole stratigraphy (Coward *et al.*, 1986).

The high-P garnet granulites of the Jijal complex are considered to be possibly related magmatically to the Chilas complex (Jan, 1980; Jan and Howie, 1981; Coward *et al.*, 1982b). The Jijal complex is probably a tectonic fragment of arc cumulates that was subducted or downthrust to a substantial depth (~35 km) against the MMT (see also Bard, 1983). The Sm-Nd mineral isochron age for the Jijal rocks is 103 $\pm$ 2 m.y. (Coward *et al.*, 1986). The Jijal granulites (800-900°C, ~ 10 kbar) are derived from pyroxene granulites rather than directly from igneous rocks. Therefore, the pyroxene granulite facies metamorphism in Kohistan must pre-date 103 m.y. Thus the time gap between the formation of the Chilas-Jijal complexes (~130 m.y.) and their first metamorphism in pyroxene granulite facies (~110 m.y.) is rather short. Bard (1983a) proposed that the cause of the first episode of the regional metamorphism in Kohistan may be the remnant magmatic heat associated with the still hot Chilas complex. The pyroxene granulites were equilibrated at 800°C, 5-7.5 kbar (Jan and Howie, 1980), and Bard (1983b) suggested that geothermal gradients within and on the near borders of the Chilas complex were 80-100°C/km.

Bard (1983b) correlated the early Kohistan metamorphism and the blueschist metamorphism (~80 m.y.) in the underlying trench melange with Upper Cretaceous obduction of the Kohistan arc. However, considering the approximately 25 m.y. gap between the granulite facies and blueschist metamorphism and secondary-hornblende ages reaching up to 100 m.y. in the granulite belt, obduction of the arc may

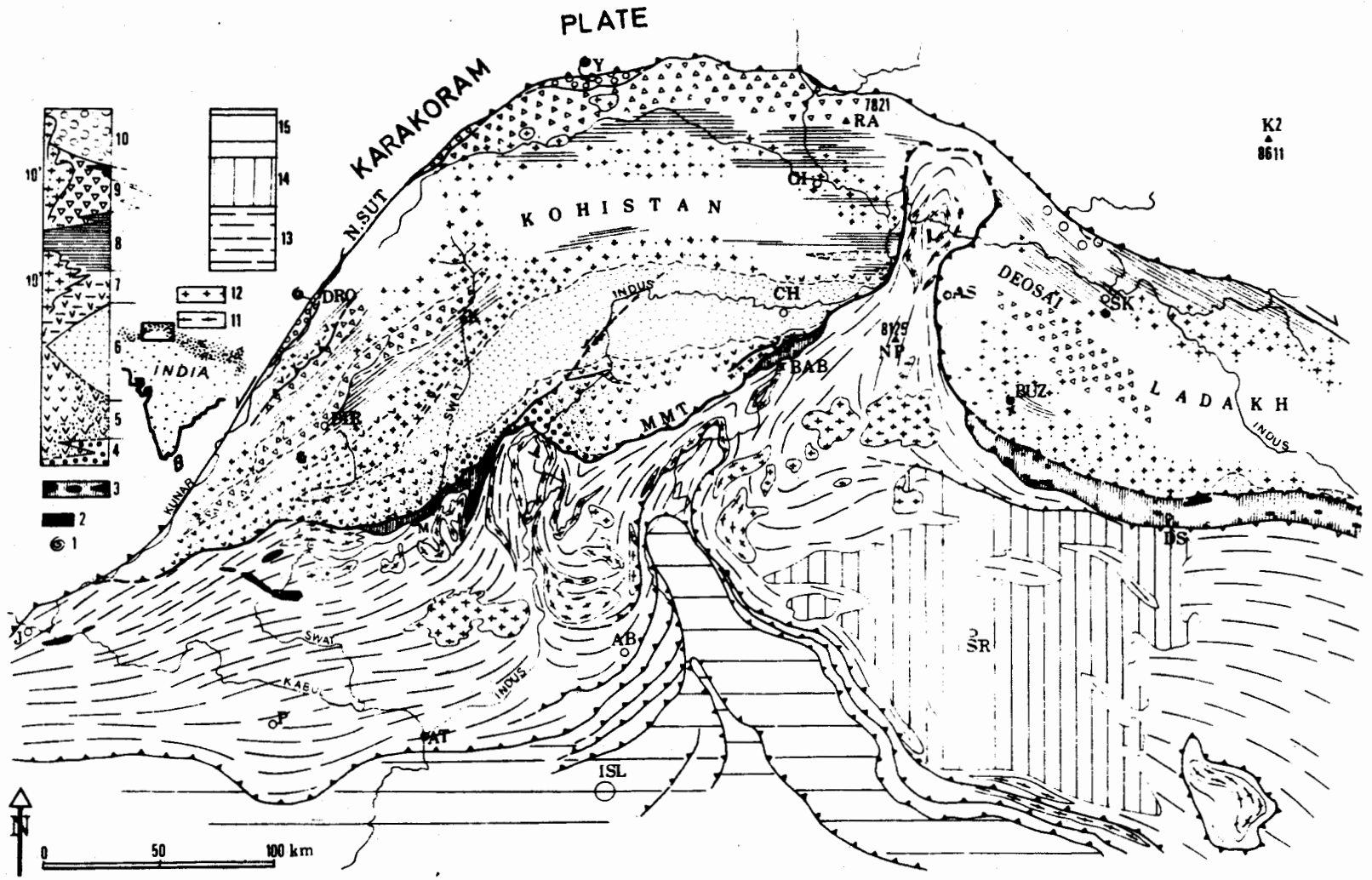

Fig. 1

Geological sketch-map of northern Pakistan and Kashmir with special reference to the Kohistan area (modified after Bard, 1983a). 1 = fossil localities (Cretaceous to Lower Eocene); 2 = serpentinite and allochthonous ultrabasics; 3 = blueschist belt and associated tectonic mélange under the Main Mantle Thrust (MMT) palaeosuture; 4 = Jijal-Patan mafic-ultramafic complex (high-P granulites) and western equivalents; 5 = southern amphibolite belt; 6 = Chilas complex (layered and pyroxene-granulite facies metamorphosed "lopolith"); 7 = northern amphibolite; 8 = Cretaceous Kalam sediments; 9 = Chalt (Jurassic-Cretaceous) and Utrot (Eocene) volcanics; 10 = Cretaceous to middle Tertiary calc-alkaline plutons covering much of the blank area in the middle Kohistan; 10 = Yasin Group (middle Cretaceous); 11 = Indo-Pak plate orthogneisses (Precambrian and Cambrian); 12 = younger Indo-Pak plate granitoids; 13 = Indo-Pak plate metasediments (Precambrian to Palaeozoic); 14 = Upper Palaeozoic to Triassic series of Srinagar and Panjal Traps; 15 = Foreland Cenozoic deposits (Murree Formation, etc.).

AB = Abbottabad; AS = Astor; AT = Attock; BAB = Babusar Pass; BUZ = Burzil Pass; CH = Chilas; DRO = Drosh; DS = Dras; GI = Gilgit; Isl = Islamabad; J = Jallalabad; K = Kalam; M = Mingora; NP = Nanga Parbat; P = Peshawar; R = Rakaposhi Mountain; SR = Srinagar; SK = Skardu; Y = Yasin.

have started in the Middle Cretaceous. Jan (1987) regards that the high-P (blueschist) metamorphism is subduction related.

The granulite facies rocks underwent a second phase of medium- to low-grade metamorphism when they were hydrated to amphibolites (Jan, 1977, 1982). This metamorphism has the following features according to Bard (1983b): (a) it was Barrovian-type overprinting associated with the Oligocene collision of India with Asia, (b) the geotherm approached 25° C/km within a re-equilibrated thermal structure, and (c) it was retrogressive and produced amphibolite ± epidote ± garnet at the expense of granulites, especially in the Kamila-Patan area of the southern amphibolite belt. Although the presence of pyroxene granulite outcrops in several places and of Jijal-like (garnet-clinopyroxene ± plagioclase) high-P granulites in Lilauni area N of the Shangla blueschists lend support to Bard's hypothesis, the situation in the southern amphibolite belt may be too complicated (cf. Jan 1977, 1982, 1988). There also is the likelihood that some retrograde metamorphism was connected with the collision of Indo-Pak plate and Kohistan and uplift of the latter block about 53 to 40 m.y. ago (Powell, 1979; Molnar, 1986).

In this paper we present an account of the chemistry of 52 garnet, epidote, mica and feldspar analyses from the amphibolites, granulites and early clac-alkaline dioritic rocks of southern half of the Kohistan zone. In addition, 38 analyses of garnets and 18 epidotes published from Kohistan have also been taken into consideration. Wet chemical analyses were performed by combining classical and atomic absorption methods described by Jan and Howie (1982). Microprobe analyses were carried out using the energy dispersive system. Trace elements in wet-analysed samples were carefully measured and their values are presented in the Tables. The energy dispersive analyses of trace elements do not appear to be of high quality and are therefore not included in the Tables. However, their values are presented in the descriptions following the Tables.

GARNETS

Three wet and 10 microprobe analyses are presented in Table 1. US25 has a brick-red powder and is reddish-pink in thin section whilst the almandines (369, 177, 587) have pinkish and grossular (324) whitish powder. The first seven analyses are from the amphibolite belt (with a dubious status of SI96), 587 is from an unusal granulite containing essential quartz+bytownite+garnet+hypersthene+biotite, and the last five are from high-p garnet granulite of Lilauni area. Compared to their host rocks the first three garnets, together with 597 and 324, have higher MnO, and FeO/MgO and (FeO+MgO)/CaO ratios. Such relations have already been found by Buddington (1952), Subramaniam (1952), Howie and Subramaniam (1957) and Jan and Howie (1981). They are, except 25, poorer in TiO_2 and Cr_2O_3 than their host rocks.Rocks analyses are not available for the remaining garnets. Microprobe analyses suggest that only four of the analysed garnets from Kohistan are appreciably zoned (cf. Fig. 2).

The compositions of the garnets, along with 16 more analyses from the amphibolite belt and 22 from the high-P granulites of Jijal (Ahmed and Ahmad, 1975; Jan and Howie, 1981; Bard, 1983b) have been plotted on the triangular pyrope-(almandine + spessartine)-(grossular + andradite) diagram (Fig. 2) of Dobretsov *et al.*, (1982). Those from the amphibolite belt straddle the fields of garnets from amphibolite and epidote amphibolite facies but US25, SI324 and two more analyses plot outside these fields because of their higher grandite contents. Garnets from the Lilauni area are generally similar to those from Jijal; these high-P garnets mostly plot in the overlapping fields of garnulite and eclogite garnets. Garnet from SK587 plots in the field of amphibolites rather than of granulites. The analysis of a garnet from a similar rock (garnet-hypersthene-biotite gneiss) about 15 km to the S of 587 has a very similar composition (point x) to 587 (Bard, 1983b). The higher FeO and MnO contents of these two garnets from pyroxene granulites must be in response to the bulk chemical control.

Some distinct differences are found when garnets from the amphibolite belt are compared with those from the high-P granulites of Jijal and Lilauni. The former (except 324, 25 and 27) are almandine-rich (Alm 54-68%) and have lower pyrope (8-25%) and grossular (12-19%) than those of Jijal (Alm_{28-43} Pyr_{28-46} $Gros_{17-35}$). However, four of the Lilauni area high-P granulites have lower pyrope (15-24%) with two having almandine content of 51 and 54% (Table 1). The MnO content of the amphibolite garnets is comparatively higher than those of the granulites (ignoring the two hypersthene-biotite gneisses) irrespective of the MnO content of their host rocks. These differences thus appear to reflect differences in metamorphic conditions. For example, the MgO/FeO ratio of rock 177 (0.71) is similar to some rocks from Jijal whilst the CaO content of this rock (12.74%) is higher than the Jijal rocks but their garnets show different relations. Within the particular range of metamorphic conditions, however, bulk chemistry and associated minerals have controlled the garnet composition. The high MnO content of 25 and CaO content of 177 reflect the richness of their host rocks in these components as well as the lower accommodation of these components in the remainder of the minerals in the two rocks (cf. Jan 1977).

Experimental work and garnet analyses from eclogites and glaucophane-bearing rocks provide ample evidence for the incorporation of more grossular and, probably, pyrope in garnets with increasing pressure (cf. Jan and Howie, 1981). A number of workers have also reported that lower grade garnets are enriched in MnO (Barth, 1936; Miyashiro and Shido, 1973) although the composition of host rock plays an important role in determining the MnO content of garnets (Hsu, 1968; Misch and Onyeagocha, 1976). Saxena (1968) suggested that the mixture (Fe^{2+} , Mn Ca) garnet tends to be ideal at low T and P.

The occurrence of garnet in the amphibolite belt is sporadic and not restricted geographically to a particular area. In some cases, garnet-bearing bands are intimately associated with and alternating with those without it. It seems that bulk chemistry has been important for its development, as has already been suggested by other workers. The various factors considered to have helped the development of garnet in other areas include higher Al_2O_3, MnO, normative anorthite; and lower oxidation ratio, H_2O^+, TiO_2, Ca + Na + K, SiO_2 and, above all, lower Mg/(Mg + Fe^{2+}) (Engel and Engel, 1962; Leake, 1963, 1972; Buddington, 1965; Binns, 1965; Manna and Sen, 1974; Martignole and Schrijver, 1973). According to Glassley and Sorensen (1980), the role of garnet in high-grade metabasites is complex, being either generated or consumed, depending upon P_{H_2O} , P_{total} , temperature pathways and bulk composition.

Of the 33 amphibolites and associated gneisses analysed from Swat Kohistan (Jan, 1977), only five contain garnet. In three of these the lower Mg/Fe^{2+} appears to be the essential factor along with high MnO in US25; in 324 it may be the high normative an/ab and high CaO. The cause of garnet development in one non-homogeneous amphibolite is not clear, unless it is assumed that either selective migration of elements or higher concentration of iron in certain bands has taken place. That the lower Mg/Fe ratio is responsible for garnet development in Kohistan is also obvious from the observation that, in general, leucocratic bands and veins carry garnet more frequently than dark amphibolites. It is worth mentioning, however, that garnet is more abundant and found over a wider range of composition in Lilauni area This area of amphibolites has garnet granulite relics and, like the Jijal high-P granulites, has undergone a higher pressure metamorphism. High-P is also obvious from the occurrence of glaucophane schists in a thrust belt imediately to the S of Lilauni amphibolites. Comparing Connemara with Dalradian, Leake (1972) similarly found that garnet is more abundant and present over a wider range of composition in Dalradian due to a higher-P metamorphism as also evidenced by the presence of kyanite.

The Fe^{2+}/Mg ratios in all analysed garnet-clinopyroxene and garnet-hornblende pairs from Swat-Kohistan (Jan and Howie, 1981, 1982; Bard, 1983b; Jan, unpublished data) are plotted in Fig. 3. The straight-line relationship suggests attainment of equilibrium except in a few pairs,

Table 1. Analyses of garnets from Swat-Kohistan.

	SI 369	SI 177	US 25	US 27	SS 96 Core	SS 96 Margin	SI 324	SK 587	SS 121	SA 24	SA 2	SS 123	SI122
SiO_2	38.29	--	37.75	39.31	38.91	38.81	38.46	38.88	37.80	38.63	38.99	38.37	38.81
TiO_2	0.22	0.17	0.14	0.09	0.07	0.05	0.44	0.00	0.22	0.05	0.06	0.10	0.14
Al_2O_3	21.39	21.95	19.36	21.56	21.22	21.33	16.89	23.11	20.40	21.07	21.24	21.01	21.06
Fe_2O_3	0.48	0.00	2.68	1.56	2.00	1.33	6.97	0.00	1.78	1.78	1.89	2.11	1.61
FeO	26.88	27.18	14.63	22.45	21.02	22.30	0.89	28.19	24.69	23.60	21.00	19.33	18.58
MnO	1.18	1.46	11.06	0.44	0.56	0.84	0.66	1.10	1.48	0.58	0.56	0.22	0.25
MgO	6.29	5.61	2.28	8.42	8.01	6.07	0.08	7.52	3.72	5.79	8.40	5.85	6.15
CaO	5.12	5.99	12.04	7.44	8.73	9.89	34.89	2.21	9.98	9.52	8.09	12.93	13.21
Na_2O	0.03	0.00	0.15	--	--	--	0.03	0.00	--	--	--	--	--
Total	99.88	--	100.09	101.27	100.52	100.62	99.31	101.01	100.07	101.02	100.23	99.92	99.81
Trace Elements (ppm)													
Co	31	28	41				--	--					
Cr	20	23	60				68						68
Cu	16	18	11				--	--					
Li	1	1	1				--	--					
Ni	20	17	24				--	--					-
Pb	5	23	11				--	--					
V	130	79	98				--	--					
Zn	118	63	158				241	1366					
Numbers of ions on the basis of 24(0)													
Si	5.981	6.000	5.998	5.961	5.946	5.974	5.986	5.936	5.962	5.959	5.960	5.921	5.972
Al	0.019	0.000	0.002	0.039	0.054	0.026	0.014	0.064	0.038	0.041	0.040	0.079	0.028
ΣZ	6.00	6.00	6.00	6.00	6.00	6.00	6.00	6.00	6.00	6.00	6.00	6.00	6.00
Al	3.920	3.988	3.624	3.816	3.768	3.844	3.086	4.095	3.756	3.791	3.788	3.743	3.793
Fe^{3+}	0.056	0.000	0.321	0.178	0.230	0.154	0.816	0.000	0.211	0.206	0.217	0.245	0.186
Ti	0.026	0.020	0.017	0.010	0.007	0.006	0.052	0.000	0.026	0.006	0.007	0.012	0.016
ΣY	4.00	4.01	3.96	4.00	4.00	4.00	3.95	4.10	3.99	4.00	4.01	4.00	4.00
Mg	1.464	1.288	0.539	1.903	1.824	1.392	0.018	1.711	0.875	1.331	1.913	1.345	1.410
Fe^{2+}	3.511	3.503	1.944	2.847	2.687	2.871	0.116	3.676	3.257	3.045	2.685	2.494	2.391
Mn	0.157	0.191	1.488	0.056	0.072	0.109	0.088	0.142	0.198	0.076	0.073	0.029	0.032
Ca	0.857	0.989	2.050	1.209	1.430	1.632	5.820	0.361	1.687	1.574	1.326	2.138	2.179
Na	0.009	0.015	0.046	-	-	0.010	0.000	-	-	-	-	-	-
ΣX	6.00	5.99	6.08	6.01	6.01	6.00	6.05	5.89	6.02	6.03	6.00	6.01	6.01
Mole per cent end-members													
Alm	58.6	58.7	32.3	47.3	44.7	47.8	1.9	62.4	54.1	50.5	44.8	41.5	39.8
Andr	2.0	0.5	8.4	4.7	5.9	4.0	21.5	-	5.9	5.3	5.6	6.4	5.0
Gro	12.3	16.1	25.6	15.4	17.9	23.2	74.8	6.1	22.1	20.8	16.5	29.2	31.2
Pyr	24.5	21.6	9.0	31.6	30.3	23.2	0.3	29.1	14.5	22.1	31.9	22.4	23.5
Spess	2.6	3.2	24.7	0.9	1.2	1.8	1.5	2.4	3.3	1.3	1.2	0.5	0.5

Explanation Table 1.

369, 177 and 25 analysed by wet chemistry and the rest by micro-probe. Analyst M.Q. Jan (anal. 587 and 324 by J.P. Bard). In microprobe analyses the FeO :Fe_2O_3 ratio was estimated to maintain the ionic charge-balance. SiO_2 was not determined in 177 but an assumed value of 38.93 was taken to give Si (in Z) = 6.00.

SI 369 Almandine-rich garnet from a banded plagioclase-quartz-aluminotschermakite-epidote-garnet gneiss, 3.5 km NW of Kayal-Indus confluence, Karakoram Highway (KKH). D 4.005 g/cm³.

SI 177 Almandine-rich garnet from a plagioclase-epidote-garnet amphibolite, 1.7 km N of Jalkot, Indus valley.

US 25 Garnet from a quartz-plagioclase-garnet-opaque-amphibole-epidote-clinopyroxene rock in amphibolite belt, between bridge and Lilbanr, along road W of Harnoi stream, Upper Swat. D 3.971 g/cm³.

US 27 Garnet from a garnet-hornblende vein in two-pyroxene-plagioclase granulite lens in amphibolite, 5 km S of Matta, Upper Swat. Contains 0.02% K_2O, 0.08% NiO, 0.18% CuO, 0.05% ZnO, 0.9% Cr_2O_3.

SS 96 Garnet from a edenitic hornblende-epidote-garnet-rutile-chlorite amphibolite or granulite, 2 km NW of Lilauni, Swat (amphibolite belt). Contains 0.04% Cr_2O_3, 0.1% NiO, 0.06% CuO, and 0.11% ZnO.

SI 324 Grandite from a quartz-garnet-calcite-clinopyroxene-microcline-albite horizon in amphibolites, 10 km N of Patan, Indus Valley.

SK 587 Almandine-rich garnet from a bytownite-quartz-biotite-hypersthene granulite, in stream 5 km W of Asrit, Swat-Kohistan.

SS 121 Almandine-rich garnet from a high-pressure (ferroan pargasitic hornblende-plagioclase-garnet-clinopyroxene-opaques-secondary epidote) granulite, 4 km W of Lilauni, Swat, in amphibolite belt.

SA 24 Garnet from a high-P (ferroan pargasitic-hornblende-plagioclase-garnet-clinopyroxene-rutile) granulite NW of Lilauni in amphibolite belt.

SA 2 Garnet from a high-P (garnet-clinopyroxene-plagioclase-rutile-quartz-opaques granulite boulder collected near Lilauni.

SS 123 Garnet from a high-P (garnet-ferroan pargasitic hornblende-clinopyroxene-epidote-rutite-opaques-sphene) granulite, 5km W of Lilauni in amphibolite belt.

SS 122 Garnet from a high-P (garnet-pargasitic hornblende-clinopyroxene-epidote-opaques) granulite, 5 km W of Lilauni in amphibolite belt.

but these might depart due to analytical inaccuracy. Strangely, the garnet-hornblende pairs from ambphibolites and garnet granulites do not seem to have different K_D Fe^{2+}-Mg.

EPIDOTES

Ten wet chemical (four of them partial) and five microprobe analyses of the epidotes are present in Table 2. SI290 and 291, SA122 and 123 are from the garnet granulites of Jijal and Lilauni, the remainder from the amphibolite belt. The Ps content, i.e. hypothetical pistacite molecule $Ca_2Fe_3^{3+}Si_3O_{12}(OH)$ calculated as 100 $Fe^{3+}/(Fe^{3+} + Al)$, ranges from 0.07 to 31.7. All but DIR1 and SA30 are monoclinic, have high 2V and, according to the nomenclature of Deer *et al.* (1962), are epidotes. Holdaway (1972) has classified the monoclinic Fe-Al epidote minerals into al-clinozoisite (Ps_{0-5}), Fe-clinozoisite (Ps_{5-10}), Al-epidote ($Ps_{10-22.5}$), and Fe-epidote ($Ps_{22.5-35}$). Myer (1966) noted that the Fe^{2+}/Fe^{3+} ratio in epidotes (0.08) is lower than that (0.15) in zoisite. The Swat epidotes, except 369, are similar in this respect to Myer's analyses but the zoisite (DIR1) is unusual for its much higher ratio.

All the analyses have been recalculated on an anhydrous basis of 25 (O) per two formula units. This approach is more realistic when uncertainties in H_2O determination are involved.

Table 2. Analyses of epidotes from Swat-Kohistan

	DIR 1	SA 30	SI 122	SI 355	SI 355V	SI 291	US 19A	SS 96	SI 369	SI 177	SI 290	US 4	US 12	SS 123	SS 123
SiO_2	39.76	39.62	38.88	39.04	38.60	39.28	38.22	38.42	38.50	-	-	-	38.22	38.03	37.24
TiO_2	0.02	0.05	0.15	0.23	0.38	0.40	0.24	0.40	0.22	0.22	1.14	3.22	0.37	0.57	0.11
Al_2O_3	33.96	32.43	30.75	28.32	28.77	27.11	27.13	26.90	26.02	28.05	26.35	22.38	22.22	26.22	21.59
Fe_2O_3	0.05	0.50	2.63	5.17	5.51	7.24	7.61	7.88	8.49	9.19	9.92	10.04	13.01	8.32	15.70
FeO	0.52	-	-	0.37	0.29	0.53	0.65	-	1.60	-	-	-	0.29	-	-
MnO	0.02	0.00	0.04	0.08	0.06	0.08	0.11	0.11	0.19	0.13	0.03	0.12	0.26	0.01	0.14
MgO	0.74	0.42	0.06	0.65	0.21	0.33	0.28	0.33	0.16	0.20	0.63	0.80	1.00	0.29	0.18
CaO	24.05	24.63	24.73	23.69	24.07	23.12	23.58	24.13	22.68	22.16	21.97	22.93	23.08	23.93	22.78
Na_2O	0.05	0.21	0.18	0.11	0.02	0.08	0.10	0.13	0.08	0.08	0.14	0.12	0.24	0.02	0.23
K_2O	0.02	0.00	0.05	0.01	0.01	0.01	0.02	0.02	0.00	0.00	0.01	0.00	0.02	0.01	0.06
H_2O^+	1.42	-	-	1.88	1.58	1.77	1.92	-	-	-	-	-	1.61	-	-
P_2O_5	0.11	-	-	0.00	0.00	0.05	0.00	0.00	-	0.01	0.03	0.00	0.01	-	-
TOTAL	100.72	97.86	97.47	99.55	99.50	100.00	99.86	98.32	98.11	-	-	-	100.33	97.40	98.03
D	-	-	-	3.36	3.37	3.39	3.40	-	-	-	-				
Numbers of ions on the basis of 25 oxygens															
Si	5.951	6.023	5.998	6.060	5.984	6.095	5.980	5.985	6.041				6.051	5.988	5.985
Al	0.049	-	0.002	-	0.016	-	0.020	0.015	-				-	0.012	0.015
Al	5.914	5.604	5.587	5.182	5.242	4.958	4.984	4.927	4.812				4.147	4.855	4.079
Ti	0.002	0.006	0.017	0.027	0.044	0.047	0.028	0.046	0.048				0.044	0.068	0.012
Fe^{3+}	0.004	0.056	0.304	0.604	0.643	0.845	0.897	0.923	1.003				1.550	0.986	1.898
Mg	0.166	0.096	0.014	0.150	0.048	0.076	0.065	0.077	0.038				0.236	0.068	0.044
Fe^{2+}	0.065	-	-	0.048	0.037	0.071	0.085	-	0.210				0.038	-	-
Mn	0.003	0.000	0.004	0.010	0.007	0.010	0.015	0.014	0.025				0.035	0.001	0.019
Ca	3.858	4.012	4.088	3.940	3.998	3.844	3.954	4.027	3.813				3.916	4.037	3.921
Na	0.014	0.031	0.054	0.034	0.004	0.024	0.030	0.040	0.025				0.037	0.057	0.071
Z	6.00	6.02	6.00	6.06	6.00	6.10	6.00	6.00	6.04				6.05	6.00	6.00
Y	5.92	5.76	5.91	5.81	5.93	5.85	5.91	5.90	5.86				5.74	5.91	5.99
X	4.10	4.14	4.16	4.18	4.09	4.02	4.15	4.16	4.11				4.03	4.16	4.06
(100 Fe^{3+}/ Fe^{3+} + Al)	0.07	0.99	5.16	10.44	10.90	14.56	15.18	15.74	17.25	17.28	19.29	22.27	27.21	16.85	31.68
Trace elements (ppm)															
Co	6			7	5	6	6		6	10	40	48	14		
Cr	-			103	65	33	18		29	27	61	101	747		
Cu	7			12	8	27	16		69	15	66	16	30		
Li	-			1	1	1	1		1	1	1	1	12		
Ni	-			28	18	17	17		20	21	40	32	50		
Pb	-			5	6	5	5		41	47	-	5	5		
V	20			176	196	379	261		278	114	303	329	193		
Zn	23			8	8	21	14		50	45	90	58	46		

30, 122, 96 and 123 by microprobe, the rest by wet chemistry Analyst M.Q. Jan. DIR 1 by plasma (analyst J.N. Walsh)
All Fe taken as Fe^{3+} in probe analyses.

Explanation Table 2.

DIR-1	Zoisite from a magnesio-hornblende-zoisite amphibolite near Kotgram, 10 km N of Chakdara, Dir. Contains o.1% F, 0.6% Cr_2O_3 and (in ppm) Ba 4, La 7, Sr 126, Y 3, Zr 13.
SA 30	Zoisite from a tschermakitic hornblende-corundum-epidote- secondary margarite amphibolite, Shisham stream, W of Lilauni, Swat. Contains 0.03% Cr_2O_3, 0.03% NiO, 0.07% CuO and 0.13% ZnO.
SI 122	Fe-Clinozoisite from a high-P granulite described under Table 1. Contains 0.7% NiO and Cr_2O_3, 0.5% CuO and 0.4% ZnO.
SI 355	Al-Epidote from an amphibolite 2.5 km N. of Kiru, KKH. Contains 0.5% cloudy calcic-plagioclase and magnesio-hornblende as impurity.
SI 355V	Al-Epidote from an epidote pegmatite in 355; contains traces of saussuritized plagioclase.
SI 291	Al-Epidote from a high-P retrograde granulite composed of Al-tschermakitic hornblende, garnet, plagioclase (An_{24}), paragonite, rutile, ore. Contains 0.5% quartz and hornblende + rutile inclusions.
US 19A	Al-Epidote from an epidote-Al-tschermakite pegmatite in amphibolites, 3km S of Matta. Contains 0.5% Amph + Ilm.
SS 96	Al-Epidote from a high-P granulite or amphibolite described under Table 1. Contains 0.12% Cr_2O_3, 0.10% NiO, 0.11% CuO, 0.15% ZnO.
SI 369	Al-Epidote from a banded gneiss described under Table 1. Contains 0.5% rutile impurity.
SI 177	Al-Epidote from an amphibolite described under Table1. Contains 0.5% rutile + cloudy labradorite.
SI 290	Al-Epidote from a high-P garnet granulite of the Jijal complex, 3 km N of Sandar, KKH. Contains about 1.5% rutile + ilmenite and 0.5% hornblende impurity.
US 4	Al-Epidote from an amphibolite 6 km N of Khwaza Khela, Upper Swat. Contains 5% sphene.
US 12	Fe-Epidote from an amphibolite near Chuprial, NW of Matta, Upper Swat. Analysis corrected for 10% diposide impurity.
SS 123	Primary Al-epidote and secondary Fe-epidote from a high-P garnet granulite described under Table 1. The primary phase contains 0.06% NiO, 0.14% CuO, 0.08% ZnO, 0.09% Cr_2O_3 and the secondary epidote contains 0.09% NiO, 0.05% Cr_2O_3.

Although epidote minerals are retentive of H_2O^+ and in some only a fraction of water is released after heating for an hour at 1000°C (Deer *et al.*, 1962), three of the six water determinations are in good and two in fair agreement and the analyses approach the ideal formula $Y_2X_3Z_3O_{12}(OH)$ when recalculated on 13(O, OH) basis. The slightly Lower Y and higher X values in all the recalculated analyses might suggest some substitution of bivalent cations in Y or undersetimation of travalent cations. The analyses also have a slight excess of Si in five of the twelve complete analyses. Whether this is due to tiny quartz inclusions or some other reason (e.g. underestimation of Al) cannot be evaluated.

The essential variation in the chemistry is the substitution of Al by Fe^{3+} (Fig. 4) as shown by a plot of 33 epidote analyses of Kohistan (including those of Bard, 1983b). There is a positive correlation between Al and Ca, as already found by Dobretsov *et al.* (1972). There also is a positive correlation between total Fe_2O_3 and MnO in our analyses (Fig. 5). However, if Bard's analyses are also plotted, this correlation disappears. FeO and MnO do not seem to be significantly correlated with each other but more FeO determinations would have better asessed this relation. The minor variation in FeO and drastic variation in Fe_2O_3 in epidotes has been interpreted by Myer (1966) as an evidence for different sites in the crystal structure for the Fe^{2+} and Fe^{3+} ions.

Compared to others clinozoisite-epidote analyses (Deer *et al.*, 1962; Myer, 1966; Rambaldi, 1973; Hietanen, 1974; Enami and Banno, 1980; Bard, 1983b), the Swat Kohistan epi-

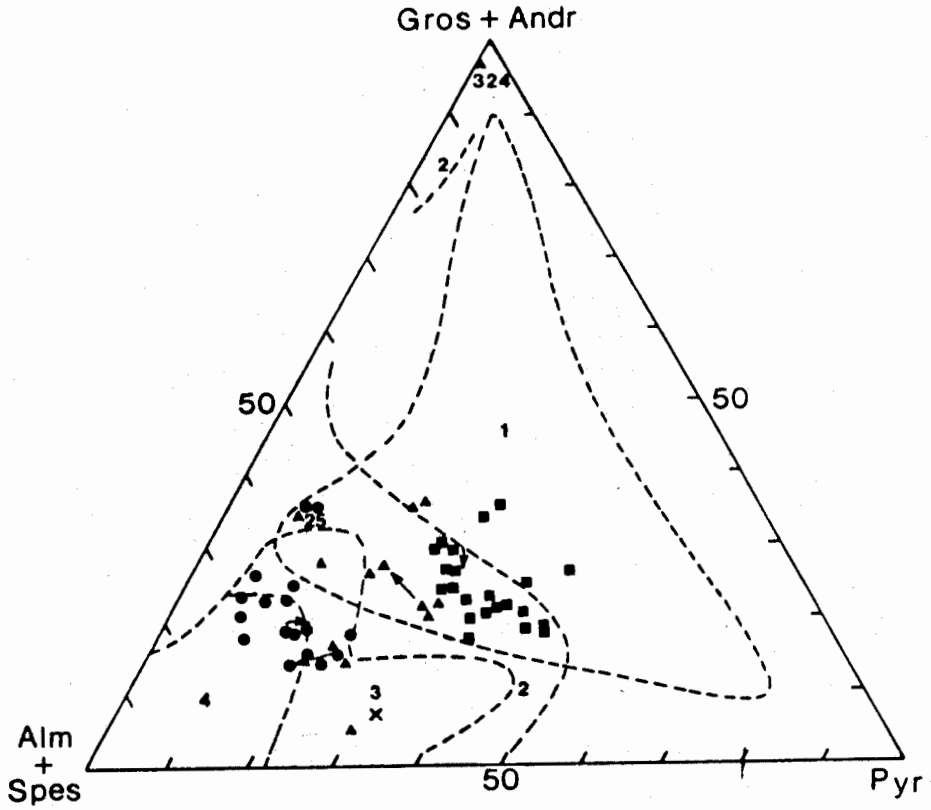

Fig. 2 Garnets from Swat-Kohistan on almandine + spessartine-pyrope-grandite triangle showing the fields of granets from (1) eclogites, (2) granulites, (3) amphibolites, and (4) epidote amphibolites (after Dobretsov *et al.*, 1972). The plots include published analyses in Ahmed and Ahmed (1975), Jan and Howie (1981), and Bard (1983).

- ■ garnets from high-P granulites of Jijal and Lilauni
- ● garnets from amphibolites, gneisses and pegmatites of the southern amphibolite belt
- ▲ garnets from this study. X garnet from hypersthene-biotite gneiss; for further details, see text.

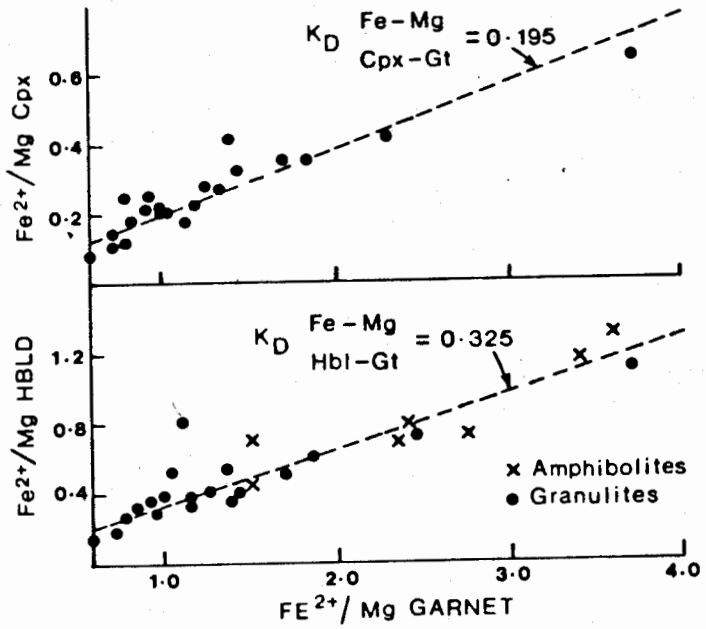

Fig. 3 Plot of Fe^{2+}/Mg in clinopyroxene and hornblende against that of garnet. The relationships are suggestive of attainment of equilibrium between Cpx-GT and Hbl-Gt pairs; however, the latter pairs from amphibolites (crosses) do not seem to have a different K_D from those of granulites (dots). Source of data; Jan and Howie (1981), Bard (1983) and Jan (unpubl. data).

dotes have more TiO_2. In some samples this can be connected with rutile/ilmenite impurities but 355V has none of these. So the excess TiO_2 is at least partly due to over-estimation. The epidotes are also higher in MgO than the microprobe analyses presented by Rambaldi, Hietanen, Enami and Banno, and Bard. When the trace elements of the wet analyses are compared with those of Myer (1966), the Swat Kohistan epidotes are richer in Cu and, especially, V and comparable in Pb and Cr. Hydrothermal epidotes, according to Myer, have lower Cr contents. Co, Ni, and Zn were not detected in the epidotes studied by Myer. The presence in small amounts of Na and K in these as well as in some microprobe analyses of other workers suggests their accomodation in the stucture rather than being due to impurities. P might also be in sturcture rather than in apatite impurities (cf. Koritnig, 1964; Myer 1966). Epidote 12 and, especially, DIR1, have high Cr (reflecting Cr substitution for Al in the M(3) site according to Grapes, 1981) due to a high Cr content of their hot rocks, and 369 and 177 are rich in Pb.

The stability of the epidote minerals has been investigated in recent years (Boettcher, 1970; Liou, 1973; Newton, 1965, 1966; Holdaway, 1972). It is now thought that the Fe^{3+}/Al ratio is influenced by a number of factors (and hence some conflict in the data). Many workers (Miyashiro and Seki, 1958; Hietanen, 1974; Liou *et al.*, 1975; Raith, 1976; Coombs *et al.*, 1976) have found that the Fe^{3+} content of epidotes decreases with increasing metamorphism but the data of Rambaldi (1973) suggest an opposite effect. Similarly, zoisite has been found by a number of workers to be stable to higher temperatures than clinozoisite; however, Tanner (1976) found the reverse in the Moinian calcpods. Dobretsov *et al.* (1972, p. 313), on a composite diagram based on the experimental investigation of the reaction epidote + quartz = Ca garnet + anorthite + hematite + H_2O, have shown that the boundary curve passes through 620°C, 2 kbar for epidote with Ps_{33}; 650°C, 4 kbar for Ps_{25}; 700°C, 6 kbar for Ps_{15}; and 750°C, 9 kbar for Ps_{10}.

The composition and upper stability limit of the epidotes can be influenced by metamorphic grade, bulk composition especially Fe_2O_3/Al_2O_3 ratio and fugacity of oxygen. Other components in the complex rock systems (Mg, Fe^{2+}, Ti, Na, K, OH) may also have an influence although the effect is not known. Holdaway (1972) considered that the persistence of epidote to higher grades in calc-silicate rocks is in large part a function of the Ca/Na ratio of the host rocks. The coexisting mineral phases (Hietanen, 1974) and their Fe^{2+}/Fe^{3+} ratios (Rambaldi, 1973) have also some influence.

On the basis of epidote composition alone, it is hard to reach conclusions regarding the grade of metamorphism in Swat Kohistan. The oxidation and, especially, Fe^3/Al ratios of the host rocks have considerably influenced the composition of the epidotes (Fig. 5). The positive correlation between total iron in all the hornblende-epidote pairs, and Fe_2O_3 in the completely analyse pairs also suggests the influence of fO_2 (Fig. 6). The Jijal and Lilauni granulites have equilibrated at higher temperatures and much higher pressure (800-900°C, ~ 10 kbar) than the amphibolites (550-700°C, 4-7 kbar except locally) but their epdotes do not have much different Ps contents. Similarly, temperature estimates for rocks 177 and 96 are higher than the rest of the amphibolites but their epidote is in no way exceptional.

The Swat Kohistan rocks generally contain only one epidote mineral. In a few rocks, as indicated by colour and birefringence difference, a second variety does occur. However, textural relations of the two epidotes suggest disequilibrium relations, either as zones (with generally Fe-rich cores), replacement features or secondary growth (anal. 123). Occurence of more than one epidote mineral in equilibrium in rocks has been interpreted to be due to miscibility gap (Strens, 1965). The composition of such epidotes varies in different cases due to asymmetrical solvus with its top at Ps_{22} (Holdaway, 1972). Raith (1976) suggested that immiscibility in epidotes takes place at low temperatures (≤ 550°C). Enami and Bano (1980) found that with increasing temperature, in the range of low-to medium-grade metamorphism, the compositional gap between coexisting zoisite-clinozoisite enlarges and shifts towards higher Fe^{3+}. On the basis of three zoisite-clinoepidote pairs from Jijal, Bard (1983b) extended the im-

Table 3. Analyses of biotitic micas from Swat Kohistan

%	SI 352	SK 462	SI 337	SI 193	SK 592	SK 587	SI 192	SK 528	SK 525	SK 448	SK 476
SiO_2	-	-	34.89	35.88	36.29	36.15	-	37.94	36.26	36.04	36.94
TiO_2	3.88	5.03	1.89	5.04	3.39	6.10	6.42	4.45	3.47	4.10	4.26
Al_2O_3	17.37	17.78	18.21	14.82	14.15	14.83	15.78	16.70	16.42	14.94	15.72
Fe_2O_3	8.16	1.66	-	3.05	-	-	0.94	-	3.33	0.46	1.65
FeO	12.13	13.28	18.50*	15.51	17.41*	14.66*	14.43	15.08*	15.06	17.47	14.58
MnO	0.23	0.20	0.02	0.07	0.09	0.07	0.05	0.09	0.29	0.14	0.16
MgO	9.70	16.71	11.52	11.52	13.02	12.18	13.60	14.60	11.62	13.57	13.10
CaO	1.46	1.14	0.21	0.21	0.08	0.04	0.36	0.00	0.19	0.92	0.63
Na_2O	0.21	0.16	0.10	0.08	0.09	0.19	0.08	0.03	0.14	0.12	0.18
K_2O	4.72	5.14	8.17	8.94	8.79	9.67	9.05	9.83	9.36	7.34	8.21
H_2O^+	-	-	-	-	-	-	-	-	3.34	4.33	3.48
P_2O_5	0.00	0.00	0.00	0.01	0.00	0.13	0.00	0.00	0.00	0.00	0.00
F	-	-	-	-	-	-	-	-	0.30	0.36	0.039
O=F	-	-	-	-	-	-	-	-	0.13	0.15	0.16
TOTAL	-	-	93.51	95.13	93.34	94.02	-	98.77	99.65	99.64	99.14
Number of ions on the basis of 24 (O, OH, F) or 22(O)**											
Si			5.368	5.436	5.603	5.499		5.459	5.486	5.375	5.537
Al			2.632	2.564	2.397	2.501		2.541	2.514	2.625	2.463
Σ			8.00	8.00	8.00	8.00		8.00	8.00	8.00	8.00
Al			0.669	0.084	0.178	0.158		0.292	0.415	0.003	0.315
Ti			0.219	0.574	0.393	0.698		0.482	0.395	0.460	0.480
Fe^{3+}			-	0.348	-	-		-	0.380	0.052	0.186
Fe			2.381	1.966	2.247	1.865		1.815	1.906	2.179	1.828
Mn			0.003	0.009	0.012	0.009		0.011	0.037	0.018	0.021
Mg			2.641	2.601	2.996	2.761		3.131	2.620	3.017	2.927
Σ			5.91	5.58	5.83	5.49		5.53	5.75	5.73	5.76
Ca			0.034	0.034	0.013	0.006		0.00	0.031	0.147	0.101
Na			0.030	0.024	0.029	0.057		0.009	0.042	0.036	0.052
K			1.603	1.728	1.725	1.881		1.805	1.807	1.396	1.571
Σ			1.65	1.79	1.77	1.94		1.81	1.88	1.58	1.72
OH			-	-	-	-		-	3.371	4.307	3.481
F			-	-	-	-		-	0.144	0.169	0.185
Fe_t/Mg	1.13	0.50	0.90	0.89	0.75	0.68	0.63	0.58	0.87	0.74	0.69
Trace Elements (ppm)											
Cp	57	78	-	114	-	-	122	-	79	88	95
Cr	59	496	-	67	480	205	346	-	38	188	88
Cu	325	16	-	417	-	-	87	-	110	62	120
Li	18	155	-	12	-	-	28	-	65	55	84
Ni	148	-	-	219	-	-	638	-	100	228	176
Pb	5	-	-	6	-	-	13	-	5	5	5
V	220	315	-	734	-	-	782	-	524	601	432
Zn	329	252	-	290	400	400	86	400	326	272	316

*Total Fe as FeO **Analyss with water recalculated on 24 (O,OH,F); others on the basis of 22(O)

592, 528, 537 and 587 analysed by microprobe by J.-P. Bard. Rest analysed by wet chemistry by M.Q. Jan.

SiO_2 and Al_2O_3 in 193 are microprobe values.

352 and 462 from amphibolitic rocks, 337 to 528 and, possibly, 647 from pyroxene granulites, and 713 to 448 from quartz diorites. Locations and modes of rocks 337, 193, 592, 587, 528 and 647 (Density = 2.996) given under other tables.

352. Altered biotite from a banded gneiss containing plagioclase, quartz, hornblende, epidote, mica, etc. Along KKH, 1/2 km N of Kiru, Indus valley.

462. Altered biotite from streaky amphibolite. From isolated outcrop between road and river at Asrit, Swat Kohistan.

192. Biotite from pyroxene granulites, along KKH, 2 km E of Thor stream.

525. Biotite from a quartz diorite along stream 4 km W of Kedam, Swat Kohistan. Density = 2.653.

448. Biotite from a quartz diorite 2 km S of Kalam.

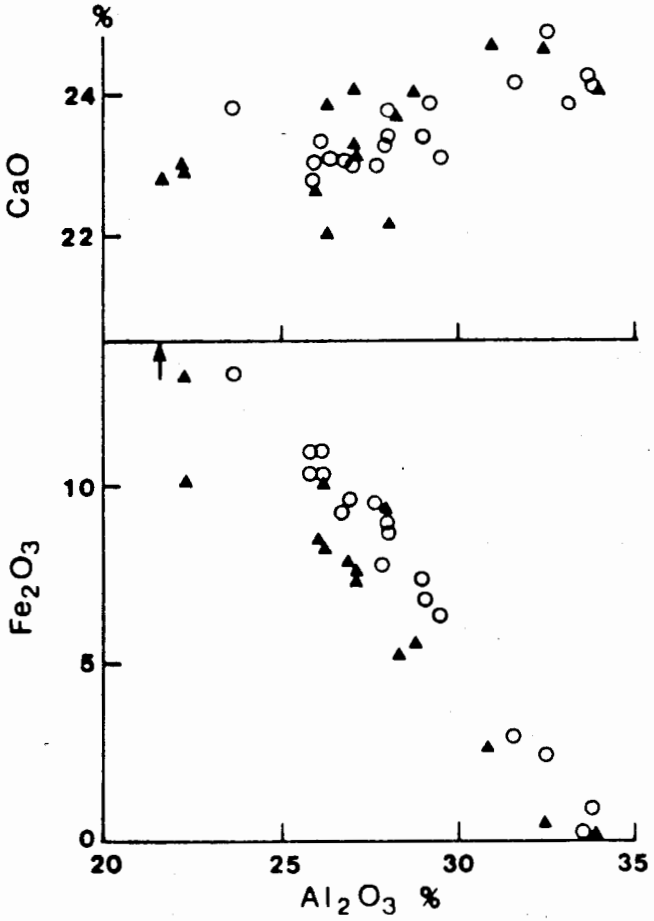

Fig. 4 Al_2O_3 ***vs.*** Fe_2O_3 and CaO (oxide percentages) in the analysed epidotes. Although the essential variation is in the Fe^{3+}/Al substitution, a positive correlation is also obvious in CaO and Al_2O_3. Triangles: this study; circles: Bard's (1983b) data.

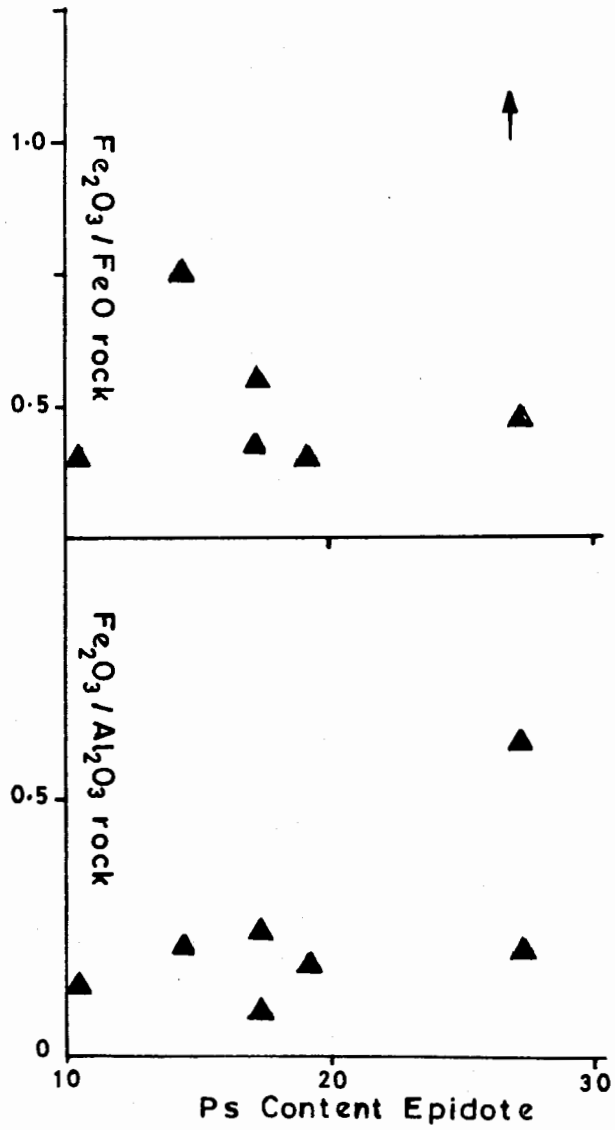

Fig. 5 Plots of Fe_2O_3/FeO and Fe_2O_3/Al_2O_3 in host rocks against Ps content (100 $Fe^{3+}/(Fe^{3+}+$ Al) of epidote. A fairly strong influence of the Fe^{3+}/Al ratio of rock on Ps content of epidote is obvious but that of oxidation ($f\,O_2$) is rather variable in this figure (but compare Fig. 6B).

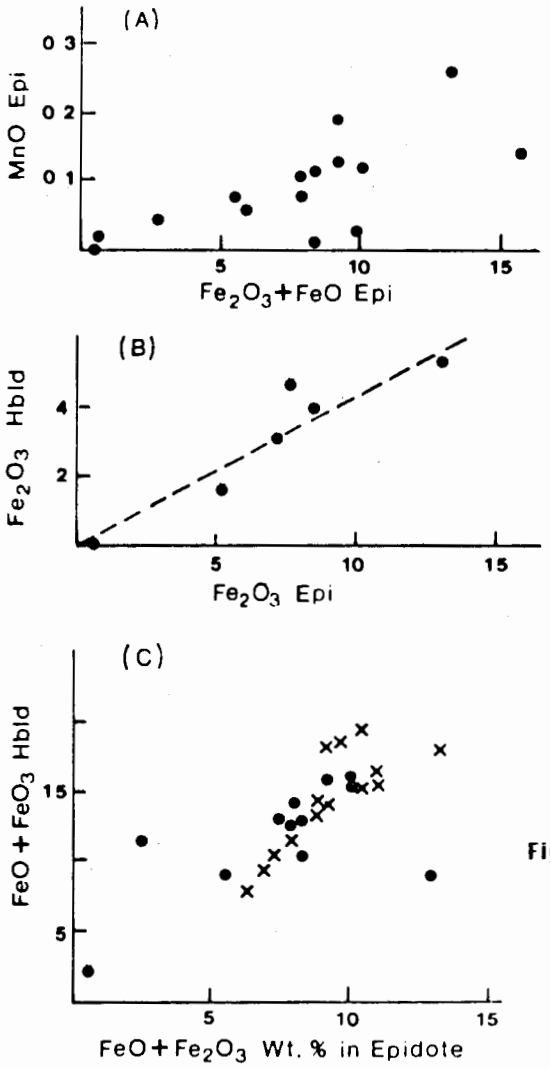

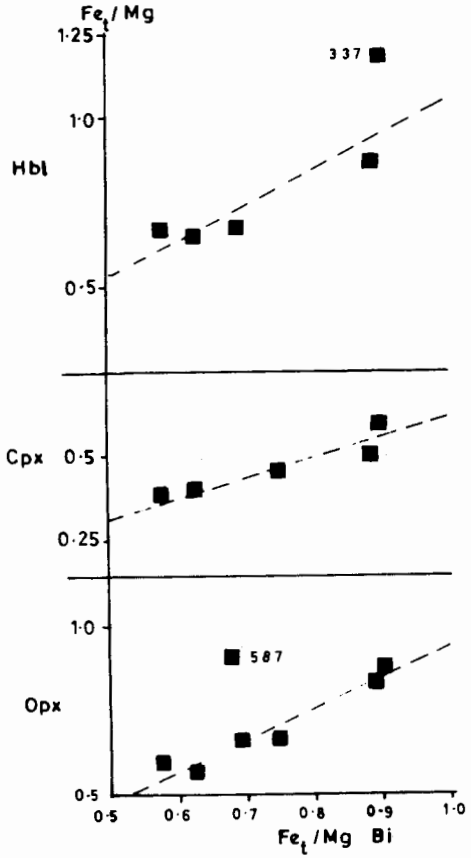

Fig. 6 A) Positive correlation between the MnO and total iron content of the epidotes of the present study. Such a relationship is not obvious when Bard's (1983b) analyses are also plotted.
B) Relation between the Fe_2O_3 contents of hornblende and epidotes. Only those hornblendes were considered in which Fe_2O_3 and FeO were wet-chemically analysed (Jan and Howie, 1982). The strong positive correlation suggests the influence of fO_2 on the two minerals.
C) Positive correlation between FeO + Fe_2O_3 contents of epidote and hornblende pairs, suggesting the influence of the host rock chemistry. Crosses: Bard's (1983) data; dots: this study.

Fig. 7 Fe_t/Mg distribution between pyroxene granulite biotite and asocited orthopyroxene, clinopyroxene, and hornblende. (Anal. 647 is included in granulites in this diagram). Dashed linear trends pass through origin. The apparently systematic distribution of Fe and Mg is indicative of equilibrium in mafic silicate-biotite pairs despite an opposing textural evidence in a few cases. Bio-Opx in 587 and bio-Hbl in 337 depart from the trends although textures (especially in the former) favour equilibrium relations. Compositions of pyroxenes and hornblende from Jan and Howie (1980, 1982) and Jan (1983).

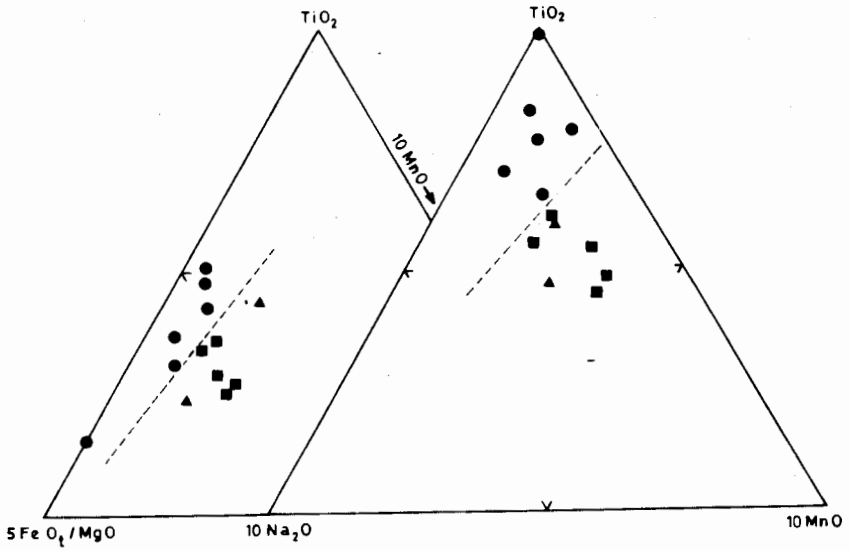

Fig. 8 TiO_2-10MnO-5FeO_t-MgO. and TiO_2-10MnO-10Na_2O triangular plots for the biotitic micas from Kohistan pyroxene granulites (circles), amphibolites (triangles), and diorites (squares). Dashes line separates granulite micas from the rest. Analysis 647 is symbolized as diorite.

miscibility gap to granulite field. His data suggest a reduction in the gap with a rather rapid Fe^{3+} increase.

MICAS

Partial to complete analyses of 13 micas, along with trace elements for nine of them, are presented in Table 3. Analyses 352 and 462 are from amphibolites, 337 to 528 from pyroxene granulites, and 713 to 448 from diorites. SK647 is of doubtful granulite origin. The granulite micas are generally in small quantity and have replacive relations with the rest of the minerals. However, their Fe/Mg distribution with the coexisting mafic silicates suggests that they may have attained chemical equilibrium (Fig. 7). Different models of geothermometry involving biotite and other mafic minerals yield high temperatures (Jan, 1983) suggesting that the biotite may have formed in the last stages of granulite facies recrystallisation/early obduction at depth.

Table 4. Microprobe analyses of some feldspars from Swat Kohistan.

	SI 337*	SI 193*	SK 528*	SK 647*	SK 592*	SI 324*	SI 324*	US 27**	US 27**	SA 24**	SS 121**
SiO_2	54.03	56.63	55.85	56.90	56.79	68.51	66.27	48.80	59.36	57.44	62.77
TiO_2	0.01	0.02	0.04	0.04	0.05	0.00	0.00	0.05	0.00	0.03	0.02
Al_2O_3	29.86	27.65	27.05	27.48	27.33	19.86	19.11	31.03	24.22	26.49	23.03
Fe_2O_3	0.11	0.11	0.21	0.14	0.04	0.00	0.03	0.66	0.00	0.16	0.21
MnO	0.00	0.02	0.00	0.00	0.00	0.09	0.03	0.05	0.09	0.02	0.00
MgO	0.01	0.01	0.04	0.00	0.02	0.00	0.00	0.10	0.22	0.07	0.01
CaO	11.80	9.55	9.74	9.15	8.96	0.16	0.03	14.99	6.28	8.31	4.63
Na_2O	4.76	5.52	5.51	5.82	6.10	11.25	0.93	3.07	7.78	6.62	8.69
K_2O	0.23	0.49	0.54	0.53	0.29	0.11	15.10	0.02	0.04	0.04	0.10
P_2O_5	0.02	0.04	0.00	0.05	0.04	0.03	0.01	-	-	-	-
Cr_2O_3	0.02	0.00	0.03	0.01	0.05	0.00	0.17	0.07	0.00	0.00	0.03
ZnO	0.01	0.00	0.08	0.07	0.00	0.00	0.08	0.05	0.38	0.00	0.03
TOTAL	100.86	100.04	99.09	100.19	99.67	100.01	101.76	98.89	98.37	99.18	99.52
Numbers of ions on the basis of 32(0)											
Si	9.691	10.167	10.153	10.209	10.221	11.955	11.985	9.051	10.777	10.362	11.159
Al	6.314	5.852	5.798	5.813	5.799	4.086	4.074	6.785	5.184	5.634	4.827
Ti	0.002	0.005	0.005	0.005	0.007	0.000	0.000	0.007	0.000	0.004	0.003
Fe^{3+}	0.015	0.015	0.029	0.020	0.006	0.000	0.004	0.092	0.000	0.022	0.028
ΣZ	16.02	16.04	15.99	16.05	16.03	16.04	16.06	15.94	15.96	16.02	16.02
Mn	0.000	0.003	0.000	0.000	0.000	0.014	0.004	0.008	0.014	0.003	0.000
Mg	0.002	0.002	0.005	0.000	0.005	0.000	0.000	0.028	0.060	0.013	0.002
Ca	2.268	1.837	1.898	1.760	1.730	0.030	0.005	2.979	1.222	1.606	0.882
Na	1.653	1.920	1.942	2.025	2.128	3.806	0.326	1.103	2.738	2.315	2.995
K	0.052	0.112	0.125	0.121	0.067	0.025	3.484	0.004	0.09	0.009	0.023
ΣX	3.98	3.87	3.97	3.91	3.93	3.88	3.82	4.12	4.04	3.95	3.90
Mole per cent end-members											
An	57.11	47.55	47.93	45.06	44.15	1.13	0.23	72.9	30.8	40.9	22.6
Ab	41.58	49.56	48.92	51.84	54.14	98.22	0.53	27.0	69.0	58.9	76.8
Or	1.31	2.89	3.15	3.10	1.71	0.65	91.23	0.1	0.2	0.2	0.6

337 Labradorite in basic pyroxene granulite lens in amphibolites, 2 km N of Patan, Indus Valley.

193 Andesine in intermediate pyroxene granulite along KKH, 6 km E of Thor stream.

528 Andesine in basic pyroxene granulite, in Bishigram (Madyan) stream, 1/2 km E of Karamai, Swat Kohistan.

647 Andesine in retrograde intermediate granulite or hypersthene diorite, along footpath in ridge 2.8 km W of Dabna, Swat Kohistan.

592 Andesine in intermediate pyroxene granulite, along southern Mankial stream. 3/4 km S of Sur Gat, Swat Kohistan.

324 Albite and microcline microperthite (description of sample given under Table 1).

US 27 Reversely zoned (An_{73}-$An_{70.9}$) bytownite (perhaps pre-metamorphic relics) and newly formed (metamorphic) andesine, from a pyroxene granulite lens in amphibolite described under Table 1.

SA 24 Andesine from a high-P granulite described under Table 1.

SA 121 Oligoclase from high-P granulite described under Table 1.

Analyst: * = J.-P. Bard ** = Microprobe analyses by M.Q. Jan.

Analyses 639 and 713 are atypical of biotites; they contain abnormally low K_2O and high CaO. Both these micas are strongly altered to chloritic material with some prehnite, etc. The two amphibolite micas (352, 462) are also substantially poor in K_2O than normal biotites. The lower K_2O values of these analyses cannot be explained by making allowances for possibly lower K_2O due to a lower grade of metamorphism (Zakrutkin and Grigorenko, 1968), impurities, underestimation, X-site vacancies or substitution of H_2O^+ or H_3O^+ in the X-site. It seems that alteration (rather mild in thin section) is the principal cause of their peculiar chemistry. A notable feature of the four analyses is the increase in their CaO with decrease in K_2O. Analysis 713 is also low in SiO_2 and high in H_2O. It appears that the alteration process responsible was not strictly chloritization. In some diorites of Kohistan, prehnite development after biotite has been noticed; thus there is a possibility that the four micas are affected by chloritization as well as some prehnitization. The lowering of K_2O in biotitic micas in eastern Otago schists, New zealand, was also attributed to hydrothermal alternation and leaching (Craw *et al.*, 1982).

The general chemistry of the remaining micas is brodly similar to other biotites but the CaO content of the analyses is generally higher than those of the 90 microprobe analyses of biotites from different parts of the world (Misch and Onyeagocha, 1976; Guidotti *et al.*, 1975; Scharbert and Kuart, 1974; Ramsay, 1973). The possibility of unnoticed sphene impurities or something else in the wet analysed samples should not be ruled out.

Simonen and Vorma (1969) noted that biotites from Rapakivi area contain more Al^{IV}, Fe^{3+}, Ti, and $Al^{VI} + Fe^{3+} + Ti$ than the coexisting amphiboles, suggesting equilibrium conditions for the two. In Swat, Fe^{3+} (except in 352) is lower and Ti higher in the brown micas than in the coexisting amphiboles despite that the two do not show disequilibrium textures in the diorites and amphibolites. The Y site totals for the recalculated micas are lower than the ideal value for a trioctahedral mica. This is a common feature of the biotite analyses and suggestive of replacement by some dioctahedral constituents (Deer *et al.*, 1962; Windley and Smith, 1974).

A characteristic feature of the micas is their richness in Co, Cr, Cu, Li, Ni and Zn. The values for F and Pb, however, are low. The values for Co and V are highest for the granulite and lowest for the amphibolite micas. Compared to the biotites from a tonalite and two quartz monzonites of Ardnamurchan (Walsh, 1975), the Swat quartz diorite micas have higher values for Co, V, Cr and, especially, for Cu and Ni, and lower Pb. Lithium shows a greater range in Ardnamurchan biotites (42 to 142 p.p.m.). On the basis of trace element content of the biotites (and of the amphiboles), the quartz diorites cannot be mutually distinguished effectively but, perhaps, more analyses ae required.

Although Ramsay (1973) did not find a temperature control over Ti in biotites around a pluton in NW Territories, Canada, many workers have suggested an increase in Ti with metamorphic grade, mainly temperature (Best and Weiss, 1964; Zakrutkin and Grigorenko, 1968; Dobretsov *et al.*, 1972, and others). comparison between the micas of granulites and amphibolites of Swat Kohistan cannot be made because of the altered nature of the only two analyses from the amphibolites. However, the granulite biotites have more Ti than those of the diorites. The latter group of rocks has been considered on other grounds to have equilibrated finally at lower temperatures than granulites (Jan, 1977). The granulite micas are poorer also in Na_2O and MnO than the rest. Although granulite biotites are considered to be lower in Mn than those of lower grade rocks (Dobretsov *et al.*, 1972), the cause of the lower Na in the Swat Kohistan granulite biotites is not clear. On TiO_2-5FeO/MgO - 10MnO and TiO_2 - $10Na_2O$ - 10MnO plots the micas are clearly separated into two fields (Fig. 8). In agreement with Sapozhnikova's (1981) studies on pegmatite biotites, the Al_2O_3 content of the high-T (granulite) biotites from Swat is generally lower than those of the lower temperature (amphibolites and diorites) ones. The Al_2O_3 in biotite of sample 448 is lower than the rest of the diorites. This rock is a shallow, unmetamorphosed diorite yielding a higher T-estimate than

the remainder of the diorites (Jan and Howie, 1980).

FELDSPARS

Microprobe analyses of ten plagioclases and one microcline microperthite are given in Table 4. Analyses 324 are from a calc-silicate horizon in amphibolite, 24 and 121 are from garnet granulites, whilst the rest are from pyroxene granulites with a dubious status of rock 647. The analyses have been recalculated on 32 oxygen basis and all are fairly close to ideal formula where Z = 16 and X = 4. The total iron, taken as Fe_2O_3, has been considered to replace Al_2O_3 and, along with Ti, added to Z. Mn and Mg probably substitute for Ca and added to X. The anorthite contents of the analyses closely match those optically determined.

The analyses are normal but the high MnO in albite analysis of 324 and US27 andesine may reflect over-estimation. In eight of the analyses the Z totals are slightly more than 16 and X less than four. In most of the analyses Si and Al are slightly in excess even when Fe, Ti, P, and Zn are considered to substitute for Ca and added to X group. The cause of this excess has not been evaluated here but readers are referred to Deer *et al.* (1962) who have discussed the problem of excess Si in feldspar analyses.

The plagioclase of the noritic members of the pyroxene granulites shows rather a restricted range, mostly being calcic andesine. Analysis 337 (labradorite) is from a rock with distinctly higher CaO/alkalis, normative anorthite/(albite + orthoclase), and Al_2O_3/alkalis ratios than the rest, so a compositional control is responsible for its higher An content. In the rest of the cases, however, the An content cannot be tied up with these factors. In one pyroxene granulite (US27), the plagioclase occurs in two ways: (a) larger zoned and partly cloudy grains, and (b) fresh, smaller grains. The former is bytownite and may be pre-metamorphic relics, and the latter is andesine and definitely metamorphic.

Jan (1977) determined optically the composition of 60 plagioclases in basic and intermediate pyroxene granulites of the Chilas complex, none of the rocks containing modal and only six containing minor normative olivine. He found that the plagioclase commonly ranged from An_{45} to An_{54} with some up to An_{60}. This narrow range is akin to the plagioclase found in Adirondacks (Buddington, 1939) and other anorthosite massifs, although Crosby (1972) has warned against "making sweeping generalizations". The narrow range in large anorthosite massifs has been attributed to narrow temperature interval, narrow range of load or water pressure, and/or close approximation to chemical equilibrium (Buddington 1969; Yoder, 1969; Crosby, 1972). Jan and Howie (1980), Jan (1983) and Bard (1983) have also suggested rather uniform conditions of metamorphism (~800°C, 6-8 kbar) for the vast belt of pyroxene granulites. In a number of Swat pyroxene granulites the plagioclase is antiperthitic. This feature has yet not been fully investigated but it is worth mentioning that the plagioclase is similar in this respect to those from other granulites. Basic igneous rocks normally do not contain antiperthitic plagioclases.

Plagoiclase in the high-P granulites of Lilauni (anal. 24 and 121) and Jijal (see Appendices in Jan and Howie, 1981; Bard, 1983) is generally more sodic than in pyroxene granulite. The Jijal plagiopyrigarnites developed due to a reaction between plagioclase and orthopyroxene/olivine. The newly formed clinopyroxene and abundant garnet consumed Ca and Al but pressure was not sufficiently high for the accommodation of much Na in clinopyroxene (Jan and Howie, 1981). Thus the recrystallized plagioclase was left with more Na to accommodate.

The microcline and albite analyses from 324 are not unusual, but the albitic nature of the plagioclase is surprising. The presence of clinopyroxene and granet in this rock, as well as the grade of metamorphism in the surrounding rocks, suggest temperatures of almandine amphibolite facies (> 560°C). Under such conditions, it is hard to expect albitic plagioclase as a prograde product. Although garnet-clinopyroxene and two-feldspar geothermometry yield temperatures in the greenschist facies for this rock, we have no evidence to suggest

that either the minerals are in disequilibrium, the terrain has suffered such a low grade of metamorphism locally, or that the rock is tectonically emplaced. Perhaps the peculiar rock chemistry has played a role in producing such a paragenesis.

CONCLUSIONS

Analyses of garnets, epidotes, micas and feldspars complete the first major phase of investigation of the principal rock-forming minerals in Swat and southern Kohistan. Garnets from the amphibolite belt are almandine-rich (54 to 68 mole percent) but calcic and manganiferous garnets occur in calcareous and Mn-rich rocks. Compared to those from the high-P granulite facies metabasites from Jijal (Jan and Howie, 1981; Bard, 1983), the amphibolite facies garnets are poorer in Mg and Ca, and richer in Mn and Fe^{2+}. Garnet in the amphibolite belt is sporadic and bulk chemistry, especially low Mg/Fe^{2+}, is responsible for its development. In the Jijal complex, and in Lilaunai area of the amphibolite belt where pressure were higher than the rest of the belt, garnet is more abundant and developed over a wider range of composition.

The epidote minerals in the amphibolite belt and garnet granulites are generally monoclinic with Ps content ranging from 0 to 32; however, zoisite occurs in a few rocks instead or along with a monoclinic variety. No obvious difference is found in the composition of the epidotes from amphibolites and garnet granulites. The Ps content of the epidotes is controlled by Fe_2O_3/Al_2O_3 and by the oxidation state of their host rocks but other factors might also have some influence. The rocks generally contain only one epidote mineral; a second epidote, when present, shows disequilibrium relations but a few rocks (even in granulite facies) may contain coexisting Fe-poor and Fe-rich epidotes.

The analyses of biotites from the pyroxene granulites contain more Ti and less Mn and Na than those of the diorites which are considered to have equilibrated at lower temperatures than the pyroxene granulites. Four of the "biotites" show varying degrees of alteration, the process apparently a combination of chloritization and prehnitization, such that decrease in K (and Si) is accompanied by a slight increase in Ca (and H_2O). The feldspars are usual but their Si and Al are generally in excess over those required by Ca and alkalis. The plagioclase in a calc-silicate rock is much too sodic than is expected in rocks of amphibolite facies. Perhaps the peculiar composition of the host rock played a role in producing an albitic plagioclase.

ACKNOWLEDGEMENTS

Professor J.P. Bard is thanked for several microprobe analyses, and Dr. J.N. Walsh for advice during the wet chemical analyses and also for analysing epidote DIR1. M.Q. Jan wishes to acknowledge Prof. B.F. Windley and the Royal Society for the award of a guest research fellowship which enabled him to visit the University of Leicester in 1981.

REFERENCES

AHMED, Z. & AHMAD, S. (1975) Garnets from the Upper Swat Hornblendic Group, Swat district, Pakistan. Part 1: Garnets from the gneisses and pegmatites. Mineral. Mag. **40**, pp. 53-58.

ANDREWS-SPEED, C.D. & BROOKFIELD, M.E. (1982) Middle Paleozoic to Cenozoic Geology and tectonic evolution of the northern Himalaya. Tectonophysics **82**, pp. 253-275.

BARD, J.P. (1983a) Metamorphism of an obducted island arc: example of the Kohistan sequence (Pakistan) in the Himalayan collided range. Earth Planet. Sci. Letters, **65**, pp. 133-144.

——— (1983b) Metamorphic evolution of an obducted island arc: example of the Kohistan sequence (Pakistan) in the Himalayan collided range. Geol. Bull. Univ. Peshawar **16**, pp. 105-184.

———, MALUSKI, H., MATTE, PH. & PROUST, F. (1980) The Kohistan sequence: crust and mantle of an obducted island arc. In: Proc. Int. Commit. Geodynamics, Grp. 6 Mtg. Peshawar, Nov. 23-29, 1979, pp. 87-94.

BARTH, T.F.W. (1936) Structural and petrological studies in Dutchess Country, New York. Part II; Petrology and metamorphism of the Paleozoic rocks. Geol. Soc. Amer. Bull. **47**, pp. 775-850.

BEST, M.G. & WEISS, L.E. (1964) Mineralogical relations in some pelitic hornfelses from the southern Sierra Nevada, California. Amer. Mineral. **49**, pp. 1240-1266.

BINNS, R.A. (1965) The mineralogy of metamorphosed basic rocks from the Willyama complex, Broken Hill district, New South Wales, Part II. Pyroxenes, garnets, plagioclases, and opaque oxides. Mineral. Mag. **34**, pp. 306-326.

BOETTCHER, A.L. (1970) The system of CaO-Al_2O_3 SiO_2-H_2O at high pressures and temperatures. Jour. Petrol. **11**, pp. 337-379.

BUDDINGTON, A.F. (1939) Adirondacks Igneous Rocks and their Metamorphism. Geol. Soc. Amer. Mem. 7.

———— (1952) Chemical petrology of some metamorphosed Adirondacks gabbroic, syenitic and quartz syenitic rocks. Amer. Journ. Sci., Bowen Vol., pp. 37-84.

———— (1965) The origin of three garnet isograds in Adirondack gneisses. Mineral. Mag. **34**, pp. 71-81.

———— (1969) Adirondack anorthosite series. In 'Origin of Anorthosites and Related Rocks.' (Y.W. Isachsen ed.). N.Y. State Mus. & Sci. service, Mem. **18**, pp. 215-231.

COOMBS, D.S., NAKAMURA, Y. & GUAGNAT, M. (1976) Pumpellyite-actinolite facies schists of the Taveyanne formation near Loeche, Valais, Switzerland. Journ. Petrol. **17**, pp. 440-471.

COWARD, M.P., JAN, M.Q., REX, D., TARNEY, J., THIRLWALL, M. & WINDLEY, B.F. (1982a) Structural evolution of a crustal section in the western Himalaya. Nature, **295**, pp. 22-24.

———— (1982b) Geotectonic framework of the Himalaya of N. Pakistan. J. Geol. Soc. London **139**, pp. 299-308.

———— WINDLEY, B.F., BROUGHTON, R., LUFF, I.W., PETTERSON, M., PUDSEY, C., REX, D., & KHAN, M.A. (1986) Collision Tectonics in the NW Himalaya. In: Coward, M.P. and Reis, A.C. (eds.) Collision Tectonics. Geol. Soc. Spec. Pub. **19**, pp. 203-213.

CRAW, D., COOMBS, D.S. & KAWACHI, Y. (1982) Interlayered biotite-kaolinite and other altered biotites, and their relevance to the biotite isograd in eastern Otago, New Zealand. Min. Mag. (Deer, Howie & Zussman vol.), **45**, pp. 79-85.

CROSBY, P. (1972) Petrogenesis and significance of leuconorite inclusions in the main Adirondack anorthosite massif. Proc. 24th Int. Geol. Cong. Montreal, **2**, pp. 312-319.

DEER, W.A., HOWIE, R.A. & ZUSSMAN, J. (1962) ROCK-FORMING MINERALS, vols. 1,3,4. Longman, London.

DOBRETSOV, L.N., KHLESTOV, V.V., REVERDATTO, V.V., SOBOLEV, N.V. & SOBOLEV, V.S. (1972) THE FACIES OF METAMORPHISM. (Transl. by D.A. Brown). Canberra (Aust. Nat. Univ.).

ENAMI, M. & BANNO, S. (1980) Zoisite-clinozoisite relations in low- to medium-grade high-pressure metamorphic rocks and their implications. Min. Mag. **43**, pp. 1005-1013.

ENGEL, A.E.J. & ENGEL, C.G. (1962) Progressive metamorphism of amphibolite, northwest Adirondack Mountains, New York. In 'Petrologic studies' (Engel *et al.*, eds.). Geol. Soc. Amer., A.F. Buddington vol., pp. 37-82.

GLASSLEY, W.E. & SORENSEN, K. (1980) Constant Ps-T amphibolite to granulite facies transition in Ag to (West Greenland) metadolerites: implications and applications. Jour. Petrol. **21**, pp. 69-105.

GRAPES, R.H. (1981) Chromiam epidote and zoisite in kyanite amphibolite, southern Alps, New Zealand. Amer. Mineral, **66**, pp. 974-975.

GUIDOTTI, C.V., CHENEY, J.T. & CONATORE, P.D. (1975) Interrelationship between Mg/Fe ratio and octahedral Al content in biotite. Amer. Mineral. **60**, pp. 849-853.

HIETANEN, A. (1974) amphibole pairs, epidote minerals, chlorite, and plagioclase in metamprhic rocks. Northern Sierra Nevada, California. Amer. Mineral, **59**, pp. 22-40.

HOLDAWAY, M.J. (1972) Thermal stability of Al-Fe epidotes as a function of fO_2 and Fe content. Contrib. Mineral. Petrol. **37**, pp. 307-340.

HONEGGER, K., DIETRICH, V., FRANK, W., GANSSER, A., THONI, M. & TROMMSDORFF, V. (1982) Magmatism and metamorphism in the Ladakh Himalayas (the Indus-Tsang Po suture zone). Earth Planet. Sci. Lett. **60**, pp. 253-292.

HOWIE, R.A. & SUBRAMANIAM, A.D. (1957) The paragenesis of garnet in charnockite, enderbite, and related granulites. Min. Mag. **31**, pp. 565-586.

HSU, L.C. (1968) Selected phase relations in the system Al-Mn-Fe-Si-O-OH: a model for garnet equilibria. Journ. Petrol. **9**, pp. 40-83.

JAN, M.Q. (1977) The Mineralogy, geochemistry, and petrology of Swat Kohistan, NW Pakistan. Ph.D. thesis, London Univ. (Unpublished).

———— (1980) Petrology of the obducted mafic and ultramafic metamorphites from the southern part of the Kohistan Island Arc sequence. Proc. Int. Commt. Geodynamics, Grp. 6 Mtg. Peshawar, Nov. 23-29, 1979, pp. 95-107.

JAN. M.Q. (1982) Chemical changes accompanying the granulite to amphibolite transition in Swat, NW Pakistan. *In:* Sinha, A.K. (ed.) Contemporary Geoscientific Researches in Himalaya, 2, Dehradun. India, pp. 49-52.

———— (1983) Further data on ortho- and clinopyroxenes from the pyroxene granulites of Swat-Kohistan, northern Pakistan. Geol. Bull. Univ. Peshawar 16, pp. 55-64.

———— (1987) Phase chemistry of blueschists from eastern Ladakh, NW Himalaya. N. Jb. Geol. Paleont. Mh., pp. 613-635.

———— (1988) Geochemistry of amphibolites from the southern part of the Kohistan arc, N. Pakistan. Min. Mag. 52, (in press).

———— & ASIF, M. (1981) A speculative tectonic model for the evolution of NW Himalaya and Karakoram. Geol. Bull. Univ. Peshawar 14, pp. 199-201.

———— (1983) Geochemistry of tonalites and (quartz) diorites of the Kohistan-Ladakh (Transhimalayan) granitic belt in Swat, NW Pakistan. *In*: Shams, F.A. (ed.) Granites of Himalaya, Karakoram and Hindukush. Institute of Geol., Punjab Univ. Lahore, Pakistan. pp. 355-376.

———— & HOWIE, R.A. (1980) ortho- and clinopyroxenes from the pyroxene granulites of Swat Kohistan, northern Pakistan. Min. Mag. 43, pp. 715-726.

———— (1981) The mineralogy and geochemistry of the metamorphosed basic and ultrabasic rocks of the Jijal complex, Kohistan, NW Pakistan. Jour. Petrol. 22, pp. 85-126.

———— (1982) Hornblendic amphiboles from basic and intermediate rocks of Swat-Kohistan, northwest Pakistan. Amer. Mineral. 67, pp. 1155-1178.

KHAN, M.A., JAN, M.Q., WINDLEY, B.F. & TARNEY, J. (In press) The Chilas mafic igneous complex: the root of the Kohistan Island Arc in the Himalayas of N. Pakistan. Geol. Soc. Am. Spec. Publ.

KLOOTWIJK, C., SHARMA, M.L., GERGAN, J., TIRKEY, B., SHAH, S.K. & AGARWAL, V. (1979) The extent of greater India, II Palaeomagnetic data from the Ladakh intrusives of Kargil, northwestern Himalaya. Earth Planet. Sci. Lett. 44, pp. 47-64.

KORITNIG, S. (1964) Der erstz von Si^{-} durch P^{+5} in gesteinsbildenden silikat-mineralen. Naturwissenschaften 24, p. 63.

LEAKE, B.E. (1963) Origin of amphibolites from northwest Adirondacks, New York. Geol. Sco. Amer. Bull. 74, pp. 1193-1202.

———— (1972) Garnetiferous striped amphibolites from Connemara, western Ireland. Min. Mag. 38, pp. 649-665.

LIOU, J.G. (1973) Synthesis and stability relations of epidotes, $CaAl_2FeSi_3O_{12}$ (OH). Jour. Petrol. 14, pp. 381-413.

---------- HO, C.O. & YEN, T.P. (1975) Petrology of some glaucophane schists and related rocks from Taiwan. Jour. Petrol. 16, pp. 80-109.

MANNA, S.S. & SEN, S.K. (1974) Origin of garnet in the basic granulites around Saltora, W. Bengal, India. Contrib. Mineral. Petrol. 44, pp. 195-218.

MARTIGNOLE, J. & SCHRIJVER, K. (1973) Effect of rock composition on appearance of garnet in anorthosite-charnockite suites. Canad. Jour. Earth Sci. 10, pp. 1132-1139.

MISCH, P. & ONYEAGOCHA, A.C. (1976) Symplectic breakdown of Ca-rich almandines in upper amphibolite-facies Skagit gneiss, North Cascades, Washington. A study of chemical exchanges and imperfectly attained successive equilibria. Contrib. Mineral. Petrol. 54, pp. 189-224.

MIYASHIRO, A. & SEKI, Y. (1958) Enlargement of the compositional field of epidote and peidmontite with rising temperature. Amer. Jour. Sci. 256, pp. 423-430.

———— & SHIDO, F. (1973) Progressive compositional change of garnet in metapelite. Lithos, 6, pp. 13-20.

MOLNAR, P. (1986) The geologic history and structure of the Himalaya. Amer. Scientist 74, pp. 144-154.

MYER, G.H. (1966) New data on zoisite and epidote. Amer. Jour. Sci. 264, pp. 364-385.

MYSEN, B.O & HEIER, K.S. (1972) Petrogenesis of eclogites in high-grade metamorphic gneisses exemplified by the Hareidland eclogite, western Norway. Contrib. Mineral. Petrol. 36, pp. 73-94.

NEWTON, R.C. (1965) The thermal stability of zoisite. Journ. Geol. 73, pp. 431-441.

———— (1966) Some calc-silicate equilibrium reactions. Amer. Jour. Sci. 261, pp. 204-222.

PETTERSON, M.G. & WINDLEY, B.F. (1985) Rb-Sr dating of the Kohistan arc-batholith in the Trans-Himalaya of north Pakistan, and tectonic implications. Earth Planet. Sci. Lett. **74**, pp. 45-57.

POWELL, C. McA (1979) A speculative tectonic history of Pakistan and surroundings: Some consraints from the Indian Ocean. *In:* Farah, A. & DeJong K.A. (eds.). Geodynamics of Pakistan Geol. Surv. Pakistan. Quetta, pp. 5-24.

REITHER, M. (1976) The Al-Fe (III) epidote miscibility gap in a metamorphic profile through the Penninic series of the Tauern window, Austria. Contrib. Mineral. Petrol. **57**, pp. 99-117.

RAMBALDI, E.R. (1973) Variation in the composition of plagioclase and epidote in some metamorphic rocks near Bancroft, Ontario. Canad. Jour. Earth Sci. **10**, pp. 852-868.

RAMSAY, C.R. (1973) Controls of biotite zone mineral chemistry in Archaean metasediments near Yellowknife, Northwest Territories, Canada. Jour. Petrol. **14**, pp. 467-488.

RICKWOOD, P.C. (1968) On recasting analyses of garnet into end-member molecules. Contrib. Mineral Petrol., **18**, pp. 175-198.

SAPOZHNIKOVA, L.N. (1981) Characteristics of the chemical composition of biotite from Mica-bearing plagioclase pegmatites of Mamski-Chukotsky region (in Russian). Zap. Vses. Min. Obs. **110**, 453-460. M.A. 82M/3249.

SAXENA, S.K. (1968) Distribution of elements in coexisting minerals and the nature of solid solution in garnet. Amer. Mineral. **53**, pp. 994-1014.

SCHARBERT, H.G. & KUART, G. (1974) Distribution of some elements between co-existing ferromagnesian minerals in Maldanubian granulite facies rocks, Lower Austria, Austria. Tschermaks Min. Petr. Mitt. **21**, pp. 110-134.

SEARLE, M.P. & 10 OTHERS (1987) The closing of the Tethys and the tectonics of the Himalaya. Geol. Soc. Amer. Bull. **98**, pp. 678-701.

SHARMA, K.K. & GUPTA, K.R. (1983) Calc-alkaline island arc volcanism in Indus-TsangPo Suture Zone. *In:* Thakur, V.C. & Sharma, K.K. (eds.) Geology of Indus Suture Zone of Ladakh. Wadia Inst. Himal. Geol. Dehradun, India, pp. 71-78.

SIMONEN, A. & VORMA, A. (1969) Amphibole and biotite from Rapakivi. Bull. Comm. Geol. Finlande, **238**, pp. 1-28.

STRENS, R.G.J. (1965) Stability and relations of Al-Fe epidotes. Min. Mag. **35**, pp. 464-475.

SUBRAMANIAM, A.P. (1962) Pyroxenes and garnets from charnockites and associated granulites. *In:* Engel *et al.* (eds.) Petrologic Studies. Geol. Soc. Amer. A.F. Buddington vol., pp. 21-36.

TAHIRKHELI, R.A.K. & JAN. M.Q. (1979) The Geology of Kohistan. Geol. Bull. Univ. Peshawar (Spec. Issue), **11**.

———— , MATTAUER, M., PROUST, F. & TAPPONNIER, P. (1979) The India Eurasia suture zone in northern Pakistan: synthesis and interpretation of data at plate scale. *In:* Farah, A. & DeJong, K.A. (eds.) Geodynamics of Pakistan. Geol. Surv. Pak. Quetta, pp. 125-130.

TANNER, P.W.C. (1976) Progressive regional metamorphism of thin calcareous bands from the Moinian rock of N.W. Scotland. Jour. Petrol. **17**, pp. 100-134.

VIRDI, N.S. (1981) Presence of parallel metamorphic belts in the northwest Himalaya-Discussion. Tectonophysics **72**, pp. 141-146.

WALSH, J.N., (1975) Clinopyroxenes and biotites from the Centre III igneous complex, Ardnamurchan, Argyllshire. Min. Mag. **40**, pp. 335-345.

WINDLEY, B.F. & SMITH J.V. (1974) The Fiskenaesset complex, west Greenland, Part II. General mineral chemistry from Qeqerlarssuatsiaq. Grnland Geol. Under. **108**, pp. 1-54.

———— , COWARD, M.P. & JAN, M.Q. (1986) The geology and tectonic evolution of the Karakoram-Kohistan range of the Himalaya of N. Pakistan. Symp. vol. Academia Sinica, Beijing, China pp. 455-467.

YODER, H.S., JR., (1969) Experimental studies bearing on the origin of anorthosite. In: Isachsen, Y.W. (ed.) Origin of Anorthosite and Related Rocks' N.Y. State Mus. & Sci. Serv. Mem. **18**, pp. 13-22.

ZAKRUTKIN, V.V. & GRIGORENKO, M.V. (1968) Titanium and alkalis in biotite in metamorphic facies. Dokl. Acad. Sci. U.S.S.R., Earth Sci. Sect. **178**, pp. 124-127.

ZEITLER, P.K., JOHNSON, N.M., NAESER, C.W. & TAHIRKHELI, R.A.K. (1982) Fission-track evidence for Quaternary uplift of the Nanga Parbat region, Pakistan. Nature **298**, pp. 255-257.

Manuscript received on 20.10.1987
Accepted for publication on 20.10.1987

ACTA MINERALOGICA PAKISTANICA
VOLUME 3 (1987) pp. 26 - 41

MINERAL CHEMISTRY OF THE SAKHAKOT-QILA OPHIOLITE, PAKISTAN: PART 1, MONOSILICATES

ZULFIQAR AHMED
Centre of Excellence in Mineralogy, University of Baluchistan, P.O.Box 43, Quetta, Pakistan.

ABSTRACT: This paper is the first of a 4-part serial characterization of the mineral chemistry of the Sakhakot-Qila ophiolite. Monosilicates from this ophiolite include olivine, sphene and garnets. Olivine with a Fo content of 73% to 97%, shows variations in Mg and Fe contents related to the primary rock-types, and to the textural components within rock samples. Olivines with the highest Mg and lowest Fe form inclusions in chromite crystals. Olivine grains embaying into the boundaries of chromite crystals are intermediate between such inclusions and discrete grains. Olivines with the highest Fe and lowest Mg are those from the Fe-websterite dyke. Sphene is a late-stage crystallization product found only in metadolerites and plagiogranite differentiates. Its chemical variations are insignificant. Garnets are all metasomatic and present in various types of rodingitic veins and dykes. Grossular is the most common garnet and often coexists with hydrogrossular, or rarely, andraditic grossular. At interfaces of rodingites with the chromitite wall-rocks, uvarovite or Cr-rich titanian grossular may develop. The garnet compositions are commensurate with the mother fluids having a sea water source.

INTRODUCTION

The rocks and minerals of the Sakhakot-Qila ophiolite (hereafter referred to as SQO) located in the southern part of Malakand Agency, Pakistan, have been the subject of many previous studies, including those by Ahmed (1978a, 1978b, 1982, 1983, 1984); Ahmed & Bevan (1981); Ahmed & Hall (1981, 1982, 1983) and Rossman & others (1970). These studies were each focussed on specific themes of geoscientific interest. These are also a source of information on the general geological features and maps of the SQO, and form a background for a more elaborate study of the mineral chemistry presented here. This study also serves to systematically characterize the minerals of SQO.

This communication comprises four parts, each of which deals with the chemical features of specific mineral groups. This first part comprises the monosilicates of SQO which include olivine, sphene and garnet group minerals. This study is not restricted exclusively to mineral chemistry and does describe the relevant petrographic features as well.

THE SQO MINERAL ASSEMBLAGE

The rock types identified from the SQO comprise the following: chromitite, rodingitized chromitite, clinopyroxene-harzburgite, harzburgite, dunite, clinopyroxene-dunite, wehrlite, serpentinite, asbestose serpentinite, chloritized serpentinite, orthopyroxenite, clinopyroxenite, websterite, Fe-websterite, dolerite, metadolerite, grossular veins, metasomatized metadolerite, rodingite, lower-level unsaturated metagabbro, middle-level quartz-bearing metagabbro, higher-level amphibole gabbro, and plagiogranite. The mineral assemblage identified from these rock types includes: monosilicates comprising forsteritic olivine, sphene, grossular, hydrogrossular, uvarovite and andraditic grossular; polysilicates comprising enstatite, diopside, endiopside, augite, salite and a variety of amphiboles; phyllosilicates comprising serpentines, chlorites and clintonite; disilicates comprising clinozoisite and vesuvianite; tectosilicates comprising quartz, albite and altered plagioclase; and non-silicates comprising chromian spinel, 'ferritchromit', magnetite, ilmenite, magnesite, apatite, corundum, perovskite, nan-

tokite, native Cu, awaruite, heazlewoodite, pentlandite, and troilite. Some of the previous studies on the SQO have investigated some of these minerals; and have provided significant background data for the present study. These earlier studies include a study of chromite and its alteration products by Ahmed & Hall (1981); and studies on the nickeliferous opaque minerals by Ahmed & Bevan (1981) and Ahmed & Hall (1982).

MINERAL CHEMISTRY AND PETROGRAPHY

The minerals of the SQO were analyzed by the Microscan microprobe unit at the Department of Geology, University College, University of London, U.K. The unit is fitted with a Si (Li) detector and a Link Systems Ltd. energy - dispersive attachment used for peak measurement and processing. The analyses were made with 15 kV accelerating potential, 0.5×10^{-8} A specimen current, and 100 live seconds counting time for each spot analyzed. Internal standard was pure cobalt; and external standards were pure metals and synthetic and natural minerals.

Representative analyses of the monosilicate minerals are presented in tables 1 through 7; whereas more data has been utilized for construction of the diagrams and discussion in the text. The oxide weight percentages in tables 3 through 7 are reduced to the second decimal points, however, the cationic formulae listed carry three decimal digits and were calculated by the Link Systems attachment. Total iron contents are reported as divalent for olivine, and as trivalent for sphene and garnets. For olivine, sphene and anhydrous garnet, the analyses whose oxide percentages totals remained between 98.5 and 101.5 are included.

OLIVINE

The most abundant mineral of the SQO rocks is olivine and is present as an essential constituent of harzburgites, clinopyroxene-

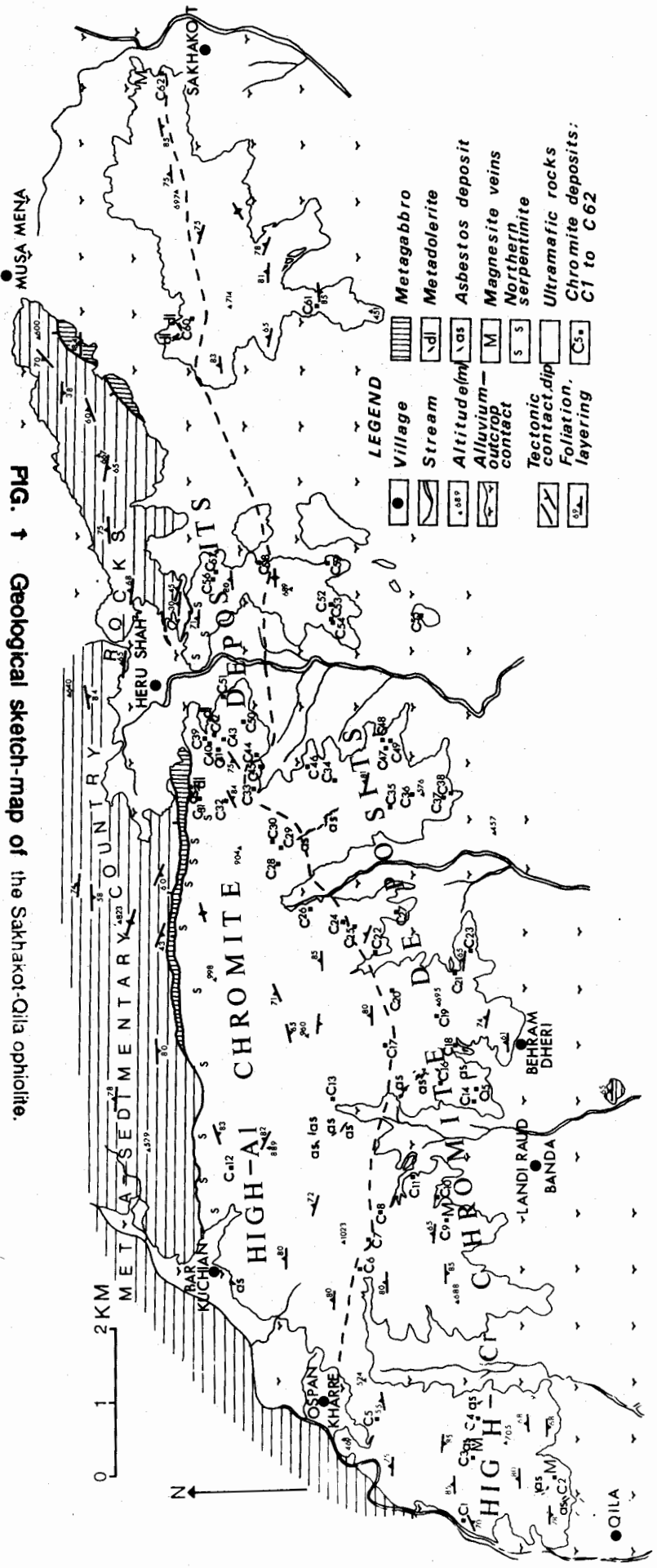

FIG. 1 Geological sketch-map of the Sakhakot-Qila ophiolite.

Table 1. Sample locations by grid reference to toposheets (GRID) and by map (fig. 1); and their analyzed mineral assemblages.

Rock Name & Sample No.	GRID	Location on fig. 1	Minerals analyzed	Descriptive remarks
Graded-layered chromitite:				
Z40A,B	4232-7374	C6	Chr,Ol,Srp.	Lower, chromite-rich part of a graded layer.
Z40C	4232-7374	C6	Chr,Ol,Srp,Chl	Upper, chromite-poor part of graded layer in Z40A,B
Z291	4275-8426	C59	Chr,Fchr,Ol.	
Z244	4210-8160	C48	Chr,Ol,Srp.	
Disseminated- textured chromitite:				
Z34	4205-7465	C8	Chr,Ol,Cpx inclusions in Chr,Srp,Chl.	
ZA228A	4454-8158	C42	Chr,Ol,Chl.	
ZA228B	4454-8158	C42	Chr,Ol,Chl,Hz	Dunite dyke crosscuttting ore sample ZA228A.
Z142	4062-7620	C14	Chr,Ol,Srp,Awr.	
Nodular chromitite:				
Z279n	4392-8412	C58	Chr,Ol,Srp.	From within the chromite nodule.
Z279	4392-8412	C58	Chr,Ol,Srp.	Matrix of nodules of Z279n.
Z120	4103-7452	C9	Chr,Ol,Srp.	
Z155	4078-7834	C23	Chr,Ol,Srp,Fchr.	
Massive chromitite:				
Z274A	4458-8390	C56	Chr.	
Z318	4543-9127	C62	Chr,Ol,Srp,Chl.	
Banded chromitite:				
Z131	4161-7509	C11	Chr,Ol,Srp.	
Z151	4188-7785	C20	Chr,Ol,Srp.	
Occluded- silicate chromitites:				
Z175	4360-7975	C28	Chr,Ol,Fchr.	
Speckled chromitite:				
Z160	4240-7870	C25	Chr,Ol,Srp.	
Z82	4205-7465	C8	Fchr,Chl,Chr,Ol.	
Z53	4219-7422	C7	Chr,Ol,Mgs.	
Chromite–net chromitite:				
Z121	4103-7452	C9	Chr,Ol,Srp.	
Clinopyroxene-harzburgite:				
Z222	4454-8158	near C42	Opx,Ol,Cpx,Chr.	
Z323	4330-8390	–	Ol,Opx,Cpx,Chr.	
Z326	4332-8388	–	Ol,Opx,Cpx,Chr,Srp,Chl, secondary Tr,Trhb.	
Harzburgite:				
Z216	4459-8146	C40	Chr,Ol,Opx.	Contains Chr 10%. Hosts chromitite.
Z324	4330-8390	–	Ol,Opx,Chr.	
Z105	4103-7452	C9	Ol,Opx,Chr,Srp,Ol inclusions in Chr.	
Z344	4484-8350	–	Ol,Opx,Chr,Srp.	
Z310	4543-9127	C62	Ol,Opx,Chr,Fchr.	
Z374	4205-7465	C8	Chr,Ol,Opx,Cpx	Sample made of cm-scale Opx-bearing bands (A) and dunite (B).
Dunite:				
Z188A	4396-8080	C33	Ol,Srp,Chr.	
Z274B	4458-8390	C56	Ol,Chr,Srp,Fchr,Chl.	Host rock of massive chromitite (sample 274A).
Z275B	4453-8400	C56	Ol,Chr,Srp,Fchr,Hz	
Z327	4310-8400		Ol,Chr,Mag,Srp, Inclusions of Chl & Cpx in	

			Chr crystals.	
Z375	4205-7465	C8	Ol,Chr,Cpx,Chl,Srp.	This dunite is Cpx-bearing.
Serpentinite:				
Z342	4495-8350	–	Srp,Ol,Chr.	
Z346	4480-8351	–	Srp,Chl,Ol,Fchr,Chr.	
Wehrlite:				
Z24	4060-7155	C4	Ol,Cpx,Chr,Fchr.	
Z147	4060-7640	–	Ol,Cpx,Chr,Srp.	
Z183	4460-8035	C32	Ol,Cpx,Fchr,Chr,Srp.	
Z188	4396-8080	C33	Ol,Cpx,Chl,Chr.	
Z202	4468-4156	C39	Cpx,Ol,Chr,Fchr,Srp.	
Z265	4150-8332	C55	Ol,Cpx,Srp,Chl,Chr.	
Z294A	4492-8774	C60	Ol,Cpx,Chr,Srp.	
Z347	4480-8360	–	Ol,Cpx,Chr,Fchr,Mag, Srp,Hz.	
Orthopyroxenite dykes:				
Z104	4103-7452	C9	Opx,Ol,Chr,Srp,Ath,Tr.	
Clinopyroxenite dykes:				
Z70B	4205-7465	C8	Cpx,Ol,Srp,Chr,Chl.	Dyke < 1 cm thick crosscuts orbicular chromitite sample Z70.
Z188B	4396-8080	C33	Cpx,Ol,Chl,Srp,Tr, Mhb,Chr,Awr,Hz.	
Z275A	4453-8400	C56	Cpx,Ol,Tr,Ed,Opx,Srp, Chr,Ol inclusions in Chr.	Dyke crosscuts chromitite.
Fe-Websterite dyke in dunite:				
Z36	4232-7374	C6	Opx,Cpx,Ol,Chr,Edhb, Prghb,Ol inclusions in Opx,Tro,Pn.	
Metadolerite:				
Z219	4454-8160	–	Fprg,Fedh,Fed,Edhb, Fprhb,Czo,Spn,Ilm,Chap.	
Plagiogranitic differentiates:				
Z339	4540-8160	–	Qtz,Ep,Ab,Ilm,Ap,Spn,Chl.	
Rodingitic rocks:				
Z41A	4232-7374	C6	Chr,Cpx,Chl,Srp,Uvr, Hgrs,Prv,Ap.	Rodingitic-veined massive chromitite.
Z235	4454-8158	C42	Chr,Di,Grs,Hgrs,Chl,Hz.	Rodingitic- veined pseudoclastic chromitite.
Z400	4480-8080	–	Grs,Adrg,Chl,Srp.	
Z371	4530-8750	–	Grs,Hgrs,Uvr,Chl,Ilm, Cu,Ntk,Grs inclusions in Cu.	Rodingitic vein crosscuts metadolerite dykes.
Z372	4510-8770	–	Fsp,Ab,Fedhb,Edhb, Fprhb,Hgrs,Ed,Fedhb, Fed,Fprg,Grs,Spn,Cpx.	Rodingitozed metadolerite dyke.
Z383	4490-7560	–	Grs,Chr,Cnt.	Rodingite dyke in serpentinite of outer contact of ophiolite.
ZA222	4454-8158	–	Grs,Hgrs,Uvr,Cpx,Chl, Cnt,Crn,Fchr,Ves.	Rodingite dyke hosted by clinopyroxene harzburgite.
Z361A	4470-8165	–	Di,Grs,Hgrs,Chl,Uvr.	
Z399	4480-8010	–	Gr,Hgrs,Chl,Uvr.	Rodinigite vein.

Mineral symbols are: Ab, albite; Adgr, andraditic grossular; Math, magnesio-anthophyllite; Aw, awaruite; Chap, chlorapatite; Chl, chlorite; Chr, chromite; Cpx, clinopyroxene; Czo, clinozoisite; Cnt, clintonite; Crn, corundum; Cu, native copper; Di, diopside; Ed, edenite; Edhb, edinitic hornblende; Fsp, feldspar; Fchr, "ferritchromit"; Fed, ferroedinite; Fedhb, ferroedinitic hornblende; Fprg, ferroan pargasite; Fprhb, ferroan pargasitic hornblende; Grs, grossular; Hz, heazlewoodite; Hbl, hornblende; Hgrs, hydrogrossular; Mhb, magnesiohorblende; Mag, magnetite; Mgs, magnesite; Nkt, nantokite; Ol, olivine; Opx, Orthopyroxene; Prghb, pargasitic hornblende; Pn, pentlandite; Prv, perovskite; Srp, serpentine; Tr, tremolite; Trhb, tremolitic hornblende; Tro, troilite; Uvr, uvarovite; Ves, vesuvianite; Zo, zoisite.

Table 2. Olivine composition representing various rock types listed in table 1. Certain grain-types are indicated by symbols: n = inside the chromite nodules of nodular chromitite; m = matrix of chromite nodules; d = dunite host rock of chromitite; h = harzburgite host rock of chromitite; dd = dunite dyke cutting across chromitite and carrying about 10 modal % finer-grained chromite; c = grains with clinopyroxene inclusions; ic = euhedral olivine inclusion in chromite crystal; io = inclusion in orthopyroxene host crystal.

Sp.No.	Z274A	Z274B	Z318	Z310	Z34	Z279n	Z279	ZA228A	ZA228B	Z222
No. Anal	$\bar{x}$(4)	$\bar{x}$(8)	$\bar{x}$(14)	$\bar{x}$(10)	$\bar{x}$(14)	(1)	$\bar{x}$(8)	$\bar{x}$(4)	$\bar{x}$(12)	$\bar{x}$(8)
SiO_2	40.14	39.71	41.49	40.39	41.65	41.72	41.82	41.00	40.63	40.65
FeO	7.56	9.50	4.67	9.77	4.73	6.16	6.83	5.83	8.08	8.97
MnO	0.08	0.14	0.09	0.14	0.05	n.d.	n.d.	0.05	0.12	0.11
MgO	50.44	48.99	52.00	48.63	53.78	51.23	50.51	52.04	51.08	49.11
NiO	0.50	0.24	0.81	0.29	0.50	n.d.	n.d.	0.41	0.32	0.36
Total	98.72	98.58	99.06	99.22	100.71	99.11	99.16	99.33	100.23	99.20
Fo(%)	92.257	90.201	95.095	89.743	95.294	93.674	92.950	94.036	91.729	90.652

Sp.No.	Z323	Z326	Z324	Z216	Z344	Z142	Z188A	Z275B	Z327	Z375
No.Anal.	$\bar{x}$(26)	$\bar{x}$(12)	$\bar{x}$(8)	$\bar{x}$(14)	$\bar{x}$(8)	$\bar{x}$(6)	$\bar{x}$(16)	$\bar{x}$(10)	$\bar{x}$(12)	$\bar{x}$(10)
SiO_2	40.52	39.89	40.36	39.79	40.74	40.78	40.33	40.40	40.72	40.78
FeO	9.09	9.94	8.96	9.35	8.15	8.48	11.15	9.33	7.38	8.41
MnO	0.15	0.14	0.18	0.12	0.08	0.05	0.20	0.12	0.13	0.12
MgO	48.87	50.13	48.90	49.24	49.68	50.25	47.87	49.15	49.78	50.38
NiO	0.39	0.41	0.39	0.35	0.29	0.40	0.30	0.33	0.43	0.34
Total	99.02	100.51	98.79	98.85	98.94	99.96	99.85	99.33	98.44	100.03
Fo(%)	90.483	89.848	90.586	90.274	91.547	91.319	88.475	90.265	92.176	91.340

Sp.No.	Z147	Z188	Z202	Z265	Z294A	Z294A	Z294A	Z183	Z24	Z347
No.Anal.	$\bar{x}$(14)	(1)	$\bar{x}$(22)	$\bar{x}$(4)	(1)	(1)	(1)	$\bar{x}$(4)	$\bar{x}$(12)	$\bar{x}$(4)
SiO_2	40.88	39.86	40.28	40.71	40.73	40.74	39.54	40.61	40.47	40.53
FeO	9.62	11.92	9.98	8.39	9.37	10.04	14.00	11.09	9.42	9.06
MnO	0.14	n.d.	0.18	0.20	0.08	0.19	0.22	0.11	0.16	0.24
MgO	50.07	48.52	47.92	50.79	49.29	48.76	45.61	48.32	48.56	48.87
NiO	0.30	0.31	0.43	0.42	0.40	0.50	0.48	0.17	0.39	0.41
Total	101.01	100.61	98.79	100.51	99.87	100.23	99.85	100.30	99.00	99.11
Fo(%)	90.129	87.876	89.362	91.340	90.371	89.673	85.300	88.549	90.027	90.351

Sp.No.	Z342	Z346	Z104	Z70B	Z188B	Z188B	Z275A	Z275A	Z36a	Z36
No.Anal.	$\bar{x}$(8)	$\bar{x}$(14)	$\bar{x}$(14)	$\bar{x}$(4)	$\bar{x}$(6)	(1)	(1)	$\bar{x}$(14)	(1)	(1)
SiO_2	38.91	41.28	40.47	38.65	40.31	39.00	40.87	40.48	38.17	38.09
FeO	17.81	5.25	9.47	14.20	10.53	16.21	7.02	8.28	22.90	23.38
MnO	0.34	0.47	0.16	0.26	0.09	0.28	0.10	0.16	0.26	0.44
MgO	42.37	51.66	48.67	45.28	48.24	44.23	50.50	49.46	38.76	38.01
NiO	0.04	0.33	0.38	0.35	0.27	0.00	0.52	0.61	0.06	0.07
Total	99.47	98.99	99.15	98.74	99.44	99.72	99.01	98.99	100.15	99.99
Fo(%)	80.624	94.121	90.006	85.052	88.99	82.682	92.652	91.259	74.876	73.952

Table 3. Olivine analyses from samples of speckled (Z53), nodular (Z120, Z155) and chromite-net textured (Z121) chromitites, harzburgite (Z105), dunite (Z142), and harzburgite bands (Z374B) in dunite (Z374A). The analyzed grain-types are: g = discrete grains; i = inclusions in chromite crystals; m = grains from olivine-rich matrix interstitial to chromite-nodules; e = olivine grains embaying into margins of chromite crystals; cn = grains from net-forming area of chromite-net chromitites; oc = grains from olivine-rich area bordered by the net of chromite-net chromitites. Number of analyses averaged is given in parentheses with each grain-type.

Sp.No.	Z53	Z53	Z120	Z120	Z120	Z155	Z155	Z155	Z121	Z121
Grain-type	i	g	i(6)	g	m	i	e	g(10)	i,cn(4)	e,cn
SiO_2	43.57	41.67	42.14	41.41	41.30	42.64	40.81	41.19	41.47	42.12
FeO	4.86	5.28	3.37	4.70	5.51	3.16	3.79	4.22	3.87	4.14
MnO	–	–	0.00	0.11	0.08	–	–	–	–	–
MgO	50.22	51.48	54.74	53.11	51.54	53.82	53.55	53.26	53.17	53.67
NiO	0.39	0.57	0.54	0.47	0.46	0.57	0.49	0.50	0.47	0.48
CaO	0.00	0.01	0.13	0.09	0.05	–	–	–	–	–
Total	99.04	99.01	100.92	99.89	98.94	100.19	98.64	99.17	98.98	100.41
Cations based on 4 oxygens:										
Si	1.048	1.011	0.996	0.995	1.004	1.012	0.989	0.994	1.000	1.002
Fe	0.098	0.107	0.067	0.096	0.112	0.063	0.077	0.085	0.078	0.082
Mn	–	–	0.000	0.002	0.002	–	–	–	–	–
Mg	1.800	1.861	1.928	1.901	1.868	1.903	1.935	1.916	1.912	1.904
Ni	0.008	0.011	0.010	0.009	0.009	0.011	0.009	0.009	0.009	0.009
Ca	0.000	–	0.003	0.002	0.001	–	–	–	–	–
Fo(%)	94.840	94.560	96.642	95.098	94.248	96.795	96.173	95.752	96.080	95.871

Sp.No.	Z121	Z121	Z105	Z105	Z105	Z374A	Z374A	Z374B	Z142	Z142
Grain-type	g,cn	g,oc	i	e	g(4)	i	g	g(10)	i	g
SiO_2	41.72	41.35	40.83	41.12	40.66	40.10	40.64	40.46	40.68	40.79
FeO	4.97	5.78	7.40	7.94	9.19	11.25	9.32	8.90	7.21	9.96
MnO	–	–	0.16	0.14	0.10	0.18	0.20	0.18	0.07	0.02
MgO	52.99	52.60	50.63	50.74	49.23	47.33	48.72	48.95	50.86	49.17
NiO	0.51	0.56	0.49	0.46	0.47	0.13	0.45	0.39	0.41	0.38
CaO	–	–	–	–	–	0.00	0.00	0.00	–	–
Total	100.19	100.29	99.51	100.40	99.65	98.99	99.33	98.88	99.23	100.32
Si	1.000	0.994	0.997	0.997	0.999	1.000	1.002	1.002	0.994	0.998
Fe	0.100	0.116	0.151	0.161	0.189	0.235	0.192	0.184	0.147	0.204
Mn	–	–	0.003	0.003	0.002	0.004	0.004	0.004	0.001	0.000
Mg	1.892	1.885	1.842	1.833	1.802	1.759	1.790	1.803	1.853	1.793
Ni	0.010	0.011	0.009	0.009	0.010	0.003	0.009	0.008	0.008	0.007
Ca	–	–	–	–	–	0.000	0.000	0.000	–	–
Fo(%)	94.980	94.203	92.285	91.788	90.483	88.038	90.131	90.558	92.604	89.785

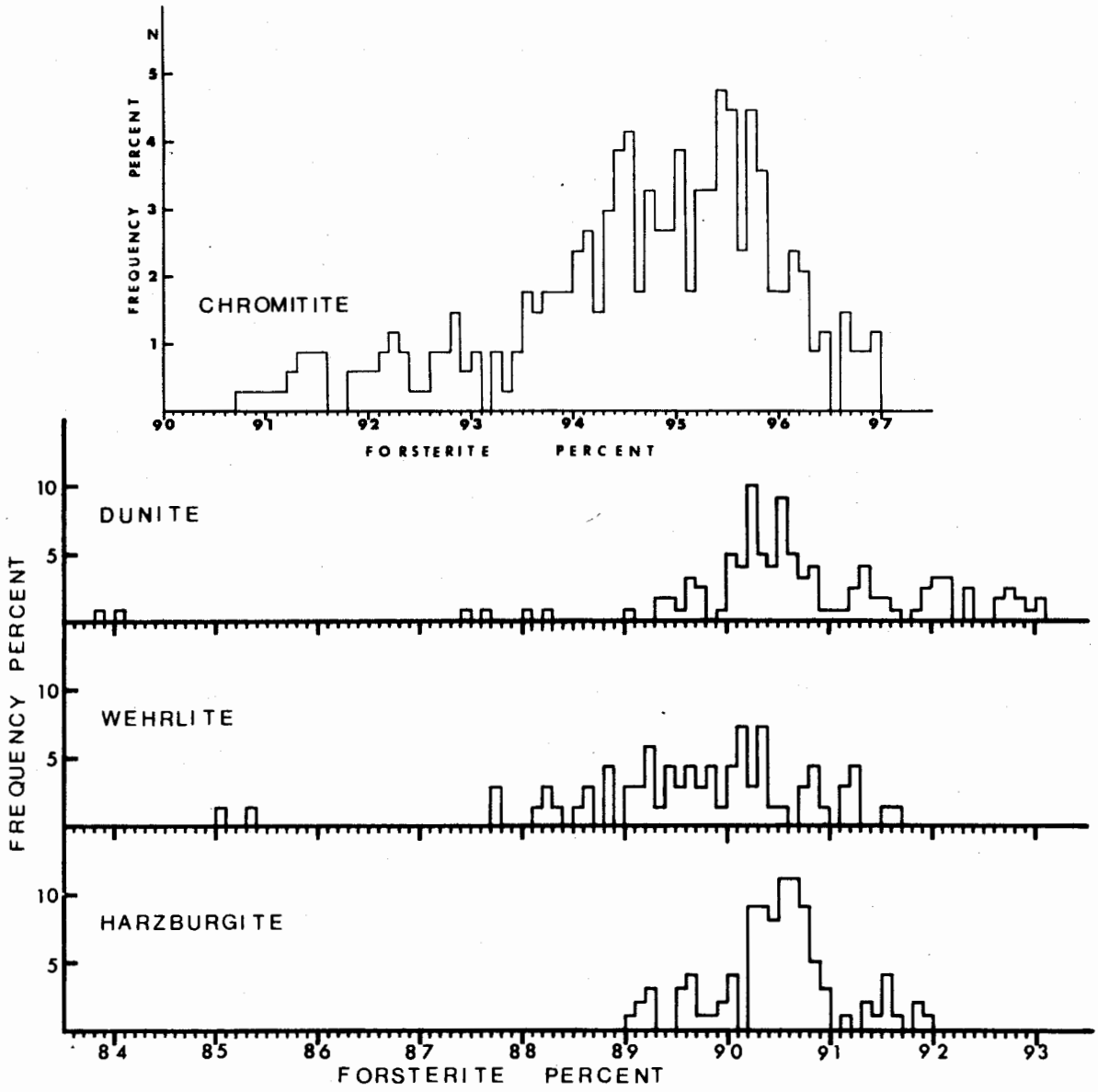

Fig. 2. Frequency histograms showing the variation in Fo content of olivines from :

(A) Chromitites and matrix dunites (500 analyses) with maximum frequency at 95.4 %.

(B) Dunite wall rock sheaths of chrome ore bodies as well as barren dunite bodies (125 analyses) with maximum frequency at Fo 90.2 %.

(C) Wehrlites (70 analyses) with maximum frequency at 90 2 %

(D) Harzburgites including clinopyroxene-harzburgites (105 analyses) with maximum frequency at 90 6 % and a narrow spread .

Table 4. Analyses of olivine from graded-layered chromitites. Alphabets after each sample number represent level in each graded layer; from chromite-rich bottom (A) towards olivine-rich top (D).

Sample No.	Z291-A	Z291-B	Z291-C	Z291-D	Z40-A,B	Z40-C	Z244-A	Z244-B
No. Anal	(1)	(1)	(1)	(1)	$\bar{x}$(6)	$\bar{x}$(6)	$\bar{x}$(4)	$\bar{x}$(2)
SiO_2	42.86	41.92	41.58	42.71	41.62	40.91	41.06	40.94
Cr_2O_3	0.03	0.00	0.00	0.00	–	–	0.14	0.24
FeO	4.10	5.13	6.26	6.34	4.01	5.88	4.53	5.03
MnO	–	–	–	–	0.09	0.15	–	–
MgO	52.00	51.47	50.99	50.01	53.85	51.86	52.69	52.40
NiO	0.28	0.42	0.50	0.43	0.57	0.33	0.45	0.54
CaO	0.06	0.04	0.05	0.05	–	0.04	0.04	0.10
Total	99.33	98.98	99.38	99.54	100.15	99.13	98.91	99.25
Cations to 4 Oxygens:								
Si	1.048	1.015	1.009	1.031	0.993	0.994	0.996	0.994
Fe	0.084	0.104	0.127	0.128	0.080	0.119	0.092	0.102
Mn	–	–	–	–	0.002	0.003	–	–
Mg	1.896	1.800	1.857	1.844	1.917	1.879	1.903	1.897
Ni	0.006	0.008	0.010	0.008	0.011	0.007	0.009	0.010
Ca	0.001	0.001	0.001	0.001	–	0.001	0.001	0.002
Fo (%)	95.758	94.538	93.599	93.509	95.898	93.903	95.389	94.897

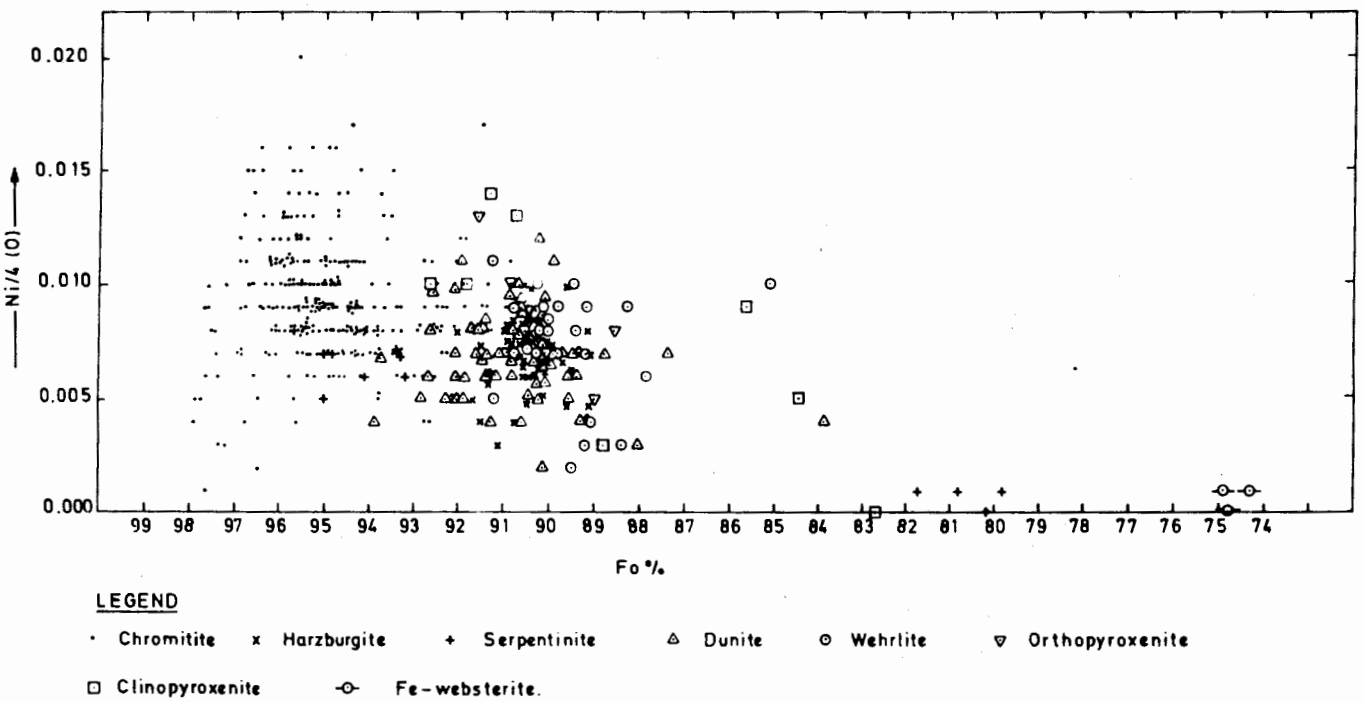

Fig.3. Plot of percentage of Fo against Ni cations per formula unit of olivines from various rock-types of SQO.

harzburgites, dunites, clinopyroxene-dunites, wehrlites, chromitites, and as minor constituent of pyroxenites and serpentinites. It often contains inclusions of chromite. The olivine in these rocks is closely similar to that from the ultramafic portions of ophiolites. The olivine in the chromitites and the host dunites is always highly magnesian with forsterite content showing an overall range of 91.7% to 97.0% by mass. A plot of 500 microprobe analyses from chromitites on the frequency histogram (fig. 2A) shows maximum frequency at 95.4% Fo. Analyses with lesser Fo content are mainly from the dunitic sheaths at the contact of chromitites; as in the rocks away from the chromitite contacts, the olivine shows relatively lesser forsterite proportion. Similar plots for the other rocks on the frequency histogram are given in fig. 2 B-D, for comparison purpose. In harzburgite, olivine shows a much restricted range in Fo content than that in dunite or wehrlite. The wehrlites contain more Fe-rich olivines than the dunite samples from the same localities. Assumption of total Fe as FeO in the analyses given here is further justified by the observation that Fe^{3+} is usually at undetectable or very low levels in natural olivines (Brown, 1980) as shown by the ^{57}Fe Mossbauer studies and optical absorption studies.

Most pyroxenite dykes contain minor amounts of olivine which shows very low Fo content. In orthopyroxenites, the olivine-range from 88.34 to 91.50% Fo was observed. In clinopyroxenites, the olivine range is from 82.68 to 89.40% Fo. In the Fe-websterite sample Z36, the olivine is exceptionally Fe-rich with Fo content of 74.32 to 75.10% and accompanies similarly Fe-rich pyroxenes and accessory primary chromite. The olivine is Fe-rich compared to the other websterites of SQO which show more magnesian olivine just like the rest of the pyroxenites.

In various textural varieties of chromitites described from SQO by Ahmed (1982, 1984), the olivine compositions in texturally different components are separately determined. Generally, only slight but quite consistent differences in MgO and FeO contents were observed between the coarser chromite and the finer-chromite units of such textural varieties. Olivine grains often occur as inclusions inside coarser chromite grains. The inclusions tend to be slightly richer in Fo than the discrete olivine grains outside their host chromite crystals. However, such variation is sometimes not distintly apparent.

Minor elements contained in the olivine of SQO rocks are below the following maximal amounts observed from spot analyses: TiO_2, 0.14%; Cr_2O_3, 0.27%; Al_2O_3, 0.2%; V_2O_3, 0.1%; MnO, 0.56%; NiO, 0.81% and CaO, 0.19%. Maximum TiO_2 content of 0.14% was observed in the olivine from Fe-websterite sample (Z36) which also shows maximum Al_2O_3 content of 0.2%. The Cr content tends to correlate positively with the Mg content. Maximum Cr_2O_3 content of 0.27% was found in a graded-layered chromitite sample (Z244), in an olivine grain with 95.4% Fo. The CaO content of SQO olivines seldom exceeds 0.05% and is nil in 80% measurements. Maximum CaO content noticed is 0.155% equivalent to 0.004 Ca ions per formula unit. The low Ca content is compatible with the plutonic nature of these olivines, as the earlier works (e.g., Simkin & Smith, 1970) show that plutonic olivines contain less Ca than the hypabyssal and volcanic olivines. The metamorphic olivines are also known to contain lesser Ca (Brown, 1980). Clinopyroxene-bearing dunite sample (Z375) contains the olivine with maximum CaO (0.19%) although the same sample contains olivine with CaO as low as 0.07%.

V_2O_3 is ordinarily below the detection level for most analyses of olivine. The maximum value of 0.1% is from a dunite sheath (sample Z274B) around a massive chromitite. Maximum MnO content of 0.56% is contained in an olivine relict in serpentinite (sample Z 346).

The variation of Ni with varying Fo content of olivine analyses from SQO is exhibited graphically in fig. 3. The general Ni content of olivine is fairly high. Maximum NiO value of 1.05% is observed in a sample of massive chromitite (Z318). Its overall range varies from nil to 0.02 cations per formula unit calculated to 4 oxygens. The plot shows higher Ni values for

Table 5. Olivine analyses from samples of banded chromitites (Z131, Z151), occluded-silicate chromitite (Z175), and speckled chromitites (Z160, Z82). The grains–types analyzed are from: c = chromite-rich bands; o = olivine-rich bands; oo = chromite-rich parts outside the olivine - rich occlusions; io = inside the olivine- rich occlusions; cc = speckles rich in coarse-grained chromite; fc = patches rich in fine grained chromite and, dd = chromite–lacking dunite dyke that runs across speckled chromitite. Number of analyses averaged are given in parentheses with each grain–type symbol.

Sample No.	Z131	Z131	Z151	Z151	Z175	Z175	Z160	Z160	Z160	Z82	Z82
Grain-type	c(10)	o(2)	c	o	oo(6)	io	cc	fc	dd(4)	cc	fc
SiO_2	41.41	41.13	41.51	41.88	41.02	41.12	41.13	41.51	41.15	41.51	41.33
FeO	3.92	4.61	6.47	6.98	4.73	5.01	4.41	4.75	5.57	4.68	5.38
MnO	0.09	0.51	0.20	0.08	–	–	0.00	0.07	0.00	0.07	–
MgO	53.27	52.53	52.14	51.25	52.83	52.53	52.87	52.98	51.62	53.34	52.40
NiO	0.55	0.45	0.44	0.60	0.48	0.37	0.41	0.39	0.36	0.58	0.44
CaO	0.09	0.15	0.00	0.16	–	–	–	–	–	–	–
Total	99.33	99.02	100.76	100.95	99.06	99.03	98.82	99.70	98.70	100.18	99.55
Cations based on 4 Oxygens:											
Si	0.998	0.997	0.996	1.005	0.994	0.997	0.996	0.998	1.002	0.994	0.998
Fe	0.079	0.093	0.130	0.140	0.096	0.102	0.089	0.096	0.114	0.094	0.108
Mn	0.002	0.003	0.004	0.002	–	–	0.000	0.002	0.000	0.001	–
Mg	1.911	1.898	1.864	1.833	1.907	1.898	1.906	1.897	1.875	1.905	1.886
Ni	0.011	0.009	0.009	0.011	0.009	0.007	0.008	0.008	0.007	0.011	0.008
Ca	0.002	0.004	0.000	0.004	–	–	–	–	–	–	–
Fo(%)	95.934	95.186	93.293	92.810	95.207	94.900	95.525	95.088	94.269	95.250	94.584

chromitites, lower values for other rock types and lowest for the Fe-websterite dyke. A diffuse trend of increase of Ni with increase in Mg content is indicated. This trend is not displayed by chromitites plotted alone; but by all the rock types plotted together.

The chromite crystals in chromitites almost invariably contain olivine inclusions. In table 3 are set out the olivine analyses to compare the compositions of crystal inclusions inside chromite grains with those from the adjacent discrete olivine grains. Generally the inclusions are more magnesian and less ferriferous than discrete olivine grains. Analyses of olivine grains embaying into the margins of coarse chromite crystals are also given in table 3. Their compositions are more magnesian than those of olivine grains outside chromite crystals; but less magnesian than those of olivine inclusions in chromite crystals. However, at least in one of the samples (Z374A, table 3) the olivine inclusions show less magnesian and more Fe-rich compositions than the olivine grains outside chromite crystals. This is a trend reverse to that noted above for most of the samples. This aberrant sample (Z374A) is of a dunite that bears pyroxene-rich bands and possibly represents crystallization from the magmatic fluid independent of the main ophiolitic rock crystallization.

The olivine analyses from the graded layered chromitites are listed in table 4. The samples may be regarded as variants of banded chromitites in which the chromite: olivine ratio and chromite crystal size decrease gradationally upwards in each band. The appearance strongly points towards magmatic gravity settling as the main process involved in its formation. The olivine is either absent or present in very small amounts in the lower part of each graded layer, but increases gradually towards its top. Often the top has a sharp contact with the chromite-richer base of the next graded layer. In some samples, each graded layer has one or two levels at which there is sharp change in the modal contents of chromite and olivine. Cusp texture is also common in forming the bases of graded layers. Analyses presented in table 4 show that relatively more magnesian olivines crystallize

earlier towards the basal parts of graded layers. The later-crystallized upper parts of graded layers contain more Fe-rich olivines. In sample Z291, analyses of olivines from four successively upward levels within a graded layer show this trend. Olivines in sample Z40 show, for the lower part of its graded layer, a composition with more MgO, NiO, SiO_2 and less FeO, MnO. A similiar variation is shown by sample Z244 (table 4).

Olivine compositions given in table 5 are from chromitite textural varieties constituted by chromite-rich and olivine-rich components. The banded chromitites possess coarser-chromite olivine-poor rhythmic bands that alternate with finer-chromite olivine-rich bands. The former type of bands possess olivine with higher Mg and lower Fe contents compared to the latter type. The speckled chromitites with irregular patches or 'speckles' made of coarser-chromite with lesser olivine are set in the finer-chromite olivine-rich parts. These show more magnesian olivine in the 'speckles'. The occluded-silicate chromitite as defined by Thayer (1969), and including the clot texture of Mukherjee (1969) consists of spherical, ellipsoidal or irregular shaped occlusions of fine grained disseminated chromite, usually richer in olivine, that are surrounded by coarser-chromite olivine-poor bounding areas. Some occlusions have cores of olivine without associated chromite. Sample Z175 in table 5 shows less magnesian and more Fe-rich olivine of the occlusions than their bounding parts.

Table 6. Sixteen microprobe analyses of sphene. $\bar{X}$ gives mean values for the number of analyses given in parentheses. S = standard deviation, EOCR = effective octahedral cation radius. All iron is supposed to be trivalent. b.d. = below detection level.

Sr. No.	$\bar{X}(2)$	$\bar{X}(4)$	S	$\bar{X}(10)$	S
Sp. No.	Z339	Z219		Z372	
SiO_2	30.71	30.76	0.23	30.57	0.22
TiO_2	37.60	36.44	1.11	40.19	0.13
Al_2O_3	2.22	2.93	0.72	0.80	0.14
V_2O_3	0.60	0.42	0.21	0.34	0.17
Fe_2O_3	0.24	0.56	0.09	0.35	0.07
MnO	0.04	0.06	0.04	0.00	
MgO	0.05	0.10	0.04	0.00	
NiO	b.d.	b.d.		0.04	0.02
CaO	29.17	28.92	0.25	28.79	0.23
Na_2O	0.03	b.d.		0.14	0.11
K_2O	b.d.	b.d.		0.04	0.02
Total	100.66	100.19		101.26	
Number of ions on the basis of four Si:					
Si	4.000	4.000		4.000	
Ti	3.683	3.563		3.954	
Al	0.341	0.449		0.123	
V	0.042	0.029		0.024	
Fe^{3+}	0.024	0.055		0.034	
Mn	0.004	0.006		0.000	
Mg	0.010	0.019		0.000	
Ni	–	–		0.004	
Ca	4.070	4.029		4.036	
Na_2	0.008	–		0.035	
K	–	–		0.007	
O	20.062	19.981		20.242	
(EOCR)	0.599	0.597		0.603	

SPHENE

Accessory sphene is present in the metadolerites and the quartz-rich plagiogranitic differentiates as a late-stage crystallization product (sample Z339). Analyses are consistent with its chemistry known from similar occurrences described in literature (e.g., Deer *at al.*, 1982). In table 6, analyses from 3 samples are given and are consistent with the data on igneous sphenes from literature (Deer *et al.*, 1982). One metadolerite rock (sample Z372) shows relatively higher TiO_2 and lower Al_2O_3. Cr_2O_3 is negligible in sphene. Al + Fe^{3+} (with predominant Al) apparently substitute for Ti, as they show a reciprocal relationship (table 6).

The sphene composition from SQO (table 6) is quite close to the theoretical Ca Ti SiO_3 and thus, resembles the compositions exhibited generally by the sphenes from basic and ultrabasic rocks (Deer *et al.*, 1982). The sphene is different from that often found in the syenitic rocks which contains appreciable Fe^{3+}, Al and Nb. It also differs from the sphene of granitic rocks which is often rich in REE.

GARNET

The SQO rocks do not contain primary garnet of magmatic derivation; garnets are associated abundantly with the rodingitic rocks. Rodingitic rocks of the SQO are composed mainly of grossular and hydrogrossular garnets whose analyses are listed in table 7. Rodingite dyke samples in table 7 are Z383, ZA222, Z361A and Z399. The grossular and hydrogrossular analyses in table 7 show that andraditic substitution is generally low in these samples. Some analyses are of highly pure grossulars. TiO_2 is usually low and ranges from nil to 0.6%. Within sample variations in TiO_2 are, however, large. MnO is always low; one sample contains 1.3% MnO whereas the rest of the samples contain from nil to 0.33% MnO. V_2O_3 content is below 0.07%, although the associated uvarovite contains 0.2% V_2O_3.

Two-garnet rodingites containing both hydrogrossular and grossular are common. Such two-garnet rodingites are also known from other areas of the world (e.g., Duffield & Beeson, 1973; Leach & Rodgers, 1978). The SQO rodingites contain all the three phases, grossular, hydrogrossular and vesuvianite, known to occur in rodingites from the Archaean ultramafic complexes in the Barbeton Mountainland, South Africa (Anhaeusser, 1979). Z400 contains a rodingitic vein with two garnets: one, a transparent, colourless grossular with FeO content varying from 1.27% to 1.47%; the other, a brown, transparent, euhedral, andraditic garnet with FeO content varying from 7.35% to 9.93%.

Small, cm-scale white veins composed almost entirely of hydrogrossular and grossular that occur in chromitite samples (Z41A, Z235); in serpentinite sample Z400; in metadolerite sample Z372; and in metasomatized metadolerite sample Z371B, are also listed in table 7. The metasomatized metadolerite sample Z372 contains grossular distributed pervasively in the rock in addition to veins. No regular compositional difference was noticed between these two types of grossular.

The white grossular veins crosscutting the chromitite sample Z41A attain green colouration due to Cr content at the interface between the vein and the chromitite host and become Cr-enriched leading often to the formation of uvarovite. The mode of occurrence indicates development of uvarovite through the reaction of chromitite wall rock with the parent aqueous solutions of the rodingite vein. Analyses of coexisting grossular and uvarovite from the same sample are given in table 7. Uvarovite is rich in Cr_2O_3 and has higher TiO_2, but lower Al_2O_3, MgO, FeO and CaO than the associated hydrogrossular. Uvarovite shows solid solution chiefly with the grossular molecule, with very little andradite and pyrope molecules indicated by the low Fe and Mg contents, respectively. However, its high Ti content is noteworthy and an exceptional feature (cf. Deer *et al.*, 1982). The greenish, Cr-bearing titanian hydrogrossular at the wall zone of another similar vein in chromitite is analyzed from sample Z235c (table 7). Its comparison with the coexisting white hydrogrossular (Z235b) shows it to have higher Cr_2O_3, TiO_2 and MgO, but lower Al_2O_3, FeO and CaO. The Cr-bearing titanian hydrogrossular has exceptionally high TiO_2 content. The high TiO_2 content is usually associated with andraditic garnets (Deer *et al.*, 1982). However, in the present analyses of both uvarovite and Cr-bearing titanian garnet, low iron content indicates very low andradite component.

Within-sample variations of rodingitic garnets are large. The rodingite dyke sample ZA222 contains coexisting grossular and hydrogrossular; the former possesses higher Al_2O_3, CaO, SiO_2, and lower FeO and MgO than the latter. Similar variations of hydrogrossular and grossular are noticed in the sample Z371B where the FeO and MgO also show noticeable variation. SiO_2 percentage of all hydrogrossular analyses is lower than that of grossular analyses. This supports the substitution $Si \rightleftharpoons 4H$.

DISCUSSION AND CONCLUSIONS

At SQO, the olivine mineralogy and chemistry has mainly developed from primary magmatic processes; whereas the garnets seem to display the influence of later metasomatic processes. Essentially similar compositions are revealed by sphene from both rock types: the quartz-rich plagiogranitic differentiates and the metadolerites effected by magmatic and metasomatic processes.

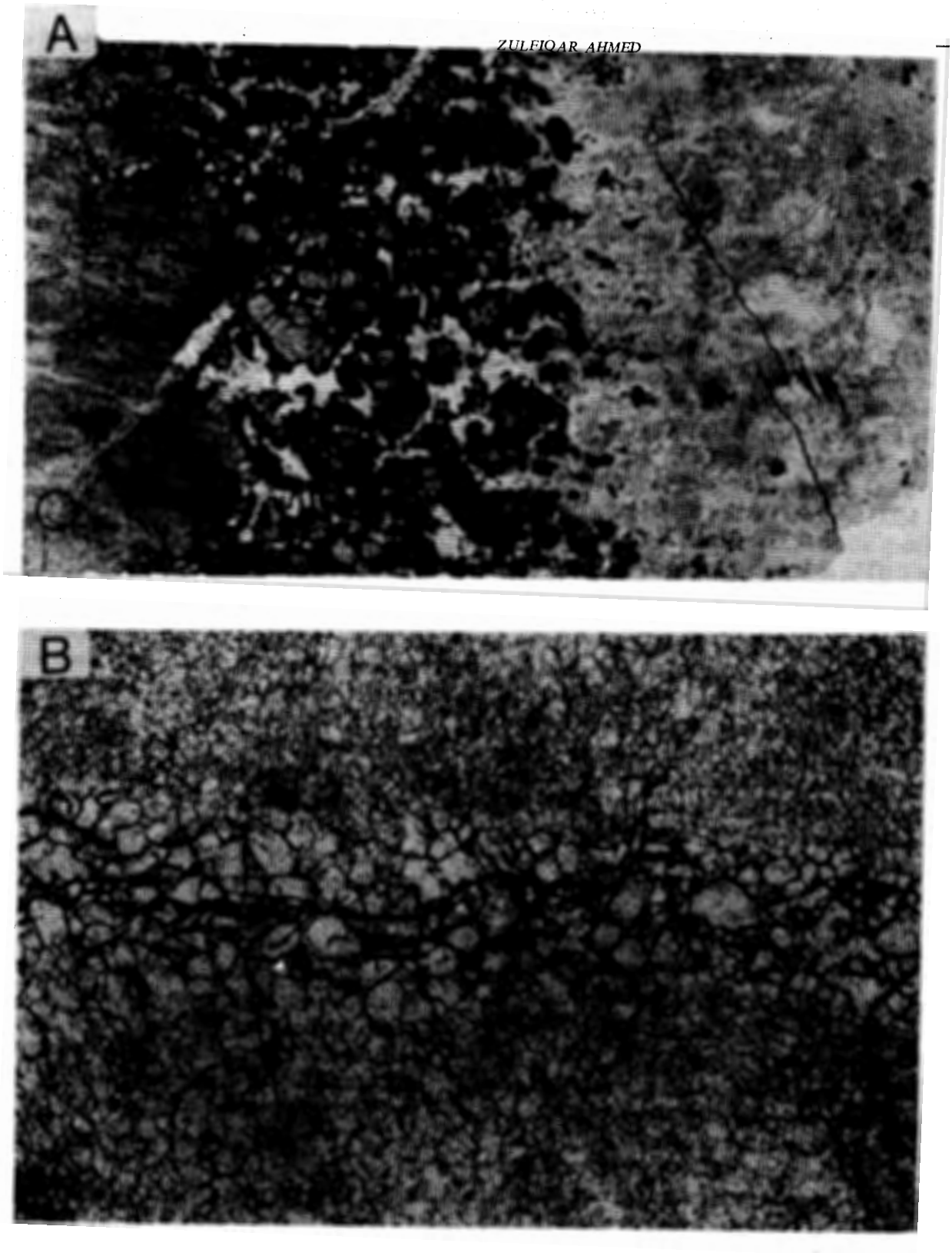

Fig. 4 . (A) Transmitted light photomicrograph of rodingite (sp no. Z399) displaying the chlorite wall of the dyke (towards right) grading inwards to to grossular-rich rock, with an in between zone of grossular and hydrogrossular grains and granular aggregates carrying vesuvianite druses and chlorite matrix. The ferritchromit opaque specks are seen in the chlorite margin. (B) Detail of recrystallized hydrogrossular along a crack seen in (A) towards the left hand bottom part.

Table 7. Garnet analyses. Na_2O and K_2O are below detection level.

Sp. No.	Z41Ai	Z41Aii	Z235a	Z235b	Z235c	Z383	ZA222a	ZA222b	Z361Ai
No. Anal.	$\bar{X}$(10), s	$\bar{X}$ (2)	$\bar{X}$ (2)	(1)	$\bar{X}$ (2)	$\bar{X}$ (4), s	$\bar{X}$ (2)	$\bar{X}$ (20), s	$\bar{X}$ (22), s
SiO_2	36.38 (0.60)	36.82	39.74	37.20	35.97	39.87 (0.14)	39.30	36.39 (0.40)	37.18 (0.35)
TiO_2	2.58 (0.84)	0.16	0.06	0.06	6.50	b.d.	0.07	b.d.	b.d.
Al_2O_3	9.42 (0.30)	17.27	21.82	17.92	11.70	22.55 (0.09)	21.50	17.28 (1.30)	19.03 (0.41)
Cr_2O_3	13.98 (0.96)	0.50	0.08	0.08	1.44	0.05 (<0.01)	0.06	b.d.	b.d.
V_2O_3	0.20 (0.07)	0.07	0.00	0.04	b.d.	n.d.			
Fe_2O_3	1.49 (0.12)	1.74	0.96	1.58	1.21	0.38 (0.08)	0.96	2.70 (0.30)	1.67 (0.22)
MnO	b.d.	b.d.	b.d.	0.02	0.00	0.06 (0.03)	0.00	b.d.	0.08 (0.05)
MgO	0.72 (0.50)	3.09	0.09	2.64	3.48	0.23 (0.16)	0.08	2.32 (0.65)	2.13 (0.34)
NiO	b.d.	b.d.	0.00	0.06	b.d.	b.d.	b.d.	b.d.	0.00
CaO	35.18 (0.73)	36.69	37.75	36.86	35.50	37.65 (0.08)	37.54	36.79 (0.36)	36.40 (0.27)
Total	99.95	96.34	100.50	96.46	95.80	100.79	99.51	95.48	96.49

Sp. No.	Z361Aii	Z399	Z372	Z371Bi	Z371Bii	Z371Biii
No. Anal.	$\bar{X}$ (10), s	$\bar{X}$ (11), s	$\bar{X}$(8), s	(1)	(1)	$\bar{X}$(9), s
SiO_2	38.73 (0.43)	36.54 (0.59)	39.20 (0.63)	39.58	38.42	35.68 (0.39)
TiO_2	b.d.	b.d.	0.04 (0.02)	0.00	n.d.	0.41 (0.31)
Al_2O_3	20.56 (1.02)	17.79 (0.52)	21.69 (0.78)	21.69	14.09	15.54 (0.69)
Cr_2O_3	b.d.	0.05 (0.04)	b.d.	0.08	0.00	b.d.
Fe_2O_3	1.62 (0.30)	2.26 (0.40)	4.50 (0.89)	1.46	12.30	5.63 (0.68)
MnO	b.d.	b.d.	0.95 (0.33)	0.14	0.33	b.d.
MgO	1.31 (0.95)	2.37 (0.33)	0.16 (0.16)	0.00	0.10	2.04 (0.35)
NiO	0.08 (0.06)	0.00	b.d.	0.03	0.00	b.d.
CaO	36.94 (0.41)	36.67 (0.33)	33.33 (1.44)	36.42	35.29	35.60 (0.57)
Total	99.24	95.68	99.87	99.40	100.53	94.90

Sp.No.	Z371Biv	Z400i	Z400ii
No.Anal.	$\bar{X}$(8), s	$\bar{X}$(9), s	$\bar{X}$(4), s
SiO_2	36.85 (0.91)	39.13 (0.30)	39.61 (0.35)
TiO_2	0.11 (0.09)	0.07 (0.03)	0.06 (0.06)
Al_2O_3	20.18 (1.19)	16.93 (0.93)	20.14 (0.10)
Cr_2O_3	b.d.	b.d.	0.02 (0.02)
Fe_2O_3	2.31 (1.80)	8.91 (1.29)	1.50 (0.08)
MnO	0.23 (0.23)	b.d.	0.36 (0.06)
MgO	b.d.	0.08 (0.06)	0.03 (0.03)
NiO	0.00	0.00	0.03 (0.04)
CaO	35.46 (1.44)	35.89 (0.57)	36.88 (0.18)
Total	95.14	101.01	98.63

The normal trend of crystallization of olivine is generally considered to be towards Fe-enrichment. In the ophiolitic ultramafic cumulates, olivine generally increases in Fe stratigraphically upwards (Coleman, 1977; Himmelberg & Loney, 1980) and the olivine in gabbros may carry 70 to 85% Fo. At SQO, olivine in the metagabbros was not observed, and therefore the most Fe-rich olivine of the complex is that of Fe-websterite which contains about 74% Fo.

From chromite-bearing zones of the stratiform complexes, it has been shown that olivines have higher Fo content in the chromite-olivine cumulates than in the adjacent chromite-poor olivine cumulates (Cameron & Desborough, 1969; Hamlyn & Keays, 1979; Jackson, 1969). Table 2 documents the olivine compositional variations amongst different rock types and different components of the samples. Minor but consistent differences in MgO and FeO contents of olivines are recorded in tables 3 to 5 for the textural components of chromitites.

All garnet in SQO rocks is rodingitic, and developed through the activity of metasomatic aqueous solutions, richer in Ca and Al, resulting in the formation of grossular and hydrogrossular garnets. Uvarovite has developed metasomatically at some hydrogrossular-chromitite contact-points; Cr being supplied from its adjacent chromite grains. Cr is also higher in a titanian hydrogrossular that occurs in similar manner to uvarovite. The compositions are also compatible with the experimental existence of extensive solid solution between uvarovite and grossular. Complete solid solution is observed between uvarovite and grossular below 855± 5°C at 1 atmosphere total pressure by Huckenholz & Knittel (1975). Such compositions are also reported from natural garnets. Ti-bearing hydrogarnet has been reported from a fissure in a rodingite dyke at Bric Canizzi, Liguria, Italy, by Basso *et al.*, (1981).

REFERENCES

AHMED, Z. (1978a) Chromite from Sakhakot-Qila-area, Malakand Agency, Pakistan. Min. Mag. **42**, pp. 155-157.

———— **(1978a)** Geological investigations of the chromite ore deposits of the Malakand Agency, Pakistan Sci. Found. Proj. Rep. P-PU/EARTH (17), 38 p.

———— **(1982)** Porphyritic nodular, nodular, and orbicular chrome ores from Sakhakot-Qila Complex, Pakistan, and their chemical variations. Min. Mag. **45**, "Deer, Howie & Zussman Vol.", pp. 167-178.

———— **(1983)** Geology and chromite deposits of the Sakhakot-Qila ophiolite, Pakistan (Summary). Ofioliti **8** (2), pp. 261-262.

———— **(1984)** Stratigraphic and textural variations in the composition of the Sakhakot-Qila Complex, Pakistan. Econ. Geol. **79** (6), pp. 1334-1359.

———— **& BEVAN, J.C. (1981)** Awaruite, iridian awaruite and a new Ru-Os-Ir-Ni-Fe alloy from the Sakhakot- Qila complex, Malakand Agency, Pakistan. Min. Mag. **44**, pp. 225-230.

———— **& HALL, A. (1981)** Alteration of chromite from the Sakhakot-Qila ultramafic complex Pakistan. Chemie der Erde **40**, pp. 209-239.

———— **& HALL, A. (1982)** Nickeliferous opaque minerals associated with chromite alteration in the Sakhakot-Qila complex, Pakistan, and their chemical variation. Lithos **15**, pp. 39-47.

———— **& HALL, A (1983)** Petrology and mineralization of the Sakhakot-Qila ophiolite Pakistan. ***In:*** Gass, I.G., Lippard, S.J. & Shelton, A.W. (eds.) OPHIOLITES AND OCEANIC LITHOSPHERE. Geol. Soc. London Spec. Publ. **13**, pp. 241-252.

ANHAEUSSER, C.R. (1979) Rodingite occurrences in some Archaean ultramafic complexes in the Barberton Mountain Land, South Africa. Precambrian Res. **8**, pp. 49-76.

BASSO, R., DELLA GIUSTA, A. & ZEFIRO, L. (1981) A crystal chemical study of a Ti-containing hydrogarnet. Neues Jahrb. Min. Mh., p. 230-236.

BROWN JR., G.E. (1980) Olivines and silicate spinels. ***In:*** Ribbe, P.H. (ed.) ORTHOSILICATES. Min. Soc. Amer. Reviews in Mineralogy **5**, pp. 275-381.

CAMERON, E.N. & DESBOROUGH, G.A. (1969) Occurrence and characteristics of chromite deposits--- Eastern Bushveld complex. ***In:*** Wilson, H.D.B. (ed.) MAGMATIC ORE DEPOSITS. Econ. Geol. Monograph **4**, pp. 23-40.

COLEMAN, R.G. (1977) OPHIOLITES----Ancient Oceanic Lithosphere? Springer--Verlag, Berlin. 229 p.

DEER, W.A., HOWIE, R.A. & ZUSSMAN, J. (1982) ROCK-FORMING MINERALS: Volume **1A**, Orthosilicates. Second Edition Longman London, 919p.

DUFFIELD, W.A. & BEESON, M.H. (1973) Two-garnet rodingite from Amador County, California. Jour. Res. U.S. Geol. Surv. **1**, p. 665-672.

HAMLYN, P.R. & KEAYS, R.R. (1979) Origin of chromite compositional variation in the Panton Sill, Western Australia. Contrib. Mineral. Petrol, **69**, p. 75-89.

HIMMELBERG, G.R. & LONEY, R.A. (1980) Petrology of the Vulcan Peak alpine-type periodtite, Southwestern Oregon. Geol. Soc. Amer. Bull. **84**, pp. 1585-1600.

HUCKENHOLZ, H.G. & KNITTEL, D. (1975) Uvarovite : stability of uvarovite-grossularite solid solution at low pressure. Contrib. Mineral. Petrol. **49**, pp. 211-232.

Jackson, E.D. (1969) Chemical variation in coexisting chromite and olivine in chromite zones of the Stillwater complex. ***In:*** Wilson, H.D.B. (ed) MAGMATIC ORE DEPOSITS; Econ. Geol. Monograph **4**, pp. 41-71.

LEACH, T.M. & RODGERS, K.A. (1978) Metasomatism in the Wairere serpentinite, King Country, New Zealand. Min. Mag. **42**, pp. 45-62 & M 12 – M 15.

MUKHERJEE, S. (1969) Clot textures developed in the chromites of Nausahi, Keonjhar District, Orissa, India. Econ. Geol. **64**, pp. 329-337.

ROSSMAN, D.L., ABBAS, S.G. & OTHERS (1970) Geology and economic potential for chromite in the ultramafic rock complex near Dargai, Peshawar Division, West Pakistan. U.S. Geol. Surv. — Pakistan Govt. Proj. Report (IR) PK, 69p. (Unpublished).

SIMKIN, T., & SMITH, J.V. (1970) Minor element distribution in olivine. Jour. Geol. **78**, pp. 304-325.

THAYER, T.P. (1969) Gravity differentiation and magmatic re-emplacement of podiform chromite deposits. ***In:*** Wilson, H.D.B. (ed.) MAGMATIC ORE DEPOSITS; Econ. Geol. Monograph **4**, pp. 132-146.

Manuscript received on 20.10.1987
Accepted for publication on 20.10.1987

ACTA MINERALOGICA PAKISTANICA
VOLUME 3 (1987) pp. 42 - 50

PETROLOGICAL STUDY OF PART OF THE BASEMENT OF THE ARGENTERA-MERCANTOUR MASSIF, FRANCE.

ABDUL HAQUE
Department of Geology, University of Baluchistan, Quetta, Pakistan.

ABSTRACT: The petrological study of part of the basement of the Argentera-Mercantour Massif mapped on a scale of 1:20,000 is presented. The author puts together the previous petrological results as well as his own field and lab observations to introduce the phenomena of metasomatism, metamorphism, and retromorphism.

INTRODUCTION

The basement of the Argentera-Mercantour Massif has been divided petrographically into a western zone and an eastern zone by the Valleta-Moliere mylonite, which is a major dextral strike-slip fault (Faure-Muret, 1955). Each zone is further subdivided into different petrological complexes. The western zone or the *"Tinee Complex"* is composed of the following rock units from west to east: Varelios-Fourgieret gneiss: Valabre gneiss; Anelle gneiss & migmatite, and Rabuons migmatites. The eastern zone is divided into the *"Chastillon-Valmasque Complex"* and the *"Malenvern-Argentera Complex"*. The Chastilon-Valmasque Complex is further subdivided from west to east into: Adus migmatite; Chastillon gneiss; Valmasque granite. Malenvern-Argentera Complex is also subdivided from west to east into: Malenvern migmatites; Comba-Grossa anatexy, and Argentera granite.

Out of the above units, the following are exposed in the mapped area (Abdul Haque, 1984) the Valabre gneiss, the Anelle gneiss and migmatite, the Rabuons migmatites and the associated amphibolites, the Adus migmatite, the Chastillon gneiss, the Comba-Grossa anatexy, and the Argentera granite.

Various rock samples contain a large variety of minerals (table 1) and exhibit micro-features for each rock unit. This study was carried out to understand the phenomena of metasmatism, metamorphism, chloritization, sericitization and damourization related to retromorphism; progressive change in the attitude of foliation from western to eastern zones; kink-bands in biotite, muscovite and plagioclase crystals; post-foliation schistosity, fractures, and boudinage refilled by neoformed leucocratic minerals which brough about the cataclasis; distinction between mylonite and paleomylonite due to the dextral movement of major strike-slip fault of Valleta-Moliere.

WESTERN ZONE

In the western zone or "Tinee Complex" gneiss and migmatites of Valabre, Anelle, Rabuons and the associated amphibolites are mapped and are summarized below.

Valabre Gneiss

The Valabre gneiss is situated on the western side of the Tinee Valley (fig. 2).

This rock unit is composed of gneiss, amphibolites and rare migmatite (Faure-Muret, 1955) but the present author observed that it is a

homogeneous and granular gneiss in which quartzo-feldspathic assemblage is abundantly surroundee by microcrystalline dark minerals. N140, 30N oriented foliation is only visible in the blackish grey and greenish part of this gneiss with which green bands of amphibolites are also associated.

The Valabre gneiss has heteroblastic lamellar texture, and has been microscopically divided into two types: gneiss rich in green hornblende and biotite but poor in muscovite,and granular homogeneous gneiss poor in hornblende but rich in biotite (Faure-Muret, 1955). The present thin sections study reveals both leucocratic and melanocratic minerals. Leucocratic minerals are represented by xenomorphic quartz associated with orthoclase, albite, and sub-automorphic oligoclase grains all being grouped into long leucocratic lenticular shape in which feldspars have often been sericitized and damouritized. These leucocratic lenticules are seperated by melanocratic assemblage composed of green hornblende sometimes chloritized, brown biotite, rare flakes of muscovite and chloritized biotite, with accessory minerals like sphene and apatite. Accessory minerals are in the form of inclusions in leucocratic minerals. Both leucocratic and melanocratic minerals are preferentially along linear foliation within the basement of Argentera-Mercantour. The attitude of such foliation measured during field work is N130, 30N. Moreover, James (1976) described the presence of garnet in this gneiss.

All these rocks have been teared up and their openings are refilled with recrystallized altered chlorite. Retrograde metamorphism of this gneiss is characterized by chloritization of biotite, sericitization and damouritization of feldspars and recrystallization of quartz crystals.

Anelle Gneiss and Migmatite

The Anelle gneiss and migmatite outcrop on the eastern side of the Tinee (fig. 2).

Faure-Muret (1955) considered that the Anelle rocks consititute plagio-gneiss and migmatite with associated amphibolites are represented by two facies: fine grained homogeneous gneiss injected lit-par-lit, heterogeneous migmatite and injected micaschists. Bogdanoff (1980) drew also attention to the presence of marble, micaceous and feldspathic quartzites within these gneiss and migmatite outcrops.

During my field investigations, millimetric and pluricentimetric leucocratic (quartz and feldspars) ribbons being separated by an assemblage of melanocratic minerals, (biotite, chlorite, muscovite) have been observed along foliation planes. Such foliation is anterior to all sort of deformations of the Argentera-Marcantour basement (Bogdanoff, 1980).

Microscopic study of the gneiss and migmatite reveals minerals like albite, oligoclase, andesine, quartz, orthoclase, biotite, chlorite, muscovite, zircon, apatite, sphene, epidote and tourmaline. Faure-Muret (1955) mentioned the presence of sillimanite, garnet, kyanite and phenacite. These minerals are grouped together into leucocratic and melanocratic types.

Leucocratic association is present in two different forms: lenticular and amygdoloidal forms. The former one contains mosaic of xenomorphic recrystallized quartz, being associated with sub-automorphic plagioclase and orthoclase. Myrmekite is well developed at the limit of quartz and orthoclase. Ancient plagioclase crystals are stretched. fractured and these fractures are refilled by the recrystallization of neoplagioclase. The latter one is composed of sericitized porphyroblastic orthoclase, albite, oligoclase, and large crystals of quartz. Quartz grains, in the form of droplets are recrystallized both in plagioclase and in melanocratic minerals. Sericitized orthoclase giving fine poecilo-blastic texture in the midst of which small neoform sericite crystals are present. Albite and big crystals of oligoclase are saussuritized where only albite twinning is identifiable.

Melanocratic association makes the micaceous halfhogshead, and is composed of biotite, chlorite, muscovite and accessory minerals like apatite, zircon, sphene, epidote and tourmaline. Fresh automorphic muscovite crystals showing micro-kink-bands are less than chloritized and

crushed biotite crystals which are disposed in large blades, parallel to the foliation of the basement.

Rabouns Migmatites

To the west of Anelle gneiss and migmatite comes the Rabuons migmatites which outcrop in the Moliere river (Fig. 2) and are studied as below:

Megascopic study: Faure-Muret (1955), Romain (1978) and Bogdanoff (1980) have shown that the Rabuons migmatites are mainly augen type with abundant orthoclase and have been represented under three different forms: micaceous migmatite; porphyroblastic augen type migmatite, and amygdaloidal migmatite, with which amphibolitic bands are also associated. Moreover, associated marbles showing centimetric to metric ribbons which are parallel to the foliation of the basement are also described by Bogdanoff (1980). During the author's field observations (Abdul Haque, 1984) one lenticular band of amphibolite outcrops over the contact of Anelle gneiss and migmatite and Rabuons migmatites.

Microscopic study: Microscopically, I observed minerals like, quartz, orthoclase very abundant, albite, oligoclase, perthite, biotite, muscovite, chlorite and sericite, garnet, sphene, zircon, apatite. Amongst the aforesaid minerals, Faure-Muret (1955) mentioned sillimanite and kyanite, Romain (1978) described epidote, Bogdanoff (1980) observed rutile, tourmaline and sillimanite which is in the form of myrmekitic fibre. Bogdanoff also observed dominant calcite with crystals of pistacite, amphibolite, zoisite, and finally epidote. During my laboratory study lepidoblastic biotite (automorph to subautomorph) is more frequent than muscovite and micaceous fibres in these migmatites. Sericitized sillimanite is also present in it in the form of fibre. This lepidoblastic arrangement of minerals (biotite, muscovite etc.) which separate xenomorphic porphyroblasts of alkalic feldspars more or less perthitic from the amygdales which are composed of quartz, damouritized orthoclase, albite, oligoclase, biotite, apatite, and garnet, giving to the whole rock a granblastic texture arranging themselves parallel to the foliation of the basement. Such foliation has been laterly transcepted obliquely by strain-slip schistosity or crenulation cleavage which materializes itself by the alignment of neoformed minerals, like quartz, muscovite, biotite and fresh plagioclase. Plagioclase crystals (albite, oligoclase) are stretched in such a way that the voids produced are refilled by recrystallized microcrystals of quartz agains defining the above schistosity. Micro-kink-bands are also visible in biotite and in muscovite crystals.

Porphyroblasts of quartz are present in microgranoblastic ground mass which is made of orthoclase, albite, oligoclase, losangic sphene, and rare fractured garnet. Subautomorph apatite and zircon without plaeochroic aureol are present in the form of small inclusion in muscovite. On the contrary grains of zircon with concentric aureol are present in biotite crystals.

Amphibolites

In my mapped area dark green amphibolites with variable orientations are associated with the gneiss and migmatites belonging to the western zone (Fig. 2). These amphibolites sometimes homogenous (green compact massive) sometimes heterogeneous (alternating decametric light and dark bands) are probably in the form of sills have been studied under the polarizing microscope and summaritized as below:

Microscopic study: In these amphibolites microscopically I studied minerals like quartz, feldspar, and green hornblende (main constituent), albite, biotite, zircon, apatite, kyanite, sphene, garnet and opaque minerals. Besides diposide and labradorite described by Faure-Muret (1955), whereas muscovite, chlorite, epidote, idocrase, prehnite, pistacite, zoisite, and a undetermined carbonate have been mentioned by Bogdanoff (1980).

Xenomorphic crystals of felspars (orthoclase) being sericitized and damouritized showing porphyroclasts in which two generations of plagioclase crystals have been observed. The

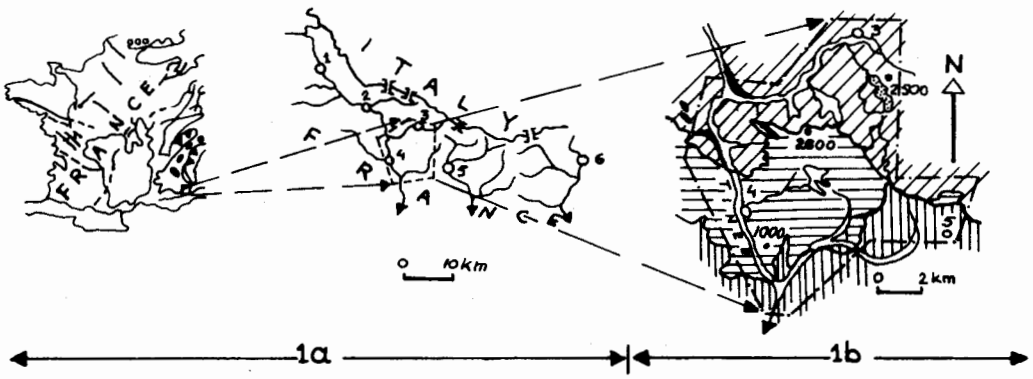

Explanations of Figures 1a and 1b

1. Saint Etienne de Tinée; 2. Isola; 3. Molière; 4. Saint souveur sur Tinée; 5. Saint Dalmas; and 6. Saint Martin Vésubie. (⌒ = Saddle)

Legend of Figure 1b

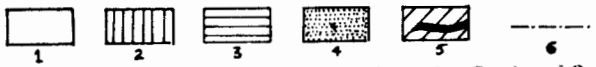

1. Recent. 2. Sedimentary Cover. 3. Permo-Triassic. 4. Carboniferous. 5. Basement rocks with amphibolites. 6. Limit of the mapped area.

Figure 1a: Schematic geological map of France and geographical limits of mapped area. 1b: Geological map of the studied domain between Saint Sauveur sur Tinée, Molière and Saint Dalmas.

Figure-2: Geological map of part of the basement of Argentera-Mercantour, French maritime Alps.

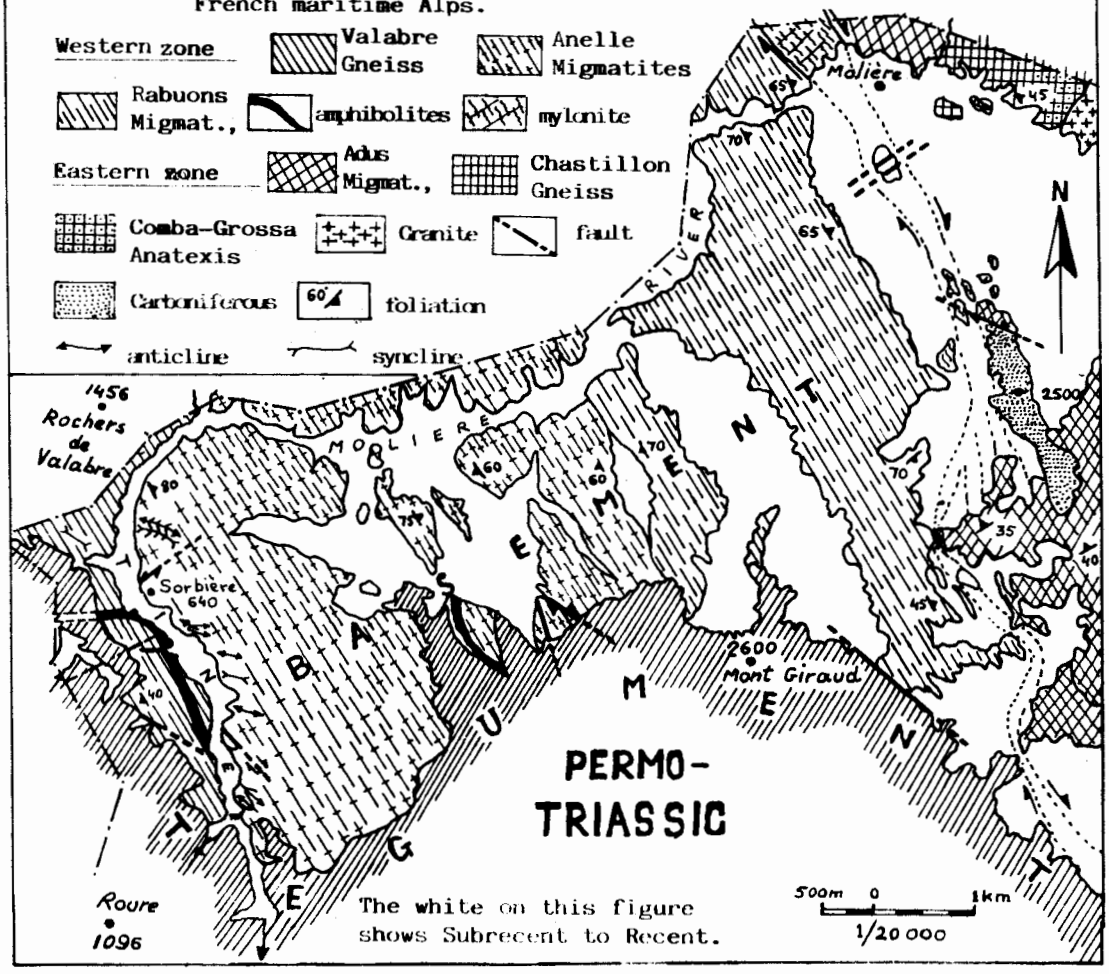

first generation is represented by big saussuritized while that of second generation are fresh one. Fresh hornblende crystals sometimes develop themselves at the expense of biotite grains, specially observed near the contact of garnet crystals.

Velleta-Moliere Mylonite

Valleta-Moliere mylonite within the massif of Argentera-Mercantour is represented by a crushed zone, being the product of dynamome tamorphism. The material derived by such metamorphism within such zone is called mylonite. This mylonitic zone divides the massif of Argentera-Mercantour into two different petrographical zones, the western zone and the eastern zone. This crushed zone is a major dextral strike-slip fault, oriented NW-SE, being 45 to 50km long with variable width from few centimentres to 100-150 metres. The petrological and structural studies of this mylonitic zone have already been discussed (Abdul Haque 1986a & 1986b).

EASTERN ZONE

The eastern zone is defined by two complexes, to the west *"Chastillon-Valmasque Complex"* and to the east *"Malenvern-Argentera Complex"*. The former one is further subdivided from west to east into: Adus migmatite; Chastillon gneiss; Valmasque granite, while the latter one is also subdivided from west to east into: Malenvern migmatites; Comba-Grossa anatexy, and Argentera-granite (Faure-Muret, 1955). In the mapped area, surroundings of Moliere (fig. 2), only Adus migmatite, Chastillon gneiss belonging to Chastillon-Valmasque Complex and Comba-Grossa anatexy, Argentera-granite having appurtenances to the Malenvern-Argentera Complex have been successively studied in detail in the following paragraphs.

Adus Migmatite

Megascopic study: To the west of Moliere (fig. 2) outcrops Adus migmatite being characterized by greenish compacted millimetric sheets which are separated by the alignment of quartzo-feldspathic assemblage. Here quartz crystals are visible in the lens but feldspars and other dark minerals remain microscopic. Thus, such alternation of these leucocratic and melanocratic assemblages define linear foliation being oriented N135, 30E and N155, 40E and which becomes rough and irregular towards east where Chastillon gneiss outcrops.

A mappable melanocratic lens within the Adus migmatite near the Mercera saddle made Faure-Muret (1955) to interpret it as ancient enclave of eruptive rocks. She has also demonstrated that this migmatite has been intercepted by non-retromorphosed aplitic and granulitic veins which are related to the Anataxis granite situated in the east (Fig. 2) In the west of Molière, a fine grained leucocratic vein, plurideci-metric thick intercepts obliquely the aforesaid foliation has been observed during the field work (Abdul Haque, 1984).

Microscopic study: The following minerals have been microscopically identified in the Adus migmatite, namely: quartz, orthoclase, microcline albite, oligoclase, biotite, muscovite, chlorite, sericite. Biotite grains slightly chloritized associated with muscovite are in abundance. Small crystals of orthoclase associated with them are also sericitized. All these minerals together give a pseudo-lepidoblastic texture. Big crystals of quartz always xenomorph, sometimes with correded contour are cataclized and oriented according to preferential direction, thus, giving the trend of linear foliation. These quartz grains associated with automorphic albite, oligoclase and big altered crystals of orthoclase producing porphyroblastic structure. Sometimes this assemblage makes elongated well preserved eyes being parallel to the foliation. Moreover, microcrystals of quartz, mica, sericite are synkinematically recrystallized in the voids and fractures of big crystals of quartz. These fractures have been produced during cataclastic phenomenon.

On going towards east, biotite crystals are going to change themselves into chlorite, whilst muscovite remains identifiable. Quartz crystals become more and more rounded while other

leucocratic minerals become abundant and the color of the rock changes from greenish to white, showing already commencement of the zone of anatexis, where the foliation becomes completely blurred.

Post foliation deformations which give to this migmatite an orthogneissic aspect, are manifested by different phenomena such as:
(1) formation of kink-bands within micas,
(2) synimematic recrystallization of quartz and micas in the voids, and in the fractures of porphyroblasts and,
(3) development of boundinage in feldspars and in quartz crystals.

Chastillon Gneiss

Chastillon gneiss (outcrop in the east) being narrowly associated with Adus migmatite (in the west) containing abundant light minerals, therefore, giving it a clear white color. In the field Chastillon gneiss shows millimetric alternance of very fine light and dark elements, which are ascribed as of sedimentary origin (Faure-Muret, 1955). The same author also points out rare remains of amphibolites and metamorphic carbonates which are enclosed in these gneiss. During mapping (Abdul Haque, 1984) one folded metamorphic carbonate lens is wedged out of Chastillon gneiss, outcroping in the SE of Molier (Fig. 2), as wel as unmappable outcrops of leucocratic lenses of ancient vestige being also associated with these gneiss.

Microscopic study: Microscopically I observed small secondary xenomorphic quartz crystals which are recrystallized in the middle of large dirty xenomorphic quartz and illitized. Microcrocline is also present. These light colored phenocrysts are crushed and cataclized in steps. Albite is saussuritized lately by dynamometamorphism.Secondary sericite grains develop at the expense of retromorphosed plagioclase crystals. The rough orientation of all these minerals, gives a blurred and irregular foliation to the Chastillon gneiss. Biotite crystals are completely changed into chlorite. Muscovite is present in two forms: either in lath shape of primary origin but rare in quantity, or in small secondary flakes developed at the expense of a mass of sericite. Very small grains of zircon and rutile are rarely present. Moreover, Faure-Muret (1955), Romain (1978), and Bogdonoff (1980) have mentioned the presence of sillimanite, either asociated with sericite or in the form of recrystallized needles within the quartz crystals.

Post foliation deformations are very abundant, which have been represented by 1) fractures in quartz and in felspar crystals, 2) microkink-bands in muscovite laths and, 3) cataclization of other crystals. These phenomena have completely obliterated the structure as well as the composition of original rocks from which the Chastillon gneiss has been derived.

Comba-Grossa Anatexy

Megascopic study: To the west of Chastillon gneiss outcrops Comba-Grossa anatexy which shows progressive contact with the former gneiss. They are also called *"transition anatexy"* because they are petrologically situated between Chastillon gneiss to the west, and Anatexis granite to the east. Comba-Grossa anatexy is represented by equigranular leucocratic rocks which have already been taken granitic aspect. The presence of enclaves of Chastillon gneiss in the Comba-Grossa anatexy shows that the latter one is derived from the former one.

Microscopic study: Microscopically chloritized biotite becomes very accessory which are associated with muscovite and giving undulatory extinction. Albite and oligoclase crystals are auto- to sub-automorph. The rocks sometimes give granoblastic aspect where microscopically recrystallized ground mass made of xenomorphic quartz crystals reveal undulatory extinction. Quartz are equally recrystallized into large crystals, oftenly crushed and reweld by leucocratic microelements Orthoclase is also crushed and sericitized.

Microcline is always abundant and present in two forms: primary microcline of dirty color showing paecilitic structure, and secondary prophyroblastic microcline very fresh which enclose few old crystals of untwined microperthetic microcline. Finally the albite twins are

TABLE–I: RESUME OF THE GEOLOGY OF THE PART OF BASEMENT OF ARGENTERA–MERCANTOUR, FRENCH MARITIME ALPS

W	WESTERN ZONE					VALLETA–MOLIERE MYLONITE	EASTERN ZONE				E
	TINEE COMPLEX						CHASTILLON–VALMASQUE COMPLEX MALENVERN–ARGENTERA COMPLEX				
	Saint Anne		TINEE VALLEY	Molière river			Molière				
	West of Tinée			West	East		Adus Migmat.,	Chastillon Gneiss	Combe-Grossa Anatexy	Anataxis Granite	
	Valabre Gneiss			Anelle Gneiss & Migmatites	Rabuons Migmatites						
FACIES	Gneiss with amphibolites.			Migmatite & Plagioclase. (associated amphibolites)	Migmatites with potash.		Migmatite	Gneiss	Anatexy	Granite	
	–do–			heterogeneous migmatite / homogeneous migmatite / greiss plus migmatite (associated marble)	heterogeneous migmatites / homogeneous migmatites / plus greiss (augen type)		–do–	Gneiss with enclave	Transition Anatexy	–do–	
MINERALS Leucocrates		qtz.,orth.(=).,alb.(++) oligo., (+).		qtz.,orth.(*) alb.(*)(++)., oligo.(*)(++)., and. (acc.).	Qtz.,orth.(***) (+++).,alb.(+)or (p)., oligo.(+)., per.(acc.).		qtz.(cat.), (±++)., orth.(*)., alb.,oligo micl.(acc).	qtz.(sec) orth.(*), (=).,alb. oligo., micl.(++)	qtz., orth.(*)., (cat.)., alb., micl.(++)	qtz., alb., oligo., micl., anor..	
MINERALS Melanocrates		hord., biot., mus.(=).chl. (sec.).,grt. (acc.).,sph. (acc.).,apt. (acc.).		biot.,mus.,chl., grt.,sph.,apt., zir.,sill.,kyn., epd.,serc., tour.,.	biot.,mus.,chl., grt.,sph., apt., zir., sill.,kyn., epd., serc.,rut., tour.,.		biot.(++). mus.(=)., chl.(=)., zir.(acc.). serc.(+)., rut.(acc.).	biot.(+)., mus.(=)., chl.(++)., serc.(++).	biot.(acc) chl.(+++).	biot., mus., grt., sph., epd.,.	
MINERALS Charact;		hord.(+++)., biot.(++)., mus.(=).,.		sill.(acc.)., kyn.(acc.)., grt.(acc.)., tour.(acc.).,	sill.(++)., kyn. (acc.).,grt.(acc.), tour.(acc.).,.		sill., according to B,F & R.	sill., according to F.	micl.,.	micl., biot., grt.,	
Foliation	(1)	NW–SE		NW–SE	NW–SE		NW–SE	blurred	absent		
Foliation	(2)	roughly NW–SE		NW–SE to NE–SW	NW–SE to NE–SW		(±)	blurred & irregular	–do–		
Derived from		homogeneous schist (F).		alternated schist and arenaceous & calcareous schist (F).		sed.,schist(B)		phyllateous schist, poor in quartz(F).			

alb.	albite	orth.	orthoclase	(=)	poor	(B)	Bogdanoff(1980)
and.	andesine	per.	perthite	(+)	more or less	(F)	Faure–Muret (1955)
anor.	anorthite	qtz.	quartz	(sec.)	secondary		
apt.	apatite	rut.	rutile	(acc.)	accessory	(P)	Prunac (1976)
biot.	biotite	serc.	sericite	(p)	present	(R)	Romain (1978)
chl.	chlorite	sill.	sillimanite	(*)	sericitized		
epd.	epidote	sph.	sphene	(**)	sausuritized		
grt.	garnet	tour.	tourmaline	(***)	damouritized		
hord	hornblende	zir.	zircon	(al)	altered		
kyn.	kyanite			(cat)	cataclized		
micl.	microcline	(+)	very little				
mus.	muscovite	(++)	abundant	(1)	regional		
oligo.	oligoclase	(+++)	very abundant	(2)	local		

deformed in micro-kink bands and show some traces of zonal structures and myrmekites.

Argentera Granite

Finally holoeucocratic (0-10% black minerals) Comba-Grossa anatexy transforms itself towards east into Anatexis granite which is also called Argentera granite. Field study shows that this granite is leucocratic, granular and homogeneous and the crystals like quartz, rose feldspar and biotite are easily visible by necked eye while plagioclase grains remain microscopic.

Microscopically this granite has a granblastic texture and rarely porphyraceous. The granoblasts are essentially represented by microcline, albite, oligoclase, anorthite and quartz, which is sometimes automorph. Microcline is microperthetic and albite-microcline twin is well developed. Orthoclase encloses sericitized albite either in the form of spots or ribbons.

Biotite crystals being dark brown and dark red in color, are of high temperature and high pressure which sometimes enclose small zircon crystals encircled by concentric pleochroic aureol. Myrmekite is developed in the acid plagioclase sometimes of greenish color, probably due to phenomenon of sericitization. Accessory minerals are muscovite, garnet, apatite, zircon, sphene and epidote.

Thus, this leucocratic garnetiferous granite of Carboniferous age (Debelmas, 1974) is granoblastic and has anatectic origin, although its form reminds us like a batholith in the midst of migmatites (Faure-Muret, 1955).

CONCLUSION

The petrological and structural results obtained through megascopic and microscopic studies of the gneiss, migmatites and granite belonging to the western and eastern zones have been summarized in Table-I. Nevertheless, the given paragraphs sum up the other geological results having been apprehended in the course of study of relevant literatures regarding the basement of the massif of Argentera-Mercantour. Since the maped area is situated in the centre of this massif, the given results are closely inter-related for both the western and eastern zones.

Western Zone

Megascopically, foliation is not too precisely define within Valabre gneiss (by the alignment of grey and greenish bands) which becomes well developed to the east where Anelle-Rabuons gneiss and migmatites have been mapped Here it is represented by alternative leutcocratic and melanocratic bands of centimetric thicknesses.

Microscopically, these light and dark bands representing lenticular shapes being composed of quartz, orthoclase, microcline, albite, oligoclase, andesine, muscovite, biotite, hornblende, garnet, sillimanite, kynite, tourmaline, sphene, zircon, etc. Amongst them hornblende is abundant in Valabre gneiss; albite, oligoclase, andesine are essential minerals in Anelle gneiss and migmatite; orthoclase and microcline are the main constituants of Rabuons migmatites. High grade metamorphic minerals are characterized by the presence of garnet, sillimanite, kyanite in Anelle and Rabuons gneiss and migmatites.

During the major phases of migmatization accompanied with metasometism (may be of Caledonian age), all the rock constituents of the basement had been set up right to the vertical (Bogdanoff, 1980).

The degree of metamorphism (Hercynian age) and retromorphism (Alpine age) augments from Valabre gneiss on the west to the Rabuons migmatites to the east. Retromorphism of these gneiss and migmatites is characterized by: chloritization of biotite and sometimes of hornblende crystals; sericitization and damouritization of orthoclase and sillimanite crystals; saussuritization of albite and oligoclase crystals.

Cataclastic phenomenon is manifested by synkinematic recrystallization of quartz and other light and dark minerals within the voids and fractures, as well as in the plane of strain-slip

schistosity which cuts obliquely the preexisting foliation.

Valleta-Moliere mylonite which divides the massif of Argentera-Mercantour into western and eastern petrological zones and is the product of successive dynamometamorphism of Caledonian, Hercynian and Alpine ages, has entirely changed paleomylonite and mylonite to ultramyonite (Romain, 1978; Abdul Haque, 1986b).

Eastern Zone

On going right to left (table 1) foliation within the eastern zone is oriented NW-SE (within Adus migmatites) to the right, which becomes irregular and blurred (within Chastillon gneiss) and finally becomes absent towards left (within Comba-Grossa anatexy and Anataxis granite).

The characteristic minerals are successively sillimanite, microcline, and garnet; chlorite, sericite become very abundant towards east, while quartz crystals become secondary. Albite is saussuritized, orthoclase is sericitized, biotite is slightly chloritized, and development of sericite at the expense of retromorphosed plagioclase.

The effects of cataclastic phenomenon are prominent than that of retromorphism in the eastern zone and are characterized by: development of micro-kink-bands in micas and in twined plagioclase crystals; porphyroblasts of quartz (showing correded contour), orthoclase (showing boundinage), chlorite and biotite (crushed and fractured in steps) and all are reweld by micro-leucoratic elements which are developed due to synkinematic recrystallization.

Non retromorphic apalitic and granulitic viens issued from Anataxis granite of Carboniferous age have been intercepted the whole eastern zone. The form of this granite which is centrally situated within these gneiss and migmatites belonging to this massif reminds us as a batholith but in fact, it has been derived from preexisting rocks and thus, has anatectic origin.

ACKNOWLEDGEMENTS

I am extremely grateful to messieurs M. Rioult and L. Dupret Professors at the University of CAEN, for their worthy discusions during the microscopic study regarding petrological problems. My gratitudes equally go to Madam A. Faure-Muret, Professor, University of Orsay, Paris, for her considerable assistance during the preparation of my Ph.D. thesis in France.

REFERENCES

ABDUL HAQUE, (1984) Analyse des structures Alpines du socle-tegument de l' Argentera-Mercantour et de la couverture sur la transversale de la Tinee (Alpes-Maritimes, France). These 3 cycle, Univ. Caen, 153p. (Unpublished).

————,**(1986a)** Some structural and petrographical aspects of the massif of Argentera-Mercantour situated in the French maritime Alps. Presented 15 Dec, 1986, in the 4th Miami Inter. Sym., Miami Beach, Florida USA.

———— **(1986b)** Microstructures of Valeta-Moliere Fault of France & Italy. Acta Mineralogica Pakistanica, **2,** pp. 153-157.

BOGDANOFF, S. (1980) Analyse structurale dans la partie occidentale de l' Argentera-Mercantour (A.M). Thèse Doct. es-sciences Univ. Paris- sud, 317p (Unpublished).

DEBELMAS, J. (1974) GÊOLOGIE DE LA FRANCE, Douin, 250p.

FAURE-MURET, A. (1955) Etudes geologiques sur le massif de l' Argentera-Mercantour et ses enveloppes Sedimentaires. Mem. Expl. Carte Geol. France, 336p.

JAMES, O. (1976) Etude geologique des bordures du massif de l'Argentera et du dome de Barrot (A.M). These 3 cycle, Univ. Nice, 139p. (Unpublished).

PRUNAC, M. (1976) Analyse structurale dans le socle de l'Argentera-Mercantour (A.M). These 3 cycle, Univ. Paris-sud, 198p. (Unpublished).

ROMAIN, J. (1978) Etude petrographique et structural de la bordure sud-occidentale du massif de l'Argentera, de Saint-Martin Vesubie a la cime du Diable (A.M) These 3 cycle, Univ. Nice, 365p. (Unpublished).

Manuscript received on 16.10.1987
Accepted for publication on 15.12.1987

ACTA MINERALOGICA PAKISTANICA
VOLUME 3 (1987) pp. 51 - 54

KINK-BANDS IN THE PERMIAN RED SCHIST OF THE ARGENTERA-MERCANTOUR MASSIF, FRANCE

ABDUL HAQUE
Department of Geology, University of Baluchistan, Quetta, Pakistan.

ABSTRACT: The Alpine orogeny has left considerable structural effects on the Permian red schist (Capeirotto serie) part of the tegument of Argentera-Mercantour massif. The late vertical compressive phase of this orogeny being directed N-S, has produced kink-bands deforming the preexisting axial plane schistosity or cleavage within the Capeirotto serie. Such schistosity is itself the product of major horizontal N-S compressive phase of Alpine tectonics.

INTRODUCTION

Unconformably overlaying the folded, faulted and fractured gneisses, migmatites and granites belonging to the basement of the Argentera-Mercantour massif, are the Carboniferous and Permo-Triassic continental rocks which define the tegument of this massif.

Carboniferrous detritic rocks enveloped by basement series are represented by grey to black schist, fine sandstone and variegated conglomerate which have been intensely deformed along with the basement during Hercynian and Alpine orogenies. These Carboniferous rocks situated at the base of tegument have been radiometrically dated 290 at ± 10 Ma (Debelmas, 1967).

After the deformation of Carboniferous continental rocks, comes the deposition of Permo-Triassic detritic formations. These unfossiliferous Permo-Triassic rocks have been unconformably deposited either directly over already deformed basement, or over folded Carboniferous rocks. Detailed lithological descriptions of these rocks have been done by Abdul Haque (1988).

Faure-Muret (1955) has divided the Permian continental rocks into four different series according to the law of superposition. These are:

1) ***The Inferno series:*** (the lower most) mainly composed of conglomerate with passage of dacitic lava; thickness varies from 0 to 7m.

2) ***The Marveilles series:*** constitutes green schist at the base, red at the top; thickness varies from 0 to 500m.

3) ***The Bego series:*** defined by sandstone and arkose with rare passage of pebble-beds at the base; thickness fluctuates from 400 to 1000m.

4) ***The Capeirotto series***: (at the top) containing red schist; thickness varies from 0 to 2000m.

Only the last two series are present in the mapped area, in which the Capeirotto series has been lithologically and structurally studied, and is summarized below.

GEOLOGY OF CAPEIROTTO

The Capeirotto series constitutes red to violet homogeneous schist and pelite which is locally called red roofing slate because of its use as roofing stone in the buildings of the surounding area. Greenish bands of thickness centimetric to decimetric as well as greenish oval spots (marker beds) both define the original bedding planes within this schist. These marker beds are due to reduction and are not only folded (N-S to NNE-SSW compression) but also displaced along the

axial plane schistosity (the same compression), thus, giving micro-similar folds. Moreover, fine sandstone bands are also observed within the Capeirotto series, which are due to the *reworking* of underlying Permian rocks. These marker beds have been folded along with the Permian schist into anticlines and synclines with an axial plane schistosity or cleavage.

KINK-BANDS WITHIN THE CAPEIROTTO SERIES

A part from axial plane cleavage and fracture cleavage which are associated with the folding produced by the N-S to NNE-SSW compression of Alpine age, kink-bands are also present in the Capeirotto series. Kink-bands differentiate itself from the above two types of cleavages both by its nature, and by its origin.

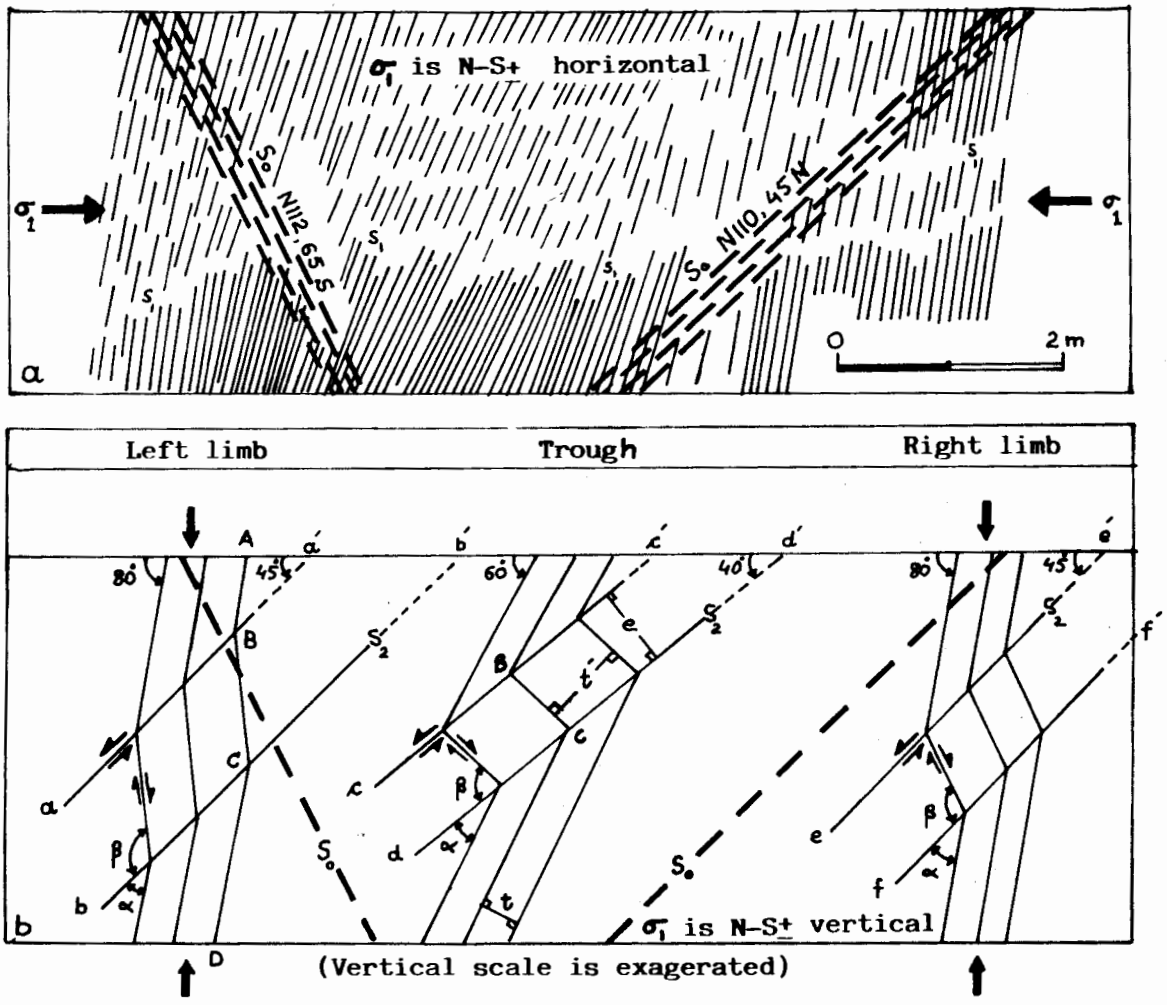

Figure–1 Schematic representation of kink-bands in the Permian red schist of Argentera-Mercantour. 1a) Synschistaceous syncline in the Permian red schist. The axis of this syncline is N113 ± horizontal, 1b) Schematic representation of kink-bands associated with synschistaceous syncline in the Permian red schist: aa', bb', cc', dd', ee' and ff' are planes of kink (kink-bands); AB or CD is the original schistosity plane while BC is the reoriented schistosity plane; t is the orthogonal thickness between original schistosity planes; t' is the orthogonal thickness between reoriented schistosity planes, and the angles α and β, the surface S_0, the thickness e are selfexplainatory.

The conditions for the development of kink-bands are, the rock to be texturally fine grained and subjected to an anisotropic planary tectonics. Moreover, these planes (textural or structural) must be perpendicularly confined on both sides in order to avoid extension of the rock (Paterson & Weiss, 1962; Boucarut, 1967; Ramsay, 1967).

In the Permian red schist (Fig. 1a) textural planes are defined by bedding planes (S_o) and structural planes are represented by secondary surfaces (S_1). In figure 1b the anisotropic planes are materialized by an axial plane schistosity or cleavage being denoted by AB or CD which itself gives shaly or phyllitic nature to the Capeirotto series. Such schistosity is due to the major N-S compression, more or less horizontal, of Alpine age. This schistosity is posteriorly deformed by the development of kink-bands which are produced by late N-S vertical compressive stresses of Alpine period.

Figure 1b shows the same syncline as well as the associated kink-bands in which two opposite rotations can be observed. The external sinistral rotation along the kink-planes, symbolised by aa' bb', etc., and the internal dextral rotation along the planes of reoriented schistosity denoted by BC, etc. Thus, the axes of external and internal rotations are nearly parallel to the E-W oriented axis of the pre-existing fold, though the tectonic phase responsible for the formation of these kink-bands is post-folding. This is due to the rotation (relaxation) of compressive stress axes from horizontal (major Alpine phase) to vertical (late Alpine phase) position.

In figure 1b, angle β is everywhere greater than angle α measured either in the trough or in the two limbs of fold. Thus, the orthogonal thickness t´ will also be greater than the orthogonal thickness t (compared only in one part of figure 1b). This augmentation of thickness t´ consequently creates perpendicular spaces in the reoriented cleavage planes BC, which are in fact, materialized by filling of fine films of important as well as gangue minerals. In addition, the relationship between angles α & β between the thickness t and t´ is only valid where there is no movement or gliding along the planes of kink. According to Ramsay (1967), in kink-bands t´ is less than 10cm, as in the present case; if t´ is above 10cm it is called knee-fold.

According to the hypotheses forwarded by various geologists (Fourmarier, 1923 & 1953; De Sitter, 1958; Ramsay, 1967; anderson, 1964) when angle β is less than angle α, shearing takes place along the planes of kink (which is not the present case). When conjugated kink-bands are present in the field, the difference is such, if one is dextral kink-band, the other will be sinistral fault and vice versa.

CONCLUSION

Kink-bands symbolized by aa', bb', and so on in fig. 1b are the product of late vertical N-S compressive stresses and posterior to the axial plane schistosity AB or CD, which are itself the product of major horizontal N-S compressive phase of Alpine orogeny. This change of horizontal to vertical N-S compressions is due to the relaxation of stresses in the late stage of Alpine orogeny.

ACKNOWLEDGEMENTS

I express my thanks to Messieurs F. Dore, M. Rioult and L. Dupret Professors in the University of Caen, Calvados, France for their assistance both in the field and in the laboratory investigations during my Ph.D. thesis in France. The author is also grateful to the anonymous referee for his valuable comments and suggestions for the amendment of this paper.

REFERENCES

ABDUL-HAQUE (1986) Some structural and petrographical aspects of the massif of Argentera-Mercantour situated in the French Maritime Alps. 4th Miami Intern. Symp. Miami Beach, Florida, USA., pp. 433-438.

——— , **(1986)** Lithostratigraphy of the part of tegument of the massif of Argentera-Mercantour, France. Kashmir Jour. Geol., **6** (In press).

ANDERSON, T.B. (1964) Kink-bands and related geological structures. Nature. **202,** April 18.

BOUCARUT, M. (1967) Structure du granite de l' Argentera et style tectonique de l' ensemble de ce massif (Alpes-Maritims). C.R. Acad. Sci. Paris, **264 (D),** pp. 1573-1576.

DEBELMAS, J. (1967) GÊOLOGIE DE LA FRANCE. Douin, 250p.

DE SITTER, L.U. (1958) Boudins and plastic folds in relation to cleavage and folding. Geol. en Mijnb. 8, pp. 277-285.

FAURE-MURET, A. (1955) Etudes geologiques sur le massif de l' Argentera-Mercantour et ses enveloppes sedimentaires. Mem. Expl. Carte Geol. France, 336p.

FOURMARIER, P. (1923) De l' importance de la charge dans le development du clivage schisteux. Bull. Acad. Roy. Belgique, cl. sci., ser. 5, t.g, p. 454.

_____ (1953) schistosite et grande tectonique. Ann. Soc. Geol. Belgique, t. 7 p. B 275.

PATERSON, M.S. & L.E. (1962) Experimental folding in rocks. Nature 195, sept. 15.

RAMSAY, J.G. (1967) FOLDING AND FRACTURING OF ROCKS. Mc-Graw Hill, 568p.

Manuscript received on 16.10.1987
Accepted for publication on 15.12.1987

ACTA MINERALOGICA PAKISTANICA
VOLUME 3 (1987) pp. **55 - 160**

PROCEEDINGS OF THE SYMPOSIUM ON MINERAL RESOURCES AND GEOLOGY OF PAKISTAN

ORGANIZED BY THE
Center of Excellence in Mineralogy, University of Baluchistan, Quetta, Pakistan.
20-28 October, 1987

INCLUDING:

A. PROGRAMME OF THE SYMPOSIUM
(SEE PAGES 56 - 61)

B. ABSTRACTS OF THE ORAL PRESENTATIONS
(SEE PAGES 62 - 71)

C. REVISED FULL-LENGTH PAPERS CONTRIBUTED TO THE SUMPOSIUM
(SEE PAGES 72 - 160)

MINERAL RESOURCES AND GEOLOGY OF PAKISTAN

A national symposium organized by the
Centre of Excellence in Mineralogy, University of Baluchistan, Quetta.
October 20 - 28, 1987.

PROGRAMME WITH ABSTRACTS

The first Pakistan national symposium on "Mineral Resources and Geology of Pakistan" was organized by the National Centre of Excellence in Mineralogy, University of Baluchistan, Sariab Road, Quetta.

The symposium was inaugurated by the General (Retd) Muhammad Musa, Governor of Baluchistan, on 20th October, 1987. The session, held at the University Law College, Khojak Road, Quetta, was opened by recitation from Holy Quran and the welcome address by Mr. Muhammad Hassan Baluch, Vice Chancellor, University of Baluchistan. Dr. Zulfiqar Ahmed, Director of the Centre of Excellence in Mineralogy, delivered the keynote address. General Muhammad Musa, in his inaugural address, laid emphasis on the need to enhance mineral resources exploration activities in Pakistan. The session ended with a group photograph and refreshments for all the guests, which numbered about 250. The national and local press, T.V. and radio elaborately reported the inaugural session.

The scientific paper reading sessions started on the afternoon of 20th October were actively persued till the late evening of 22th October. The titles of papers, names of authors are reported in the "Programme with Abstracts" which was included in the bags distributed to the registered delegates. Total 68 professional geoscientists registered for the symposium. They came from all over Pakistan and represented most of the mineral- related Organizations. Each registered delegate received symposium bag with included symposium literature and stationary items. The themes of the scientific paper reading sessions were as under:

1. Geology of oil and gas in Pakistan.
2. Minerals in relation to plate tectonics.
3. Marine geology and coastal areas of Pakistan.
4. Application of mineral exploration techniques in Pakistan.
5. Minerals of acidic rocks.
6. Base metal deposits and geology of Baluchistan.
7. Sedimentary minerals and stratigraphy of Pakistan.
8. Ophiolites of Pakistan.

A total of 22 papers were presented. A poster session was also organized.

A geological field excursion attended by 25 delegates and 5 organizational staff was held from 23rd to 28th October, 1987. The excursion visited the fluorite deposits of Kohi Maran area, barite deposits of Gunga area and nearby gossans overlying the Mississippi Valley type lead-Zinc deposits; Mesozoic sedimentary rocks of Ferozabad area; barite mill at Khuzdar; ophiolitic melange, gabbro and harzburgite bodies with chromite mines near Nal with its underlying strata and overlying strata, especially the Eocene limestones rich in fauna. Observations were also made alongside a 200 kms long north-south road section of the gigantic and spectacular Bela Ophiolite featuring thick sequence of pillow lavas, sheeted dykes, pyroxenite horizon and dykes, typically granitic differentiates, rodingitic dykes and mines and deposits of chromite and magnesite.

The success of the symposium strongly suggested its recurrence.

ACKNOWLEDGEMENTS

The Director, Centre of Excellence in Mineralogy and Secretary of the Organizing Committee for Symposium wishes to express feelings of deep gratitude to the following for the courtesies mentioned in each case.

1. *Honourable Governor of Baluchistan, & Chancellor of the University, for inaugurating the symposium.*

2. *University Grants Commission, Islamabad, for the allocation of necessary funds to the Centre of Excellence in Mineralogy and for permission to organize the Symposium.*

3. *National Institute of Oceanography, Karachi, for an active participation by their senior scientists and for donating a sum of Rs. 10000/- towards one dinner and part of the field excursion expenditure.*

4. *Pakistan Science Foundation, Islamabad, for sending a delegate and donation of Rs. 20,000 only towards the publication cost of the proceedings of the Symposium.*

5. *The National Academy of Higher Education, Islamabad, for approving funds for the Symposium.*

6. *Baluchistan Development Authority, Quetta, for donating Rs. 5,000/- towards the Symposium expenditure, for arranging guided tour and refreshments at the Kohi Maran fluorite mines and Mangocher town. Also their geologists participated actively.*

7. *The Geological Survey of Pakistan, Quetta, for participation by their geoscientific staff and provision of three 2-cabin pick up vehicles which made the field excursion programme successful. The Director General, Mr. Waheedud Din Ahmed, chaired one session and delivered a paper himself in addition to other staff from G.S.P., Quetta.*

8. *Pakistan Mineral Development Corporation, Quetta kindly provided one vehicle for the field excursion programme and also their mining engineers and geologists participated in the Symposium.*

9. *Khuzdar Engineering College, for extending generously their logistic facilities at Khuzdar during the field excursion from 23rd to 28th October, 1987.*

10. *Bolan Mining Enterprises Ltd. Quetta and Khuzdar for invitation to a dinner for field excursion party at Khuzdar and for arranging a guided tour to the barite mine at Gunga and milling plant at Khuzdar.*

11. *The S&GAD Department, Government of Baluchistan, for providing two staff cars.*

12. *The University Law College, Quetta, for providing their premises and venue for the Symposium.*

MONDAY OCTOBER 19, 1987

REGISTRATION OF DELEGATES
Centre of Excellence in Mineralogy, Quetta.

TUESDAY OCTOBER 20, 1987

INAUGURAL SESSION	**11.00 a.m. - 12.30 p.m.**
RECEPTION (Hosted By C.E.M.)	12.30 p.m.
LUNCH BREAK	1.00 p.m. - 3.00 p.m.
SCIENTIFIC PAPER READING SESSION	3.00 - 4.30 p.m.

Chairman: AFTAB AHMAD BUTT, PUNJAB UNIVERSITY, LAHORE.
Theme: **MINERALS IN RELATION TO PLATE TECTONICS.**

1. Waheeduddin Ahmad G.S.P., Quetta: A review of geology and metallic minerals of Pakistan related to plate tectonics.

2. Abul Farah; National Institute of Oceanography, Karachi: & Geological Survey of Pakistan, Quetta: Plate geology and mineral deposits of Baluchistan, Pakistan.

Theme: **GEOLOGY OF OIL AND GAS IN PAKISTAN**

3. Arif Kemal and M. Azam Malik; Oil & Gas Development Corporation, Islamabad. Geology and gas resources of Marri-Bugti Agency.

DINNER 7.30 p.m.
HOSTED BY: CENTRE OF EXCELLENCE IN MINERALOGY.

WEDNESDAY OCTOBER 21, 1987

SCIENTIF PAPER READING SESSION 9.30 - 11.00 a.m.
Chairman: G.S. QURAISHEE, N.I.O., KARACHI.

Theme: **MARINE GEOLOGY AND COASTAL AREAS OF PAKISTAN.**

4. Abul Farah; National Institute of Oceanography, Karachi: Recent advances in marine geology.

5. M. Akram Chaudry & Qasim Memon; National Institute of Oceanography, Karachi: Study of heavy minerals concentration along the Baluchistan coast, Pakistan; from Gadani to Phornala.

TEA BREAK 11.00 - 11.30 a.m.

6. G.S. Quraishee; N.I.O., Karachi: Progress of oceanographic studies by N.I.O. on the Indus delta region.

LUNCH INTERVAL 1.00 - 3.00 p.m.

SCIENTIFIC PAPER READING SESSION 3.00 - 4.30 p.m.

Theme: **APPLICATION OF MINERAL EXPLORATION TECHNIQUES IN PAKISTAN.**

7. TARIQ MAHMOOD; R.D.F.C., Islamabad: Role of financial organizations towards mineral development.

8. S.A.K. Alizai; SUPARCO, Karachi: Use of satellite imagery for geological mapping in the coastal Makran region of Baluchistan.

DINNER 7.30 p.m.
COURTESY: NATIONAL INSTITUTE OF OCEANOGRAPHY, KARACHI.

THURSDAY OCTOBER 22, 1987

SCIENTIFIC PAPER READING SESSION 9.30 - 11.00 a.m.
Theme: **MINERALS OF ACIDIC ROCKS**
Chairman: S.A.K. ALIZAI, SUPARCO, KARACHI.

9. Khurshid Alam Batt PAE Min. Cen. Peshawar: Pleistocene thrusting in Himalayas and its relation to uranium mineralization.

Chairman: WAHEEDUDIN AHMED, G.S.P., QUETTA.

10. Tehseenullah Khan, Imtiaz Ali, Rehanul Haque Siddiqui and Haider Kamal; Geological Survey of Pakistan, Quetta: Pink zoisite (thulite) occurrence at Nomal, Gilgit District, Pakistan.

TEA BREAK 11.00 - 11.30 a.m

SCIENTIFIC PAPER READING SESSION 11.30 - 1.00 p.m

Theme: **BASE METAL DEPOSITS AND GEOLOGY OF BALUCHISTAN.**

Chairman: WAHEEDUDIN AHMED, G.S.P., QUETTA.

11. Rehanul Haq Siddiqui, Jan Mohammad Mengal, & Heshamul Haque; G.S.P., Quetta: Paragenetic and petrochemical study of phyllic alteration of Dashte Kain porphyry copper-molybdenum prospect, Baluchistan, Pakistan.

12. S. Iqbal Ali, Resource Development Corporation, Saindak; & Wazir Khan, Geological Survey of Pakistan, Quetta; & Centre of Excellence in Mineralogy, Quetta: Alteration zoning in polymetallic deposit, Saindak, Chagai District, Baluchistan, Pakistan.

13. Rehanul Haque Siddiqui, Syed Anwer Hussain & Munirul Haque; Geological Survey of Pakistan, Quetta: Geology and petrography of Eocene mafic lavas of Chagai island arc, Baluchistan, Pakistan.

LUNCH BREAK 1.00 - 3.00 p.m.

SCIENTIFIC PAPER READING SESSION 3.00 - 5.00 p.m.

Theme: **SEDIMENTARY MINERALS AND STRATIGRAPHY OF PAKISTAN.**

Chairman: CH. MOHAMMAD NASEEB, D. MIN. DEV. LAHORE & M. AZAM MALIK, O.G.D.C., ISLAMABAD.

14. Aftab Ahmad Butt, Punjab University, Lahore: The Palaeogene stratigraphy of the Kala Chitta Range, northern Pakistan.

15. Akhtar Mohammad Kassi, Abdul Salam Khan & Abdul Haque, University of Baluchistan, Quetta: Petrology and provenance of Siwaliks of Kach and Zarghun areas, northeast Baluchistan.

16. Aftab Ahmad Butt, Punjab University, Lahore: Some observations on the genus Ranikothalia.

17. Syed Afzal Ahmad, & Mohsin Anwar Kazim; Geological Survey of Pakistan, Quetta: Geology of coal bearing "Ghazij Formation" of Mach area, Baluchistan, Pakistan.

18. M. Khurshid Khan Raja, A.J.K. University, Muzaffarabad: General geology and petrography of Cham Traran area, Jhelum Valley, Muzaffarabad, Azad Kashmir.

19. Jan Muhammad, & Malik Abdul Hafeez; Geological Survey of Pakistan, Quetta. Geology of Kalat area, Baluchistan, Pakistan.

20. **TEA BREAK** 5.00 - 5.30 p.m.

Theme: **OPHIOLITES OF PAKISTAN.**

SCIENTIFIC PAPER READING SESSION 5.30 - 7.00 p.m.

Chairman: MAHMOODUD DIN AHMAD SIDDIQUI, G.S.P., QUETTA.

21. S. Ghazanfar Abbas; Geological Survey of Pakistan, Quetta. Chromite deposits of Muslimbagh ophiolites.

22. Zulfiqar Ahmed, Centre of Excellence in Mineralogy, Quetta: Compositions of pyroxenes and pyroxenite dykes from the Sakhakot-Qila ophiolite, Malakand Agency, Pakistan.

DINNER 7.30 p.m.

HOSTED BY: CENTRE OF EXCELLENCE IN MINERALOGY.

FRIDAY OCTOBER 23, 1987.

GEOLOGICAL FIELD EXCURSION:

START UNIVERSITY OF BALUCHISTAN, QUETTA 8.00 a.m.
MANGOCHER TOWN
KOHI MARAN FLUORITE DEPOSITS & MINES OF BALUCHISTAN DEVELOPMENT AUTHORITY,
LUNCH DURING FIELD WORK
KALAT (TEA : COURTESY: PAKISTAN NATIONAL CENTRE, KALAT).
STAY AT KHUZDAR
DINNER (COURTESY : BOLAN MINING ENTERPRISES).

SATURDAY OCTOBER 24, 1978.

GEOLOGICAL FIELD EXCURSION:

START KHUZDAR ENGINEERING COLLEGE 9.00 a.m.
BARITE MILL AT BOLAN MINING ENTERPRISES
GUNGA BARITE DEPOSIT
SURMAT LEAD–ZINC GOSSANS
SHEKRAN LEAD–ZINC GOSSANS
STAY AT KHUZDAR
DINNER 8.00 p.m.
(HOSTED BY CENTRE OF EXCELLENCE IN MINERALOGY)

SUNDAY OCTOBER 25, 1987.

GEOLOGICAL FIELD EXCURSION:

START KHUZDAR ENGINEERING COLLEGE 9.00 a.m.
KHUZDAR - NAL ROAD SECTION
OPHIOLITIC ROCKS SECTION
LUNCH AT NAL
FIELD EXCURSION WEST OF NAL
STAY AT KHUZDAR
DINNER 8.00 p.m.
(HOSTED BY CENTRE OF EXCELLENCE IN MINERALOGY)

MONDAY OCTOBER 26, 1987.

GEOLOGICAL FIELD EXCURSION:

START KHUZDAR ENGINEERING COLLEGE 9.00 a.m.
ROAD TO PIR UMAR REST HOUSE AND WAD
RODINGITES AND LIMESTONES SOUTH OF WAD
PLAGIOGRANITES AT PURWAIT BHUT
ORNACH - CROSS ULTRAMAFIC ROCKS
CHROMITE MINES AT BARAN LAK
MAGNESITE DEPOSITS/ASBESTOS LOCATIONS
SONARO
LUNCH AT ROADSIDE HOTEL
BORA JHAL PILLOW LAVAS AND SHEETED DYKES
KARARO REST HOUSE
NIMMI JHAL
RETURN TO KHUZDAR
DINNER BY CENTRE OF EXCELLENCE IN MINERALOGY 9.00 p.m.

GEOLOGICAL FIELD EXCURSION:
RETURN FROM KHUZDAR TO QUETTA
HANNA LAKE VISIT
BREWERY-GORGE SECTION
DINNER AT QUETTA 8.00 p.m.
(HOSTED BY CENTRE OF EXCELLENCE IN MINERALOGY)

WEDNESDAY OCTOBER 28, 1987.

DEPARTURE OF THE DELEGATES.

ABSTRACTS

Themes of sessions portray a diversity of topics. Three out of five gas fields of Marri Bugti Agency possess 6.5 trillion cubic feet reserves likely to be revised upwards from their reservoirs in Upper Cretaceous - Lower Tertiary clastics and carbonates (Azam Malik). The Baluchistan Province is divisible into five plate tectonic units: volcano-plutonic arc of Chagai; arc -trench system of Kharan -Makran region; Chaman strike-slip zone; ophiolitic zone; and, continental shelf of Pakistani plate (Abdul Farah). Gravity, magnetic and resistivity surveys of lead-zinc deposits of Besham area yielded low geophysical signals, but were typified accumulatively and useful in demarcating ore zones which occur in places of low gravity and low magnetic relief around structurally weaker zones (M. Ali et al.). A new occurrence of pink zoisite, thulite, was reported from Nomal from calc-silicate pockets in quartz veins in granodiorite (T. Khan *et al.*). The phyllic alteration sequence in tonalite porphyry at Deshte Kain Cu-Mo prospect is due to Si- and K- metasomatism (R.H. Siddiqui *et al.*). The sulphide mineralization at Saindak polymetallic deposit is related to hydrothermal alteration; and K-silicate alteration correlates with high Cu content (S.I. Ali).

The geology of Kala Chitta Range, which evolved from Early Mesozoic till Miocene, integrates with adjacent regions with small differences. The major Cenomanian–Turonian regression, and Coniacian-Campanian transgression in north caused epidiagenetic changes in lower Cretaceous rocks and secondary porosity in sandstone. Another regression in Late Cretaceous formed residual deposits over micritic Kawagarh Formation; and a transgression during Thanetian deposited shallow shelf carbonates. Marine deposition in Kala Chitta Range stopped from Late Eocene to Oligocene; and in Miocene it formed hinterland to adjacent Potwar basin (A.A. Butt).

Lithic- arenites and calc-lithites identified in Siwaliks, derived detritus from nearby mountains (Kassi *et al.*). The Nummulitid genus Ranikothalia from Upper Palaeocene of Pakistan and its significance in the Palaeocene stratigraphic correlation scale was highlighted (A.A. Butt).

For finding new chromite ore bodies in the Muslimbagh ophiolite, it was suggested to prospect within dunites along the hinges of isoclinal folds. This ophiolite, underlain by melange, was emplaced in Palaeocene or Early Eocene (S.G. Abbas). The Sakhakot-Qila ophiolite has strongly magnesian ultramafites with certain unique features in pyroxenes and pyroxenites (Z. Ahmed).

Studies were presented on heavy minerals in sands of Makran Coast showing variations in grain size, sorting and petrography (M.A. Chaudhry & Q. Memon); on engineering characteristics of soils from Karachi city (M. Arshad & S.A. Sheikh); on basaltic flows overlying Eocene pryoclastics of Chagai arc (R.H. Siddiqui *et al.)*; on 18 coal seams in Eocene shales near Mach with lignitous to subbituminous coals deposited under swampy to shallow marine conditions (S.A. Ahmed & M.A. Kazmi); and on regional geology of parts of Azad Kashmir (M.K.K. Raja) and Kalat (J. Muhammad & M.A. Hafiz).

Certain unique geological features of Makran region showed up by effective application of satellite imageries which surpass conventional geological methods in utility (S.A.K. Alizai).

RECENT ADVANCES IN MARINE GEOLOGY

ABUL FARAH
National Institute of Oceanography, Karachi.

STUDY OF HEAVY MINERALS CONCENTRATION ALONG THE BALUCHISTAN COAST, PAKISTAN, FROM GADANI TO PHORNALA

M. AKRAM CHAUDRY AND QASIM MEMON
National Institute of Oceanography, Karachi.

Sorting and concentration of a variety of heavy minerals along the coast between Gadani and Phornala, Baluchistan, are facilitated by the coincidence of the periods of maximum turbulence and wave activity, maximum precipitation and sediment discharge. Sediments samples from different intertidal zones between Gadani and Phornala were collected for grainsize analysis and petrographic/petrological study. Variations in grain size and mineral assemblage in the intertidal zones have been noted in fine grained sediments; light coloured minerals are rather ubiquitous. The sediments exhibit wide range of sorting, poor to very well.

ENGINEERING CHARACTERISTICS OF SOIL OF WEST WHARF AND PORT TRUST AREAS, KARACHI.

MUHAMMAD ARSHAD
Institute of Geology, University of Azad Jammu & Kashmir, Muzaffarabad
AND
SHAMIM AHMED SHEIKH
Department of Geology, University of Karachi, Karachi.

Engineering characteristics of soils and subsoils of West Wharf and Karachi Port Trust areas have been investigated to evaluate the suitability of these soils and subsoils for civil engineering structures and designing of foundations of these structures. The study also includes the evaluation of safe bearing capacity of these soils. The study was based on the analyses of distrubed and undisturbed samples collected from ten different boreholes at different depths.

It is concluded that deeper pile foundations shall be more suitable for the construction of huge structures (high rise buildings) in this area. It is recommended that piles of 66 cms diameter and 15 m depth would carry a safe working load of 90 tons and for 48 cms diameter, 13 metres deep piles are required to carry a safe working load of 39 tons. Hence the design of foundations should be computed to carry safe working load conditions.

USE OF SATELLITES IMAGERY FOR GEOLOGICAL MAPPING IN THE COASTAL MAKRAN REGION OF PAKISTAN.

S.A.K. ALIZAI
Remote Sensing Applications Centre, SUPARCO, Karachi.

Satellites imagery provides a view of the Earth's surface which gives more detail of landforms and regional physiography than a topographic map of the same scale. Over large areas, this information can be used together with geological maps to provide a new method of viewing features important in defin-

GEOLOGY AND GAS RESOURCES OF MARRI BUGTI AGENCY

ARIF KAMAL AND M. AZAM MALIK
Oil & Gas Development Corporation, Islamabad, Pakistan.

The largest gas production of the country comes from Marri Bugti Agency in Eastern Baluchistan. Out of five known gas fields namely Sui, Zin, Uch, Pirkoh and Loti; the latter two fields were discovered by OGDC while the former three were found by Pakistan Petroleum Ltd. OGDC is actively developing Pirkoh, Loti and Uch --- till recently a dormant gas field. The cumulative recoverable gas reserves of these three fields have been estimated to be of the order of over 6.5 trillion cubic feet; but subsequently the estimates would rise as additional data after drilling more appraisal wells become available. It is firmly believed that the region as a whole still holds significant gas potential, tapping of which must await establishment of requisite infrastructure.

The current gas production from Pirkoh is about 95 MMCF/day and efforts are well underway to bring it upto 250 MMCF/day mark from 40 wells in two years time. Loti gasfield is also being rapidly developed to meet the committed target of 40 MMCF/day supply to Sui Northern Gas Pipelines Ltd. Additional gas could be delivered to supply transmission system by coming on stream of Uch field. The reservoirs are Upper Cretaceous and Lower Tertiary clastics and carbonates. The traps are structural as well as composite structural-stratigraphic.

A major thrust has been mounted by OGDC for speedy exploitation of gas resources of the region which would result in improvement of overall gas supply position of the country as a whole. OGDC has also been instrumental to a large measure in bringing about socio-economic development of Marri Bugti Agency.

This paper presents geology, prospect potential and technical aspects of exploratory and development operations. It also highlights the measures adopted by OGDC for the welfare of the local inhabitants.

PLATE GEOLOGY AND MINERAL DEPOSITS OF BALUCHISTAN, PAKISTAN

ABUL FARAH
National Institute of Oceanography, Karachi.

Baluchistan possesses an excellent and outstanding geological scenario where various principles and tenets of the theory of "plate tectonics" can be studied and tested and the natural resources potential be assessed. The concept of plate movement and interaction popularly known as "plate tectonics" has developed during the last two decades and is being vigorously pursued to understand and explore man's own habitat. This concept purports to provide a single framework in which we can explain such diverse phenomena as mountain building, volcanism, past climate, the youth of ocean floors (less than 200 million years), pulsation of the Earth in the form of earthquakes and the distribution of Earth's mineral and energy resources.

In Baluchistan five main units in the framework of plate tectonics can be identified --- (1) Volcano-plutonic arc of Chagai; (2) Arc-trench system of Kharan-Makran region; (3) Chaman strike slip zone; (4) Zone of ophiolites; and (5) Continental shelf of Pakistani plate. In this paper, these units have briefly been described and their mineral potential discussed.

RECENT ADVANCES IN MARINE GEOLOGY

ABUL FARAH
National Institute of Oceanography, Karachi.

STUDY OF HEAVY MINERALS CONCENTRATION ALONG THE BALUCHISTAN COAST, PAKISTAN. FROM GADANI TO PHORNALA

M. AKRAM CHAUDRY AND QASIM MEMON
National Institute of Oceanography, Karachi.

Sorting and concentration of a variety of heavy minerals along the coast between Gadani and Phornala, Baluchistan, are facilitated by the coincidence of the periods of maximum turbulence and wave activity, maximum precipitation and sediment discharge. Sediments samples from different intertidal zones between Gadani and Phornala were collected for grainsize analysis and petrographic/petrological study. Variations in grain size and mineral assemblage in the intertidal zones have been noted in fine grained sediments; light coloured minerals are rather ubiquitous. The sediments exhibit wide range of sorting, poor to very well.

ENGINEERING CHARACTERISTICS OF SOIL OF WEST WHARF AND PORT TRUST AREAS, KARACHI.

MUHAMMAD ARSHAD
Institute of geology, University of Azad Jammu & Kashmir, Muzaffarabad
AND
SHAMIM AHMED SHEIKH
Department of Geology, University of Karachi, Karachi.

Engineering characteristics of soils and subsoils of West Wharf and Karachi Port Trust areas have been investigated to evaluate the suitability of these soils and subsoils for civil engineering structures and designing of foundations of these structures. The study also includes the evaluation of safe bearing capacity of these soils. The study was based on the analyses of disturbed and undisturbed samples collected from ten different boreholes at different depths.

It is concluded that deeper pile foundations shall be more suitable for the construction of huge structures (high rise buildings) in this area. It is recommended that piles of 66 cms diameter and 15 m depth would carry a safe working load of 90 tons and for 48 cms diameter, 13 meters deep piles are required to carry a safe working load of 39 tons. Hence the design of foundations should be computed to carry a safe working load conditions.

USE OF SATELLITES IMAGERY FOR GEOLOGICAL MAPPING IN THE COASTAL MAKRAN REGION OF PAKISTAN.

S.A.K. ALIZAI
Remote Sensing Applications Centre, SUPARCO, Karachi.

Satellites imagery provides a view of the Earth's surface which gives more detail of landforms and regional physiography than a topographic map of the same scale. Over large areas, this information can be used together with geological maps to provide a new method of viewing features important in defin-

ing structural and petrological regions.

Dominant rock types can be distinguished by their shape and character, while faults, folds lineaments, sedimentary and geomorphic patterns can be mapped accurately over large areas. This ability together with the physiographic and geologic deails can be of great importance in mineral exploration.

The extent to which satellites imagery could be used in mapping geological phenomena of coastal Makran region of Baluchistan has been investigated. Geological interpretation of the study area was carried out using standard photointerpretation techniques. The results of this study have demonstrated that satellites imagery is an effective tool in mapping geological structures as well as geological phenomena.

GEOPHYSICAL STUDY OF LEAD-ZINC DEPOSIT OF BESHAM AREA.

MUBARIK ALI, A.A. KHAWAJA, ZULFIQAR AHMAD, JUNAID AKHTAR,
KH. MAZHARULHAQ AND EHSAN FRAZ
Department of Earth Sciences, Quaide Azam University, Islamabad.

The Pb-Zn prospect of Lahor- Serai area of Besham encompasses an area of about 150,000 sq. metres. The small surface exposures of the ore are found at the northern and southern ends, while the intervening area is mostly covered by overburden. For searching the promising sites of subsurface ore the geophysical investigations were carried out using gravity, magnetic and electrical resistivity methods. As the ore deposit makes small volume fraction of the host rock, and the structural/lithologic complexities are dominant, the intensity of geophysical signal is found very low. However, the nature of signals generated in all the three methods over the ore outcrops were typified in an accumulative sense, and have been used as correlators for the demarcation of promising zones. The results suggest that the places of low gravity and low magnetic relief around structurally weaker zones may be the ore-bearing sites. The sites which had been recommended previously as ore-bearing ones, but proved unsuccessful in later drilling, trenching, and aditing are associated contrarily with gravity and magnetic highs.

THE COUNTRY ROCK IN PEGMATITIC AREA OF EVJE-IVELAND, SOUTHERN NORWAY.

SHARJIL AHMAD KHAN LODHI
Glass & Ceramics Division, P.C.S.I.R. Laboratories, Lahore.

The country rock in pegmatitic area of Evje-Iveland, southern Norway, was supposed to be a strongly banded amphibolite. In this study, the bands are classified into mela-, intermediate- and leuco-bands. Petrographic and geochemical data on these bands have been used to decipher their probable mode of origin. It is concluded that the mela-bands are derived from the medium grade metamorphism of the norite during the first period of deformation. In the second period of deformation, when the metamorphism was in its full swing and the foliation planes were developing, intruded along these foliation planes some melts of acidic composition and thus formed the intermediate- bands. After that when the metamorphism was descending intruded along the foliation planes again to new melts and thus formed the leuco-bands. Therefore, the amphibolite must now be called as injection migmatite as the country rock of the pegmatites.

PINK ZOISITE (THULITE) OCCURRENCE AT NOMAL, DISTRICT GILGIT, PAKISTAN.

TEHSEENULLAH KHAN, IMTIAZ ALI, REHANULHAQUE SIDDIQUI
AND
HAIDER KAMAL
Geological Survey of Pakistan, Quetta.

Pink zoisite (thulite) mineralization has been located in hydrothermal calc-silicate rock pockets of varied size within the quartz vein traversing the granodiorite stock. Petrographic and chemical studies have been conducted on the calc-silicate and the pink zoisite. The pinkish colour of the zoisite is due to the presence of Mn as in manganic oxide. Owing to the poor quality and quantity of the pink zoisite of Nomal, the exploitation of the pinkish mineral for the gemstone purposes can be ruled out. However, detailed investigation to locate better prospects of pink zoisite in the Nomal area is recommended.

PEGMATITIC ALBITITES AND APLITES OF MANSEHRA AREA, N.W.F.P., AS INDIGENOUS RAW MATERIALS FOR POTTERYWARES (CORNISH STONE).

M. AYUB, M. YUSUF, S.A.K. LODHI
Glass & Ceramics Division, P.C.S.I.R. Laboratories, Lahore.
AND
MOHAMMAD ASHRAF
Institute of Geology, A.J.K. University, Muzaffarabad.

Various samples were collected from Mansehra area of N.W.F.P. It was found that only pegmatitic albitites, albite-aplites and albite-microcline-aplites were the rocks suitable for making potterywares. For this purpose petrographic and chemical analyses were carried out. The materials were crushed and various compositions were prepared and their firing behaviour were studied. Owing to the simple compositions and less iron, these rocks were found most suitable for the manufacture of pottery, tiles, glazes, etc. in conjunction with pottery clay.

PARGENETIC AND PETROCHEMICAL STUDY OF PHYLLIC ALTERATION OF DASHTE KAIN PORPHYRY COPPER-MOLYBDENUM PROSPECT, BALUCHISTAN, PAKISTAN.

REHANUL HAQ SIDDIQUI, JAN MUHAMMAD MENGAL,
AND
HESHAMUL HAQUE
Geological Survey of Pakistan, Quetta.

At Dashte Kain, a newly discovered porphyry copper-molybdenum prospect, phyllic alteration is mainly developed in two comagmatic tonalite porphyry stocks. The following paragenetic sequence is suggested for phyllic alteration in the western tonalite porphyry stock:

> Sericite and quartz (quartz continuous throughout the course of alteration) kaolinite anhydrite and calcite.

Petrological and petrochemical study of phyllic alteration suggests that Si- and K-metasomatism was mainly involved in the process of phyllic alteration.

ALTERATION ZONING IN POLYMETALLIC DEPOSIT AT SAINDAK, CHAGAI DISTRICT, BALUCHISTAN, PAKISTAN.

S. IQBAL ALI
Resource Development Corporation, Saindak.
AND
WAZIR KHAN
Geological Survey of Pakistan, Quetta.

The prophyry copper deposit of Saindak in the northwestern extremity of Chagai calc-alkaline belt is limited to three ore bodies, namely East, North and South ore bodies, in tonalite porphyry and siltstone of Miocene. 75 core samples were collected from these 3 bodies and polished thin sections were prepared for detailed ore microscopy. On the basis of microscopic studies, relationship between hydrothermal alteration and sulphide/magnetite mineralization was established.

Four types of hydrothermal alterations --- propylitic, sericitic-quartz, retrosericitic and potassic silicate were recognized. It has been observed that a perfect correlation exists between K-silicate alteration and high grade of Cu mineralization in all of the three ore bodies. Chalcopyrite is the major Cu-bearing mineral. Bornite occurring as large inclusions and free grains is associated with chalcopyrite in the extreme potassium silicate alteration stage.

Chalcopyrite occurs mainly as disseminated grains with subordinate amounts in veinlets, and pods form within K-silicate alteration zones. The pyrite occurring as disseminations is lesser in amount as compared to its quantity in the form of pods and veinlets within K-silicate alteration zone/zones in all the three ore bodies. Chalcopyrite is generally intergrown with non-opaque silicates, whereas pyrite has no common intergrowth with these silicates.

Significant quantities of magnetite are associated with K-silicate alteration zone in South ore body, while the East ore body contains minor magnetite. An inverse relationship exists between pyrite and magnetite in all the three ore bodies.

Retro-sericitic alteration is confined only to the East ore body and covers a considerable part of alteration. It superimposes the biotitized zone and/or K-silicate alteration. Chalcopyrite has intergrown with sericite and chlorite.

Gold occurs as independent phase and was observed only in two samples.

GEOLOGY AND PETROGRAPHY OF EOCENE MAFIC LAVAS OF CHAGAI ISLAND ARC, BALUCHISTAN, PAKISTAN.

REHANUL HAQ SIDDIQUI, SYED ANWER HUSSAIN & MUNIRUL HAQUE
Geological Survey of Pakistan, Quetta.

Two basaltic lava flows are found towards the top of the lower pyroclastic sequence of Saindak Formation of Eocene age, which occur at about 15 km NW of Amalaf. Both the flows are elongated in NW-SE direction and crop out for more than 6 km. The older or earlier flow is about 100 m thick and extends upto 2 kms. The younger flow is upto 700 kms thick and extends beyond 6 kms. Both the flows are transected by numerous ENE trending strike-slip faults and are slightly folded.

The flows are dark brown to black and weather brown to maroon. These are fine grained merocrystalline, porphyritic and amygdaloidal in nature. Under microscope, flows are vitrophyric to subpilotaxitic and cumulophyric. Subautoclastic texture is also developed in the younger flow. Clusters of plagioclase phenocrysts and isolated phenocrysts of clinopyroxene are embedded in micro- to cryptocrystalline and devitrified groundmass. Labradorite is the main plagioclase accompained by minor andesine and bytownite. Clinopyroxene is generally represented by augite and minor diopside. Vesicles are generally filled with zeolites, chlorites, chalcedony, quartz, malachite, and occasionally with palagonite. Apatite, ilmenite and magnetite are common accessories. Uralite and chlorite are the major alteration products of pyroxene, whereas plagioclase exhibits minor argillization and sericitization. Magnetite is partially limonitized.

THE PALEOGENE STRATIGRAPHY OF THE KALA CHITTA RANGE, NORTHERN PAKISTAN.

AFTAB AHMAD BUTT
Institute of Geology, University of the Punjab, Lahore-20.

The Kala Chitta Range forms the northern edge of the Potwar Basin. It is a narrow strip of mountainous region which merges laterally into the Hazara Mountains (including Margala Hills north of Islamabad) towards the eastern direction, and extends westward into the Samana Range (the main towns located are Hangu and Kohat).

The geology of the Kala Chitta Range is an integral part of the structural units of the Kohat-Potwar-Hazara region, northern Pakistan. The sedimentary geology of the Kala Chitta Range has similarities with the adjoining areas. However, there are certain differences in stratigraphy and the geological history. The structural evolution of the Kala Chitta Range appears to have originated at the beginning of the Mesozoic and continued to develop till the Miocene. A major geological event is recorded during the Upper Cretaceous when the deposition of the Kawagarh Formation (Coniacian - Campanian) is confined to the northern part of the Kala Chitta Range. This draws attention towards draining off the sea as a major regression during the beginning of the Upper Cretaceous (Cenomanian - Turonian), while a more northerly transgression happens from Coniacian and continuing upto the Campanian to deposit the Kawagarh Formation into a narrow belt. This event exposes the Lower Cretaceous Lumshiwal Formation for a sufficient period (Cenomanian - Turonian) in northerly Kala Chitta and the entire Upper Cretaceous in the main Kala Chitta Range) for epidiagenetic changes which could have produced secondary porosity in the sandstone to improve its petrophysical characters.

The Late Cretaceous (Maastrichtian) marks a major regressive episode during which time the formation of the residual deposits "the ferruginous pisolite" over the micritic Kawagarh Formation occurs till the next major transgression during the Upper Palaeocene (Thanetian) - the time of the deposition of the shallow shelf carbonates, the Lockart Limestone. A careful persual of the K-T boundary points out the absence of the basal Paleocene (Danian) Hangu Formation.

The Upper Paleocene stratigraphy demonstrates deposition of dominant interbedding of shale and limestone causing difficulty in recognition of two-fold Upper Paleocene strata into the Lockart limestone and the Patala Formation. There is a continuity in the stratigraphy and palaeogeography across the Paleocene - Lower Eocene boundary. However, the beginning of the Middle Eocene brings a new geological setting of dominantly non-marine conditions restricting the deposition to the more southerly part of the Kala Chitta Range, which typifies the Red-Bed facies- the Kuldana Formation. The onset of Middle Eocene is reversed to the normal marine shallow shelf conditions in the same limited paleogeographic setting by laying typical Nummulitic bank beds - the Kohat Formation.

The Late Eocene and the entire Oligocene mark the end of the marine deposition in the Kala Chitta Range and this is a major geological event in the basinal history of the Kala Chitta Range when the entire area is completely drained off and brings an end to the maximum structural evolution of the range.

The Miocene characterises the Kala Chitta Range as a hinterland to the adjacent Potwar basin of active fluviatile deposition and the Kala Chitta Range is thus developed into a marginal rim of these deposits.

PETROLOGY AND PROVENANCE OF SIWALIKS OF KACH AND ZARGHUN AREAS, NORTHEAST BALUCHISTAN.

AKHTAR MOHAMMAD KASSI, ABDUL SALAM KHAN & ABDUL HAQUE
Department of Geology, University of Baluchistan, Quetta.

Thin sections of coarse clastic rocks especially sandstones of the Nagri and Dhok Pathan Formations of Kach area and the Soan Formation of Zarghun area were studied by polarizing microscope in order to identify the types of mineral constituents and rock fragments and to mutually compare and classify them. Most of them may be classified as lithic arenites and/or calclithites. Although the types of mineral and rock constituents in sandstones of the Nagri, Dhok Pathan and Soan formations are comparable, their proportions vary in different formations. It is proposed that detritus of the "Siwalik Group" in Kach area has been derived from a terrain where sedimentary, igneous and metamorphic rock fragments were available for denudation and transportation. The nearby mountain ranges are capable of providing similar detritus and the notion is supported by palaeocurrent patterns.

SOME OBSERVATIONS ON THE GENUS RANIKOTHALIA

AFTAB AHMAD BUTT
Institute of Geology, University of the Punjab, Lahore-20.

Cavelier and Pomeral (1986; see also 1983) have presented a stratigraphic correlation scale of the Paleogene stratigraphy by combining together the most valuable data of various fossil groups. It includes a column highlighting the significance of a stratigraphic distribution of the Nummulites zones and other larger foraminifera. In this column the absence of the genus Nummulites in the entire Paleocene has been brought to attention. In the present opinion, the value of the correlation would be further enhanced if the stratigraphic value of the genus Ranikothalia is taken into account.

The genus Ranikothalia is very closely related to Nummulites but it can be distinguished on account of its thick, fan-shaped marginal cord. Stratigraphically, the genus Ranikothalia (originally erected from the Upper Paleocene Ranikot beds of Sind, Lower Indus Basin, Pakistan) characterises the Upper Paleocene succession of Pakistan and elsewhere in the world. However, it does extend into the Lower Eocene. Although several species have been recorded in the literature, but a closer examination leads to conclude that the majority would be grouped into what would be identified as Ranikothalia sindensis, which essentially exhibits a complanate test.

From Pakistan, its occurrence in the Upper Paleocene (Thanetian) succession has been recorded from the stratigraphic units of the Lockhart Limestone and the Patala Formation (northern Pakistan) and the Upper Ranikot Formation of Sind, southern Pakistan. Its occurrence in the Lower Eocene Margala Hill Limestone has been noted from Hazara and the Kala Chitta Range (northern Pakistan). It would be appropriate to add this stratigraphically important Nummulitid form in the column for further elaborating the Paleogene stratigraphic correlation scale.

GEOLOGY OF COAL-BEARING "GHAZIJ FORMATION" OF MACH AREA, BALUCHISTAN, PAKISTAN.

SYED AFZAL AHMAD AND MOHSIN ANWAR KAZIM
Geological Survey of Pakistan, Quetta.

The Mach area lies about 62 kms southeast of Quetta. The rock formations ranging in age from Late Jurassic to Pleistocene are exposed. The formation is mainly composed of limestone, shale, sandstone, conglomerate, gypsiferous clays and muds. The coal-bearing horizon is restricted within the middle unit of Ghazij Formation of Eocene age, which is mainly comprised of shale and sandstone with subordinate limestone and siltstone. The coal seams range in thickness from 2.5 to 152 cms. The lateral continuity is disurbed structurally. In the Bore area, 3 km southeast of Mach, the coal seams are regular and parallel to bedding. In this area about 18 coal seams are present and only 4 coal seams are presently being mined. The chemical analyses of coal shows the carbon content ranges from 19 to 43% and averages about 33.4% which falls within the lignite to subbituminous grade. The proved coal reserves of Bore area are about 5 million tons. The environmental condition for the deposition of coal is suggested as shallow marine and swampy.

GENERAL GEOLOGY AND PETROGRAPHY OF CHAM TARARAN AREA, JHELUM VALLEY, AZAD KASHMIR.

M. KHURSHID KHAN RAJA
Institute of Geology, University of Azad Jammu & Kashmir, Muzaffarabad, A.J.K.

A geological map of the Cham Traran area, Jhelum Valley, near Muzaffarabad is prepared at a scale of 1:50,000 and a detailed description of the various rock units is given. The rocks exposed cover pelitic-psammitic, calcareous and carbonaceous rock sequence of typical Salkhala Formation intruded by Sari Nangatak granite gneiss. Basaltic to andesitic Panjal Formation is thrusted over the Precambrian Salkhala Formation and overridden by the Tertiary Murree Formation. Petrography of each rock unit is made. The conclusion drawn from mineral assemblages of the Salkhala Formation is that it comprises low grade metamorphites. Presence of gypsum and calcareous bands in deformed graphitic schist within the formation is indicative of shallow marine environment. The Panjal formation is of subaerial to submarine origin, while the Murree Formation is of molasse type deposits. Economic geology of the area is also outlined.

GEOLOGY OF KALAT AREA, BALUCHISTAN, PAKISTAN.

JAN MUHAMMAD AND MALIK ABDUL HAFIZ
Geological Survey of Pakistan, Quetta.

Rocks from Jurassic to Eocene age are present in the area. A new group, Kalat Group, is proposed after the Kalat town on RCD Highway to replace those rocks mapped by Hunting Survey Corporation (1960) as Shirinab Formation and Chiltan Limestone. The group is divisible into 3 rock units. The upper unit is named as the Anjira Formation of Middle Jurassic age. The middle unit is named as the Garrari formation of Lower to Middle Jurassic age while the lower unit is named as the Shirinab formation of Lower Jurassic age.

Faunas collected from the Kalat Group indicate that the Garrari formation occupies lower position than the Chiltan Limestone. The lithological studies of the Group shows that there is a facies change from Khuzdar to Kalat as the Ferozabad Group (Fatmi, 1986) of the same age does not correlate with this Kalat Group. An active fault, the Kalat Namatave fault is observed which trends almost N-S and transects the Quaternary alluvium besides other older rocks. The fault is left-lateral and has a displacement of about half km.

The destruction caused by the 1935 earthquake in the Kalat area is thought to be due to this fault.

CHROMITE DEPOSITS OF MUSLIM BAGH OPHIOLITES, PAKISTAN.

S. GHAZANFAR ABBAS
Geological Survey of Pakistan, Quetta

Eversince Pakistan came into existence, Muslim Bagh ophiolites have remained the largest producer of chromite in this country. Ultramafic tectonites and ultramafic cumulates of Muslim Bagh ophiolites have produced over one million tons of metallurgical grade ore.

Muslim Bagh ophiolites are the most complete ophiolite suite of rock described from Pakistan. These ophiolites are underlain by tectonic silvers of garnet amphibolite, green schist, ophiolitic melange and melange with highly sheared shale matrix. The oldest rocks found in melage are of Maestrichtian age. Early Middle Eocene Limestone unconformably overlies these ophiolites. This suggests emplacement in Paleocene or early Eocene. The ophiolites consist of ultramafic tectonites, ultramafic and mafic cumulates and a sheeted dyke complex. Pillow lavas though not found in the normal sequence are found in the melange.

Chromite is found associated with dunites of ultramafic tectonites and cumulates. In tectonites, principal ore bodies occur along the hinges of the isoclinal folds. In ultramafic cumulates, extensive layers of chromitite form the ore bodies. Presently the production of chromite from the area has gone down to very low level because new ore bodies have not been found since long. A systematic analysis of the internal structures of tectonites may however, lead to discovery of new ore bodies.

COMPOSITIONS OF PYROXENES AND PYROXENITE DYKES FROM THE SAKHAKOT-QILA OPHIOLITE, MALAKAND AGENCY, PAKISTAN.

ZULFIQAR AHMED
Centre of Excellence in Mineralogy, University of Baluchistan, Quetta.

The whole-rock major-, trace- and rare earth-element analyses of the ophiolitic rocks of the sakhakot-Qila complex show that the rocks are highly magnesian, resembling other ophiolites. The ultramafic part is dominated by harzburgite with a restricted range in chemical composition. The chemical variations are small in the dunite and wehrlite as well, although an Fe-enrichment trend is present. The TiO_2 of ultramafic rocks is low and seldom exceeds 0.02 mass %; but the mafic rock units display enrichment in Ti and appearance of phases like ilmenite, Ti-rich brown hornblende and sphene. The ultramafic rocks lack anorthite but the norms show ubiquitously small amounts of An. Alkali metal contents are very low in ultramafic rocks and Na increases in preference to K in the mafic rocks. Ba, Sr, and Zr exhibit depletion in harzburgites, but increase towards the latter fractionates which have lower Cr, Ni and Co.

The pyroxene compositions for various lithological types have been determined and exhibit more magnesian orthopyroxenes than most known from ophiolites. Most pyroxenite dykes are highly magnesian like their surrounding harzburgites, dunites and wehrlites.The pyroxene compositions are also Mg-rich. An Fe-rich websterite displays post-gabbro evolution of minerals. It shows anomalously Fe-enriched and Mg-depleted composition. All of the minerals composing this Fe-websterite are uniquely Fe-rich. Its pyroxenes show more evolved composition on the quadrilateral diagram. The Cu increase in the Fe-websterite may be thought of as due to latter metasomatic effects, parallel to the high Cu contents in the associated metasomatized metadolerite dykes. However, the Fe-websterite has SiO_2, Cr, Co and Ni contents resembling other pyroxenites. There is also an indication that the Fe-websterite dyke represents a closed system evolution independent of the main magma chamber differentiation.

Varyingly metamorphosed dolerite dykes occur below the gabbro and carry metasomatic hydrogrossular veins with Cu-bearing borders.

ACTA MINERALOGICA PAKISTANICA
VOLUME 3 (1987) pp. 72 - 81

GEOLOGY AND GAS RESOURCES OF MARI-BUGTI AGENCY, PAKISTAN.

ARIF KEMAL & M. AZAM MALIK
Oil & Gas Development Corporation, Masood Mansion, Markaz, Sector F-8, Islamabad, Pakistan.

ABSTRACT: The cumulative recoverable gas reserves of Pirkoh, Loti and Uch gas fields are estimated at 6.5 trillion cubic feet, likely to be revised upwards. The reservoirs are the clastics and carbonates of Upper Cretaceous to Lower Tertiary age. OGDC is taking measures to step up the gas production and to develop the area socio-economically. Geology, prospect potential and exploratory and development operations of OGDC are discussed.

INTRODUCTION

Gas accounts for about 36% of Pakistan's total energy consumption. The increasing consumption of gas due to rapid industrial growth is constantly widening the demand and supply gap. With the object of meeting the shortfall, it is imperative to intensify the exploratory efforts and to expeditiously develop new fields in the gas prone regions of Central Pakistan.

The Mari-Bugti Agency, the most prolific gas producing region, has contributed over 69% of the total 402.5 billion cubic feet of gas produced in the country during 1986-87. Since 1952, five gas fields have been discovered in the agency, Sui being the first and largest discovery. Out of these fields, Pirkoh is the only field other than Sui presently on production stream. The factors prohibiting intensive exploratory efforts and rapid development of the gas resources of the Mari-Bugti Agency include remote and security-sensitive territory, rugged terrain, poor accessibility, logistic problems, scarcity of water and above all non-existence of requisite infrastructure for delivery of gas to the national transmission network.

Oil and Gas Development Corporation (OGDC) had been active in the area for over a decade. Apart from geological investigations seismic surveys, exploratory and development drilling has been carried out at Pirkoh, Loti and Uch fields. Presently 95 MMCF/day of gas is being produced from Pirkoh whereas 40 MMCF/day from Loti and an additional 85 MMCF/day from Pirkoh would be made available by June, 1988.

Present energy supply position in the country has brought about a growing realization to speedily tap and exploit Pakistan's gas resources. In this context, exploration and development activities in the Mari-Bugti Agency and the adjoining areas have gained immense importance. This paper highlights these activities with a general outlook for the future.

EXPLORATION HISTORY

Exploration in the Mari-Bugti Agency started a century ago when in 1886, the then Government of India drilled 13 shallow holes (46 metres) on a surface oil seepage at Khattan. The production was discontinued after obtaining nearly 20,000 barrels of oil essentially for economic reasons. Exploratory activities in the following years remained limited to geological investigations. After independence, Pakistan Petroleum Ltd. (PPL) drilled an exploratory well at Sui which resulted in a gas discovery in 1952. This was followed by two more gas discoveries, Zin (1954) and Uch (1955). No significant exploratory work was undertaken during succeeding eight years. OGDC was established as a public sector organisation in 1961 and just 2 years after its inception, it started geological investigations in the area in 1963.

FIG. No. 1

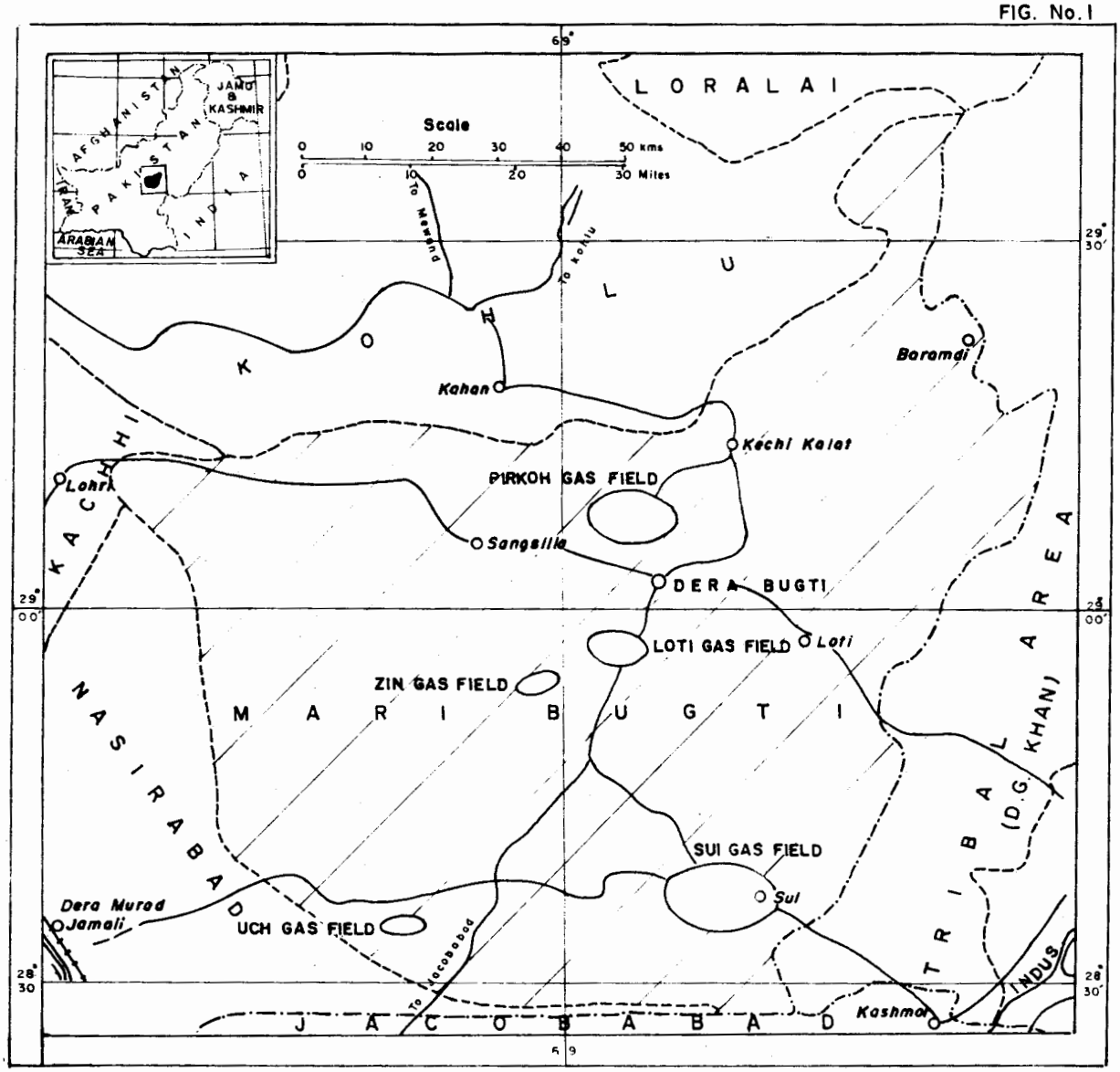

LOCATION MAP OF MARI-BUGTI AGENCY BALUCHISTAN

Further exploratory efforts remained suspended due to poor accessibility and security reasons. First ever seismic surveys in the area were conducted by OGDC using army helicopters in the mid seventies. As result of exploratory drilling, OGDC discovered the Pirkoh gasfield in 1977 and the Loti gasfield in 1985. To date about 1200 linear kms of 24 fold seismic data has been acquired by OGDC. Currently an appraisal well is being drilled at Uch.

GEOLOGY

Regional Setting

Within the context of the tectonic zonation of Pakistan, the Mari-Bugti area represents a transverse uplift lying between the Sulaiman and Kirthar Fold Belts. It exhibits stronger affinities with the Sulaiman Belt. Its rather anomalous E-W orientation has probably originated due to movements along the two transcurrent fault systems of the Sulaiman and Kirthar Fold Belts, having a general N-S alignment. The zone of foredeeps flanking the fold belts lies to the east-south and west of the uplift. Further south of the area, two parallel running Mari-Kandhkot and Jacobabad highs form prominent positive trends. To the northwest, the Mari-Bugti Uplift is limited by the deep Sibi Trough. The axial belt is located to the north where Upper Paleozoic and Mesozoic rocks are exposed (Andrieux and Maurice, 1977).

The overall tectonic evolution of Mari-Bugti Transverse Uplift is closely associated with that of the Sulaiman fold belt.

FIG. No. 2

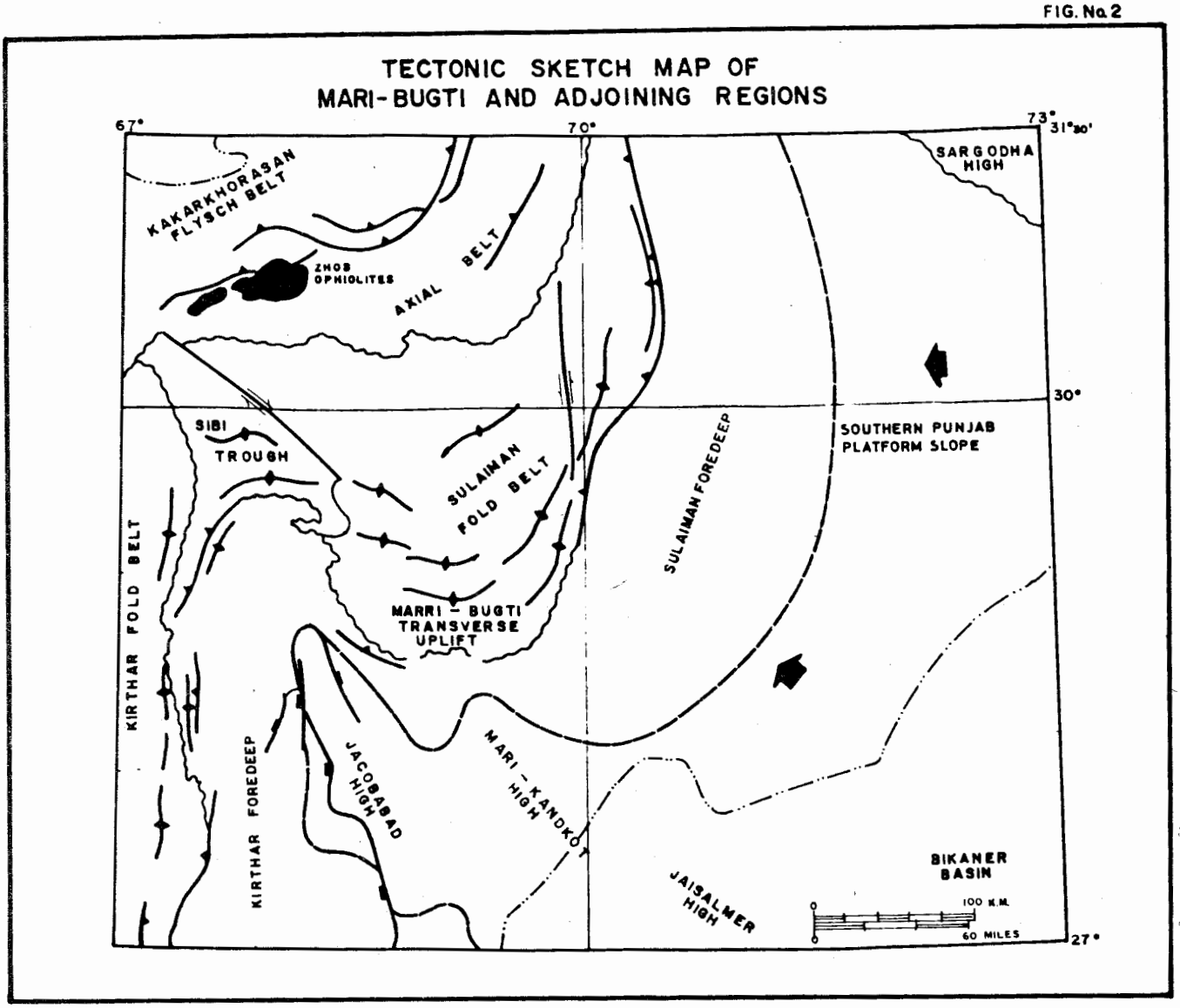

Outline of Depositional History

None of the wells in the region under discussion was drilled deep enoough to have reached Jurassic strata, however, to the north, in Kohlu Agency two wells, i.e. Jandran-1 and Tadri Main-1 drilled through a thick limestone section of the Upper Jurassic Chiltan Formation.

To begin with, the Chiltan Formation comprises massive, oolitic grey to brown dense limestone with subordinate shale and marl interbeds. These were laid down in shallow shelf environments. The contact with the overlying Lower Cretaceous Sembar Shales is disconformable. The prevailing conditions by Lower Cretaceous times had become restricted marine in nature. The succeeding Goru sequence of shales and marl indicate that the environment by then had turned open marine. These gave way to sedimentation of cream to light grey pelagic Parh Limestone. Towards early Campanian times conditions became suitable for shales, limestone and marl of the Mughalkot Formation deposited on a continental slope. The regressive trend caused shallowing of the sea making it favourable for development of shelf limestone of the Fort Munro Formation. Towards late Upper Cretaceous time, deltaic environments became prevalent, wherein Pab Sandstone was deposited. This regressive episode finally came to an end and the area became exposed to erosion by early Paleocene.

Next, the trangressive nature of the environments excercising their influence brought about the deposition of the reworked Pab clastics as

FIG. No. 3

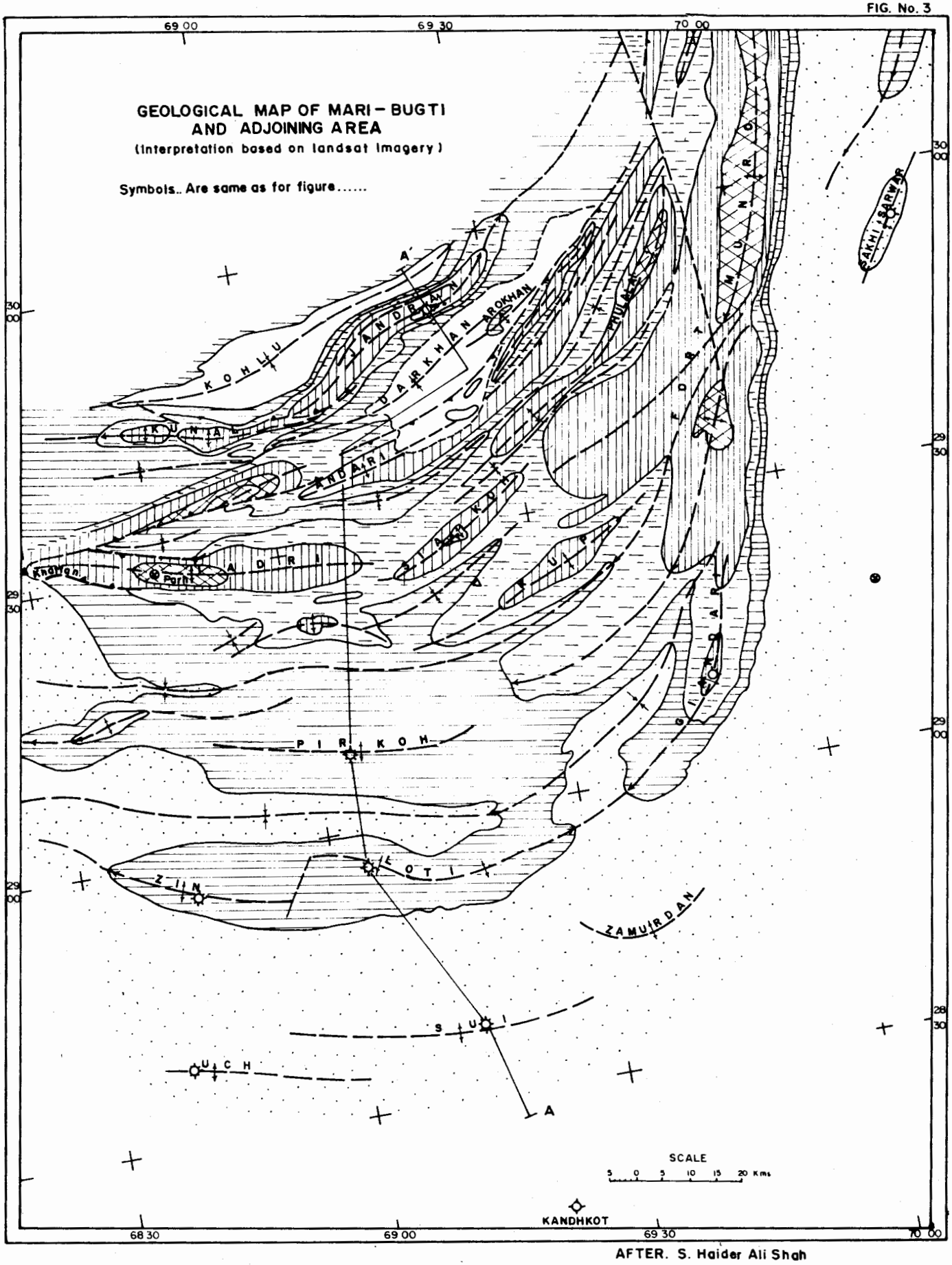

AFTER. S. Haider Ali Shah

FIG. No. 4

GENERALIZED STRATIGRAPHIC SEQUENCE OF MARI – BUGTI AGENCY SURFACE AND SUBSURFACE

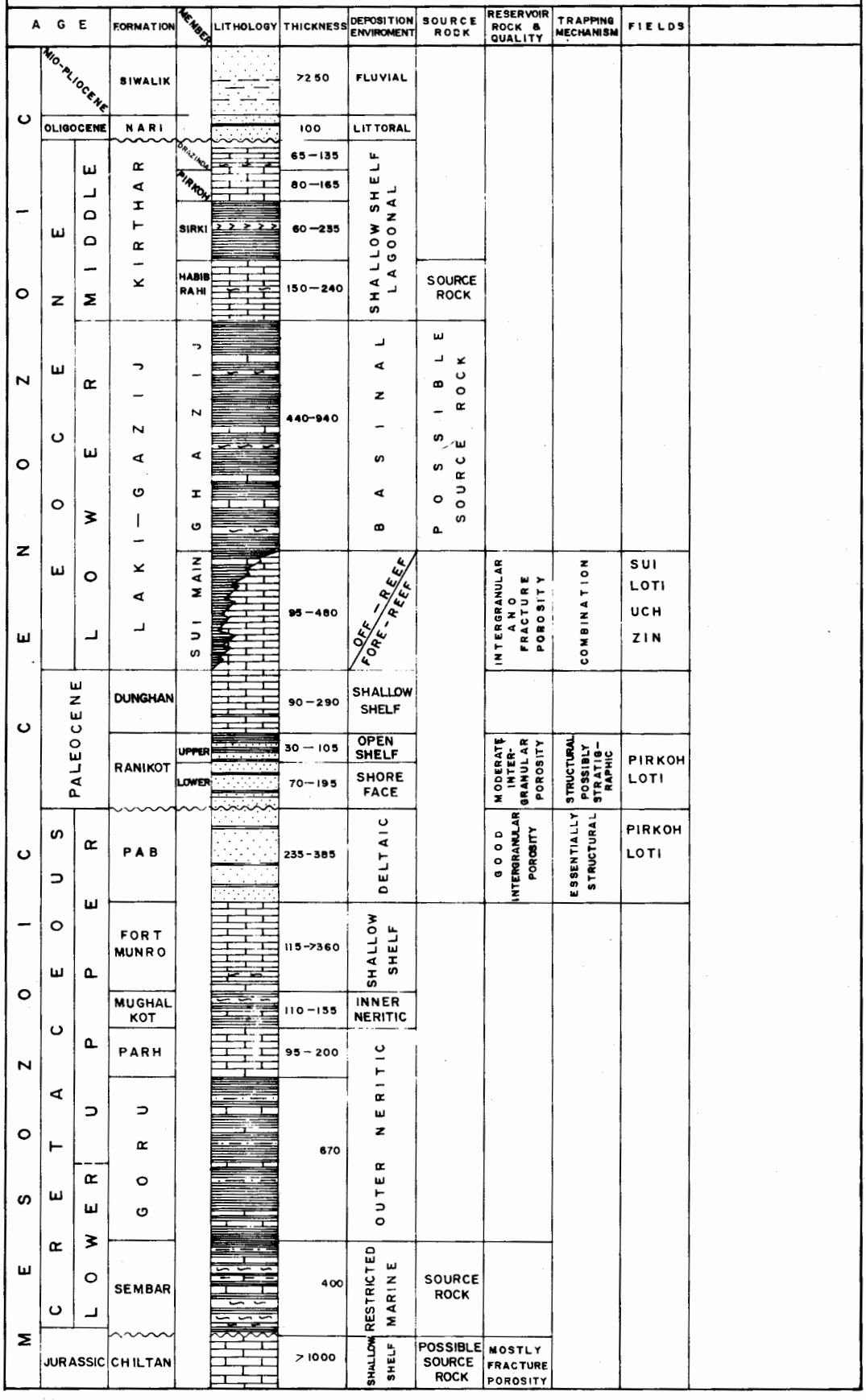

FIG. No. 5

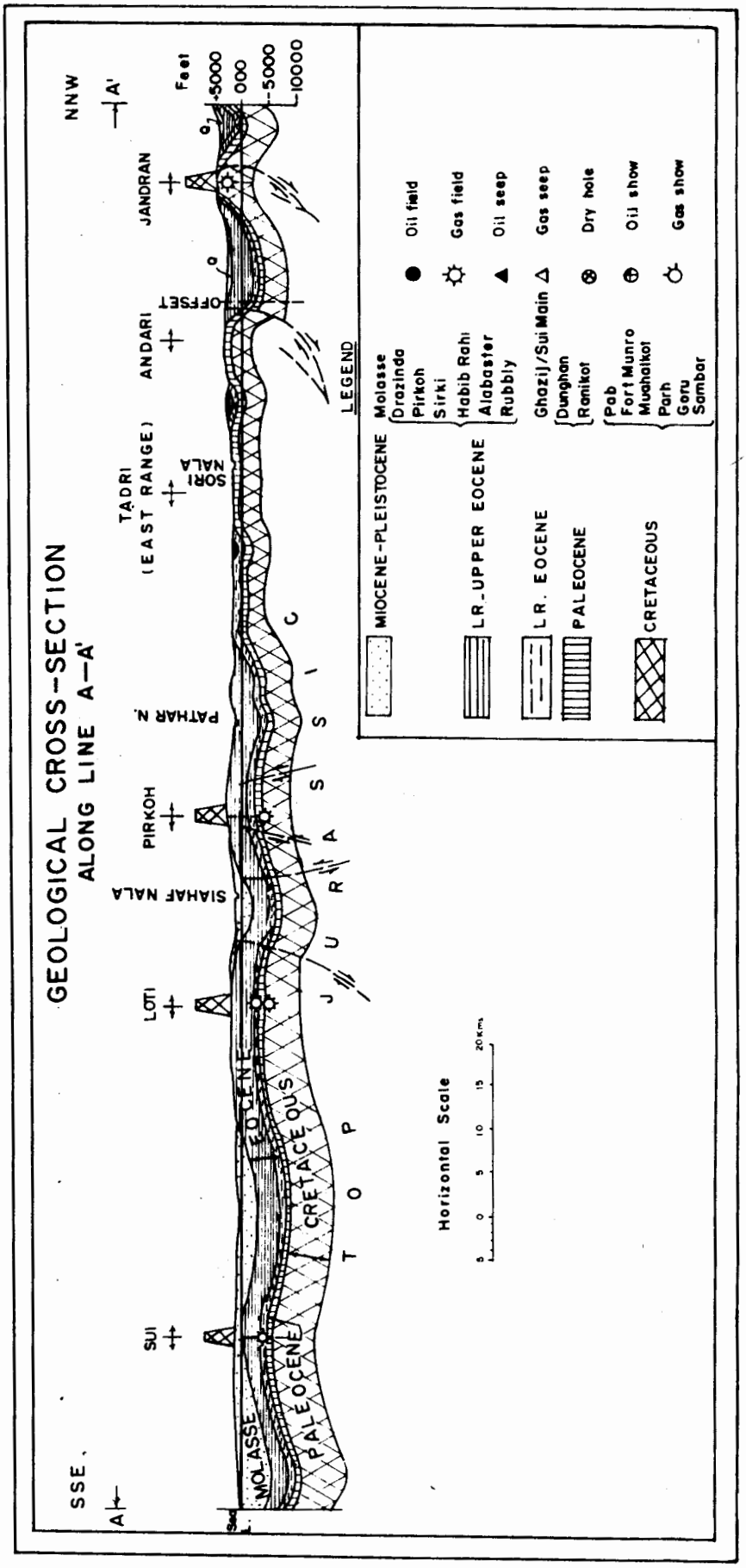

sandstones and pyritic shales of the basal Ranikot Formation representing shore face conditions. The Ranikot overlies the Pab Formation with a hiatus.

Later, with the establishment of shelf environments and paucity of clastic supply, limestone with shale interbeds of the Dunghan Formation were laid down. Towards the early Eocene, the southern part of the Mari-Bugti, environments became conducive for reef development as the area was located in the fore-reef zone. To the north, in the vicinity of Pirkoh, on the contrary, off-reef condition prevailed. Thus Sui Main Limestone reefal in nature is well developed in Sui, Uch, Zin and Loti whereas in Pirkoh only shaly facies are present. Under the influence of advancing sea, the reef succumbed and the entire area was covered with basinal Ghazij shale. In the localities to the northwest the occurrence of coal in Ghazij formation is indicative of lagoonal influence. During Middle Eocene, limestone and gypsiferous shales were deposited in shallower marine environments. The regressive trend became more pronounced and littoral environments prevailed in Oligocene, as a consequence of which sandstones of the Nari Formation were deposited.

Finally the sea retreated and continental environments became fully entrenched. As a result of Late Tertiary tectonic movements, clastic supply from north and west became abundant and fluvial sedimentation took place extensively. The deposition of fresh water Siwalik sediments, particularly in the flanking foredeeps, kept pace with the rapid subsidence. (Movshovitch & Malik, 1965; Sarwar & De Jong, 1979).

Structure

The area in general is characterised by a series of en echelon broad to very broad usually asymmetrical anticilinal folds. The southern flanks are usually steep and the axes have a general E-W alignment. The structures are mostly faulted, with significant faults running more or less parallel to the axes, whereas the transverse faults are mostly of smaller magnitude. The cores of anticlines expose progressive older formations from south to north.

Table 1. Composition of gas from fields in Mari-Bugti area.

FIELDS	PERCENTAGE COMPOSITION						
	METHANE C_1	ETHANE C_2	PROPANE C_3	BUTANE & HIGHER C_{4+}	NITROGEN N_2	CARBON DIOXIDE CO_2	GROSS HEATING VALUE BTU/CFT
PIRKOH	84.40	0.48	0.20	0.15	8.01	6.76	840.0
LOTI *	78.22	0.43	0.10	0.01	17.23	3.84	801.4
SUI *	88.52	0.89	0.26	0.37	2.46	7.35	933.0
UCH *	27.3	0.7	0.30	0.15	25.2	46.2	308.0
ZIN *	46.1	0.4	0.15	0.15	8.5	44.7	484.0

* H_2S in minor quantities

Table 2. Natural gas reserves of the gas fields of Mari-Bugti Agency, Pakistan.

GAS FIELD	YEAR OF DISCOVERY	RESERVES IN PLACE TCF				RECOVERABLE RESERVES TCF	
		PROVEN	PROBABLE	POSSIBLE	TOTAL	ORIGINAL	REMAINING ON JULY 87
SUI	1952	11.830	—	—	11.830	8.624	4.706
ZIN	1954	0.100	—	—	0.100	0.100	0.100
UCH	1955	2.550	—	—	2.550	2.550	2.550
LOTI	1985	3.834	—	—	3.834	0.800	0.800
PIRKOH	1977	3.756	6.558	0.883	11.197	3.470+	3.400+
TOTAL		22.070	6.558	0.883	29.511	15.544	11.556

The present structural configuration can be largely attributed to Plio-Pliestocene tectonic movements. There are, however, indications that in a few cases structural growth in embryonic form, might have taken place during the Cretaceous. To unravel the structural evolution on a broader scale substantial additional information, particularly good quality seismic data will have to be acquired.

Source Rocks

A source rock is a sediment which contain a certain quantity of organic matter and is capable of producing appreciable quantities of oil or gas. The hydrocarbon generating capability of a source rock depends on its preservation in anaerobic conditions, a certain depth of burial and suitable temperature. The maturity level of a source rock at a particular time is directly related to the extent it has been cooked.

According to the geochemical studies carried out so far, the shales of the Sembar formation of Lower Cretaceous age are the best known source rock in the region, and are reported to be in the peak gas generating phase. Habib Rahi Limestone Member is also regarded as a good source. To a lesser extent the shales of upper Cretaceous Mughal Kot formation could also be a possible source. Ghazij Group containing coal toward the northwest of Mari-Bugti shales of the Paleocene Ranikot formation and Upper Jurassic Chiltan Limestone are also likely sources of hydrocarbons.

Reservoir Rocks

The reservoir rocks are those possessing voids or fissures interconnected with each other through which fluids can circulate and accumulate. The porosity and permeability are two petrophysically fundamental factors which define the reservoir quality. The reservoir characteristics of a rock are in a general manner, result of geological history of a basin which include depositional environment, later diagenetic influence, and the effect of tectonics.

In Mari-Bugti, both clastic and carbonate reservoirs are encountered. The sandy reservoirs of Upper Cretaceous Pab Formation and Paleocene Ranikot formation are deltaic and shallow water sediments. The porosity of these reservoirs is essentially intergranular, though some fracture porosity also exists. The porosity of calcareous reservoir of Sui Main Limestone, deposited in fore-reef environments is intergranular as well as of secondary nature induced by fracturing as a result of folding and faulting.

The various stimulation techniques such as acidization of carbonate reservoir and sandfraccing of clastic reservoirs have yielded encouraging results in the form of enhanced gas production.

Trapping Mechanism

The hydrocarbons, after expulsion from the source rock travel through migration conduits till they are either caught in various types of traps such as anticlines, stratigraphic pinchouts, permeability barriers, etc. or escape to the surface. The traps in the area are essentially structural but composite structural-stratigraphic traps are also present. The transgressive sequences in particular the reefal type, constitute stratigraphic traps as in the case of Sui Main Limestone. On the other hand regressive sequences in general form structural traps (Chapman, 1972).

The existence of traps prior to hydrocarbon influx is a pre-requisite to entrapment. The severe underfilling of the structures of the region, indicates mostly late structural growth which caught only the later fraction of hydrocarbon influx pertaining to gas generation phase. The solubility of gas in water with low salinity increases rapidly with pressure, thus 13 m^3 of gas would get dissolved in 1 m^3 of water at a depth of around 5000 m (Magara, 1978; Perrodon, 1980). At excessive depths gas dissolved in water may attain enormous proportions. With the uplift and subsequent drop in pressure, a part of the dissolved gas is liberated and fed into the traps located on the migration path. The gas may have possibly accumulated in this manner in the lately formed traps of the area.

Gas Quality

Gases from Sui, Pirkoh and Loti are rich in methane, (78-88%), whereas the gases from Zin and Uch are deficient in methane (27-46%) but rich in carbon dioxide and nitrogen. The high content of CO_2 is considered to be the result of deep burial of carbonate rocks in the adjoining Sibi Trough. The nitrogen content is attributed to certain diagenetic changes of mostly carbonate and evaporitic sequences. The identical composition of gases from Cretaceous, Paleocene and Eocene reservoirs indicate a common source.

GAS FIELD DEVELOPMENT

Sui

This is the first field which came on production in 1956. Since then 78 development wells have been drilled. It has now reached a mature stage in its production life. The entire production is from Sui Main Limestone. The average depth of the wells is about 1400 metres. The average daily production is nearly 700 MMCF/day.

Pirkoh

This is the second producing field in the Mari-Bugti Agency. Pirkoh was discoverd by OGDC in 1977. This was the first ever Paleocene and Cretaceous discovery in the area. Exploration and development of the field posed a formidable challenge. In this rugged terrain and remote location, logistics and security were the major concerns. Scarcity of water was another main hinderance. After the establishment of the necessary infrastructure, the field was put on production stream in 1984. Till now, 20 wells have been drilled. The average depth of the wells is 2400 metres. The drilling was hazardous mainly due to severe loss of circulation. This causes the drilling mud to be lost partially or completely in the highly vuggy, cavernous or underpressured strata. This not only results in loss of mud containing expensive chemicals but also results in pipe sticking, fishing and damage to reservoir. Apart from this, scarcity of water makes the situation all the more difficult as enormous quantities of water are required to make fresh mud. Precious loss of rig time, mud chemicals and other related technical problems caused tremendous setback to the development of the field. With the object to resolve the problem, OGDC has recently resorted to the improved technique of air-mist drilling which has resulted in cutting back the rig time to 1/3, and substantial saving of mud chemicals. This has immensly speeded up development drilling operations. At least 20 more wells are planned to be drilled in next 2 years. The present gas production of 95 MMCF/day would rise to 180 MMCF/day by end of the fiscal year (1987-1988)

Expansion of the infrastructure needed to cope with the increased production in the near future is in hand.

Loti

OGDC discovered this field in 1985. It was an important discovery due to the fact that all the three known reservoirs were gas-bearing. Eight wells have been driled so far. The average depth of wells is 2200 metres. The production is due to commence by June 1988 when 40 MMCF/day of gas would be delivered to Sui Northern Pipelines Ltd. for supply through its transmission network.

Uch

Uch gasfield was discovered by Pakistan Petroleum Ltd. in 1955. The area was relinquished by the company and field remained dormant since then. OGDC realised that though gas has high CO_2 and N content, its appreciable estimated reserves make the development of the field, a viable proposition particularly for power generation. An appraisal well is currently being drilled to fully assess the reservoir potential of the field with techniques not available at the time of its discovery more than 30 years ago.

Zin

Discovered in 1954, this field remained dormant due to the reason of its having relatively

low estimated reserves and higher CO_2 and N content. Its development may become feasible at a later stage when comprehensive infrastructure would have been established at the neighbouring fields or with some new discovery in the vicinity.

RESERVES

Cumulative remaining recoverable gas reserves of the five known gasfields are estimated to be of the order of over 11.5 trillion cubic feet. With availability of additional data from appraisal/development wells this estimate may further rise. The outlook for availability of gas reserves in future is promising in view of the fact that development of Pirkoh gasfield is in its infancy as its potential is yet to be fully assessed. Loti gasfield has yet to enter the production phase and appraisal of Uch gasfield is still underway. Moreover, exploration of the adjoining areas may lead to discovery of additional resources. It is anticipated that even with increased offtake, the gas resources of the region may last for several decades.

REFERENCES

ANDRIEUX J. & MAURICE, B. (1977) L'Evolution des Chaines Occidental du Pakistan Mem. H. Ser. Soc. Geol. France, Paris, **8**, pp. 189-207.

CHAPMAN, R.E. (1972) Primary migration of petroleum from clay source rocks. Bull. Amer. Assoc. Petroleum Geol., **56(11)**, pp. 2185-2191.

MAGARA, K. (1978) COMPACTION AND FLUID MIGRATION. Elsevier Scientific Publishing Company, Amsterdam. 319 p.

MOVSHOVITCH, E.G. & MALIK M.A. (1965) Thickness and Facies Variation of molasse sediments of the Sibi Re-entrant, West Pakistan. Geol. Bull. Punjab University., **5**, pp. 31-42.

PERRODON, A. (1980) GEODYNAMIQUE PETROLIER, Masson, Elf Aquitine, Paris, 381 p.

SARWAR, G. & DE JONG, K.A. (1979) Arcs, Oroclines, Syntaxes. The curvature of mountain belts in Pakistan. ***In:*** Farah A. & De Jong K.A. (eds.) GEODYNAMICS OF PAKISTAN, Geol. Surv. Pakistan, Quetta. pp. 341-349.

Orally presented on 20.10.1987
Manuscript revised on 31.12.1987

ACTA MINERALOGICA PAKISTANICA
VOLUME 3 (1987) pp. 82 - 89

USE OF SATELLITE IMAGERY FOR GEOLOGICAL MAPPING IN THE COASTAL MAKRAN REGION OF BALUCHISTAN

SAEED AKHTAR KHAN ALIZAI
Remote Sensing Applications Centre,
SUPARCO, P.O. Box 8402, Karachi - 32, Pakistan.

ABSTRACT: Satellite imagery provides a view of the Earth's surface which gives more detail of landforms and regional physiography than a topographic map of the same scale. Together with geological maps, this information can be used, to provide a new method of viewing important features that define structural and petrological regions. Dominant rock types can be distinguished by their shape and character, while faults, folds, lineaments, sedimentary, and geomorphic patterns can be mapped accurately over large areas.

The extent to which satellite imagery can be used in mapping geological phenomena of the coastal Makran region of Baluchistan has been investigated. Geological interpretation of the study area was carried out using standard photointerpretation techniques. The results of this study have demonstrated that satellite imagery is an effective tool in mapping geological structures as well as geological phenomena.

INTRODUCTION

Since 1972 geoscientists around the world have been evaluating the utility of Landsat data for Earth resources inventory and subsequent management. Pakistani scientists have assessed the utility of these data in a broad spectrum of disciplines (Alizai & Mirza, 1986).

The report that follows is the result of one such experiment in evaluating the capabilities of Landsat data for investigation of geological structures, rock type discrimination, drainage distribution patterns and moisture concentration. The above data results in a geohydrological map.

STUDY AREA

An area of approximately 5600 km^2 covering the extreme south eastern part of Baluchistan Province bounded by longitude 65° E to 67°E and latitude 24°25'N to 26°30'N comprising the Lasbela Valley and the coastal plain in the Makran region, was chosen for the present study (fig. 1).

The study area has a triangular shape which is formed by the Mor and Hala mountain ranges. These two ranges 100 km apart at the coast merge 130 km to the north to enclose the plain (fig. 1). Physiographically, the area can be divided into (i) the low, sandy, coastal plain which includes beach ridges and shifting sand dunes; (ii) the central plain covered with alluvial deposits derived mainly from the waters of the Porali, Kharrari and Winder rivers and their tributaries, (iii) the upper plain comprising older and higher sand and gravel foothills that flank the central plain (fig. 2).

METHODS AND PROCEDURES

Most of the work presented here is based on the analysis of Landsat MSS images with and without enhancement techniques. Two Landsat data sets covering the geographic area were selected for analysis (165-42 and 164-42; NASA, 1979). An approximate plot of the geographic area is shown in fig. 1.

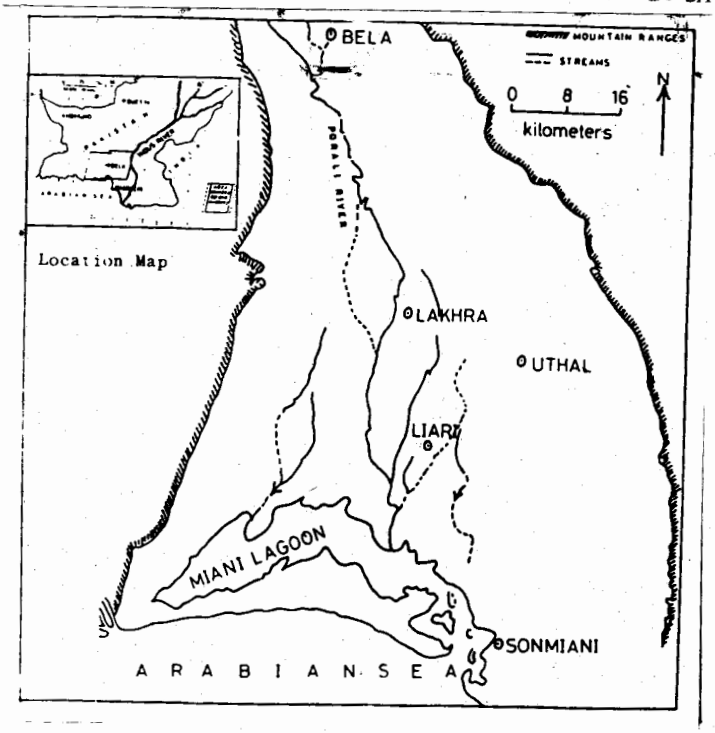

Fig. 1 Sketch map of the study area.

The analysis is based entirely on manual/ visual interpretation of Landsat images. Landsat MSS band 5 and 7 data have been used for the study of geological structures, drainage, soil moisture, etc; band 7 is the best band for rock type discrimination and has been used to delineate rock types and lithological units (Alizai & Ali, 1984).

RESULTS OF INTERPRETATION

Delineation of Geomorphic Features

The study area is a triangular level plain approximately 110 km long. From a width of 55 km at Liari, it narrows northward to a width of about 18 km at Bela. The plain is made up largely of alluvial deposits which include older and younger gravels, fine, loose brown silt, and eolian sands. The silts overlie boulder fans and attain thickness of between 1.5 m and 30 m and thicken towards west. North of the town of Bela, Pleistocene and Recent gravel and boulder fans form a continuous belt around the north end of the plain. Upslope fans lead into uplifted Pleistocene gravels that flank the valley all the way to the coast (fig. 2).

The geomorphic features most readily identifiable from the Landsat imagery corresponded directly with (i) abrupt changes in topography and structure, (ii) abrupt changes in lithology and (iii) vegetational and landuse patterns. Seasonal coverage was useful in identifying geomorphic features more precisely because vegetation changes tended to highlight the topography and landuse patterns.

Geological Framework

The study area (fig. 2) forms a segment of the Indian - Eurasian collision zone of Baluchistan. Thick sequences of marine sediments which accumulated from Paleozoic to Tertiary times underwent folding in the Cenozoic Era (Farah & De Jong, 1979).

The region surrounding the Bela Plain has highly variable relief and landforms; the major drainage system drains into the Arabian Sea. Belts of north-northeast trending topographic, textural and tonal expressions are visible on Landsat imagery, while mountains generally form high elevated linear topographic ridges on the Landsat imagery. The Lasbela Valley separates two mountain ranges (fig. 2); calcareous Jurassic and Cretaceous rocks form the eastern mountain while highly fossiliferous arenaceous Tertiary and Pleistocene rocks form the western mountain. Series of mafic and ultramafic intrusive rocks are present in the Central Lasbela Valley.

The eastern mountains have relatively simple stratigraphy. The north to south trending Kirthar, Pab and Mor Ranges are denuded anticlines of Jurassic and Cretaceous limestones, shales, etc. Mountain elevations range from 670m to 1400m, decreasing in elevation near the coast. The highest elevation in the Lasbela District is in the northeast and exceeds 1500m. The Kirthar Range extends to Cape Monze, and an outlier of the Pab Range is present at the coast at Gadani; the lower Mor Range is buried under Pleistocene sand near the coast.

The western mountains of the Lasbela Valley, comprise an arenaceous belt of Pliocene and Pleistocene rocks consisting of weak, poorly cemented sandstones with interbedded conglomerates, silstones, mudstones, shales and shelly limestones. The Haro and Hala Ranges are anticlines separated by a syncline through

which the Phor River flows. The elevation of the Hala Range varies from 600 to 1100m in the section north - west of the valley. The Haro Range is a small northeast - southwest striking anticline 55 km long, with maximum width of 8 km, the average elevation is about 500 m with a maximum of 800 m.

Identification of Lineaments

Photogeologic lineaments are lines chosen from the satellite images on the assumption that they originate through geological processes; they are often a fracture (fault or joint) or a linear expression of a fracture system. Satellite imagery makes it possible to observe lineaments of regional extent which otherwise cannot be rec-

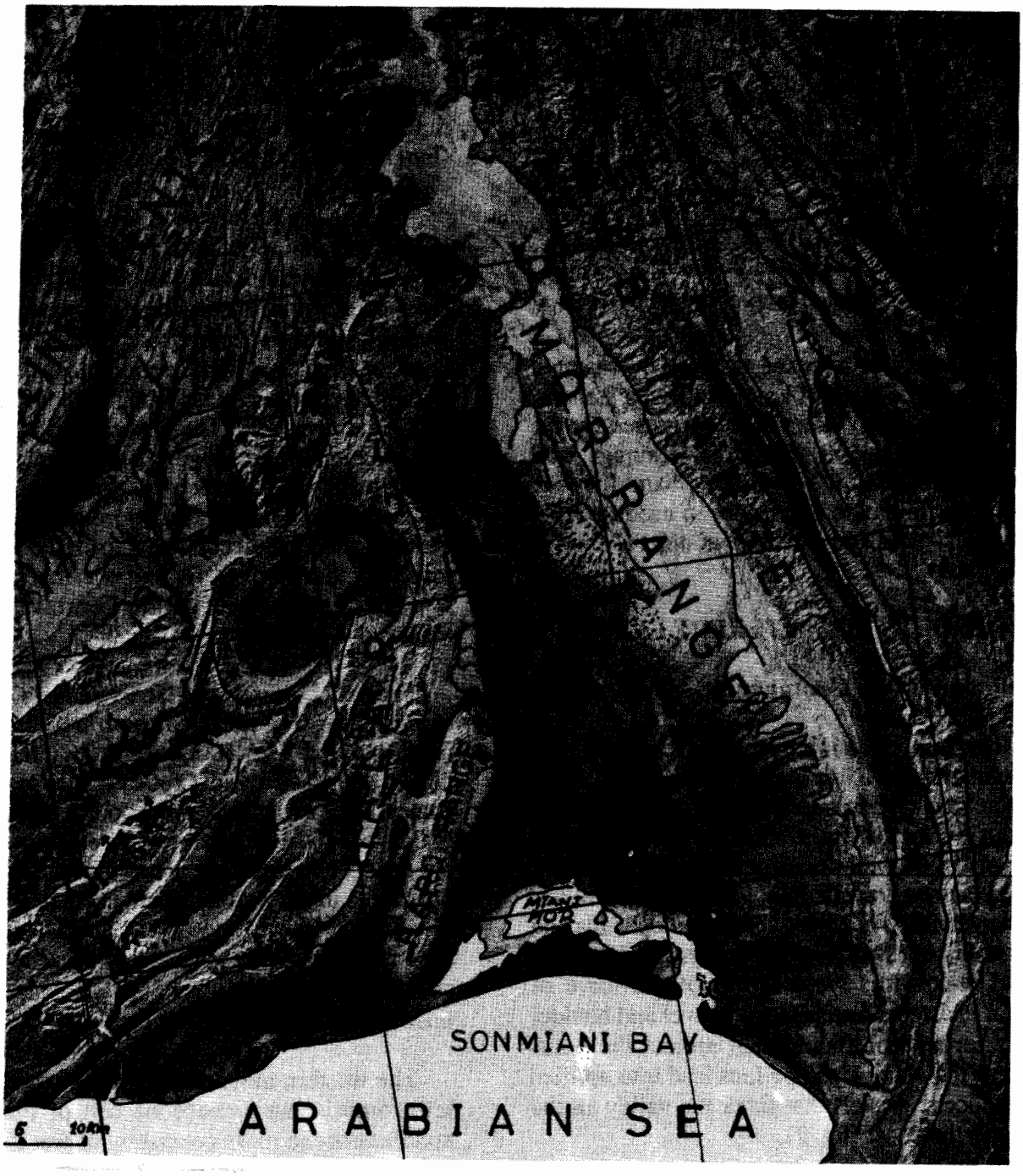

Fig. 2 Landsat MSS imagery of the Lasbela Valley and surrounding area showing distinct geological and geomorphic features.

Fig. 3 Lineament map of the Lasbela Valley and surrounding area derived from the Landsat MSS Band-7 image.

ognised by conventional techniques. It is essential to verify the nature of lineaments by field study. Four primary characteristics viz location, orientation, length and curvature contribute to the structure and pattern of lineaments. The surface features making up a lineament may be geomorphic (caused by relief) or tonal (caused by contrast difference) and presumably reflect subsurface phenomena (Sabins, 1978). Straight stream valleys and aligned segments of valleys are typical geomorphic expressions of lineaments. Difference in vegetation, moisture content and soil or rock composition account for tonal contrasts (fig. 3).

The interpreted imagery generated many previously unmapped lineaments. Most of these were of regional extent crossing many geomorphic and geological units and structures. Because of their magnitude many could not be effectively verified on the ground. Some of the major faults lying within and adjacent to the study area which are easily identifiable on the Landsat imagery include the Sonmiani, Ornachnal, Hudishi, Agher and Ras Malan faults (fig. 4).

Aquifer Rock Identification

Zall *et al.* (1980) described the use of surface drainage patterns as an important key element in the identification of rock lithology. These drainage patterns can be a qualitative indication of rock permeability. The surface drainage patterns developed on a particular terrain are composed of major streams, their tributaries, and their head waters.

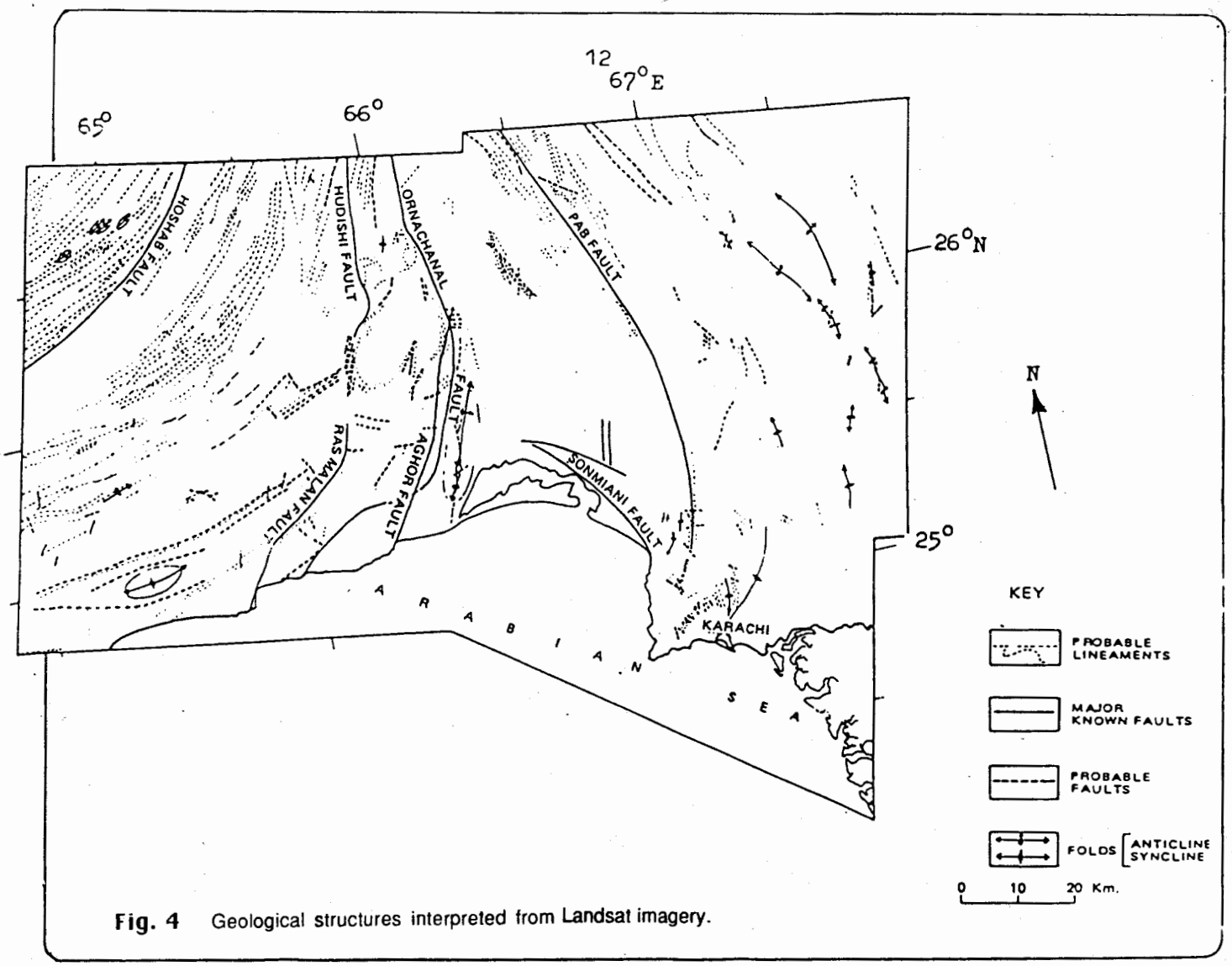

Fig. 4 Geological structures interpreted from Landsat imagery.

The type of a particular drainage pattern developed on a terrain is largely a function of the amount of precipitation which can infiltrate to the ground, versus that which becomes surface run-off. This infiltration/run-off relationship is controlled largely be the permeability of the terrain. For example, an area comprising two terrain types which contain the greater number of drainage channels per unit surface are usually less permeable. Surface run-off, in this case dominates over infiltration, and a more densely textured drainage pattern results (Salomonson & Bhavsar, 1980).

Fractured or jointed terrain creates a controlled drainage pattern consisting of straight or angular segments. For geohydrological study, the presence of these angular tributary channels in an otherwise impermeable water tight bedrock may indicate fractured or faulted zones containing groundwater.

For regional geohydrologic interpretation, drainage patterns are a powerful tool for delineating lithologic boundaries. It is important to note that on Landsat imagery, changes in surface drainage may indicate a complete change in

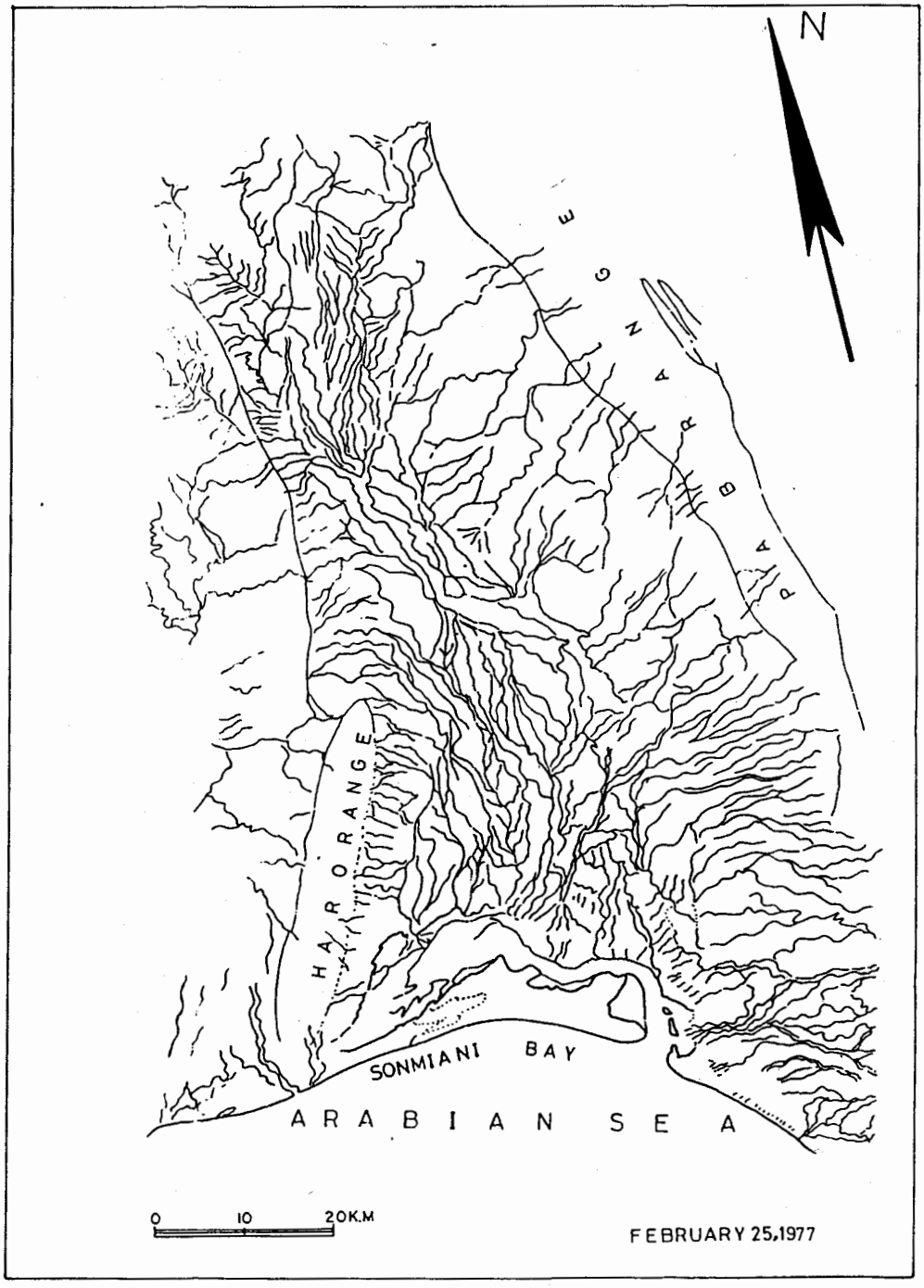

Fig. 5 Drainage map of the Lasbela Valley derived from the Landsat MSS Band-7 image.

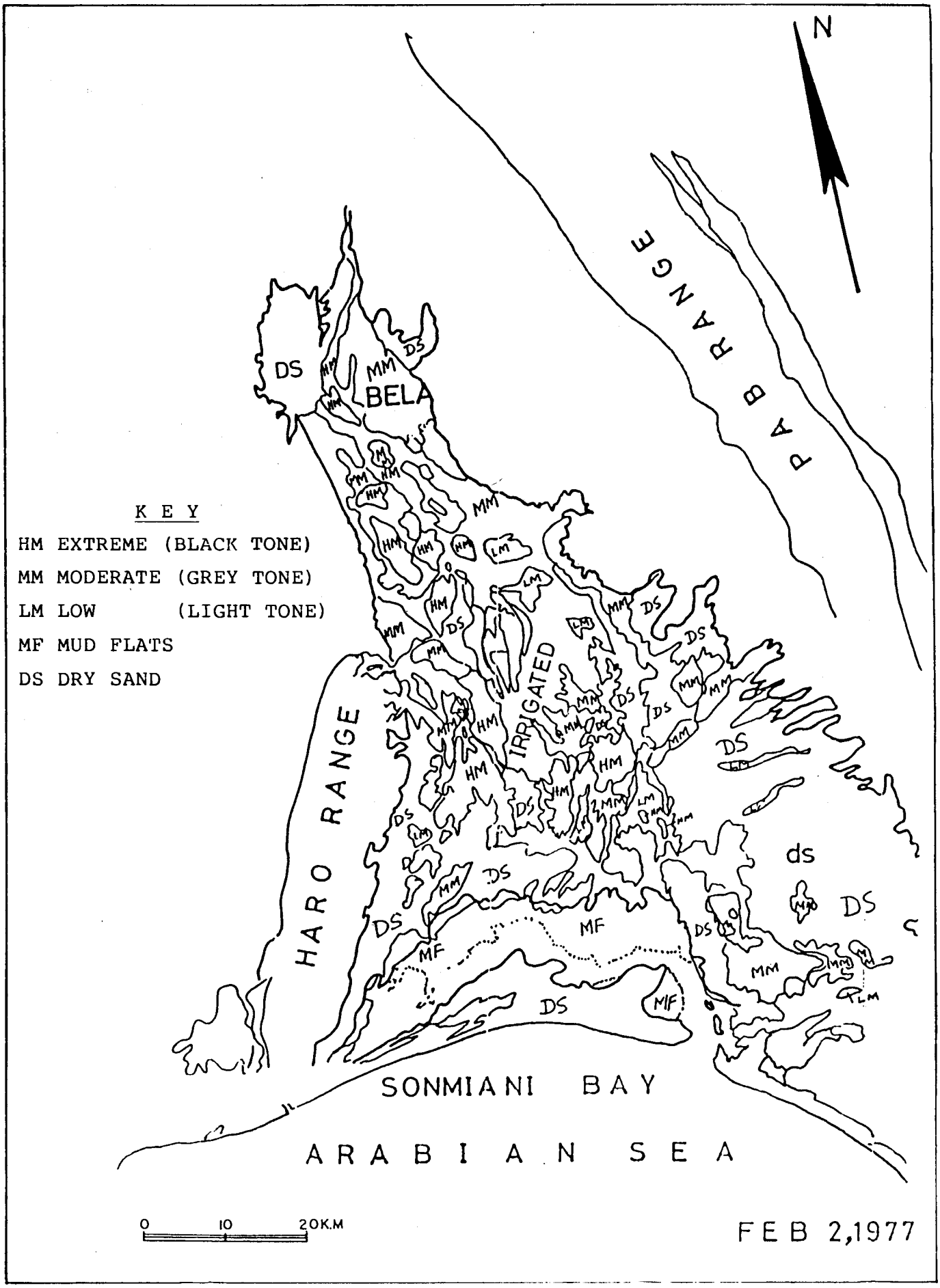

Fig. 6 Moisture distribution map of the Lasbela Valley derived from the Landsat MSS Band-7 image.

lithology. The drainage network in the study area is extensively controlled by the geomorphic as well as geologic structures which reflect the topography of the map area (fig. 5). Here, the drainage pattern in the sandstones as in many sandstones, is widely spaced, and it follows the more easily eroded joints and bedding found in the sandstone bedrocks.

Soil Moisture Concentration

Satellite image iterpretation of soil moisture is possible through physical properties of the water soil mixture. Soil moisture distribution in the study area was mapped through darkening (decreased reflectance) of soil as it is progressively moistened. Significant variation in the soil moisture content based on tonal and texture discrimination of the area have been observed (fig. 6). Based on darkening, the moist soil was classified on Landsat images as: (i) extreme moisture (black tone), (ii) moderate moisture (grey tone) and (iii) low moisture (bright tone).

A demarcation of a high moisture content zone may identify potential area for groundwater exploration. Such information, in conjunction with field data, may be used to determine soil permeability and their related parameters quantitatively (Alizai & Ali, 1986).

CONCLUSION

As pointed out in several instances throughout this presentation, Landsat imagery is definitely useful for regional geologic reconnaissance, provided the user is familiar with the subject matter, the landsat system, and imagery specifications. Field verification of interpreted results is definitely an integral part of the imagery interpretation task.

All of the imagery used in this study consisted of Landsat data. The Landsat imagery provides information only in the reflected region of the electromagnetic spectrum and at a resolution (80m) insufficient for detailed prospecting requirements. Interpretation of such imagery will result in information in only the "horizontal" plane, such as lineaments, surface drainage, soil moisture, etc., without any depth penetration. Thermal, passive, microwave and other types of imagery (TM/SPOT, etc.) must be examined together with Landsat MSS imagery for a conclusive evaluation of such technology to groundwater and mineral exploration potentials.

REFERENCES

ALIZAI, S.A.K. & ALI, J. (1984) Comparative interpretability of SIR-A and Landsat images for terrain analysis in Pakistan. Space Horizons I(No. 2 & 3), pp. 33-44.

_____ (1986) Use of remote sensing technology for hydrogeological mapping in Pakistan. Space Horizons III, No. 1 & 2, pp. 32-43.

_____ & MIRZA, M.I. (1986) Remote sensing applications in Pakistan: Current status and future programmes. Intern. Jour. Remote Sensing 7 (No. 9), pp. 1145-1150.

FARAH, A & DEJONG, K.A. (1979) GEODYNAMICS OF PAKISTAN. Geological Survey of Pakistan Quetta, 361 p.

NATIONAL AERONAUTICAL AND SPACE ADMINISTRATION, NASA (1979) Landsat Newsletters 23, 24, 25.

SABINS, F.F. (1978) REMOTE SENSING: PRINCIPLES AND INTERPRETATION. W.H. Freeman and Company, San Francisco, USA, 426 p.

SALOMONSON, V.V. & BHAVSAR, P.D. (1980) The contribution of space observations to water resources COSPAR: Advances in Space Exploration 9, 280 p.

ZALL, L. & MICHAEL, R. (1980) Space remote sensing system and their applications to engineering geology. Bull. Assoc Engrs. Geols. XVII (No. 3).

Orally presented on 21.10.1987
Manuscript revised on 31.12.1987

ACTA MINERALOGICA PAKISTANICA
VOLUME 3 (1987) pp. 90 - 96

STUDY OF HEAVY MINERALS CONCENTRATION FROM GADANI TO PHORNALA, ALONG THE BALUCHISTAN COAST, PAKISTAN.

M. AKRAM CHAUDRY & M. QASIM MEMON
National Institute of Oceanography, 37-K, Block 6, PECHS, Karachi-29, Pakistan.

ABSTRACT: Sorting and concentration of a variety of heavy minerals along the coast between Gadani and Phornala, Baluchistan, are facilitated by the coincidence of the periods of maximum turbulence and wave activity, maximum precipitation and sediments discharge. Sediment samples from different intertidal zones between Gadani and Phornala were collected for grain size analysis and petrographic/petrological study. Variations in grain size and mineral assemblage in the intertidal zones have been noted. Concentration of dark colour heavy minerals has been noted in fine-grain sediments, light-coloured minerals are rather ubiquitous. The sediments exhibit wide range of sorting, poor to very well.

INTRODUCTION

The heavy mineral placers have been explored from the marginal areas of many countries bordering the Indian Ocean. Many of these placers such as tin, ilmenite, rutile, zircon, magnetite, monazite, garnet, etc., are already being exploited (Siddiqui *et al.*, 1984). However, no comprehensive study for the exploration of heavy mineral placers has been attempted in the marginal areas of Pakistan.

The present study concentrates within the intertidal zones along the modern coast from Gadani to Phornala (fig. 1). The samples of beach sediments are collected from 9 stations from distinguishable 3 to 4 intertidal zones such as surf, wet dry and berm zones.

The laboratory analysis shows that sediments exhibit large variations in grain size, ranging from very coarse sand to very fine sand. These variations are reflected along the length of the coast as well as within the intertidal zones of a single station. The sediments also show wide range of sorting and different mineral assemblages. It is observed that the heavy minerals are concentrated in the finer fraction of the sediments.

FIELD AND LABORATORY PROCEDURES

Systematic sampling is carried out at low tide periods to cover the optimum intertidal distances. On each station three to four samples are collected covering the different intertidal zones, such as surf, wet, dry and berm zones. The location of stations from where samples are collected is shown in fig. 1. The sampling area covers a stretch of about 50 km along the modern coast line. The definition of the various intertidal zones are understood by the authors as follows:-

Surf zone: Where the wave breaks.
Wet zone: Approximately at the mid-tide stages.
Dry zone: Just below the line of water mark.
Berm zone: A nearly horizontal portion of the beach or back shore formed by the deposition of

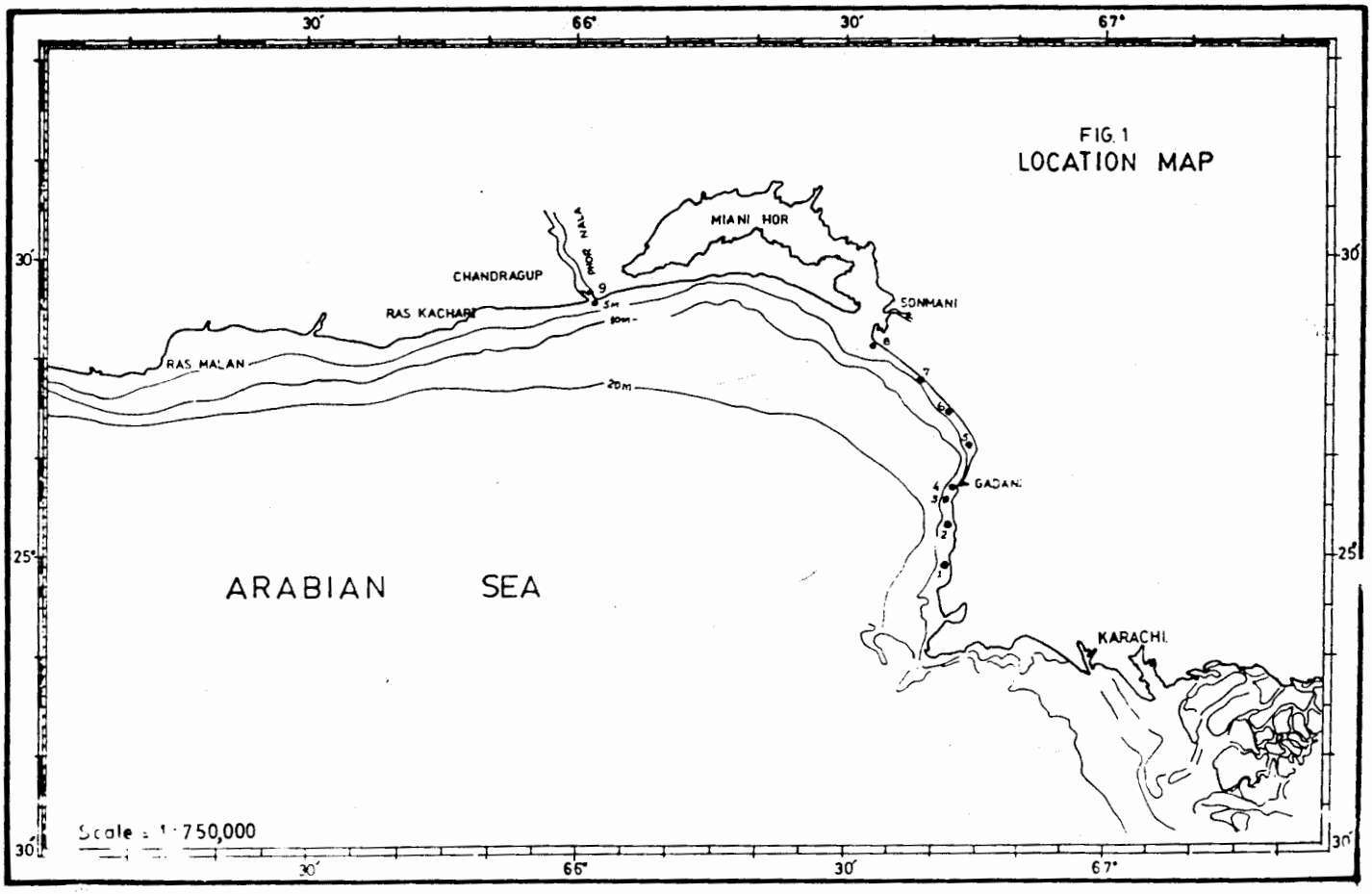

material by water action.

Grain size analysis has been carried out by sieving, using a set of six sieve meshes on electric sieve shaker for 20 minutes at vibration 40.

Each sample is washed in distilled water, dried in an electric oven at 100°C; 30-50 grams of sample is taken for the determination of grain size. The separation of heavy and light minerals has been carried out by following the sink and float method, using tetrabromethene, (S.G.2.94).

RESULTS AND DISCUSSION

The occurrence of heavy mineral placer deposits on beaches essentially results from the selective sorting of the detrital material by waves and currents action (Dunham, 1969). The North Arabian Sea receive significantly high load of detrital sediments from variety of sources in variable quantities (Milliman *et al.*, 1984; Siddiqui *et al.*, 1984). These sediments are reworked by wave and current action and may selectively concentrate along the beaches under favourable conditions. The result of grain size analysis is presented in table 1, whereas the result of heavy mineral percentage is presented in fig. 3.

An examination of the results obtained shows the following features: the relative abundance of different grain size fractions on various stations vary widely, for example; on stations 1 and 2 most of the sediments from all intertidal zones (almost 80% of the total weight) are very coarse to coarse and medium sands and poorly sorted whereas a shift is clear on station no. 3 (fig. 2). On station no. 3 most of sediments are medium to fine sands and there is a notable trend of dominating finer fraction towards Phornala, leading to the significant abundance of fine to very fine sand on the locations of station 8 and 9. This shows an overall trend of gradual change in improved sorting. This also reflects probably the gradual change in energy level of beach environment (waves and currents); because the lower the energy level of a wave or current system, the better will be the sorting of the sediments (Pettijohn *et al.*, 1983).

TABLE 1. GRAIN SIZE ANALYSIS OF SEDIMENTS FROM GADANI TO PHOR NALA (IN %)

STATION NO	NATURE OF SAMPLE	TOTAL WT. SAMP. USED	MESH (18)	MESH (35)	MESH (60)	MESH (120)	MESH (230)	MESH LESS THAN 230	TOT.WT. AFTER SEIVING
1	SURF	50	28.06	15.56	42.64	10.96	2.64	0.00	49.93
1	WET	50	25.96	13.82	44.08	15.58	0.56	0.02	50.01
1	DRY	30	0.260	6.060	70.20	25.86	0.33	0.00	30.00
1	BERM	50	14.76	8.04.	57.60	19.50	0.10	0.02	50.01
2	SURF	50	29.68	13.34	43.20	13.48	0.32	0.00	30.01
2	WET	50	20.40	13.78	50.72	14.74	0.18	0.00	49.91
2	DRY	50	28.19	20.60	20.04	7.94	0.12	0.00	49.94
2	BERM	50	8.800	7.340	59.84	23.28	0.54	0.00	49.90
3	SURF	50	3.780	7.120	55.46	32.88	0.68	0.00	49.96
3	WET	50	0.180	1.460	53.64	42.48	2.28	0.00	50.02
3	DRY	50	1.380	0.340	33.36	56.76	8.02	0.00	49.93
3	BERM	30	0.000	0.200	18.80	74.44	7.31	0.00	30.01
4	SURF	50	0.98	2.66	34.24	58.46	3.40	0.00	49.90
4	WET	50	0.640	0.600	27.81	65.34	5.44	0.00	49.92
4	DRY	50	0.000	0.080	19.98	77.86	1.96	0.00	49.91
5	SURF	50	0.300	1.740	23.84	69.20	4.80	0.00	49.94
5	WET	50	1.800	4.520	38.62	25.86	5.00	0.00	49.90
5	DRY	50	0.000	0.080	10.32	86.26	3.38	0.00	50.02
6	SURF	50	3.220	0.480	43.08	45.88	1.18	0.00	49.92
6	WET	50	2.940	9.02	47.16	39.88	0.80	0.00	49.90
6	DRY	50	0.00	0.380	11.94	81.98	5.54	0.00	49.92
7	SURF	50	1.10	2.420	36.12	56.15	3.08	0.00	49.94
7	WET	50	0.440	2.880	43.78	50.44	2.52	0.00	49.93
7	DRY	50	0.000	0.040	3.580	89.90	6.68	0.00	50.00
8	WET	30	0.230	0.260	1.130	66.76	29.4	1.00	29.91
8	DRY	30	0.00	0.060	0.960	80.43	18.6	0.13	30.05
8	BERM	30	0.030	0.060	0.900	79.60	19.4	0.03	30.00
9	SURF	30	0.200	0.130	6.930	71.16	21.0	0.16	29.90
9	WET	30	0.130	0.960	11.13	44.90	42.6	36.6	30.01
9	DRY	30	0.000	0.100	1.500	77.73	6.83	0.13	30.03
9	BERM	30	0.000	0.260	14.70	76.20	8.73	0.03	29.98

INDEX

SEIVE NO.	GRAIN SIZE (mm)
18	> 1.00
35	< 1.00 - > 0.50
60	< 0.50 - > 0.25
120	< 0.25 - > 0.125
230	< 0.125 - > 0.062
< 230	< 0.062

Table 2. Quantitative analysis of heavy minerals. All the values represent percentage of heavy minerals in the grain size fraction, 0.125–0.0625mm.

Station No. / Heavy Mineral	1	2	3	4	5	6	7	8	9
Garnet	34	30	12	10	29	30	28	27	10
Tourmaline	22	25	37	32	23	23	24	20	13
Magnetite	18	17	7	16	10	3	6	3	12
Ilmenite	10	13	12	15	10	14	14	12	15
Limonite	–	–	–	–	–	–	–	–	15
Zircon	7	6	22	25	27	24	23	27	30
Rutile	5	5	3	8	7	3	4	5	5

The variations in the sorting of sediments within the intertidal zones of every location is also notable. Sorting of sediments in all the intertidal zones (Surf, Wet, Dry, Berm) on station 1 and 2 is poor. On station 3 the sorting in all the intertidal zones is moderate, whereas the sorting of sediments in the intertidal zones from station 4 to 9 show a trend of gradual improvement from moderate to very well sorted from surf to berm.

Heavy minerals show strong association with very fine sand (fig. 3) and this association is retained on almost all the stations and for all the intertidal zones. However this relationship is relatively weak on station 4, 5, and 8.

It is observed (fig. 3) that heavy minerals are not particularly concentrated in any specific intertidal zone on station 1, 2 and 3. The contraction of heavy minerals is very random. Almost all the intertidal zones show concentration of heavy minerals in varying percentage whereas on stations 6, 8 and 9 the heavy minerals are particularly concentrated in the dry zone while on station 7 the concentration of heavy minerals is observed only in the intertidal surf zone.

Apparently the distribution of light minerals is sporadic and does not show significant relationship with heavy mineral or with any specific size fraction in the sediments.

A strong association of heavy minerals with the very fine sand (< 0.125 - > 0.0625 mm.) was confirmed (see fig. 3). Thus the heavy minerals obtained from this particular fraction were studied under the microscope for the identification and quantitative analysis. Table 2 shows the quantitative analysis of heavy minerals present in this particular fraction from all the 9 stations. It is observed (table 2) that minerals of both acidic as well as of basic igneous origin are present on almost all the stations. All the minerals such as garnet, tourmaline, magnetite, ilmenite, zircon and rutile show association with each other. The order of magnitude of this association is weak at somestations e.g. magnetite on station 6, 7 and 8 and garnet at stations 4 and 9. The mineral limonite is the only exception, which is present only on station 9. Limonite indicate the bog or lagoonal type of depositional environment.

CONCLUSIONS

The association of heavy minerals with finer fraction of the sediments shows the long distance of transportation and probably longer period of reworking by waves and currents. The gradual improvement in sorting of the sediments from Gadani to Phornala reflects the gradual decline in the energy level of beach environment (waves and currents). Sorting variation within an intertidal zone, indicates that the sediments were (station 4-9) repeatedly made available for the reworking by waves of moderate to low intensity (in between 1.5 to 3.5M). It also indicates the prevalence of the same beach environment for a long time. The absence of sediments

FIG.2. GRAIN SIZE VARIATION AT DIFFERENT INTERTIDAL ZONES.*

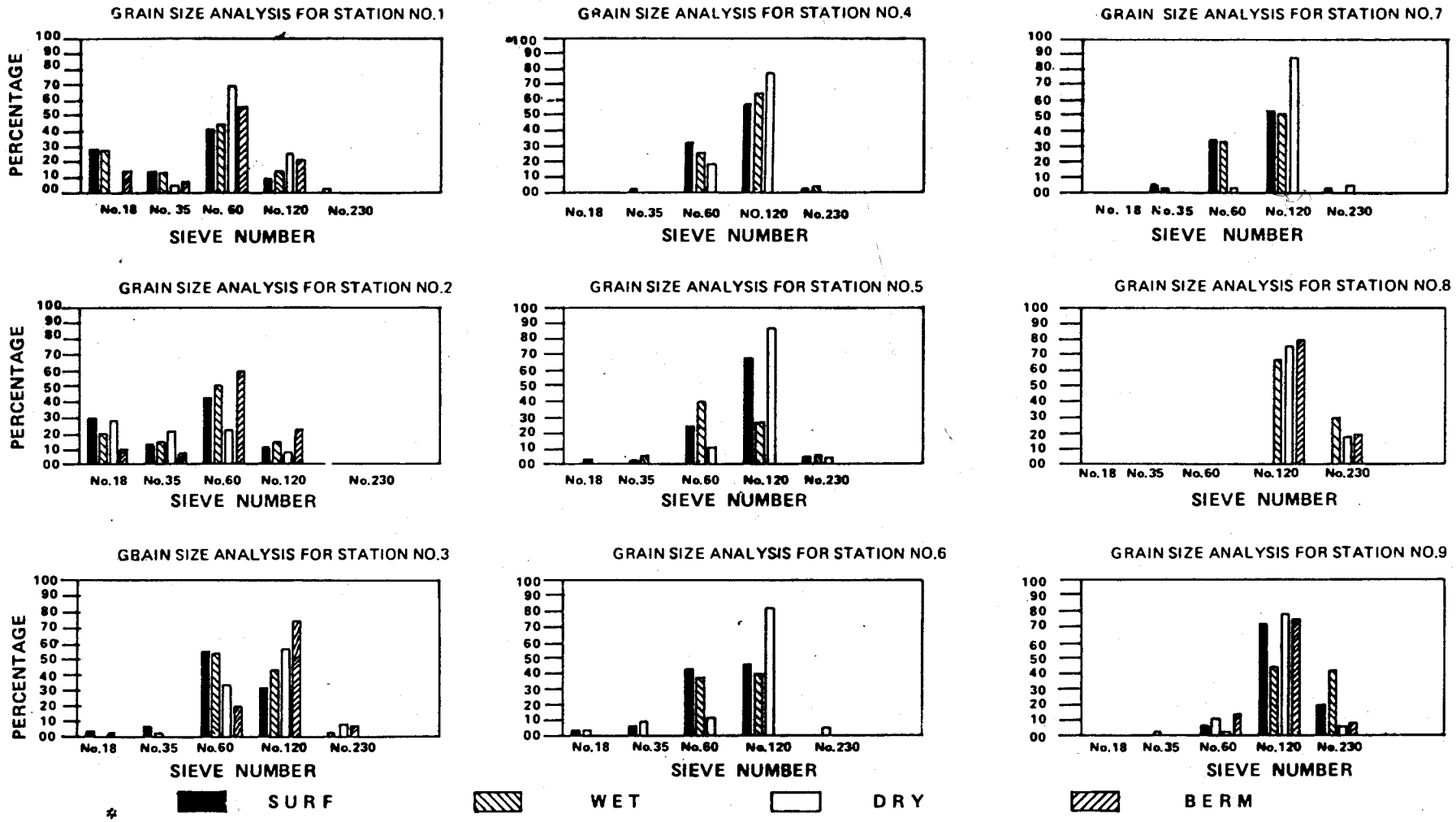

*FOR INDEX; SEE TABLE-1

FIG. 3 THE ASSOCIATION OF HEAVY MINERALS WITH GRAIN SIZE AT DIFFERENT INTERTIDAL ZONES.

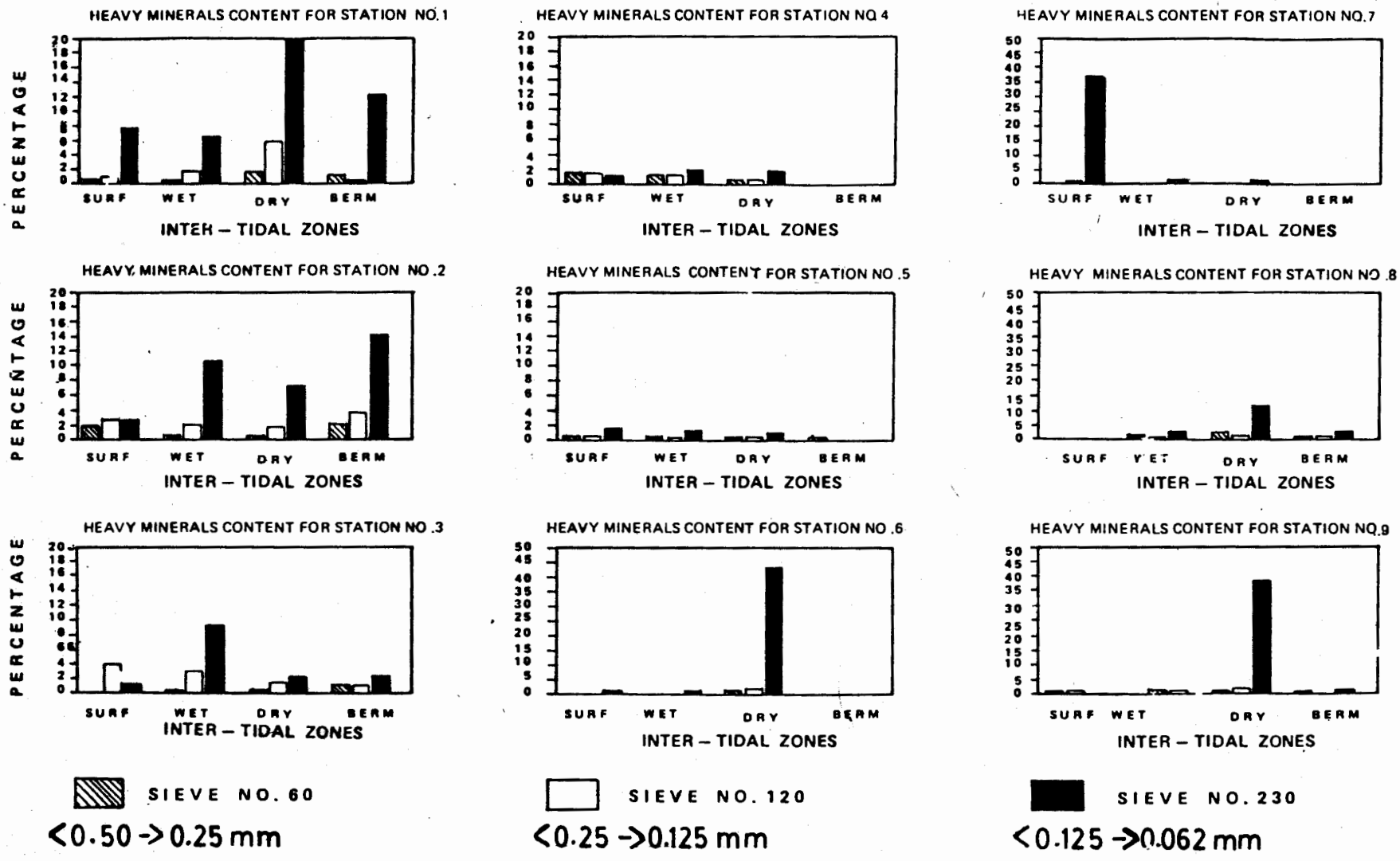

0.0625 m m fraction indicates that there is no contribution of marine sediments. Thus the detrital sediments are dominating and have their origin alongwith heavy minerals on the land. The association of ilmenite, zircon, rutile and tourmaline indicates that the provenance of the heavy minerals concentrated along this beach is the acidic as well as the basic igneous rocks. The concentration of heavy mineral placers has taken place from the reworked sediments. The exceptional occurrence of limonite on station 9 indicates the contribution from an additional source alongwith the others mentioned above. The concentration of heavy minerals in the various intertidal zones indicate the prevailing of favourable hydro-physiographic environments during the geologic development of modern coast. The results shown in table 2 represent the quantity of heavy minerals present in the size-fraction 0.125 to 0.0625 mm. The estimation of heavy mineral relative to the total volume of sample reveals, that the percentage of heavy mineral is very low (0.5 - 1.00%). On the basis of so few samples it is not possible to indicate the economic value of the deposits. It is suggested that more sampling should be carried out for further exploration of heavy minerals along the coastal areas of Pakistan.

ACKNOWLEDGEMENTS

The authors wish to thank Dr. G.S. Quraishee, Director, National Institute of Oceanography, Karachi, Mr. Abul Farah, Chief Scientist of N.I.O. and Prof. Iqbal Mohsin for their support and instructive communication during the various phases of this project. Thanks are due to Mr. A.R. Tabrez and many other staff members of N.I.O. for their assistance.

REFERENCES

DUNHAM, K.C. (1969) Practical geology and the natural environment of Man-II. Quart. Jour. Geol. Soc. London, **124**, pp. 101-129.

MILLIMAN, J.D., QURAISHEE, G.S. & BEG, M.A.A. (1984) Sediment discharge from the Indus River to the ocean: past, present and future. ***In:*** Haq, B.U. & Milliman, J.D. (eds.) MARINE GEOLOGY AND OCEANOGRAPHY OF ARABIAN SEA AND COASTAL PAKISTAN. Van Nostrand Reinhold Co. New York, pp. 65-70.

SIDDIQUI, M.N., GUJAR, A.R., HASHIMI, N.H. & VALSANGKAR, A.B. (1984) Surface mineral resources of the Indian Ocean. Deep Sea Research **31**, pp. 763-812.

PETTIJOHN, F.J., POTTER, P.E. & SIEVER, R. (1983) SAND AND SANDSTONE. Springer-Verlag, New York, 618p.

Orally presented on 21.10.1987
Manuscript revised on 31.12.1987

ACTA MINERALOGICA PAKISTANICA
VOLUME 3 (1987) pp. 97 - 110

THE PALEOGENE STRATIGRAPHY OF THE KALA CHITTA RANGE, NORTHERN PAKISTAN

AFTAB AHMAD BUTT
Institute of Geology, Punjab University, Lahore-20, Pakistan.

ABSTRACT: The geology of the Kala Chitta Range is an integral part of the structural units of the Kohat-Potwar-Hazara region, northern Pakistan. The sedimentary geology of the Kala Chitta Range has similarities with the adjoining areas. However, there are certain differences in the stratigraphy and the geological history.

The structural evolution of the Kala Chitta Range began in the Mesozoic time and attained its maximum by the end of the Eocene time. The deposition of the Upper Cretaceous (Coniacian-Campanian) Kawagarh Formation in a narrow belt along the northern part of the Range, intergradation of the Upper Paleocene (Thanetian) sedimentary facies, the continuity of the stratigraphic and the paleogeographic setting across the Paleocene-Eocene boundary, a marked shift in the paleogeographic pattern from north to south by a southward trend of younging of strata, especially during the Middle Eocene, are some of the salient geological features of this structural entity.

First major stratigraphic break between the Upper Cretaceous Kawagarh Formation (Coniacian-Campanian) and the Upper Paleocene (Thanetian) Lockhart Limestone is marked by a ferruginous pisolite. The second major break between the Middle Eocene Kohat Formation and the Miocene Murree Formation is marked by a pebbly deposit --- the Fatehjang Member.

An attempt is made to review the stratigraphic, biostratigraphic as well as the paleogeographic setting of the region in the context of basin analysis framework.

INTRODUCTION

The Kala Chitta Range forms the northern edge of the Potwar Basin (fig. 1). It is a narrow strip of mountainous region, which merges laterally into the Hazara Mountains (including Margala Hills, north of Islamabad) towards the eastern direction, and extends westward into the Samana Range (the main towns located are Hangu and Kohat). In terms of plate tectonic activity, the Kala Chitta Range is one of the epicontinental troughs developed along the collision margin as a result of continent to continent collision.

The geology of the Kala Chitta Range is an integral part of the structural units of the Kohat-Potwar-Hazara region, northern Pakistan. The sedimentary geology of the Kala Chitta Range has similarities with the adjoining areas. However, there are certain differences in the stratigraphy and the geological history. The structural evolution of the Kala Chitta Range began in the Mesozoic time and continued to develop till the Miocene. The Miocene characterises the Kala Chitta Range as a hinterland to the adjacent potwar Basin of active fluviatile deposition of the

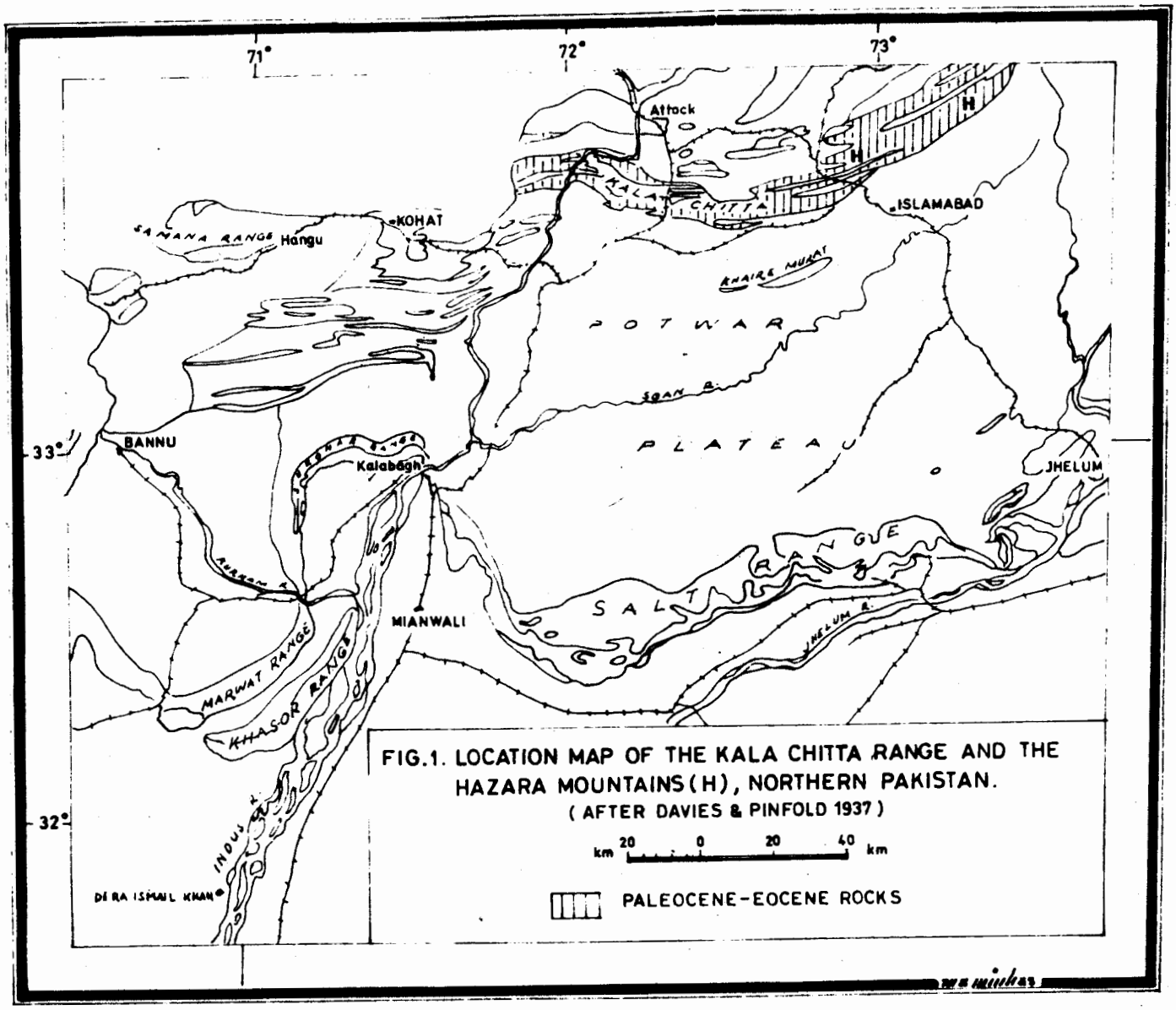

Murree Formation and the Kala Chitta Range thus develops a marginal rim of these deposits.

Cotter (1933) gave a comprehensive account of the stratigraphy of the Kala Chitta Range and reproduced a structural cross-section (fig. 2) to elucidate the difference in structural style of the Kala Chitta Range with those of the adjoining areas. According to Cotter (1933), the Jurassic sediments formed the base of the stratigraphic succession of the region, while the ammonite fauna studied by Fatmi (1973) pointed out the presence of the Triassic rocks.

First major unconformity occurs between the Upper Cretaceous (Coniacian-Campanian) Kawagarh Formation and the Upper Paleocene (Thanetian) Lockhart Limestone. It is marked by a ferruginous pisolite. The second major unconformity occurs between the Middle Eocene Kohat Formation and the Miocene Murree Formation and is marked by a pebbly deposit --- the Fatehjang Member.

Stratigraphic, biostratigraphic as well as the paleogeographic setting of the region is reviewed in the context of basin analysis framework, which includes various geological events that occurred in the region and their geological implications. The following table outlines the comparative stratigraphic setting of the Kohat-Potwar-Hazara region (fig. 3).

GEOLOGICAL NOTES

The basinal evolution of the Kala Chitta Range began in the Mesozoic time. It started with the deposition of the Triassic shallow shelf

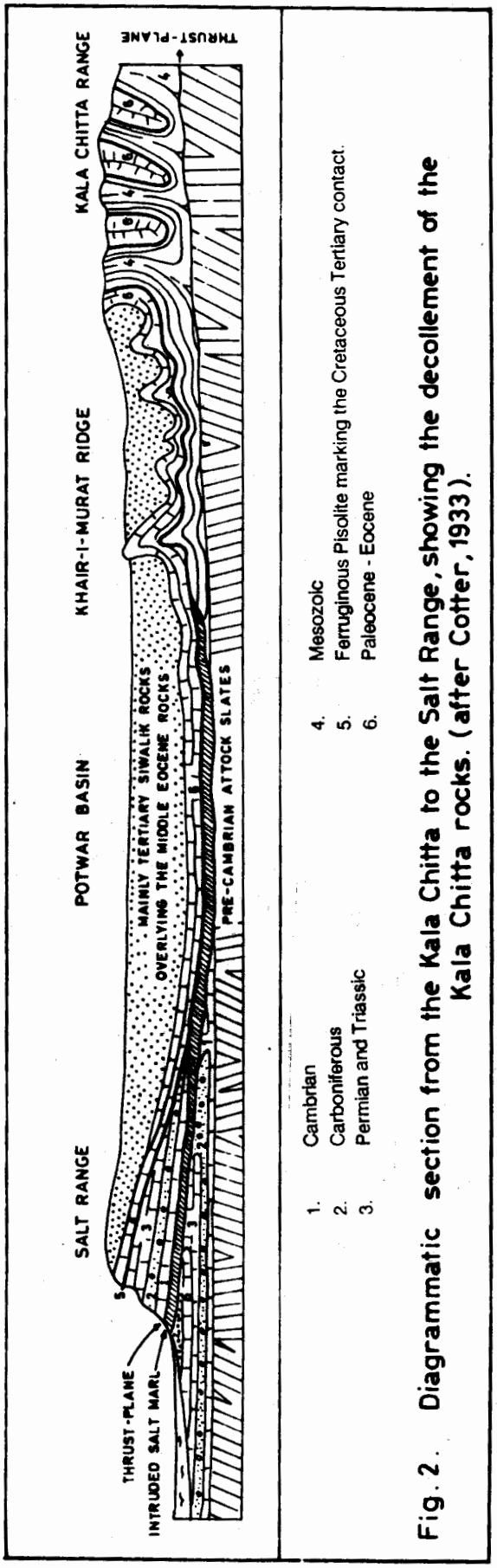

Fig. 2. Diagrammatic section from the Kala Chitta to the Salt Range, showing the decollement of the Kala Chitta rocks. (after Cotter, 1933).

carbonates of limited extent in a narrow elongated depression. The onset of the Jurassic period is marked by the shallowing of the Triassic sea. This is manifested by the Red Bed Facies (Cotter's "Ferruginous Beds" at the base of the "Kioto Limestone") indicating a continental type of environment. This facies (now called the Datta Formation) is followed by a major marine transgression in the Kala Chitta Range when the Jurassic Samana Suk Limestone (Cotter's Kioto Limestone) is deposited as shallow shelf carbonate over large area as compared to the earlier sedimentation.

The Upper Jurassic time introduces partially an anoxic event in the paleogeographic setting of the region resulting in the formation of black shale facies (Chichali Formation), a product of reducing environments of a restricted marine basinal setting, while the Lower Cretaceous period returns to normal marine conditions by depositing shallow marine glauconitic sandy beds (Lumshiwal Formation).

The beginning of the Upper Cretaceous time is a remarkable geological event in the history of the Kala Chitta Range when the entire Kala Chitta is uplifted and remains exposed from Cenomanian to Turonian time. During Coniacian and upto the Campanian there happens a marine transgression in the more northerly part of the Kala Chitta Range by depositing outer neritic micritic facies (Kawagarh Formation) in a narrow belt. The presence of planktonic foraminifera in this formation indicates deeper shelf environment. In fact, the deposition of the Kawagarh Formation in the Kala Chitta Range presents the only paleogeographic setting in the entire geological history of the Kala Chitta when deepening of the narrow trough is envisaged, otherwise the entire geological record reveals deposition of shallow water sediments in a gradually subsiding trough.

During Maastrichtian, there is a major "draining off" of the sea (event of non-deposition) by exposing the Kawagarh Formation to the chemical weathering processes while in the remaining Kala Chitta, the Lumshiwal Formation becomes exposed to the epidiagenetic changes.

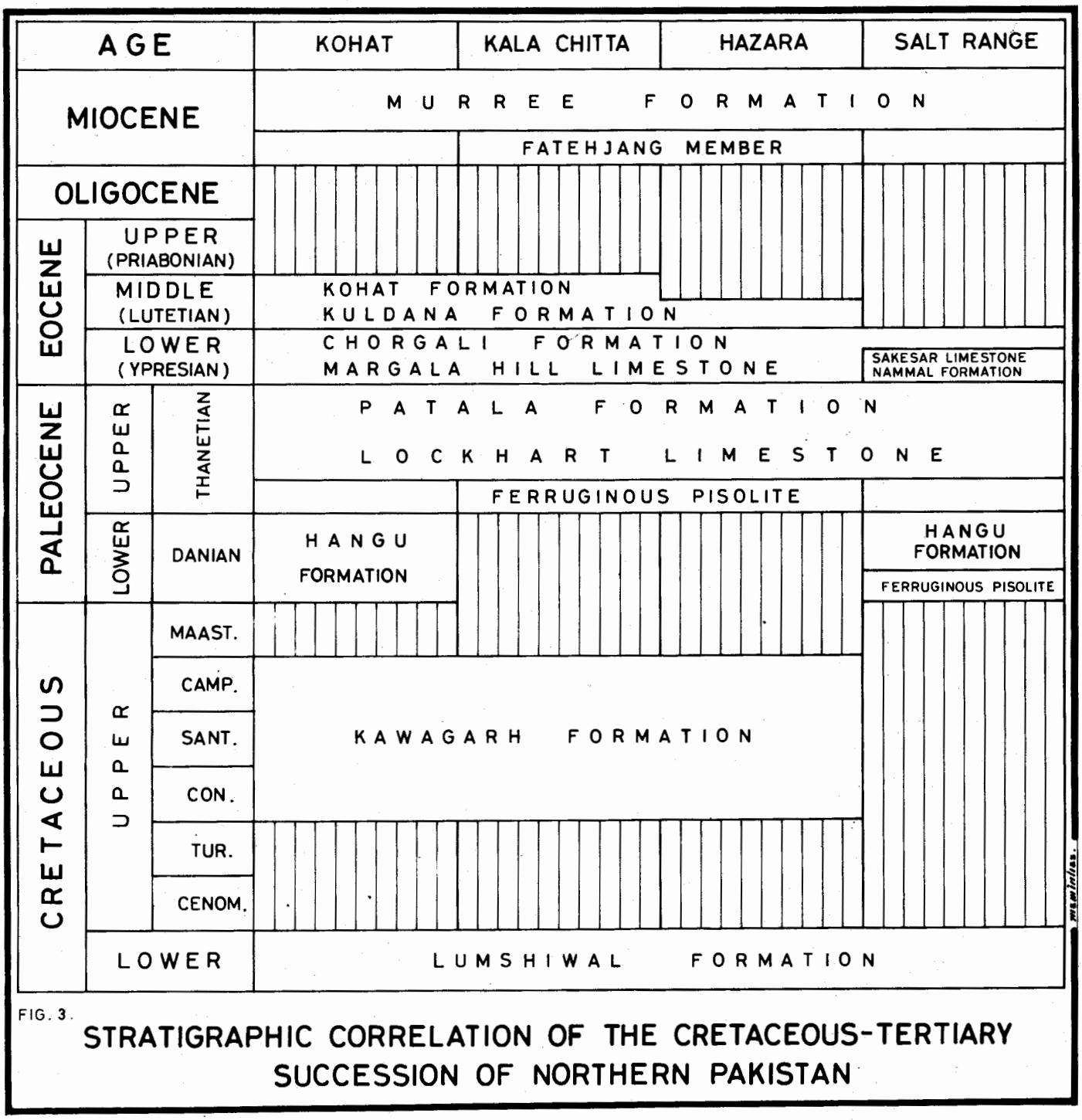

FIG. 3.

STRATIGRAPHIC CORRELATION OF THE CRETACEOUS-TERTIARY SUCCESSION OF NORTHERN PAKISTAN

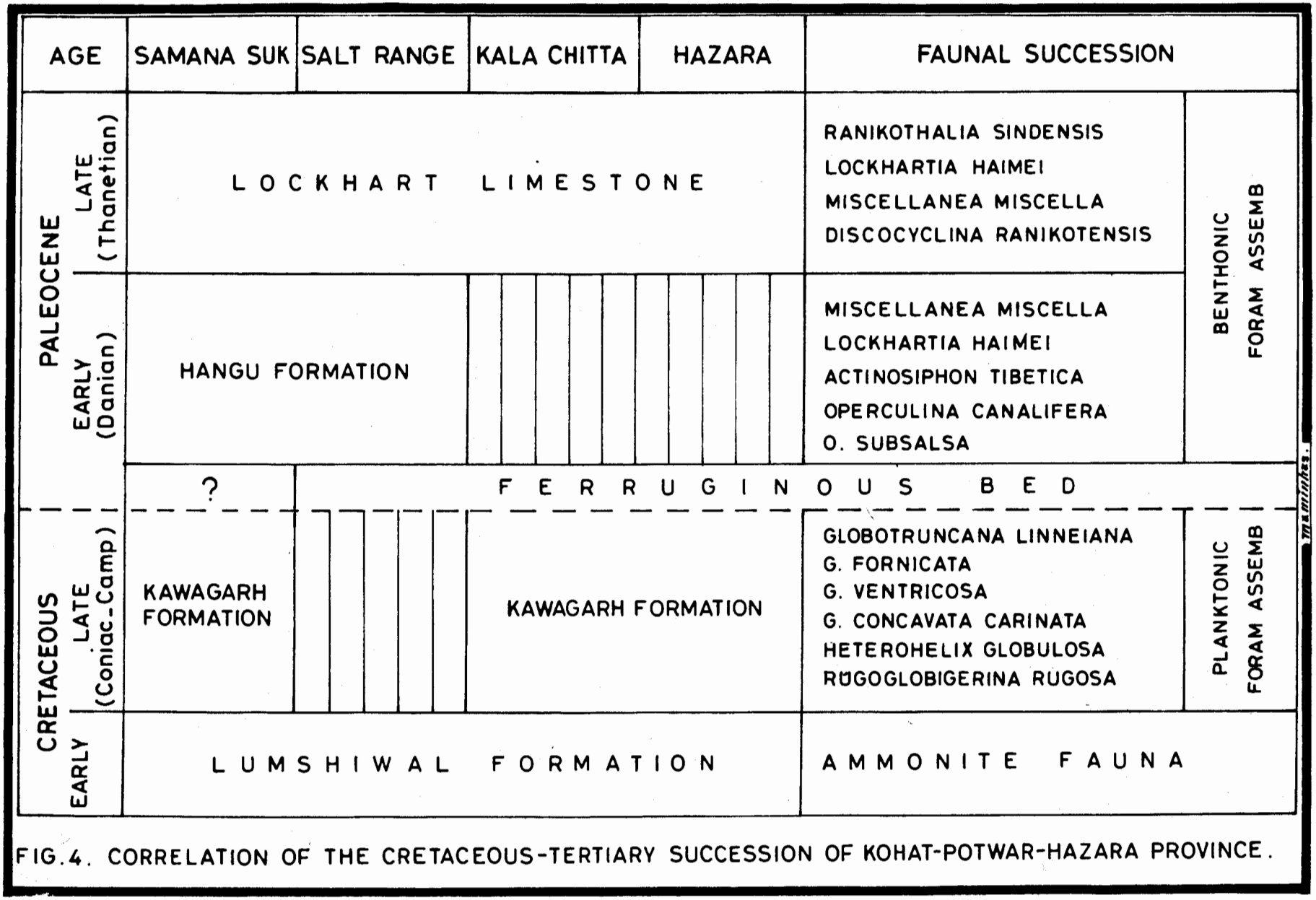

FIG. 4. CORRELATION OF THE CRETACEOUS-TERTIARY SUCCESSION OF KOHAT-POTWAR-HAZARA PROVINCE.

Description of Figures 5 — 9

Figs. 5-9 are photographs at magnification x 360.
Figs. 5 and 6 contain Paleocene forms from the Lockhart Limestone; figs. 7 to 9 contain Lower Eocene forms from the Margala Hill Limestone. {*Discocyclina ranikotensis, Assilina subspinosa, Lockhartia conditi* and *Lockhartia tipperi* range from Upper Paleocene to Lower Eocene}.

Fig. 5. A-H: *Miscellanea miscella* (d'ARCHIAC & HAIME) Lockhart Limestone, Upper Paleocene (Thanetian) Photograph C also shows *Lockhartia haimei* (DAVIES) and *Ranikothalia sindensis* (DAVIES), the latter species seen in Photograph E, as well.

Fig. 6. A-B: *Lockhartia haimei* (DAVIES)
(C) *Discocyclina ranikotensis* (DAVIES)
(D) *Miscellanea miscella* (d'ARCHIAC & HAIME)
Ranikothalia sindensis (DAVIES)
(E) *Miscellanea miscella* (d'ARCHIAC & HAIME)
Ranikothalia sindensis (DAVIES)
Lockhartia tipperi (DAVIES)
(F) *Ranikothalia sindensis* (DAVIES)
Eoannularia eocenica (COLE & BERMUDEZ)
(G) *Operculina subsalsa* DAVIES & PINFOLD

Fig. 7. (A): *Assilina graulosa* (d'ARCHIAC)
(B) *Ranikothalia sindensis* (DAVIES)
Lockhartia conditi (NUTTAL)
Assilina laminosa GILL
(C) *Assilina laminosa* GILL
(D) *Nummulites mamillatus* (FICHTEL & MOLL)
(E) *Nummulites mamillatus* (FICHTEL & MOLL)
Nummulites atacicus LEYMERIE
Assilina laminosa GILL
Assilina granulosa (d'ARCHIAC)
(F) *Discocyclina dispansa* SOWERBY
(G) *Lockhartia conditi* (NUTTAL)

Fig. 8. (A): *Assilina subspinosa* DAVIES & PINFOLD
Nummulites sp.
Lockhartia conditi (NUTTAL)
(B-D) *Ranikothalia solimani* BUTTERLIN & MONOD characterised by thick test and involute spiral. In Figs. 3-4, are also seen *Nummulites mamillatus* (FICHTEL & MOLL), *Nummulites atacicus* LEYMERIE, *Assilina laminasa* GILL
(E,F) *Lockhartia tipperi* (DAVIES)

Fig. 9. (A,B) *Fasciolites (Flosculina) ellipticus* (SILVERSTRI)
(C,D) *Discocyclina dispansa* SOWERBY
(E,F) *Nummulites mamillatus* (FICHTEL & MOLL)
Operculina spp.
(G) *Discocyclina ranikotensis* (DAVIES)
Assilina laminosa GILL
(H) *Discocyclina ranikotensis* (DAVIES)
(I) *Ranikothalia solimani* BUTTERLIN & MONOD.

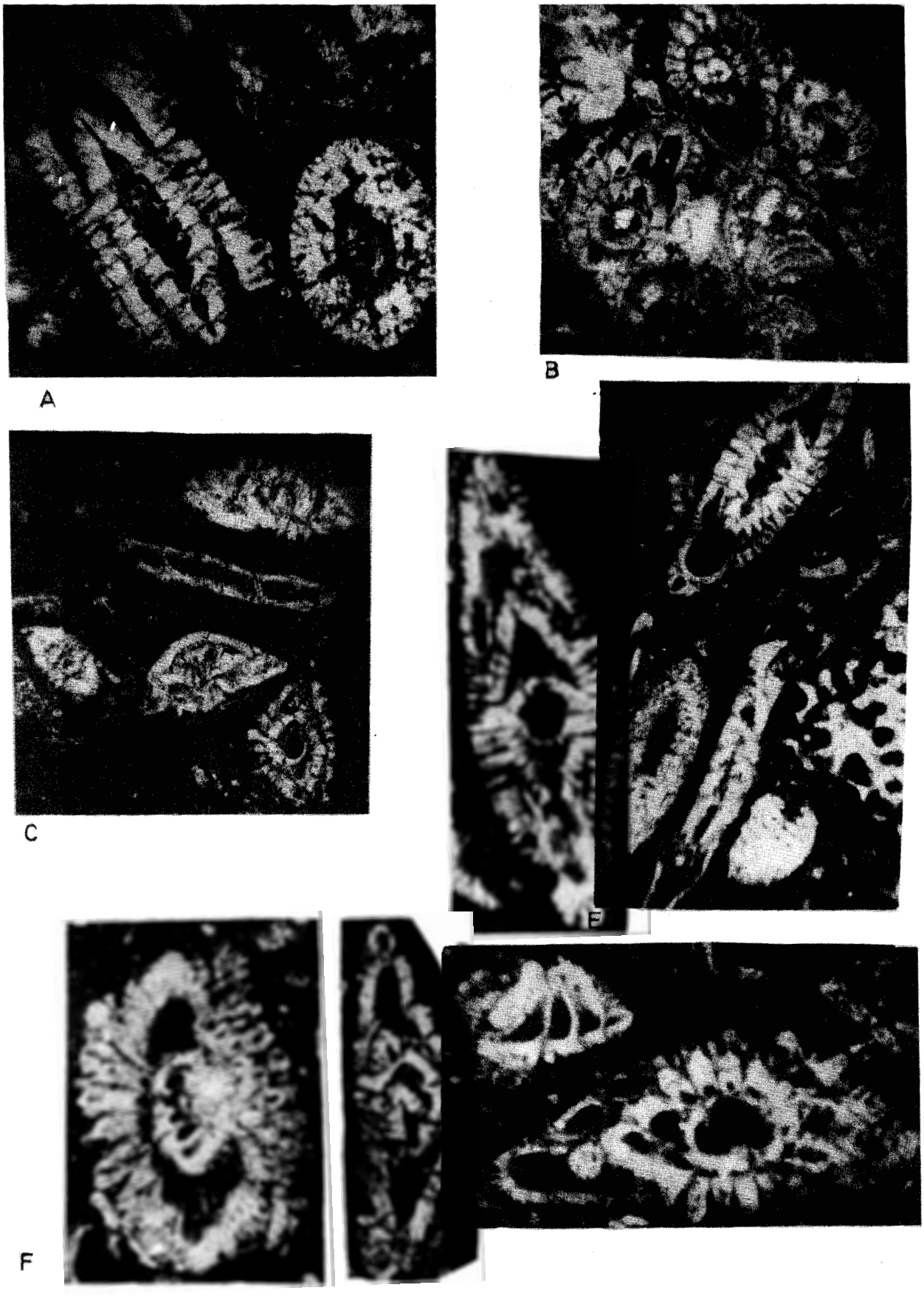

Fig. 5

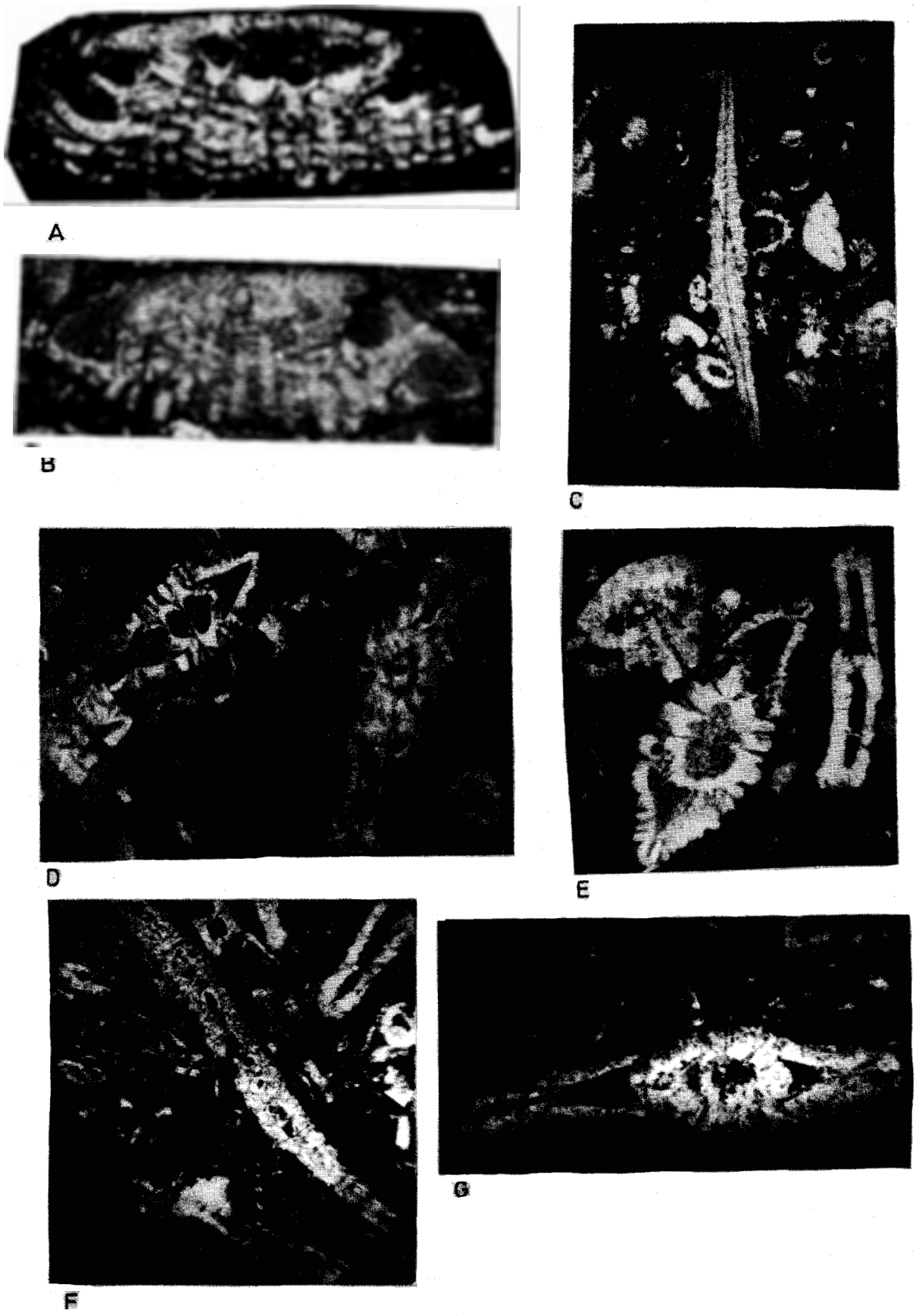

Fig. 6

A

B

C

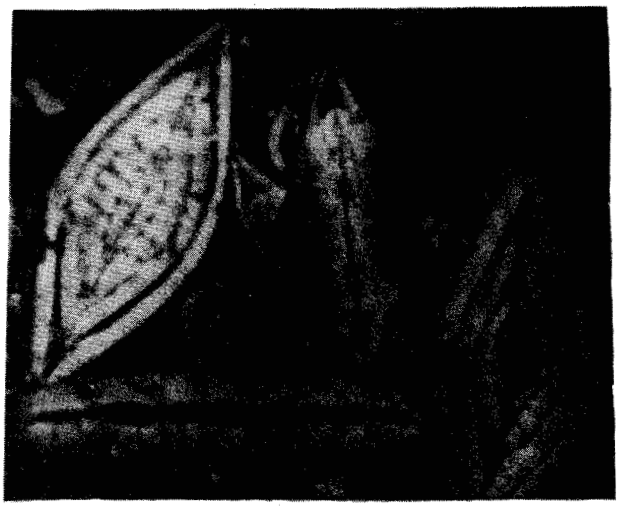

E

D

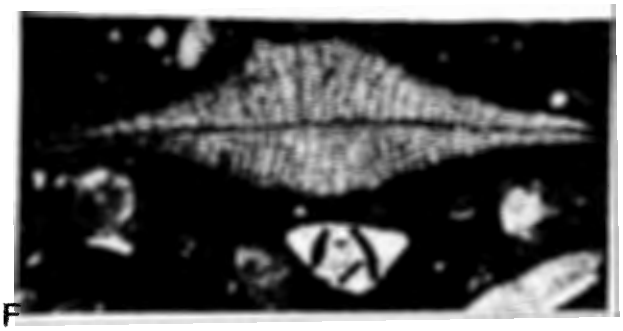

F

G

Fig. 7

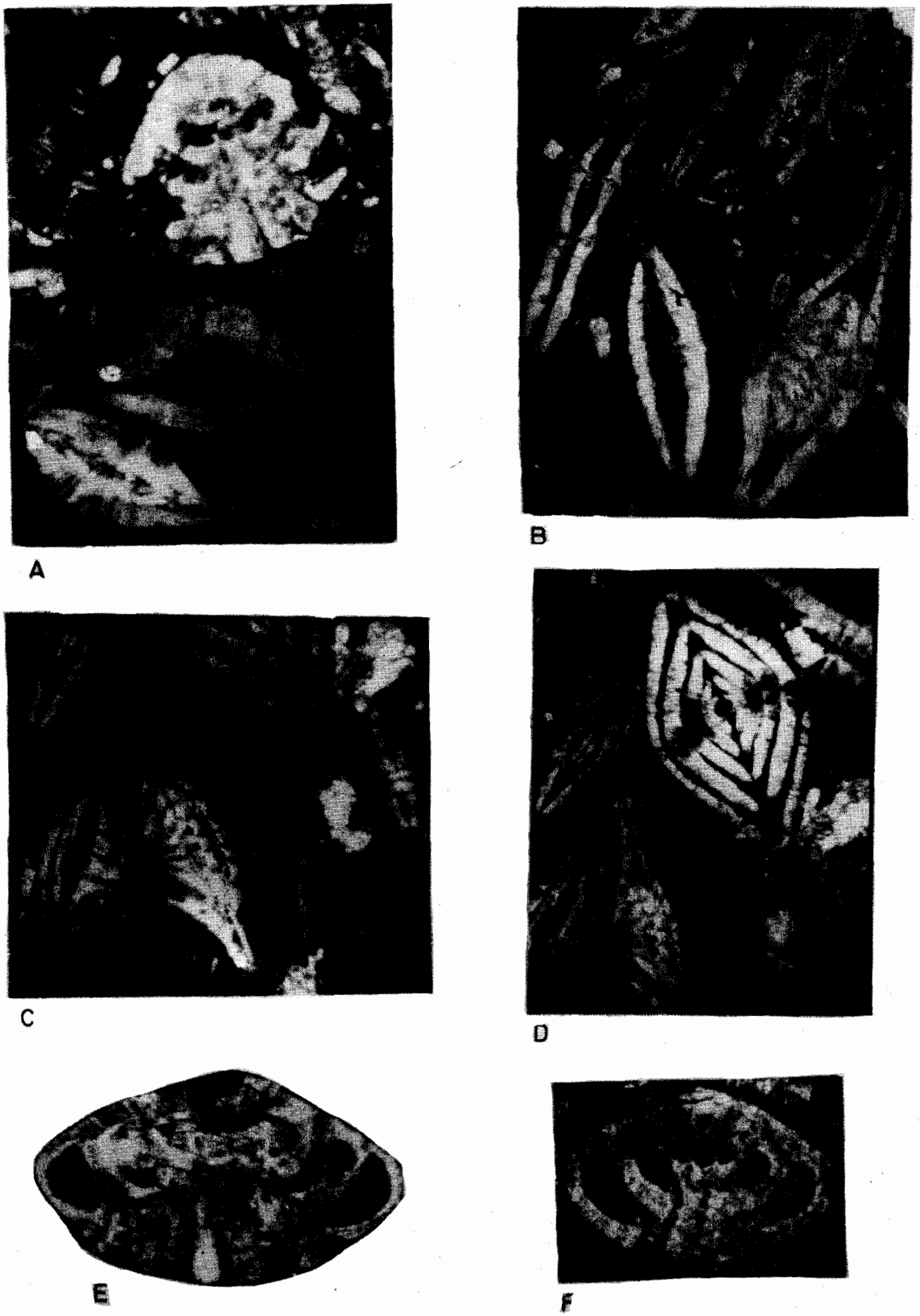

Fig. 8

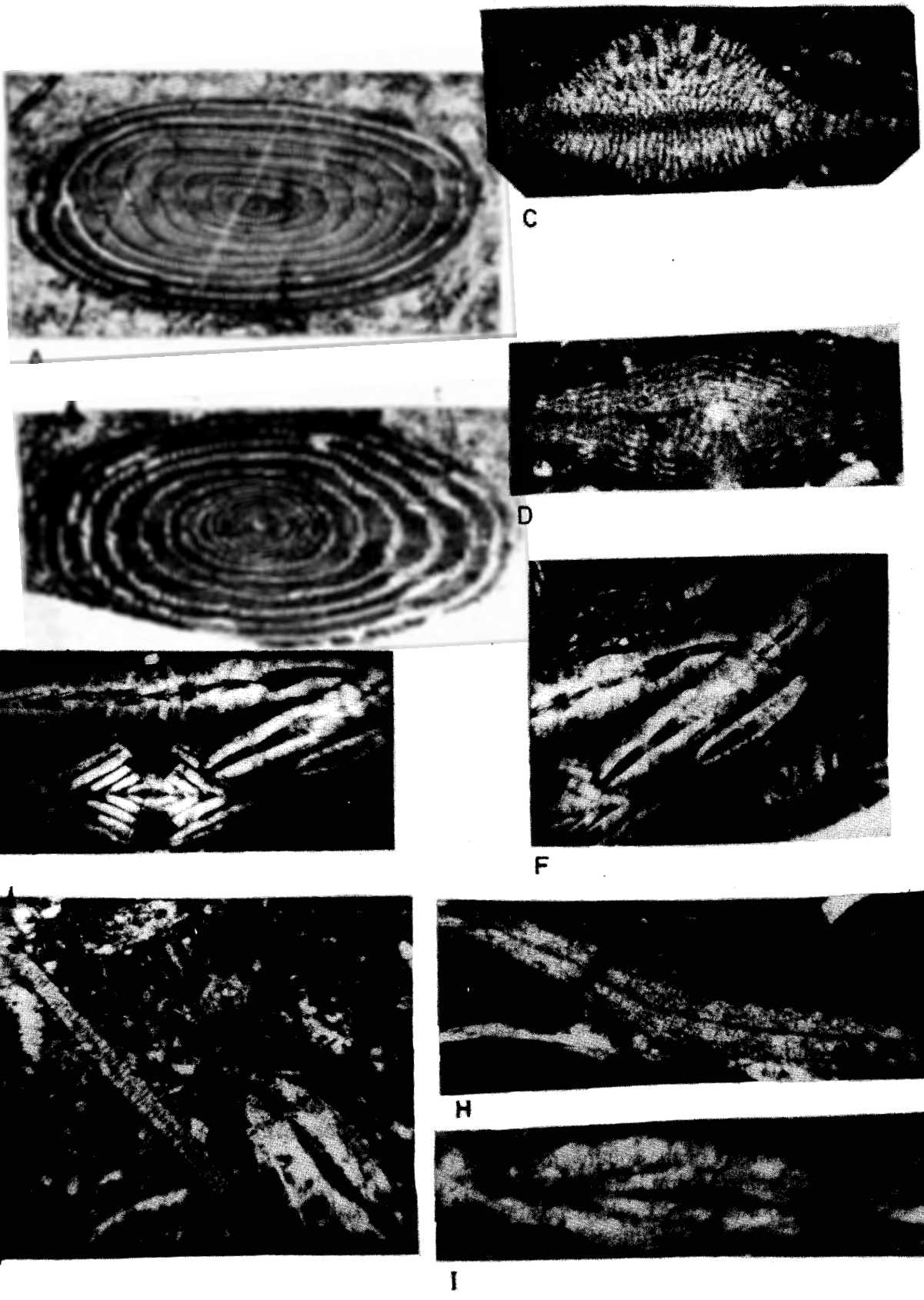
A
B
C
D
E
F
G
H
I

Given sufficient time gap (Maastrichtian to Danian), the Kawagarh Formation, subjected to chemical weathering processes, becomes overlain by ferruginous pisolite, which marks the first major stratigraphic break (unconformity) of the Cretaceous - Tertiary succession (Maastrichtian to Danian). The Cretaceous - Tertiary boundary has been outlined for a comparative study of the stratigraphic setting of these areas (fig. 4).

The Upper Paleocene (Thanetian) brings a major transgression in the Kala Chitta Range and covers a much larger area as compared to previously deposited stratigraphic units. During this time, shallow shelf carbonates (the nodular Lockhart Limestone) containing stratigraphically important benthonic larger foraminifera are laid down. It is succeeded by shaly deposits (Patala Formation) but there are inerbeds of shale and limestone. One can say that the recognition of the two fold division of the Upper Paleocene into Lockhart Limestone and the Patala Formation due to the interbedding of shale and limestone is subjective.

The Lower Eocene also displays the continued shallow shelf carbonate deposition of the nodular Margala Hill Limestone. This draws attention towards a continuity in the paleogeographic setting of the Kala Chitta Range across the Paleocene - Eocene boundary and the consistency in the basinal configuration. However, after the deposition of the Margala Hill Limestone, there is a marked change in the paleographic setting in the Kala Chitta Range. This is again a major geological event in the geological history when a trend of younging of strata towards the southerly portion of the range can be observed during the Lower Eocene. This shows a marked southward shift in the basinal configuration which is demonstrated by the deposition of the flaggy limestone (Chorgali Formation) in a narrow belt only in the southerly part of the range. The continuity of the southward shift of the paleogeographic setting is further substantiated in the Middle Eocene by the deposition of the Kuldana Formation and the Kohat Formation.

The deposition of the Kuldana Formation (Red Bed Facies) reflects dominantly a non-marine environment. This is in turn, changed into normal marine shallow-water environments when the Kohat Formation containing abundant Nummulitic fauna (predominantly coin size Assilines) is deposited as Nummulitic Bank beds. The Kohat Formation, however, marks the end of the Paleogene deposition in the Kala Chitta Range.

The Upper Eocene marks a major geological event in the geological history of the Kala Chitta Range. At this time the entire Kala Chitta is uplifted and this event also contributes towards the maximum structural modification in the region. The area remains exposed from Upper Eocene to the entire Oligocene time till the advent of the Miocene when the most southerly part of the range acts as a hinterland to the adjoining Potwar Basin of active fluviatile deposition. Interval from Upper Eocene to Oligocene marks the second major stratigraphic break in the geological record of the Kala Chitta Range.

The Miocene establishes a paleogeographic setting when the Kala Chitta Range develops a marginal rim of the Murree Formation along its southern edge. These sediments are more significant towards the geological history of the adjoining Potwar Basin which is more actively subsiding to receive sediments of greater thickness.

STRATIGRAPHIC NOTES

The stratigraphy of the Kala Chitta Range is influenced by the structural style of this mountainous belt. In this respect, reference can be made to the cross section of Cotter (1933) in which the structural style of th Kala Chitta Rage as an extremely tight isoclinal folding has been displayed (fig. 2). This structural framework happens to be the result of the intensive compressional forces applied to the sediments which were deposited into a narrow elongated depression.

As the stratigraphy of the Kala Chitta Range is a succession of limestone and shale, the isoclinal folding has been further subjected to the compressional forces, shales offering agent of lubrication, to produce structural dislocation in alignment of steeply dipping strata. This would

on one hand, produce sandwiches of limestone and shale and on the other hand, demonstrate overriding of strata. Interbedding of shale and nodular limestone, therefore, renders difficulty for recognition of the Paleocene Lockhart Limestone (nodular) and the Patala Shale as is the case around Ratta Kund. However, exposure of interbeds of the shale and bedded limestone along the Chooi-Basal Road towards the southern extremity of the Kala Chitta Range is a recognisable section of the Patala Formation. The Jurassic Samana Suk Limestone overriding the Paleocene Lockhart Limestone can be observed along the railway track from Jhalar Railway Station proceeding north, after passing couple of tunnels, beyond Ratta Kund (survey sheet 43 C/6).

In northern Pakistan (Kohat-Potwar, Hazara region) the classical locality of a complete Paleocene succession, where both lithological and paleontological control is available, is that of the Salt Range. It comprises the threefold division originally described as the Dhak Pass Beds, Khairabad Limestone (nodular) and the Patala Shales (Davies and Pinfold, 1937). The Salt Range, in fact, offers a standard Paleocene section in the Kohat-Potwar-Hazara region, to interpret the Paleocene sequence of the Kala Chitta Range or the Hazara Mountains. Davies and Pinfold (1937) described and illustrated the characteristic Paleocene benthonic larger foraminiferal species from the Salt Range, for example, *Miscellanea miscella* (d'Archiac & Haime), *Lockhartia haimei* (Davies), *Ranikothalia sindensis* (Davies), *Ranikothalia nuttali* (Davies), *Actinosiphon tibetica* (Douville), *Operculina patalensis* Davies & Pinfold, *Assilia dandotica* Davies & Pinfold, while foraminiferal species such as *Discocyclina ranikotensis* Davies, *Assilina subspinosa* Davies & Pinfold, *Lockhartia tipperi* (Davies), *Lockhartia conditi* (Nuttal) are ranging into the Lower Eocene as well.

The other locality constituting the threefold Paleocene succession (Davies 1930) is that of the Samana Range (Kohat region). Because of the nature of the depositional environments and the resulting clastic sediments, the Lower Paleocene Hangu Formation is unfossiliferous. However, the Upper Paleocene nodular Lockhart Limestone and the Patala Formation contain stratigraphically important foraminiferal species recorded and illustrated by Davies (1930) i.e., *Lockhartia haimei* (Davies), *Miscellanea miscella* (d'Archiac & Haime) and *Ranikothalia thalicus* (Davies).

In the Kala Chitta Range and the Hazara Mountains, only the Upper Paleocene strata including the Lockhart Limestone and the Patala Formation are developed. Benthonic larger foraminiferal species of stratigraphic importance have been illustrated from the Upper Paleocene Lockhart Limestone and the Lower Eocene Margala Hill Limestone of the Kala Chitta Range (fig. 5-9). In terms of biozonation, the Paleocene - Eocene boundary is characterised by the exit of *Lockhartia haimei* (Davies), *Miscellanea miscella* (d'Archiac & Haime) and the entry of *Nummulites mamillatus* (Fichtel & Moll). The Cretaceous-Tertiary contact in the Kala Chitta and the Hazara Ranges is marked by a marker bed, the ferruginous pisolite between the Upper Cretaceous Kawagarh Formation (Coniacian-Campanian) and the Upper Paleocene nodular Lockhart Limestone (Thanetian).

At present, the faunal content of the Lower Eocene Chorgali Formation (flaggy limestone overlying the Margala Hill Limestone) has not been examined in detail. From the field observation, the formation appears to be inadequately fossiliferous. As one moves up in the succession, the overlying Middle Eocene Kuldana Formation by virtue of its fluvial dominated depositional environments, is barren of foraminifera. The overlying Kohat Formation (Cotter's Upper Chharat Beds) is extremely fossiliferous. The Nummulites and large size Assilines are almost making the rock. One can conclude that the Kohat Formation has been deposited beyond any doubt, as a Nummulitic Bank Facies.

CONCLUSIONS

1. The geology of the Kala Chitta Range is quite varied. Its basinal evolution began in the Mesozoic time and continued upto the Miocene, attaining its maximum at the end of the Eocene.

2. The dominant alternating aspects of limestone and shale of the Paleocene age cause

difficulty to recognize the Lockhart Limestone and the Patala Shale. This calls for a detailed biostratigraphic study for a better understanding of the Paleocene succession.

3. The biozonation of the Paleocene-Eocene succession can be made because of the presence of several age-diagnostic foraminifera. There is also a continuity in the paleogeographic setting (shallow-water enviroment) across the boundary. The Paleocene-Eocene boundary is marked by the disappearance of *Lockhartia haimei* (Davies), and *Miscellanea miscella* (d'Archiac & Haime), and the appearance of *Nummulites mamillatus* (Fichtel & Moll).

4. The Eocene marks the end of the marine sedimentation in the Kala Chitta Range and maximum structural modification. The Miocene is the time when the Kala Chitta Range acts as a hinterland to the adjoining Potwar Basin of active fluviatile deposition to develop a marginal rim of Miocene Murree formation, which is more significant to the geology of the Potwar Basin.

5. There is a trend of younging of strata from North to South especially during the eocene time, when the Middle Eocene Red Bed Facies (Kuldana Formation) and the overlying Nummulitic Kohat Formation, while the lower Eocene Chorgali Formation underlying the Kuldana Formation were deposited in the most southerly part of the range, indicating a marked southward shift in the paleogeographic setting.

6. In view of the deposition of the Upper Cretaceous Kawagarh Formation in a narrow belt along the northern part of the Kala Chitta Range, thus exposing the underlying Lumshiwal Sandstone in the remaining part of the range for a sufficient time to weathering agencies, the Upper Paleocene transgression lends support for evaluation of reservoir characteristics of the Lumshiwal Sandstone along the unconformable contact as a result of epidiagenetic changes during the time gap (Upper Cretaceous–lower Paleocene).

REFERENCES

COTTER, G. De P. (1933) The geology of the part of the Attock District west of longitude 72° 45 E. Mem. Geol. Surv. India, 55, pt. 2, pp. 63-161.

DAVIES, L.M. (1930) The fossil fauna of the Samana Range. Mem. Geol. Surv. India, Pal. Indica, New Series, 15, pt. 1. An Introductory Note, pp. 1-15; pt. 6. The Paleocene Foraminifera, pp. 67-79.

——— & PINFOLD, E.S. (1937) The Eocene beds of the Punjab Salt Range. Mem. Geol. Surv. India, Pal. Indica, New Series, 24, pp. 1-79.

FATMI, A.N. (1974) Lithostigraphic Units of the Kohat-Potwar Province, Indus Basin, Pakistan. Mem. Geol. Surv. Pakistan, 10, pp. 1-80.

HOTTINGER. (1971) Larger Foraminifera common to Mediterranean and Indian Paleocene and Eocene formations. Ann. Inst. Geol. Publ. Hungary. (Colloque Strat. Eocene, 1969, Budapest, Hungary) 54, fasc. 4, pt. 1, pp. 145-151.

Orally presented on 22.10.1987
Manuscript revisedson 31.12.1987

ACTA MINERALOGICA PAKISTANICA
VOLUME 3 (1987) pp. 111 - 115

THE *RANIKOTHALIA SINDENSIS* ZONE IN LATE PALEOCENE BIOSTRATIGRAPHY

AFTAB AHMAD BUTT
Institute of Geology, Punjab Universtiy, Lahore-20, Pakistan.

ABSTRACT: The foraminiferal genus *Ranikothalia* characterises the Upper Paleocene (Thanetian) succession of Pakistan and elsewhere in the world, but does extend rarely into the Lower Eocene. A closer examination of several Upper Paleocene species from various world localities demonstrates that the open spiral complanate forms may be identified as *Ranikothalia sindensis* (Davies), which has been illustrated here from the Upper Paleocene Lockhart Limestone of the Kala Chitta Range, northern Pakistan. In view of its stratigraphic value, it is strongly advocated that the *Ranikothalia sindensis* Zone be incorporated within the Upper Paleocene (Thanetian) in the Paleogene stratigraphic correlation scale of Cavelier and Pomerol (1983). This would be one step forward towards refinement of the Paleogene biostratigraphy on the basis of benthonic larger foraminifera.

INTRODUCTION

Cavelier and Pomerol (1986; 1983) published a Paleogene stratigraphic correlation scale by combining the most valuable data of various fossil groups. They included both the planktonic and benthonic larger foraminiferal zonations in the scale. Within column 11, illustrating the stratigraphic distribution of the benthonic larger foraminiferal zones, are several *Nummulites* from the Early Eocene to Late Oligocene and thus attention is drawn towards the absence of the genus *Nummulites* in the entire Paleocene. The author strongly advocates that the Paleogene stratigraphy would be greatly refined if the stratigraphic value of the genus *Ranikothalia* is taken into account.

DISCUSSION

The genus *Ranikothalia* is very closely related to *Nummulites* but it can be distinguished on account of its thickened, fan-shaped marginal cord and complanate test. Originally erected by Caudri in 1944 from the Upper Paleocene Ranikot Beds of Sind, Lower Indus Basin, Pakistan, while describing the Carribbean fauna from Venezuela, the genus *Ranikothalia* characterises the Upper Paleocene succession of Pakistan and elsewhere in the world. However, it does extend rarely into the Lower Eocene. Although several species have been recorded in the literature from this stratigraphic interval from the American-Carribbean region, Indo-Pakistan sub-continent, and from Mali and Turkey, closer examination suggests that the majority could be identified as *Ranikothalia sindensis* (Davies).

From Pakistan, Davies (1927) illustrated *Nummulites nuttali, Nummulites thalicus* and *Nummulites sindensis* from the Upper Paleocene Strata in the Samana Range and the Salt Range (northern Pakistan) and Sind (southern Pakistan), which actually belong to the genus *Ranikothalia* by virtue of thick marginal cord. *Ranikothalia sindensis* (Davies) can, however, be distinguished by its rapidly expanding spiral in contrast to the gradually increasing spiral of *R. nuttali* and *R. thalicus*.

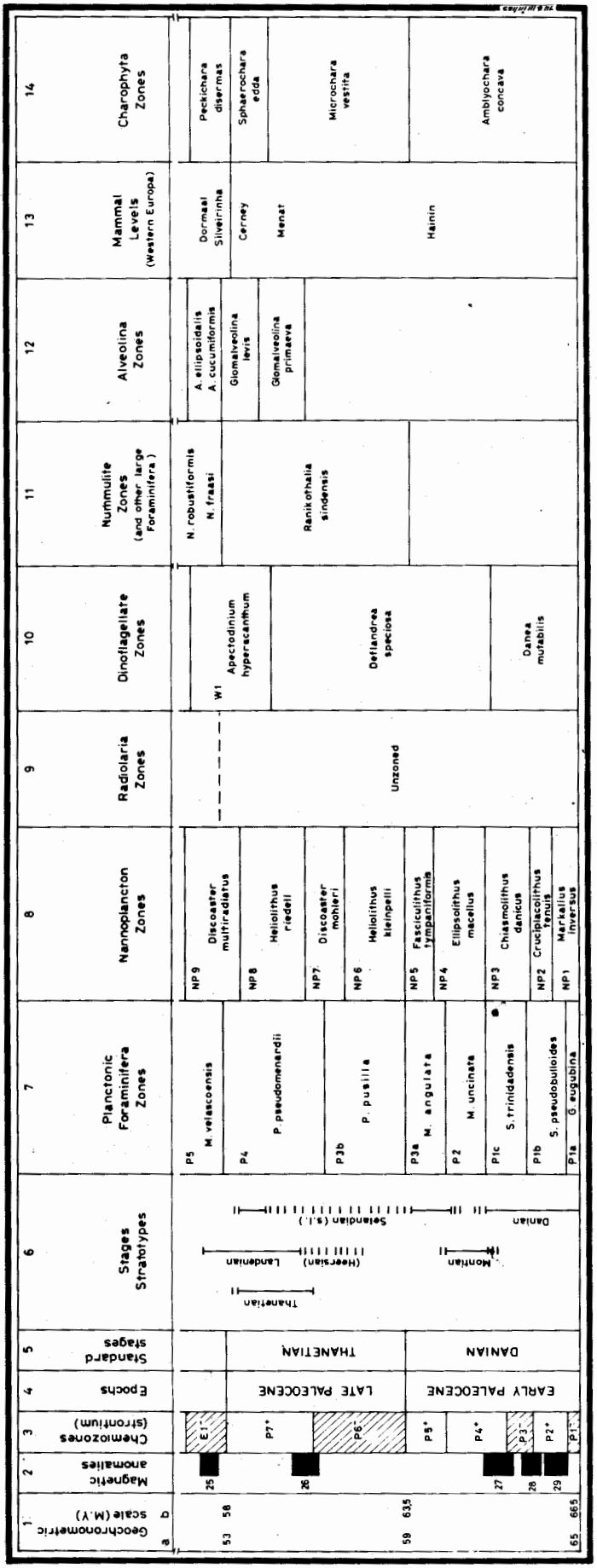

FIG. 1. INTRODUCTION OF NEWLY PROPOSED FORAMINIFERAL RANIKOTHALIA SINDENSIS ZONE IN THE PALEOGENE STRATIGRAPHIC SCALE OF CAVELIER AND POMEROL (1983)

Drooger (1960, pl. 5, figs. 1-14) has illustrated flattened form, *Raikothalia soldadensis* (Vaughan and Cole) from the Paleocene of French Guyana, while Butterlin and Mond (1969, pl. 2, figs. 1-2) have illustrated *Ranikothalia bermudezi* (Palmer), *Ranikothalia savitriae* Davies (pl. 3, figs. 1,5), *Ranikothalia sahnii* Davies (pl. 3, fig. 8) from the Lower Eocene of the Taurus Range, Turkey, all demonstrating the operculine complanate individuals. Berggren (1974) reported *Ranikothalia bermudezi* from the Upper Paleocene of Mali (Horizon III *Operculinoides bermudezi).*

The author examined a large number of specimens from the Upper Paleocene and Lower Eocene rocks of the Kala Chitta Range and Hazara Mountains, northern Pakistan. The majority of them are flattened individuals and are almost identical to the figured specimens of Drooger (1960) and Butterlin and Monod (1969). Since the name *Ranikothalia sindensis* (Davies) is oldest, it, therefore, seems appropriate to include all the above mentioned different specific names into a single species, *Ranikothalia sindensis* (Davies). This genus is illustrated here from the Upper Paleocene (Thanetian) Lockhart Limestone of the Kala Chitta Range (figs. 3,4).

In Pakistan, *Ranikothalia sindensis* (Davies) is associated with other age-diagnostic larger foraminiferal species from the Upper Paleocene (fig. 2), for example, *Miscellanea miscella* (d'Archiac and Haime), *Lockhartia haimei* (Davies), *Discocyclina ranikotensis* Davies and *Actinosiphon tibetica* (Douville), while the Lower Eocene association includes *Assilina granulosa* (d'Archiac), *Assilina laminosa* Gill, *Assilina spinosa* Davies and Pinfold, *Nummulites atacicus* Leymerie, *Nummulites mamillatus* (Fichtel and Moll). *Discocyclina dispansa* Sowerby etc.

CONCLUSION

It is proposed that the *Ranikothalia sindensis* Zone be incorporated for the Late Paleocene (Thanetian) in the stratigraphic scale (fig. 1) for further refinement of the Paleogene stratigraphic correlation scale and to acknowledge the significance of this stratigraphically important Nummulitid form.

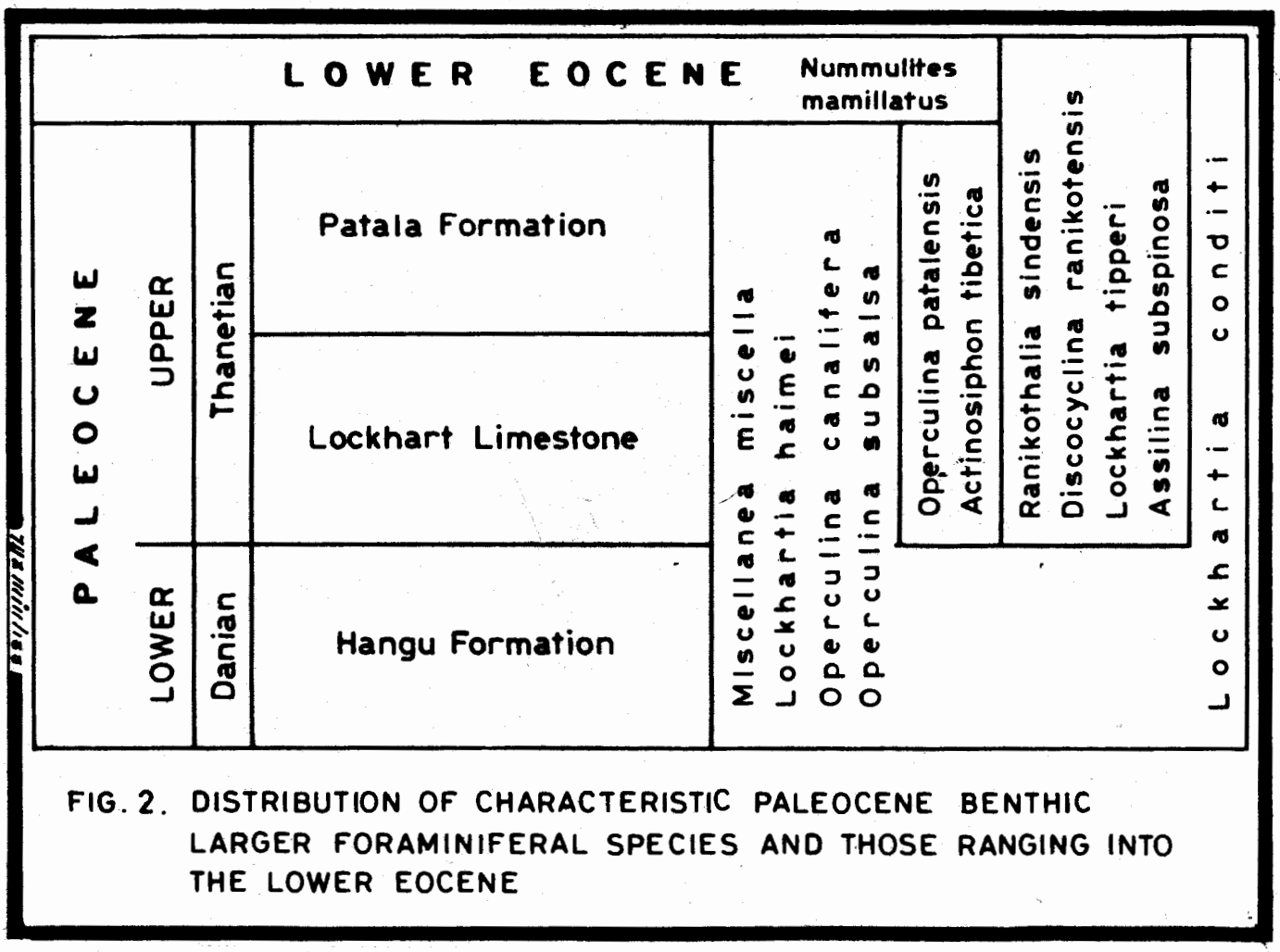

FIG. 2. DISTRIBUTION OF CHARACTERISTIC PALEOCENE BENTHIC LARGER FORAMINIFERAL SPECIES AND THOSE RANGING INTO THE LOWER EOCENE

REFERENCES

BERGGREN, W.A. (1974) Paleocene Benthonic Foraminiferal Biostratigraphy, Biogeography and Paleogeology of Libya and Mali. Micropaleontology, **20**, (4), pp. 449-485.

BUTTERLIN, J. & MONOD, O. (1969) Biostratigraphie (Paleocene d'Eocene moyen) d'une coupe dans le Taurus de Beyschir (Turquie). Etude des "Nummulites Cordelees" et revision de ce groupe. Eclogae Geologicae Helvetiae, **62**, (2), pp. 583-604.

CAUDRI, C.M.B. (1944) The Larger Foraminifera from San Juan de los Moros, State of Guarico, Venezuela. Bull. Amer. Paleont., **28**, (114), pp. 355-412.

CAVELIER, C., & POMEROL, CH. (1983) Echelle de Correlation Stratigraphique du Paleogene, stratotypes, etages standards, biozones, chimiozones, et anomalies magnetiques. Geologie de la France, **3**, pp. 261-262.

---------- **(1986)** Stratigraphy of the Paleogene. Bull. Soc. Geol. France. Ser. 8, 2, No. 2, pp. 255-265.

DAVIES, L.M. (1927) The Ranikot Beds of Thal. Quart, Jour. Geol. Soc. London, **83**, pp. 260-290.

———— **(1930)** The Fossil Fauna of the Samana Range. Mem. Geol. Surv. India, Pal. Indica, New Series, **15**, pt. 1, An Introductory Note, pp. 1-15, pt. 6, The Paleocene Foraminifera, pp. 67-79.

———— **& PINFOLD, E.S. (1937)** The Eocene Beds of the Punjab Salt Range. Mem. Geol. Surv. India. Pal. Indica, New Series, **25**, No. 1, pp. 1-79.

DROOGER, C.W. (1960) Some Early Rotaliid Foraminifera-Proc. Kon. Nederl. Akad. Wetensch. Ser. B., **63**, No. 3, PP. 287-334.

SHAH, S.M.I. (1977) Stratigraphy of Pakistan. Mem. Geol. Surv. Pakistan, **12**, pp. 1-138.

Orally presented on 22.10.1987
Manuscript revised on 31.12.1987

Fig. 3. Photographs of larger foraminifera, all are magnified to X 360.

Fig. 3. A-F,H: *Ranikothalia sindensis* (Davies).
A-C,E-F,H In association with *Miscellanea miscella* (d'Archiac & Haime) (G) *Miscellanea miscella* (d'Archiac & Haime) Lockhart Limestone, Upper Paleocene. (Thanetian) Kala Chitta Range, northern Pakistan.

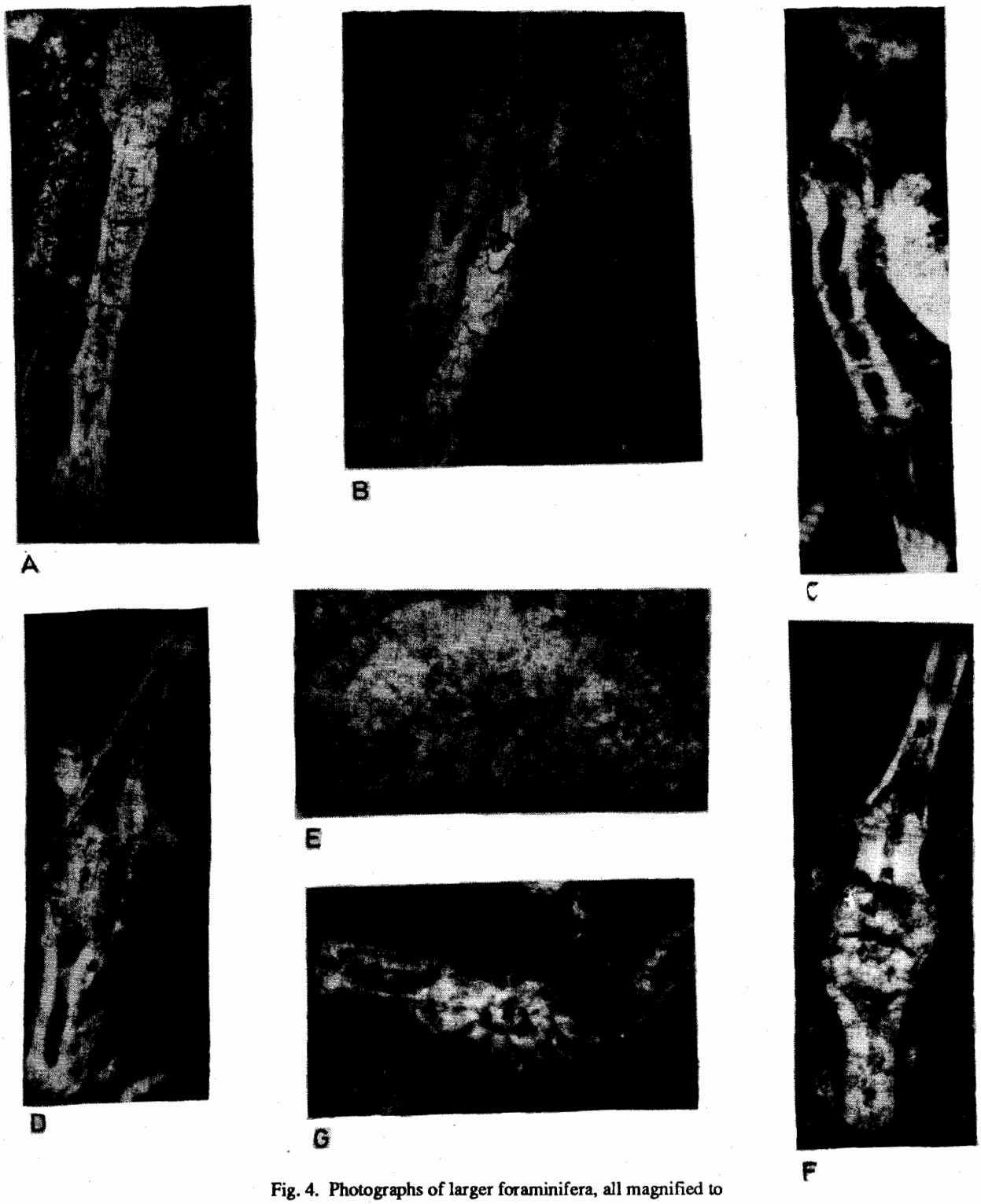

Fig. 4. Photographs of larger foraminifera, all magnified to X 360.

Fig. 4. A-D,F,G: *Ranikothalia sindensis* (Davies). (E): *Lockhartia haimei* (Davies). Lockhart Limestone, Upper Paleocene (Thanetian) Kala Chitta Range, northern Pakistan.

ACTA MINERALOGICA PAKISTANICA
VOLUME 3 (1987) pp. 116 - 122

GENERAL GEOLOGY AND PETROGRAPHY OF CHHAM-TRARAN AREA, JHELUM VALLEY, AZAD KASHMIR.

M. KHURSHID KHAN RAJA
Institute of Geology, University of Azad Jammu & Kashmir, Muzaffarabad Azad Kashmir.

ABSTRACT: A geological map of the Chham Traran area, Jhelum Valley is prepared at a scale of 1:50,000 and a detailed description of various rock units is presented. Pelitic to psammitic, calcareous and carbonaceous rock sequence of the Salkhala Formation is intruded by a body of granite gneiss. The Panjal Formation (volcanics) is thrusted over the Precambrian Salkhala Formation and over ridden by the Upper Tertiary Murree Formation. Petrography and mineral assemblages of the Salkhala Formation resemble those of low-grade metamorphites. Presence of gypsum bands in the Panjal formation is of volcanic nature. Economic Geology of the area is also outlined.

INTRODUCTION

This work includes study of rocks exposed upstream NE of Kathai Nala, on toposheet No. 43 F/16 of Survey of Pakistan, a part of Azad Jammu & Kashmir (fig. 1). A comprehensive geological and petrographic study of different lithological units is presented.

The studied area has remained unexplored by previous workers. Wadia (1931) states about the adjoining area "An oldest sedimentary formation in the Himalayas (Salkhala Series) intruded by certain patches of granitoid gneiss, which are perhaps inliers and represent the Archean basement complex. "Wadia's above statement is important in the regional aspect but not in its detailed geology.

The area lies about 50 km from Muzaffarabad via Chinari Kathai. The oldest rocks exposed in the basement belong to the Salkhala Series (Wadia 1928, 1931, 1961).

The area is accessible by road upto Chinari, 50 kms from Muzaffarabd, and from there upto Cham and Nardajian, by foot-path. Nardajian lies upstream towards Traran Nala via Gehl Jabbar. The maximum altitude in the studied area is 11,000 ft.

The mapped areas consist of areas upstream Kathai Nala, north-east of Chinari to Cham and Traran; Thare-di-Gali, north and north-west via Largucchi, Kuna, Dara Batangi areas and south-east towards Pandu (near line of control) and to Kotla via Gujar Bandi. The mapping was carried out at 1:50,000. Gypsum bands are prominently exposed.

The type locality of Salkhala formation is Salkhala village, Neelum valley, Muzaffarabad, where its dominant lithology comprises of slate, phyllite, schist, carbonaceous and calcareous material. The quartz chlorite mica-schist is exposed upward Thare-digali to Largucchi and to Khatir Nar. The mixed metamorphic sequence exposed is well bedded, light grey to grey brownish. Quartz chlorite mica schist is light green on weathered surface and light grey at fresh. This sequence is intruded by granite gneiss at Sari to Nanga Tak and onward to Cham area, generally making sharp contact with quartz chlorite mica schist. Relics of country

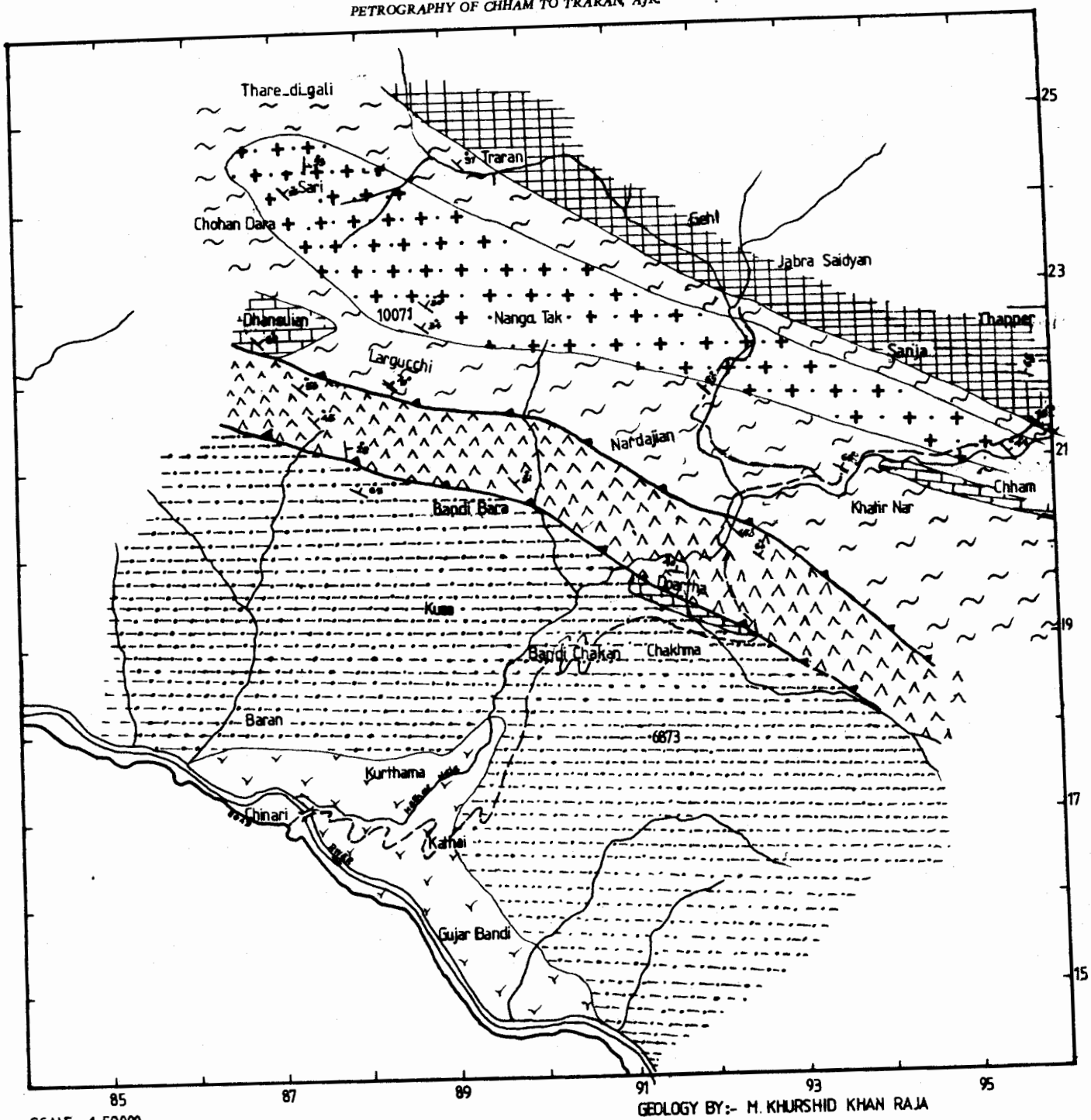

GEOLOGY BY:- M. KHURSHID KHAN RAJA

SCALE: 1:50,000

INDEX

- SALKHALA FORMATION
- ROAD TRACK
- ALLUVIUM
- THRUST
- PANJAL FORMATION
- DIP/STRIKE
- GRANITE GNEISS
- MURREE FORMATION
- RIVER/NALLA

FIG. 1. GEOLOGICAL MAP OF CHHAM_TRARAN AREA.

rock-slices in granite gneiss are seen near the contact at different places.

The graphitic schist exposed in the area is weakly bedded outcroping at the left bank of Tararan Nala towards Gehl and Sanja in mapped area. At some places it is strongly deformed, shows small fold, and looks sheared rather than well bedded.

The graphitic schist is psammitic and is grey to dark grey on fresh surface and dark grey to rusty patches on the weathered surface. Gypsum bands and limonitic patches, streaks and even beds are exposed in this rock unit. In Traran area, the limonite exposed is in the form of streaks, patches, and surficial encrustation while at Chham upstream, Nala near Mumdu bela, it is well bedded and sheared at places.

The marble bands are observed with quartz chlorite mica schist. The interbedded marble bands show light grey to white grey on weathered surface and greyish grey at fresh surface. The marble exposed in the area is saccharoidal in texture. Two exposures are near Khatir Nar and Chham area while one at Doartha near its contact with Panjal formation (thrusted contact with Salkhala Formation).

The Kathai Nala alongwith its small tributaries, receives spring and glacial-water, and falls in Jhelum river near Chinari town located at Shahrai-Kashmir from Rawalpindi to Srinagar in IHK. The area has rugged topography. A major waterfall is 100 m in Chham area. Many small and large alluvial terraces occur at Kathai, Gujar Bandi, Kotla and Karthama. Colluvial cover is prevalent at Khatir Nar and Chham to Pandu. Following stratigraphic succession is indicated:

Alluvium. Quaternary.
Murree Formation. Lower Miocene.
------ MBT (Main Boundary Thrust) ------
Panjal Formation. Permian (?)
------ Panjal Thrust ------
Granite Gneiss
Salkhala Formation. Precambrian.

Salkhala Formation

In the studied area the Salkhala formation outcrops in Khatir Nar, Nardajian, Largucchi, Thare-di-Gali. It consists of quartz mica schist, quartz chlorite mica schist (pelitic-psammitic), graphitic schist and marble (calcareous) with intruded granite gneiss. These rock units are so mixed together except graphitic schist, that they cannot be delineated at this mapping scale (i.e., 1:50000). The graphitic schist is separately exposed on eastern side of Traran Nala via Jabbar to Ainban and upward, with limonite streaks, patches and beds.

Granite Gneiss

It is exposed in Sari-Nanga Tak and near Chham area, intruded in pelites and Psammites of the Salkhala Formation. The body is a small pluton, lenticular to sheet like in shape extending from NE to SW. It is a coarse grained rock with gneissic structure, pinches and swells are commonly seen. 5 to 10 cm relics of transformed (granitised) metasediments of country rock pieces are found in the form of xenoliths near its contact with quartz chlorite mica schist near Thare-di-gali top. It is strongly foliated, leucocratic, medium to coarse-grained gneiss. The foliation is of tectonic nature (paragneiss?). At places it contains porphyroblast of potash feldspar. On way from Khatir Nar to Cham, its apophyses are seen at road side section.

It is brownish grey at weathered surface and whitish grey on fresh surface, usually making parallel to subparallel layers of quartzo-feldspathic material.

Panjal Formation

It consists of light green to dark greyish green volcanic rocks. The bedding is usually massive. Volcanic ashes, pyroclasts, and porphyroblasts of chlorite are seen at some places. Ulike its lithology in Reshian area, pillow lava is not seen in the studied area. In mapped area it outcrops throughout from Dhansuian forest to Chakhama via Dara Batangi and Doartha. It further runs towards Pandu where it crosses line of

Table 1. Modal Compositions of various rock-types. Numbers in columns below each mineral-name are percentages.

QUARTZ-CHLORITE-MICA SCHIST:

Coordinate No.	Sample No.	Quartz	Sericite	Chlorite	Biotite	Muscovite	Epidote	Sphene	Iron ore.
87752545	S 12 A	70	–	3	20	–	One grain	1	6
89602450	S 12	70	–	10	5	3	–	2	–
88502260	S L	60	2	–	33	–	–	–	5
87102484	S 13 A	70	3	–	15	7	–	1	4
89302440	S 11 A	60	1	30	1	5	–	1	3

GRAPHITIC SCHIST:

Coordinate No.	Sample No.	Quartz	Muscovite	Carbonaceous Material	Sericite	Voids
90902450	GS 5	20	5	70	1	4
96502240	GS 4A	16	2	78	2	2

MARBLE:

Coordinate No.	Sample No.	Calcite	Sericite	Iron Ore	Sphene
91801980	MR 3A	97	1	2	–
96002140	MR	96	–	2	2

GRANITE GNEISS:

Coordinate No.	Sample No.	Quartz	Plagioclase	K. Feldspar	Sericite	Muscovite	Hornblende	Biotite	Sphene	Epidote	Tour Maline	Iron Ore
87902340	GGN 8	50	18	15	–	10	–	1	4	–	1	1
95502090	GGN 16B	35	25	20	–	7	10	2	1	–	–	–
92302190	GGN 1	50	16	12	7	6	–	8	–	–	–	–
87502450	GGN 2	60	8	15	10	5	–	1	–	traces	–	1
95852125	*GGN	25	–	70	–	4	–	–	–	–	1	–

VOLCANIC ROCKS OF PANJAL FORMATION:

Coordinate No.	Sample No.	Chlorite	Epidote	Biotite	Plagioclase	Iron ore	Pyroxene	Sphene	Sericite	Orthoclase	Quartz.
89802080	PV2	16	40	15	20	3	12	2	2	–	2
92502020	PV3	20	45	2	13	4	6	2	3	–	5
87802130	*SG1	45	10	16	15	4	–	2	4	4	–

SANDSTONE OF MURREE FORMATION:

Coordinate No.	Sample No.	Chlorite	Calcite	Quartz	Muscovite	Chalcedony	Biotite	Perthite	Plagioclase	Iron ore.
87902080	MSS1	3	25	50	5	2	3	6	4	2
89201190	MSS2	8	15	58	1	8	–	2	8	–

control (L.O.C.). It has a thrusted contact with the Salkhala formation and the Murree Formation as well.

Murree Formation

The Murree Formation is under thrusted (MBT) by the Panjal formation. It consists of sandstone, siltstone and shales in cyclic alternation. Fiestmentel (1879) suggested its age as Miocene but others give its age latest Paleocene to Middle Eocene of lower part of the Murree Formation exposed in the area (i.e. lower Murree Formation).

The Murree Formation is a sedimentary rock fine to medium grained, red to purplish green in colour. Shales are to purple in colour. The siltstone is cream to light grey to dark grey in Kuna, cross beddings and ripples are commonly observed in sandstone. It outcrops in Chakhama and Kathai Gujar Bandi area.

Alluvium

Alluvium like Kathai and Karthama Terrace and adjoining near and upward Kathai Nala, consist of gravels, boulders, sand and clay. There is no marked level of consolidated from unconsolidated material. Alluvium is Recent to Subrecent in age.

PETROGRAPHY

Modal composition and co-ordinate numbers of each rock unit are given in table 1.

Salkhala Formation

(a) ***Quartz–Chlorite–Mica Schist:***

Quartz–chlorite–mica schist unit is moderately schistose, and consists of quartz, muscovite, chlorite, sericite and biotite in variable proportions with accessory iron ore and sphene. Quartz is abundant and present as subhedral to an-hedral grains. Both muscovite and biotite are present. Chlorite is sub-ordinate to micas. Epidote was noticed in one thin section.

(b) ***Graphitic Schist:***

Graphitic schist is thinly layered and folded. In consists of quartz, muscovite, carbonaceous material, sericite and a few voids. Quartz, present as fine segregated layers is subhedral to anhedral in shape. It partly looks crushed. Carbonaceous material is present as segregated and folded layers parallel to the schistosity. Some times pyrite pseudomorphs are seen. Graphitic schist also contains sericite, muscovite,etc.

(c) ***Marble:***

Marble shows uniform granoblastic to sugary texture. It is found as pure calcite usually as euhedral crystals with cleavage. Some accessories like sericite, iron ore and sphene are also present.

Granite Gneiss

Texturally, it is hypidiomorphic granuar holocrystalline, consist of quartz, plagioclase, perthite, muscovite, biotite in variable proportion. The accessories include sphene, sericite, etc.

Quartz is present as medium to coarse grained, anhedral to subhedral, generally sutured. In one thin section it shows mosaics of grains.

Plagioclase (albite to oligoclase) is euhedral to subhedral in shape, shows albite twinning. In some thin sections it shows alteration to dust like material.

K-feldspar present is perthite usually euhedral porphyroblast with some inclusions of quartz and micas.

Micas like muscovite and biotite are usually scattered in porphyroblast. Biotite is brown to reddish brown, & strongly pleochroic.

Iron ore, epidote (traces) and tourmaline are present as accessory minerals.

Panjal Formation

It shows aphanitic to microporphyrite texture, amygdaloidal with epidote/chlorite filling.

Plagioclase occurs as fine to medium, subhedral to euhedral laths.

Pyroxene occurs as subhedral, fine to medium grains altered to chlorite, epidote.

Anhedral to subhedral quartz, sphene and iron ore is also present.

Murree Formation

The Murree Formation has variegated lithology like sandstone, shales and marl, but petrography of only sandstone is presented. Sandstone is medium to coarse grained usually subangular to sub rounded clasts. The grains are quartz rock fragments, feldspar and micas alongwith chlorite and carbonaceous material.

Quartz is fine grained and recrystallized. The rocks also contain chlorite, micas, chert/ chalcedony, feldspar and iron ore.

PETROLOGIC DISCUSSION

The petrographic discussion of different rock suits exposed in the Chham-Traran area indicates low grade metamorphites. Chlorite grade is generally indicative of greenschist facies conditions. (Turner & Verhoogen, 1960; Winkler, 1965).

The graphite schist represents assemblages of greenschist facies equivalent (?) to chlorite grade. They generally indicate low grade metamorphism of reasonable amount of black shales (Harker, 1939).

The quartz-muscovite-biotite assemblage represents biotite zone of relatively high temperature under greenschist facies.

The abundant mineralogy of granite gneiss and its contact with metasediments, as well as presence of large relics at the contact shows that it is intrusive body produced by granitization of pre-existing metasediments.

To estimate the petrogenesis of the volcanics of the Panjal Formation, it needs a lot of details. The origin is not so far settled but certain volcanic features in other areas of its continuity such as pillow lavas, volcanic ashes characterize it to be submarine to subaerial conditions, is an oceanic crust of alkaline to tholeiitic basaltic association (Butt *et al.*, 1985).

They are undifferentiated material (consolidated and unconsolidated fragments). The Kathai, Gujar Bandi big terraces are result of simultaneous deposition of Kathai Nala and river Jehlum.

Economic Geology of the Area

The mapped area has got a good economic mineral potential. Among them, following are found in studied area.

1- Limonite.
2- Gypsum bands.
3- Amorphous Graphite.
4- Marble.
5- Skarn type Association (?)

Limonite

Limonite is exposed in the mapped area near Traran and Chham in the form of patches, streaks, surficial incrustations formed mainly by oxidation of pyrite.

The possible origin of the limonite can be springs originating from the pyritous graphitic schist; or it may be a gossan of some sulphide body.

It is brownish red to yellowish red can be used in paint, iron, steel and fertilizer industry. It is embedded in graphitic schist quite in the strike (NWN/SES) of Reshian limonite.

The beds are steeply inclined from 50° to 80° mainly towards ENE.

Gypsum Bands

The gypsum present in the graphite schist is in the form of bands exposed near Gehl Jabbar and upstream Tararan and Jabbar Nala. Gypsum can be exploited for proposed cement factory in Muzaffarabad as it is accessible through road links (see introduction).

Amorphous Graphite

It is in the form of beds (schistose) throughout Traran-Jabbar to Sanja, Chapper area.

It may be mixture of hypo-crystalline to amorphous, can further be exploited for commercial use.

Marble

A good quality white to off-white bandy to granoblastic texture marble is exposed near Doartha on the contact of Salkhala and Panjal formation as well as near half kilometre from Khatir Nar towards Chham in the same strike. The thickness of different outcrops ranges from 5 ft to 100 ft (approximately).

Skarn Type Rocks

Such a rock association exists right at Chham village opposite Middle School, where Nala turns further north-east. The granite gneiss (tectonic) has a contact with 5 to 10 ft thick band of marble.

ACKNOWLEDGEMENTS

The author greatly acknowledges the precious help of Abdul Latif, a senior teacher in Govt High School Nardajian whose kind guidance and help has made this field work accessible. But lovely company of two young College boys Mr. Muhammad Sharif and Muhammad Sadique (Mughals) can never be forgotten. I can also never forget the hospitality of Mr. Noor-Ullah Khan Chughtai and Rashad Kayani (Teachers) and other staff of Govt High School Nardajian.

REFERENCES

BUTT, K.A., CHAUDHARY, M.N. & ASHRAF, M. (1985) Evidence of an incipient Paleozoic ocean in Kashmir, Pakistan. Kashmir Jour. Geology 3, pp. 87-102.

DEER, W.A., HOWIE, R.A. & ZUSSAN, J., (1962) ROCK-FORMING MINERALS 1, Longmans, London.

FIESTMENTEL, O., (1879) Note on remains of palm leaves from the (Tertiary) Murree and Kasulli beds in India. Rec. Geol. Soc. India, 15, Pb, 01, pp. 51-54.

HARKAR, ALFRED. (1939) METAMORPHISM. Methuem & Co., Ltd., London.

MISCH, P. (1949) Metasomatic granitization of batholithic dimensions, Part I, Syntectonic granitization in Nanga Parbat, NW Himalayas. Amer. Jour. Sci. 247, pp. 209-245.

TURNER, F.J. & VERHOOGEN, J. (1960) IGNEOUS AND METAMORPHIC PETROLOGY. McGraw Hill, New York.

WINKLER, H.G.F. (1979) PETROGENESIS OF METAMORPHIC ROCKS. Springer-Verlag, New York, Heidelberg, Berlin. 5th Edt.

WADIA, D.N. (1928) The geology of Poonch States Kashmir and adjacent portion of Panjal. Mem. Geol. Surv. India VLI.

———— (1931) The Syntaxis of North-West Himalaya, Rec. Geol. Sury, India, 65, pp. 189-223.

———— (1961) GEOLOGY OF INDIA. Tata McGraw - Hill Publishing Co, New Dehli, 3rd Edt.

Orally presented on 22.10.1987
Manuscript revised on 31.12.1987

ACTA MINERALOGICA PAKISTANICA
VOLUME 3 (1987) pp. 123 - 127

GEOLOGY AND PETROGRAPHY OF EOCENE MAFIC LAVAS OF CHAGAI ISLAND ARC BALUCHISTAN, PAKISTAN.

REHANUL HAQ SIDDIQUI, SYED ANWER HUSSAIN & MUNIR-UL-HAQUE
Geological Survey of Pakistan, Quetta.

ABSTRACT: Two, more or less identical, basaltic lava flows are found towards the top of the lower pyroclastic sequence of the Eocene Saindak formation, 15 km NW of Amalaf town. Both the flows are elongated in a NW-SE direction and crop out for more than 6 km. The older flow is about 100 m thick and extends for 2 km. The younger flow is upto 700 m thick and extends for more than 6 km. Both the flows are transected by numerous ENE trending strike-slip faults and are slightly folded into a small scale anticline and a syncline.

Both flows are dark brown to black in colour and weather brown to maroon. They are fine-grained, hypocrystalline, porphyritic and amygdaloidal. Under the microscope, both flows are vitrophyric to subpilotaxitic and cumulophyric. Subautoclastic texture is also developed in the younger lava flow. Clusters of large phenocrysts of plagioclase and isolated phenocrysts of clinopyroxene are embedded in a micro to cryptocrystalline and devitrified groundmass. Labradorite is the main plagioclase, which is accompanied by minor andesine and bytownite. Clinopyroxene is generally represented by augite and minor, diopside. Vesicles are generally filled with zeolites, chlorite, chalcedony, quartz, malachite and occasionally with palagonite. Apatite, ilmenite, and magnetite are common accessories. Uralite and chlorite are the major alteration products of pyroxene, whereas plagioclase exhibits minor argillization and sericitization. Magnetite is partially limonitized.

INTRODUCTION

Chagai magmatic belt of northwestern Baluchistan represents several submarine volcanic episodes of eruption and explosion during late Mesozoic to late Cenozoic time.The late Cretaceous and Quaternary volcanic episodes were relatively more widespread compared to others which were very restricted and occurred intermittently in the Paleocene, Eocene, and Miocene epochs.

The present paper deals with our geologic and petrographic studies of Eocene mafic lavas of western Chagai belt.

These lava flows occur about 15 km NW of the R.D.C. Colony at Amalaf, which is about 45 km NE of Taftan, a town on the Pak-Afghan border on the RCD highway. Approximate coordinates of the area are 29° 20′N and 61° 32′ E which are within the Survey of Pakistan topographic sheet No. 30 G/11.

GEO-TECTONIC SETTING

The Chagai magmatic belt, also known as the Chagai calc-alkaline magmatic belt (Sillitoe 1974, Dykstra, 1978), is about 500 km in length, 150 km in width, and trends in an east-west direction. This belt has been postulated to be formed by the northward subduction of an oceanic lithosphere below the southern edge of the Afghan micro-continent (Stoneley, 1974; Arthurton *et al.*, 1979). It was therefore considered an Andean type magmatic belt. But recent petrological and petrochemical studies of the north central part of the Chagai belt, suggest that the Chagai belt may represent an ancient island arc constructed on oceanic crust rather than on continental margin (Siddiqui *et al.*, 1986).

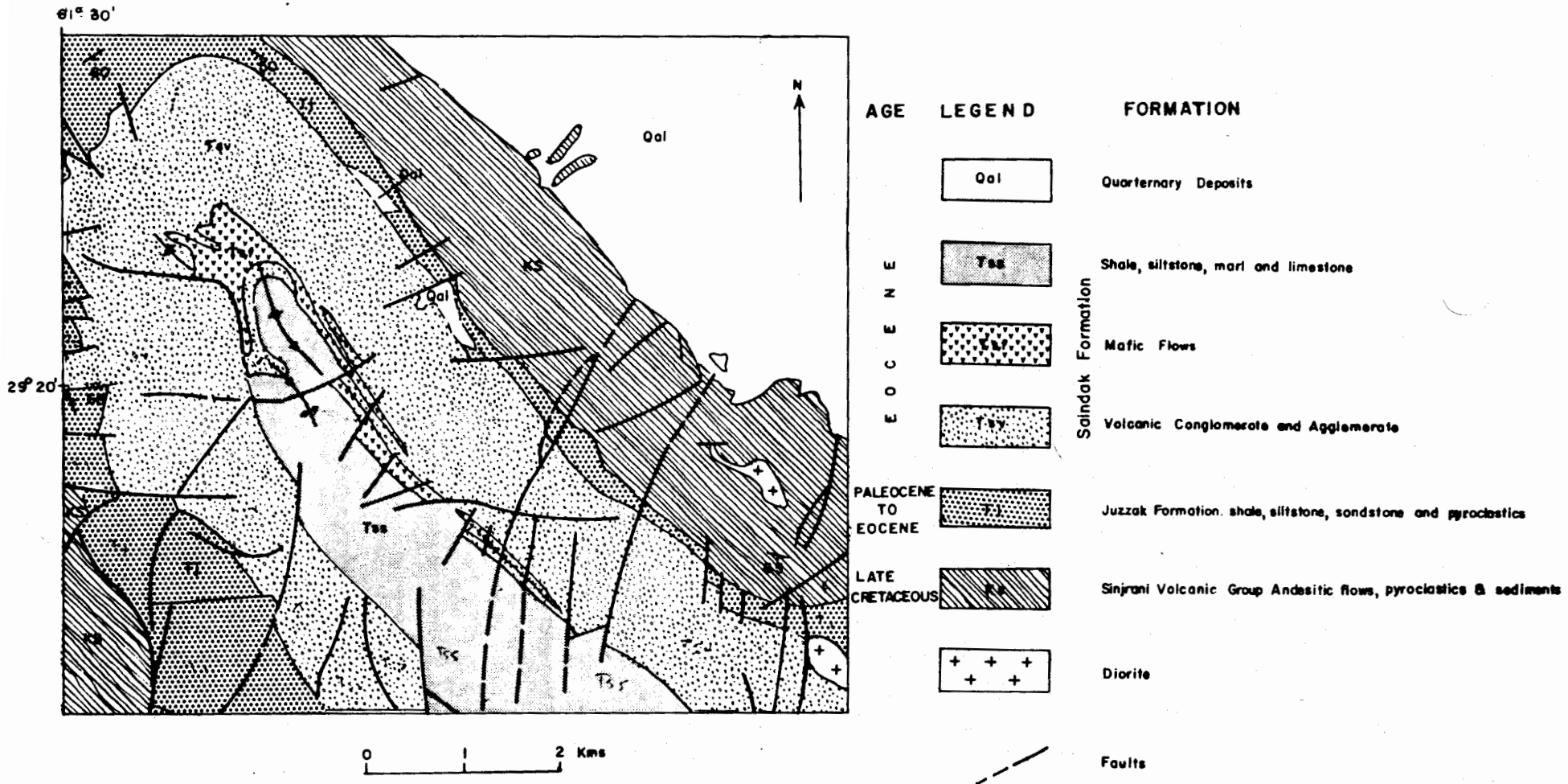

FIG.I. GEOLOGICAL MAP OF A PART OF THE SAINDAK QUADRANGLE BALUCHISTAN.
(After Schmidt *et al*, 1963)

REGIONAL GEOLOGY

The oldest rock unit of the Chagai magmatic belt is the late Cretaceous Sinjrani Volcanic Group (Hunting Survey Corporation, 1960). This group is comprised mainly of submarine, interstratified andesitic flows and pyroclastics including agglomerate volcanic conglomerate, tuff and volcanic breccias with subordinate amounts of basalt, limestone, shale, and sandstone. Total thickness of the group is about 10,000 metres (Arthurton, 1974).

The Sinjrani Volcanic Group was invaded by Chagai intrusions during pre-late Cretaceous to Miocene time. This is represented by several phases of intrusion by rock types including granite, adamellite, granodiorite, tonalite diorite and gabbro (Hunting Survey Corporation, 1960). Other rock formations exposed in the western Chagai belt include the Humai formation (Late Cretaceous), the Juzzak formation (Paleocene), the Saindak formation (Eocene), the Amalaf formation (Oligocene), and the Kamerod formation (Pleistocene), represented in the following stratigraphic sequence:–

Holocene	Recent & subrecent deposits	Boulder, gravel, sand, alluvium and sand dunes
	--Unconformity--	
Pleistocene	Kamerod formation	Volcanic conglomerate and tuffaceous sandstone.
	--Unconformity--	
Oligocene	Amalaf formation	Shale, siltstone, sandstone, and limestone.
Eocene	Saindak formation	Shale, siltstone, marl, lime-stone, mafic flows, and pyroclastics.
Paleocene to Eocene	Jazzak formation	Shale, sandstone, siltstone, limestone, mafic flows, and pyroclastics.
	Humai formation	Limestone, shale, sandstone, and conglomerate
Late Cretaceous	Sinjrani volcanic group	Andesitic and baslatic flow, agglomerate, tuff, volcanic conglomerate, and breccia with subordinate shale, sandstone, and limestone.

LOCAL GEOLOGY

Eocene mafic lava flows of the Saindak formation are interlayered towards the top of the lower pyroclastics with a minor sedimentary sequence. The Saindak formation may be divided into two parts. The lower part is composed mainly of volcanic agglomerate,mafic flow, tuffaceous sandstone and few lenses and reefs of Nummulitic limestone. The upper part consists of soft grey shale, siltstone, sandstone, marl, and thin layers of limestone. Total thickness of the formation is about 1500 m. The formation is believed to have been deposited in a shallow marine environment. It contains abundant echinoids, pelecypods, gastropods and corals (Ahmed *et al.*, 1972). The lower and upper contacts of the formation are conformable and gradational with the underlying Juzzak formation and the overlying Amalaf formation, respectively.

FIELD ASPECTS

The outcrop of the lavas of the Saindak formation is elongated in NW – SE direction, following the axis of the famous Saindak syncline. They extend about 6 km and attain a maximum thickness of about 700 m towards their northwestern end. The lavas are transected by several intermittently exposed, NE trending, andesite porphyry dykes. The flows are highly weathered and exceedingly rubbly in nature. At places spheriodal weathering has produced shapes that resemble pillow structures.

At least two more or less identical cycles of eruption are identified, separated by 100 metres thick volcanoclastic sequence of the Saindak formation (fig. 1). The rocks of the older cycle of eruption are about 100 m thick and extend upto 2 km along strike. The rocks of the younger cycle of eruption are upto 700 m thick and crops-out for more than 6 km. Both the flows are transected by numerous ENE trending strikeslip faults and are slightly folded into a small scale anticline and a syncline.

The flows are dark brown to black in colour and weather brown to maroon. These are fine-grained, hypocrystalline, amygdaloidal, and porphyritic in texture. The phenocrysts of plagioclase and pyoxenes are identifiable in hand specimen. Those phenocrysts show minor argillization and chloritization. Rounded, oval and irregular vesicles are generally filled with zeolites, chalcedony, chlorite, malachite, and crystalline quartz. At places, smoky quartz, agate,

and amethyst are also observed in cracks and cavities.

PETROGRAPHY

Under the microscope both lavas are melanocratic, vitrophyric to sub pilotaxitic, and cumulophyric in texture. They are amygdaloidal and are more or less identical in texture and mineralogy except that subautoclastic texture is also developed in later flows probably due to its more intense tectonic deformation. Alteration is also more prominent in this flow.

Clusters of large (upto 4 mm) phenocrysts of plagioclase and isolated phenocrysts of pyroxene are embedded in a micro- to cryptocrystalline and devitrified glassy groundmass, having tiny laths (less than 1 mm), microlites, and crystallites of plagioclase and pyroxene. Magnetite, ilmenite and apatite occur as accessories

Plagioclase:– Plagioclase generally ranges in composition from $An_{52} - An_{68}$ which falls within the labradorite range but a few grains show anorthite contents as low as An_{42} and as high as An_{72}, suggesting that labradorite is also accompanied with minor andesine and bytownite. Plagioclase crystals are euhedral to subhedral, lathlike and tabular in shape and exhibit polysynthetic twinning according to the albite and occasionally to the combined albite and Carlsbad laws. The plagioclase crystals are slightly fractured, corroded and a few (less than 1%) of them show resorbed and pitted margins. Oscillatory zoning is also developed in some grains. Plagioclase crystals have small inclusions of skeletal ilmenite, apatite and occasionally augite. Groundmass plagioclase generally occurs as small microlites, crystallites, and tiny columnar laths.

Pyroxenes:– Both clino- and orthopyroxenes are encountered in thin sections but clinopyroxene is dominant and is represented by augite with minor diopside. Orthopyroxene is represented by enstatite only.

Augite occurs as small euhedral to subhedral prismatic grains and eight sided basal sections. It occasionaly shows polysynthetic twinning and hourglass zoning. It is slightly fractured and fractures are filled with limonite.

Diopside occurs as small prismatic and euhedral to subhedral crystals. Polysynthetic twinning is common in diopside.

Enstatite occurs as small prismatic subhedral to anhedral and untwinned crystals.

Volcanic Glass:– Volcanic glass is generally devitrified. It has brown, yellow or green colour. Palagonite in spherulites partly shows a radiating appearance.

Accessory Minerals:– Apatite, ilmenite and magnetite are common accessories. Apatite occurs as small euhedral and prismatic crystals enclosed in larger grains of plagioclase. Ilmenite occurs as small skeletal grains in the groundmass and also as inclusions in plagioclase phenocrysts. Magnetite occurs as small subhedral and anhedral grains scattered throughout the groundmass.

Secondary Minerals:– Secondary minerals are generally developed as partial or complete replacement of primary minerals, and as infillings in vesicles. Chlorite and uralite are the common alteration products of pyroxene. Kaolinite, sericite, and carbonates have developed after partial alteration of plagioclase.

Amygdules:– Lavas are moderatly to intensely vesiculated. Vesicles are generally filled with more than one generation of zeolites (natrolite), chlorite, chalcedony, malachite, crystalline quartz, and palagonite. In some vesicles zeolites are in the centre and the lining is chalcedony, quartz, and chlorite. In others, it is reversed.

ACKNOWLEDGEMENTS

The authors gratefully acknowledge to Mr. Waheeduddin Ahmed, Director General, Geological Survey of Pakistan and Mr. S. Anisuddin Ahmad, Director of the same Department for providing field and laboratory facilities.

Mr. S. Anisuddin Ahmad, is once more thanked for critically reviewing the manuscript and for fruitful discussions.

REFERENCES

AHMED, W., KHAN, S.N. & SCHMIDT, R.D. (1972) Geology and copper mineralization of the Saindak quadrangle, Chagai District, West Pakistan. U.S. Geol. Surv. Prof. Paper 716-A, 21 P.

ARTHURTON, R.S., ALAM, G.S., AHMED S.A. & IQBAL, S. (1979) Geological history of Alam Reg Mashki Chah area, Chagai District, Baluchistan. *In:* Farah, A. & DeJong, K.A. (eds.) GEODYNAMICS OF PAKISTAN, Geol. Surv. Pakistan.

DYKSTRA, J.D. (1978) A Geological Study of Chagai Hills, Baluchistan, Pakistan using LANDSAT digital data. (Unpublished Ph. D. thesis, Darmouth College, Hanover, N.H.) 147p.

HUNTING SURVEY CORPORATION LIMITED (1960) RECONNAISSANCE GEOLOGY OF PART OF WEST PAKISTAN. A Columbo plan Cooperative project, Govt. of Canada, Toronto, Canada. 550p.

SCHMIDT, R.D., KHAN, S.N. & AHMED, W. (1963) Geological map of the Saindak quadrangle, Chagai District, West Pakistan. (Jointly prepared by United State Department of the Interior Geol. Surv. and Geol. Surv. of Pakistan).

SIDDIQUI, R.H., KHAN, W. & HAQUE, M. (1986) Petrological and petrochemical studies of north central Chagai belt and its tectonic implications. Acta Mineralogica Pakistanica 2, pp. 12-23.

SILLITOE, R.H. (1974) Metallogenic evolution of a collisional mountain belt of Pakistan. Geol. Surv. Pakistan Rec. 34, 16p.

STONELEY, R. (1974) Evolution of the continental margin bounding a former, southern Tethys. *In:* BURKE, C.I. and DRAKE, C.L. (eds.) THE GEOLOGY OF CONTINENTAL MARGINS. Springer, New York, pp. 889-903.

Orally presented on 22.10.1987
Manuscript revised on 31.12.1987

ACTA MINERALOGICA PAKISTANICA
VOLUME 3 (1987) pp. 128 - 133

PARAGENETIC AND PETROCHEMICAL STUDY OF PHYLLIC ALTERATION AT DASHT-E-KAIN PORPHYRY Cu-Mo PROSPECT, BALUCHISTAN, PAKISTAN.

REHANUL HAQ SIDDIQUI, JAN MUHAMMAD MENGAL,
RIAZ AHMED SIDDIQUI & HESHAMUL HAQUE
Geological Survey of Pakistan, Sariab Road, Quetta, Pakistan.

ABSTRACT: At Dasht-e-Kain, a newly found porphyry Cu-Mo prospect, phyllic alteration is mainly developed in two comagmatic tonalite-porphyry stocks. The following paragenetic sequence is suggested for phyllic alteration in the western tonalite porphyry stock with quartz continuous throughout the course of alteranion: sericite → kaolinite → anhydrite and calcite. This petrological and petrochemical study suggests that Si and K metasomatism was the main process involved in the phyllic alteration in the area.

INTRODUCTION

Phyllic or quartz-sericitic alteration is probably the most abundant, widespread and significant of all alteration types. It develops in nearly all types of hypogene ore-forming environments in various rock types. It is also found in the gold-quartz and massive sulphide system in Precambrian and other metamorphic terrains (Meyer and Hemley, 1967).

The present paper deals with the paragenesis and petrochemistry of quartz-sericitic alteration developed in the western ore body of the Dasht-e-Kain porphyry copper-molybdenum prospect.

The Dasht-e-Kain prospect is located 35 km NW of Chagai village, which s situated 64 km NE of Dalbandin, a town 341 km W of Quetta on the R.C.D. Highway (see Siddiqui *et al.*, 1986, for location map). The area is covered on topographic sheets Nos. 34 C/6 and 34 C/10 and approximate co-ordinates are 29° 33′ N and 64° 29′ E.

GEOLOGICAL SETTING

The prospect occurs in the north-central part of the Chagai magmatic belt in the eruptive zone of northwestern Baluchistan. This belt is about 500 km in length, 150 km in width and trends in an E-W direction. The Chagai belt is also known as the Chagai calc-alkaline magmatic belt (Sillitoe, 1974; Dykstra, 1978) and has been postulated to have formed due to northward subduction of oceanic lithosphere below the southern edge of the Afghan microcontinent (Stoneley, 1974; Arthurton *et al.*, 1979), but recent petrological studies of the north-central Chagai belt lead to the interpretation that the Chagai magmatic belt may represent an island arc, constructed on an oceanic crust rather than a continental margin (siddiqui *et al.*, 1986).

The oldest rock unit in the Chagai magmatic belt is a submarine volcanic and volcaniclastic suite known as the Sinjrani Volcanic Group (Hunting Survey Corporation, 1960), which is late Cretaceous in age and composed mainly of stratified intercalations of andesitic and basaltic flows and pyroclastics including tuff, volcanic conglomerate, volcanic breccia and agglomerate, with subordinate limestone, shale and sandsone. The Sinjrani Volcanic Group was intruded by Chagai intrusions (Hunting Survey Corporation, 1960) during late Cretaceous to Miocene times consisting of many phases of intrusion including granite, adamellite, granodiorite, tonalite, monzonite, diorite and gabbro.

Fig. 1. (A) Calcite veinlet traversing partly sericitized groundmass of tonalite-porphyry. (B) Tonalite-porphyry exhibiting feldspar-destructive sericitic alteration.

GEOLOGY OF THE PROSPECT

At Dasht-e-Kain, hydrothermal alteration is mainly associated with two comagmatic tonalite porphyry stocks. These stocks are elongated in an ENE direction and named the eastern and western stocks (Ahmed *et al.*, 1985). The stocks intrude a larger composite gabbro-diorite stock which itself intrudes the Sinjrani Volcanic Group. The eastern tonalite porphyry stock is intruded by an EW trending intrusive breccia pipe, and both the stocks are also transected by a swarm of NW and NE trending post- alteration dykes which are tonalitic, dacitic, andesitic and dioritic in composition and porphyritic in texture (Siddiqui *et al.*, 1986).

PHYLLIC OR QUARTZ-SERICITIC ALTERATION

Phyllic alteration generally occurs as a continuous or discontinuous halo around the potassium silicate alteration zone (K-zone) in a typical porphyry copper system (Lowell and Guilbert, 1970). At Dasht-e-Kain this alteration also partly surrounds the K-zone towards its southern and western sides, occupying one third of the western tonalite porphyry stock. On the northern and eastern sides it is mainly buried under alluvial cover with small outcrops of sericitized rocks (Ahmed *et al.*, 1985).

Phyllic alteration in the area is represented by the extensive development of sericite, quartz and kaolinite with minor calcite, anhydrite, pyrite, chalopyrite and molybdenite (Siddiqui, 1984). The colour of fresh quartz sericitized tonalite porphyry is white but due to the superimposed colouration of hematite, jarosite, and goethite, it generally appears reddish and yellowish brown. Sericite occurs as very fine flaky aggregates totally replacing the plagioclase, hornblende and biotite, completely bleaching the original colour of the rock and destroying its primary texture. Quartz remains unaltered but shows slight fracturing; secondary quartz is introduced as a replacement of the groundmass and in veins, veinlets and microveinlets. In places twin planes, zoning and traces of cleavage in plagioclase are retained in the preferred orientation of the sericite flakes. Kaolinite occurs as fine powdery masses replacing the groundmass and is also found on fracture planes and as isolated lenses and patches. Calcite and anhydrite generally occur on fracture planes, in veinlets and microveinlets and occasionally in the groundmass.

PARAGENESIS AND PETROCHEMISTRY OF PHYLLIC ALTERATION

Sericite appears as the earliest-formed alteration mineral in the phyllic zone, since it does not replace any other alteration mineral. Quartz is synchronous or later because it occurs interlocked with sericite in the groundmass and is also found in veinlets and microveinlets traversing the groundmass together with sericite, secondary quartz and kaolinite. Quartz and sericite are followed by kaolinite which replaces the sericite in the groundmass, kaolinite also occurs as patches and lenses transecting the groundmass. The kaolinite is followed by calcite and anhydrite, veinlets and microveinlets of which traverse the groundmass containing earlier alteration assemblages. Neither mineral shows any textural relationship with each other so they might or might not be synchronous, as in the case of the K-silicate alteration (Siddiqui *et al.*, 1986). The following paragenetic sequence is suggested for the phyllic alteration with quartz continuous throughout the course of alteration: sericite → kaolinite → anhydrite and calcite.

Chemical analyses and CIPW norms of fresh and quartz-sericitized tonalite prphyries from the Dasht-e-Kain porphyry copper-molybdenum prospect are presented in Table 1.

Comparison of the two shows marked increases in SiO_2 and K_2O contents in the altered rock, whereas FeO, MgO, CaO and Na_2O have considerably decreased. Al_2O_3, Fe_2O_3, P_2O_5, SO_2 and CuO contents show slight decreases.

The normative mineralogy of the fresh and quartz-sericitized tonalite-porphyries also show quantitative and qualitative differences. Normative quartz and orthoclase are greatly increased in the quartz sericitized rock (figs. 3, 4) while plagioclase and femic minerals in the same rock

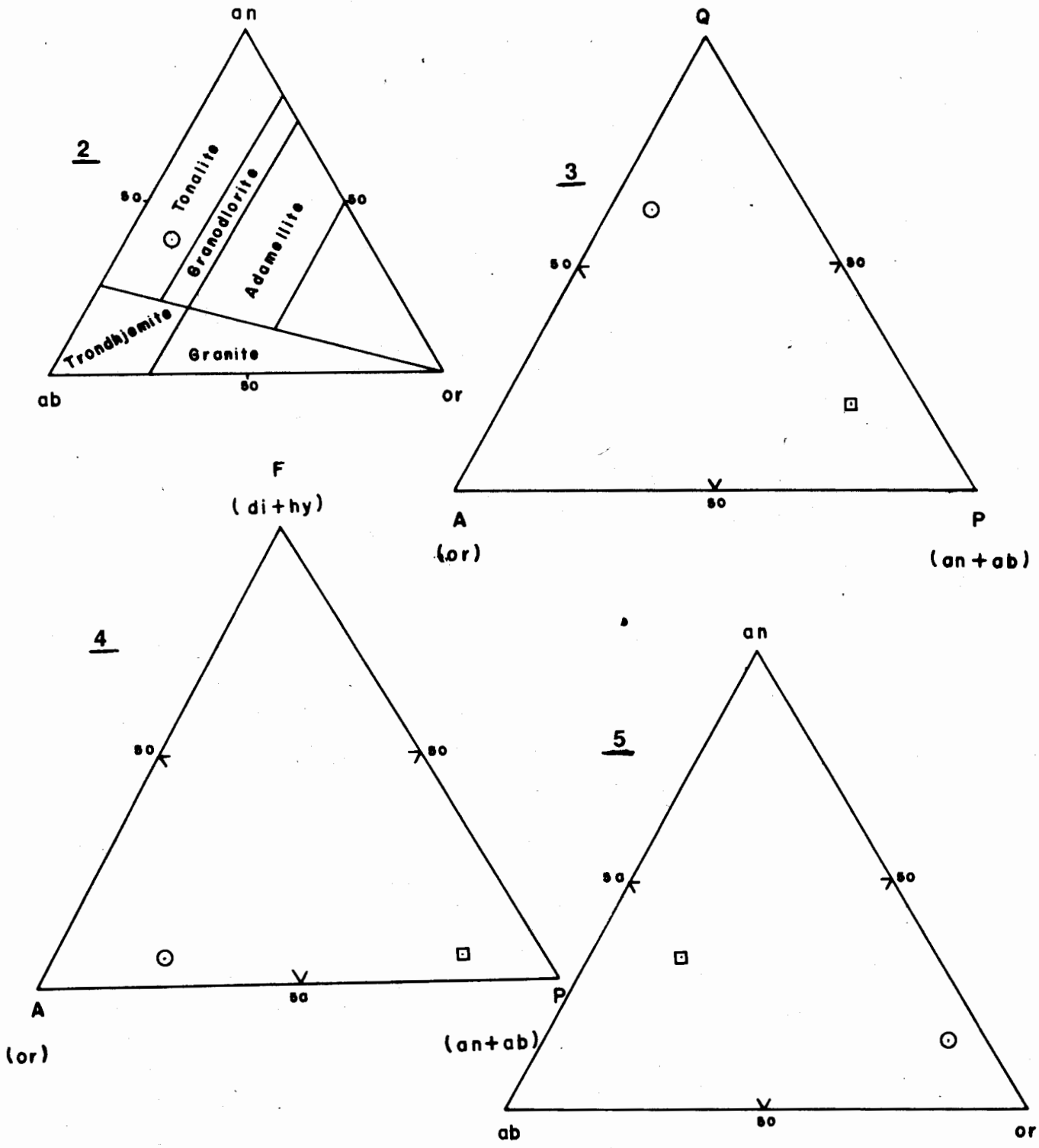

Fig. 2. Ternary plot of normative ab-an-or for tonalite porphyry of Dasht-e-Kain porphyry Cu–Mo prospect. The compositional boundries are after O' Connor (1965).

Fig. 3. Ternary plot of normative Q–A–P for fresh (⊡) and quartz–sericitized (⊙) toalite porphyry of Sash-e-Kain porphyry Cu–Mo prospect.

Fig. 4. Ternary plot of normative F–A–P for fresh (⊡) and quartz–sericitized (⊙) tonalite porphyry of Dasht-e-Kain porphyry Cu–Mo prospect.

Fig. 5. Ternary plot of normative an–ab–or for fresh (⊡) and quartz–sericitized (⊙) tonalite porphyry of Dasht-e-Kain porphyry Cu–Mo prospect.

are strongly decreased (fig. 5). Ilmenite, pyrite and apatite also show slight decreases in the quartz sericitized rock. Normative corundum and hematite are introduced in the altered rock and diopside and hypersthene are replaced by enstatite.

Table 1. Chemical compostion and C.I.P.W. norms of fresh (1) and quartz sericitized (2) tonalite porphyry from Dasht-e-Kain porphyry Cu–Mo prospect.

		1	2
SiO^2		61.85	74.25
TiO_2		0.29	0.30
Al_2O_3		18.36	14.75
Fe_2O_3		3.75	3.28
FeO		2.27	0.48
MgO		1.29	0.91
CaO		5.08	0.99
Na_2O		4.24	0.27
K_2O		2.12	4.24
P_2O_5		0.07	0.05
SO_3		0.22	0.20
CuO		0.01	0.001
H_2O^+		0.35	0.22
H_2O^-		0.12	0.04
Total		100.02	99.98
CIPW Norms:–			
	Q	16.21	53.01
	C	–	7.91
	or	12.55	25.10
	ab	35.86	2.30
	an	24.78	4.88
	wo	–	–
di	en	0.29	–
	fs	0.03	–
	en	3.09	2.28
hy	fs	0.40	–
	mt	5.43	0.39
	hm	–	3.27
	pr	0.17	0.15
	il	0.55	0.57
	ap	0.16	0.12

CONCLUSION

The study shows that phyllic alteration at the Dasht-e-Kain prophyry copper-molybdenum prospect developed according to the model proposed by Lowell and Guilbert (1970), and is similar in pattern to that at other porphyry copper mineralization areas in the Chagai belt (Siddiqui *et al.*, 1986).

Phyllic alteration in the area is represented by the extensive development of sericite and quartz, reflected in major increases in SiO_2 and K_2O in the chemical composition of the quartz-sericitized rock and in its increased normative quartz and orthoclase content. This suggests that Si and K metasomatism was the process involved in the phyllic or quartz sericitic alteration in the area.

ACKNOWLEDGEMENTS

The authors gratefully acknowledge Mr. Waheeduddin Ahmad, Direcector General, Geological Survey of Pakistan, and Dr. Mehmooduddin Ahmad, Director of the same department, for providing field and laboratory facilities.

REFERENCES

AHMED, M.U., SIDDIQUI, R.H. & CHAUDHARY, M.A. (1985) Geological and geochemical exploration and preliminary evaluation of Dasht-e-Kain porphyry copper molybdenum prospect, Chagai District, Baluchistan. Rec. Geol. Surv. Pakistan 72, 32p.

ARTHURTON, R.S., ALAM, G.S., AHMED, S.A. & IQBAL, S. (1979) Geological history of the Alam-Reg., Mashkichah area, Chagai District, Baluchistan. *In:* Farah, A. and Dejong, K.A. (eds.) GEODYNAMICS OF PAKISTAN, Geol. Surv. Pakistan, Quetta, pp. 325-31.

DYKSTRA, J.D. (1978) A geological study of Chagai hills, Baluchistan, Pakistan, using LANDSAT digital data. Unpublished Ph.D thesis, Dartmouth College, Hanover N.H., 147p.

HUNTING SURVEY CORPORATION LIMITED (1960) RECONNAISSANCE GEOLOGY OF PART OF WEST PAKISTAN, A Colombo Plan Co-operative Project, Government of Canada, Toronto, Canada.

LOWELL, J.D. & GUILBERT, J.M. (1970) Lateral and vertical alteration mineralization zoning in porphyry ore deposits. Econ. Geol. **65**, pp. 373-408.

MEYER, C. & HEMLEY, J.J. (1967) Wall rock alteration. *In:* Barnes, H.L. (ed.) GEOCHEMISTRY OF HYDROTHERMAL ORE DEPOSITS. Holt Rinehart and Winston Inc. new York, 670p.

O'CONNOR, J.T. (1965) A classification of quartz-rich igneous rocks based on feldspar ratio, U.S. Geol. Surv. Prof. Paper **525-B**, pp. B79-B84.

SIDDIQUI, R.H. (1984) Petrographic and ore microscopic studies of Dasht-e-Kain porphyry copper molybdenum prospect, Chagai District, Baluchistan, Pakistan. Inf. Rel. Geol. Surv. Pakistan, **213**, 26 p.

SIDDIQUI, R.H., CHAUDHARY, M.A. & HAFEEZ, A. (1986) Paragenetic and petrochemical study of K-silicate alteration and hypogene mineralization of Dasht-e-Kain porphyry copper-molybdenum prospect, Baluchistan. Acta Mineralogica Pakistanica **2**, pp. 107-14.

SIDDIQUI, R.H. & KHAN, W. (1986) A comparison of hydrothermal alteration in prophyry copper mineralization of Chagai calcalkaline magmatic belt, Baluchistan, Pakistan. Acta Mineralogica Pakistanica **2**, pp. 100-6.

SILLITOE, R.H. (1972) A plate tectonic model for the origin of porphyry copper deposits. Econ. Geol. **67**, pp. 189-97.

---------- (1974) Metallogenic evolution of a collisional mountain belt of Pakistan. Geol. Surv. Pakistan, Rec. **34**, 16p.

STONELEY, R. (1974) Evolution of the continental margin bounding a former southern Tethys. *In:* Burke C.A. & Drake C.L. (eds.) THE GEOLOGY OF CONTINENTAL MARGINS. Springer, New York, pp. 889-903.

Orally presented on 20.10.1987
Manuscript revised on 31.12.1987

ACTA MINERALOGICA PAKISTANICA
VOLUME 3 (1987) pp. 134 - 139

PETROLOGY AND PROVENANCE OF SIWALIKS OF KACH AND ZARGHUN AREAS, NORTHEAST BALUCHISTAN.

ABDUL HAQUE, ABDUL SALAM KHAN & AKHTAR MOHAMMAD KASSI
Department of Geology, University of Baluchistan, Quetta, Pakistan.

ABSTRACT: Sandstones and conglomerates of the Nagri and Dhok Pathan Formations of the Kach area and the Soan Formation of the Zarghun area were classified microscopically, as lithic arenites and calcithites. Although the mineral and rock constituents in sandstones of the Nagri, Dhok Pathan and Soan Formations are comparable, their proportions vary in the Nagri and Dhok Pathan Formations. The source terrain for the "Siwalik Group" in the Kach area includes sedimentary, igneous and metamorphic rocks. The nearby older mountain ranges are capable of providing Siwalik detritus and the notion is supported by palaeocurrent patterns.

INTRODUCTION

Previously the Siwalik Group in Baluchistan is represented by the "Sibi" and "Urak" groups of the Hunting Survey Corporation (1960). The name Nagri formation of Lewis (1937) has been accepted by the Stratigraphic Committee of Pakistan (1974) which in Baluchistan represents the Lowermost part of the "Sibi Group" and "Urak Group" of Hunting Survey Corporation (1960) and Uzda Pasha Formation of Kazmi and Raza (1970). Petrology and genesis (Krynine, 1937) petrology, geochemistry, faunal and palaeomagnetic studies have been carried out (Opdyke *et al*, 1979; Shah *et al.*,1979; Hussain *et al.*,1979; Abbasi *et al.*,1983; Khan, 1984) mostly in the Siwaliks of Punjab area.

This Siwalik consists of fine to coarse grained or even pebbly sandstone, conglomerate and rarely clay. The sandstone is greenish and bluish grey, poorly sorted, subangular to subrounded, fine to coarse grained having a profusion of various sedimentary structures (Kassi, 1987). Conglomerate of varied thicknesses being composed of various types of igneous and sedimentary fragments. These coarse clastic sedimentary rocks have been grouped into Siwalik and classified from bottom to top into: Nagri Formation of Lewis (1937) (mainly grey sandstone); Dhok Pathan Formation of Cotter (1933) (reddish sandstone & clay), and Soan Formation of Kravtchenkq(1964) (mainly massive conglomerate). With Dhok Pathan Formation, Nagri Formation makes a conformable and transitional contact while with that of Soan Formation is also transitional in the area near Sor Range. They are unconformably overlying different formations ranging in age from Cretaceous to Paleocene, thus, making a clear regional angular discordance (fig. 1). The Stratigraphic Committee of Pakistan (1974) has already adopted the above names. Moreover, an unpublished work of OGDC (1965) assigned Middle to Late Miocene age to these Formations.

GENERAL DESCRIPTION

1. NAGRI FORMATION:

Sandstone of the Nagri Formation is very rich in various rock fragments rather than mineral constituents,quartz and feldspars including plagioclase, orthoclase, microcline and perthite. Muscovite, biotite, green and brown hornblende, diopside and augite may also rarely be found. A few very fine grains of glaucophane are also present. Among the heavy minerals garnet showing sieve structure is common. Epidote, apatite, chrome spinel of green and brown colours and brown tourmaline are also present.

A variety of rock fragments (table 1) may be found in sandstones of the Nagri Formation. These include limestones (biomicrite and bio-

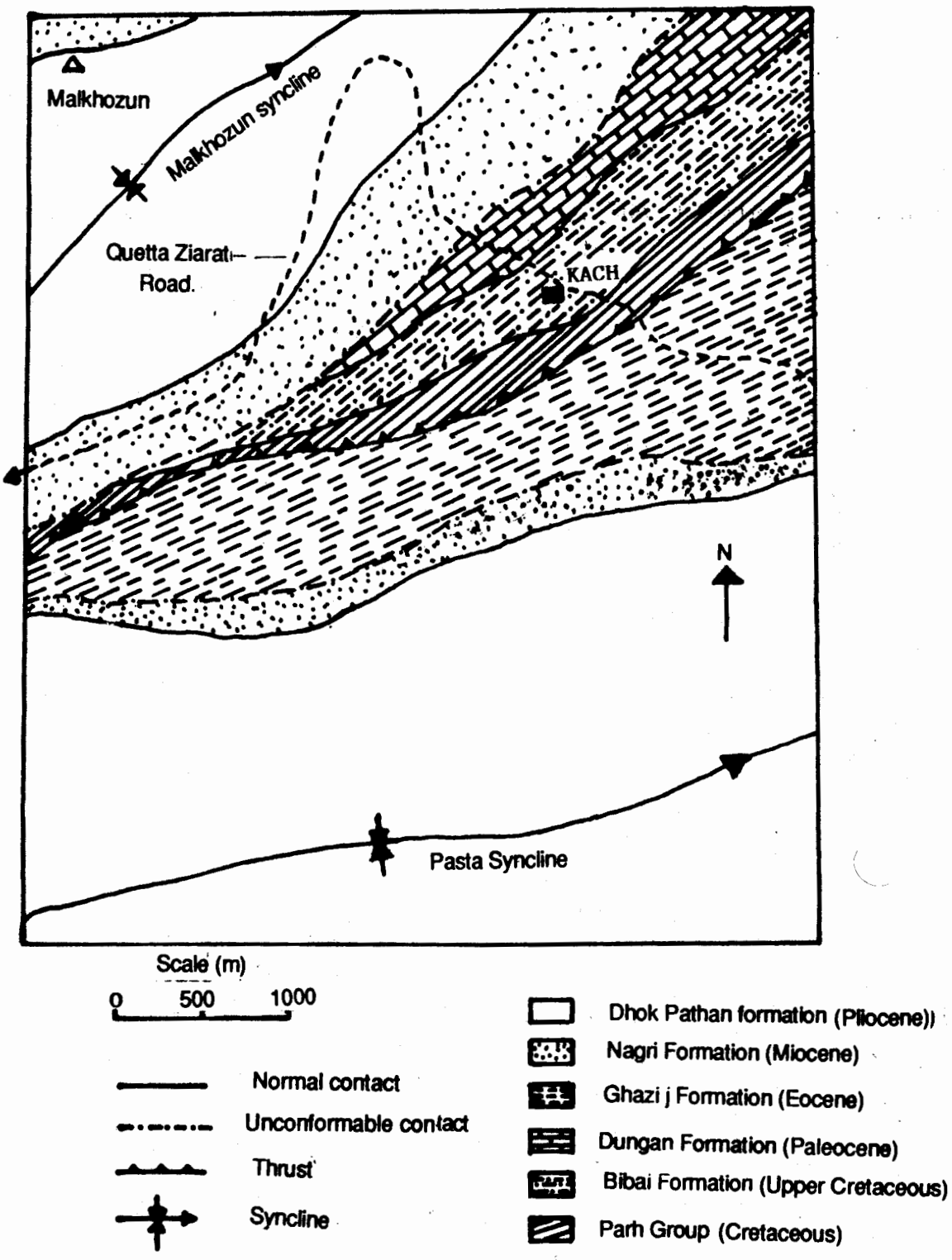

Fig. 1. Geological and structural map of Kach area.

sparite of Folk, 1959), calcarenite, marl and calcareous foraminifera, sandstone of quartz arenite and calclithite and lithic arenite, shales and siltstones which are sometimes deformed by compaction, and red to grey radiolarian cherts are recognized. Metamorphic rock fragments include quartzite, epidosite, mica schist and glaucophane schist. Among the igneous fragments granite and basic volcanic fragments are most common.

The grains are cemented by calcite being proportionally so high (50%) and mica grains are laterally displaced by the growth of calcite between the flakes. Islands of detrital grains may be seen floating within calcite cement. Lateral displacement of mica flakes and also other grains is caused by the force of crystallization of calcite cement. This may be evidence of supersaturated precipitating solutions formed due to rapid evaporation of vadose pore indicative of subaerial exposure (Watts, 1978).

2. DHOK FORMATION:

It is characterised by monotonous cyclic alternations of thick bedded sandstone and clay beds. The sandstone is brownish grey to reddish brown, moderate to well-sorted, fine to medium grained and sometimes pebbly. Various types of sedimentary structures (Kassi, 1987) may be found. The clay is reddish brown, red, maroon and yellowish grey, calcareous and sandy in places. Minor mottled yellowish brown and reddish brown siltstone intercalations may be present. The formation has a transitional and conformable contact with the underlying Nagri Formation.

Sandstones of the Dhok Pathan Formation contain more rock fragments than mineral constituents. Among the minerals quartz, feldspar, muscovite and chlorite are present in descending order of abundance. Feldspar includes plagioclase (mostly albite), perthite, microcline and rarely orthoclase. The heavy minerals include chrome spinel, garnet and epidote. In some thin sections garnet grains may be common. In this formation also a variety of rock fragments are present which include limestone of various types, sandstone, chert, metamorphic and igneous fragments, (table 1). Cementing material is calcite which is very high in proportion.

3. SOAN FORMATION:

The formation consists essentially of compact, massive conglomerate with interbeds of sandstone, siltstone and mudstone. The conglomerate is made up of moderate to well-sorted and well-rounded to sub-rounded cobbles and pebbles of limestones, sandstones, chert and igneous rocks embedded in a medium to fine grained sandy matrix. The pebbles are matrix supported and imbricated. The clay is reddish to brownish grey and light brown and occasionally light grey in colour. The mudstone is light grey to brownish grey, medium to coarse grained, subangular to subrounded and poor to moderatly sorted.

The conglomerate of the Soan Formation is very rich in pebbles and cobbles of fossiliferous limestones (sometimes oolitic) of light to dark brown, red, creamy, white, light grey and dark grey colours. Conglomerate and sandstone fragments of dark to dark brownish grey colours which closely resemble those of the Ghazi j Formation are also present. Red to black chert fragments as well as basic volcanic fragments may also be found.

Sandstone of the Soan formation is also rich in limestone fragments while quartz and feldspar are the only mineral constituents. Among feldspar, perthite and plagioclase are recognisable. The sedimentary rock fragments include various types of limestones, radiolarian cherts, sandstones, silstones and shale fragments. A few quartzite and schist fragments may also be seen. Basic volcanic and granitic fragments are among the representatives of igneous rock. These sandstones are very poor in heavy mineral content, only chrome spinel may be found. These mineral and rock fragments are cemented by a very high proportion of calcitic cement.

MODAL ANALYSES

Fresh samples within the sandstones were collected during our field work in which very coarse and very fine grained samples were excluded, and only seventeen samples were selected for modal analyses.

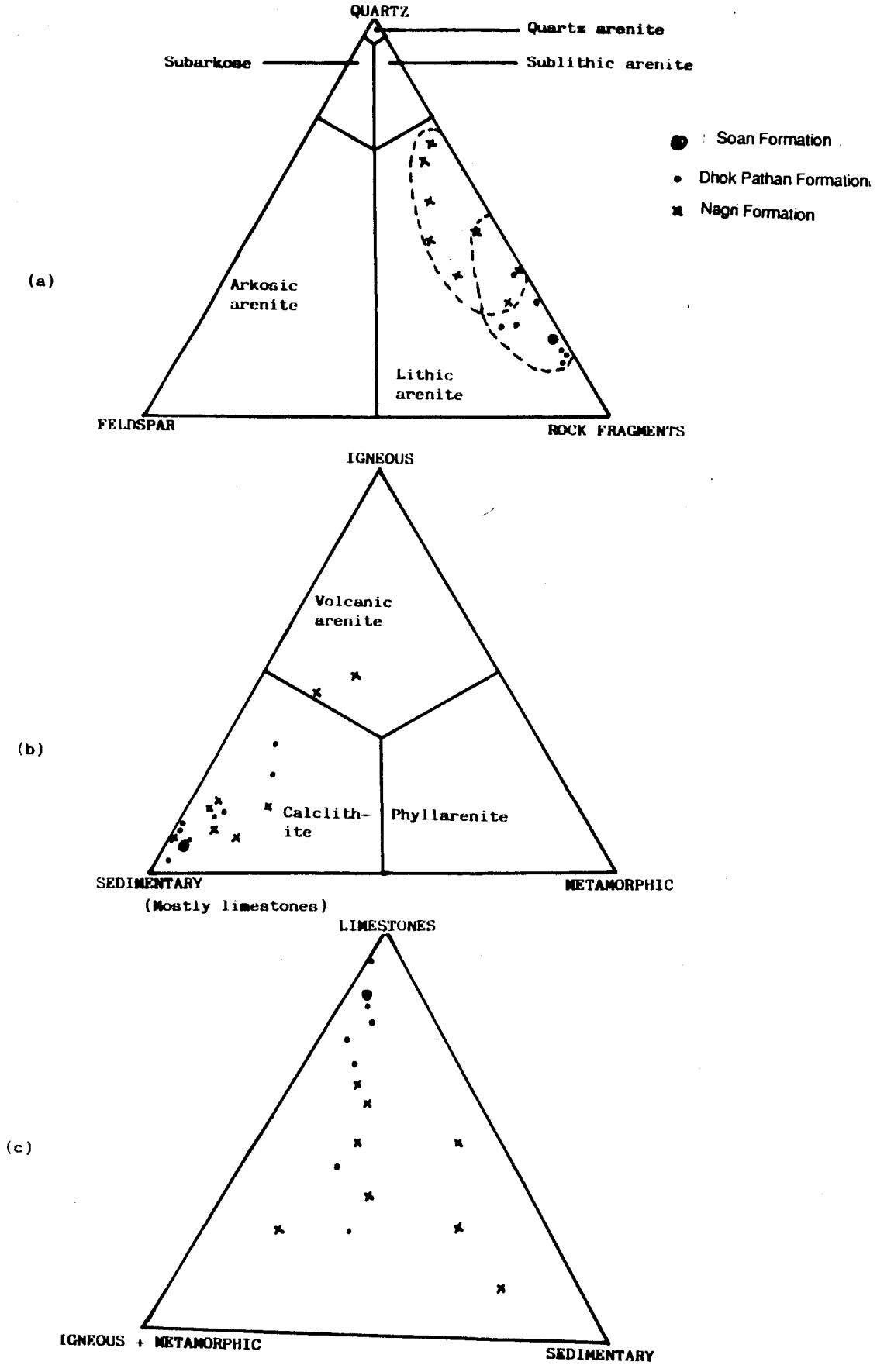

Fig. 2. Results of point counting plotted on (a) Classification diagram modified from Dott (1964) (b) Classification diagram after Folk (1968). (c) Triangular diagram to show nature of the rock fragments.

Sandstones were classified based on 500 counts per sample and plotted on triangular diagrams (fig. 2) modified from Dott (1964) and Folk (1968). The count interval was 1/3 mm and traverses 2mm apart to avoid multiple counting of coarse constituents. Although sandstones of Nagri, Dhok Pathan and Soan Formations fall into the lithicarenite field, they show marked contrasts in mineral and rock constituents (fig. 2a,c). Sandstones of the Dhok Pathan and Soan Formations are richer in rock fragments and poorer in quartz. In the majority of the samples (15 out of 17) the rock fragments are dominantly limestones, therefore, except for two samples of the Nagri Formation which are classified as volcanic arenites, most of the rocks are either calclithites and/or sedimentary arenites (fig. 2b). The rocks are highly rich in carbonate cement varying between 17% and 50% and poor in matrix (0 – 6%). The analyses include only one sample of the Soan Formation which is also classified as the calclithite variety of lithic arenite.

NATURE OF THE SOURCE AREA

Igneous, sedimentary and metamorphic rock fragments are present in sandstones and conglomerates of the Siwaliks in Kach and Zarghun areas (table 1), in which sedimentary rock fragments are dominantly limestone. The palaeocurrent's study in Siwaliks to the north of Kach in Malkhozun Syncline (fig. 1) shows a southeasterly derivation while, the Siwaliks of the Pasta Syncline south of Kach suggest a northwesterly derivation. This suggests that source area was the present mountain range being composed of sedimentary and igneous rocks (Bela Volcanic group of Cretaceous age) and which is situated between the Malkhozun and Pasta Synclines. Basic igneous and metamorphic rock fragments especially amphibolite, epidosite, mica schist, glaucophane schist and heavy minerals like chrome spinel, garnet and glaucophane indicate the possible subduction complex in the ultimate source area, which may be the Muslimbagh Igneous complex.

The palaeocurrent pattern (Kassi, 1987; fig. 7) of the Siwaliks in Kach area did not coincide with the expected source area suggested by the rock fragments. These various types of igneous and sedimentary rock fragments also include those derived most probably from the Muslimbagh Igneous Complex. Pebbles of granite are also present in the conglomeratic horizons of the Nagri Formation, which probably may have been derived from the Chaman Granite (?) associated with the Noshki-Chaman Fault. Such occurrences of rock fragments in the Siwaliks of Kach area, keeping in view the palaeocurrent pattern are concievable only through indirect (second cycle) derivation. It is suggested that such fragments may have been incorporated earlier in some of the older coarse clastic rocks like the Bela Volcanic Group which include basic igneous fragments in its sandstone and conglomerate horizons. The Bela Volcanic Group and Ghazi j Formation contain rock fragments of the Muslimbagh Igneous Complex, and also perhaps of the Chaman Granite (?) may have contributed as an indirect source of such detritus.

Table 1. Types of rock fragments found in the sandstones and conglomerates of the Siwaliks in Kach and Zarghun areas.

IGENOUS	SEDIMENTARY	METAMORPHIC
Spilite	Biomicrite limestone; Biosparite	Quartzite; Mica schist;
Andesite	Limestone; Intrasparite limestone;	Chlorite schist; Epidosite;
Granite	Oosparite limestone;	Glaucophane schist;
	Red chert; Black chert; Quartz arenite; Siltstone; Shale; Conglomerate; Fossil fragments; Plant fragments.	Amphibolite.

CONCLUSIONS

Most of the Siwalik sandstones may be classified as the calclithite/sedimentary arenite varieties of lithic arenite.

Although the nature of mineral constituents and rock fragments is comparable, their proportions vary in the Nagri and Dhok Pathan Formations.

Detritus of these rocks in Kach area may have been derived directly from the adjacent older mountain range and indirectly from the Muslimbagh Igneous Complex and Chaman Granite (?).

ACKNOWLEDGEMENTS

The authors of this present paper are extremely grateful for the anonymous referees for their valuable suggestions and comments during its publication process.

REFERENCES

ABBASI, I.A., ABID, I.A., KHAN, A.M. & SHAH, M.T. (1983) Petrography and geochemistry of Siwalik Sandstones and its relationship to the Himalayan Orogeny. Geol. Bull. Univ. Peshawar **16,** pp. 65-83.

COTTER, G.deP. (1933) The geology of part of the Attock District, West of longitude 72° 45′ E. India. Geol. Surv. Mem. **55,** pp. 63-161.

DOTT, R.H. Jr. (1964) Wacke, greywacke and motrix – What approach to immature sandstone classification? Jour. Sed. Petrology **34,** pp. 625-32.

FOLK, R.L. (1959) Practical petrographic classification of limestone. Bull. Amer. Assoc. Petrol. Geol. **43,** pp. 1-38.

HUNTING SURVEY CORPORATION (1960) RECONNAISSANCE GEOLOGY OF PART OF WEST PAKISTAN. Toronto, Canada, 550 p.

HUSSAIN, S.T., MUNTHE, J., SHAH, S.M.I., WEST, R.M. & LUKACS, J.R. (1979) Neogene stratigraphy and fossil vertebrates of the Daud Khel area, Mianwali District, Pakistan. Mem. Geol. Surv. Pakistan. **13.**

KASSI, A.M. (1987) Preliminary sedimentology of Siwaliks of Kach and Zarghun areas of northeast Baluchistan (in press).

KAZMI, A.H. & RAZA, S.Q. (1970) Water supply of Quetta Basin, Baluchistan, Pakistan. Recs. Geol. Surv. Pakistan. **20(5).**

KHAN, M. J. (1984) Brief results of Palaeomagnetic studies of the Siwalik group of the trans Indus Salt Range, Pakistan. Geol. Bull. Univ. Peshawar **17,** pp. 176-78.

KRAVTCHENKO, K.N. (1964) Soan Formation – upper unit of the Siwaliks in Potwar. Science and Industry, **2(3),** pp. 230-33.

KRYNINE, P.D. (1937) Petrography and genesis of the Siwalik series. Amer. Jour. Sci. 5th Ser., **34,** pp. 422-46.

LEWIS, G.E. (1937) A new Siwalik correlation (India). Amer. Jour. Sci., 5th Ser. **33,** p. 191-204.

OPDYKE, N.D., LINDSAY, E., JOHNSON, G.D., JOHNSON, N., TAHIRKHELI, R.A.K. & MIRZA, M.A. (1979) Magnetic polarity stratigraphy and vertebrate palaeontology of the upper Siwalik sub-group of north Pakistan. Earth and Planetary Science Letters **27.**

SHAH, S.M.I. PILBEAM, D., & OTHERS (1979) Miocene sediments and faunas of Pakistan. Peabody Mus. Natural Hist., Yale. Univ. Postilla. 179 p.

STRATIGRAPHIC COMMITTEE OF PAKISTAN (A.N. FATMI, COMPILER) (1974) Lithostratigraphic units of the Kohat-Potwar Province, Indus Basin, Pakistan. Mem. Geol. Surv. Pakistan **10,** pp. 1-80.

WATTS, N.L. (1978) Displacive Calcite: evidence from recent and ancient calcretes. Geology **6,** pp. 699-703.

Orally presented on 22.10.1987
Manuscript revised on 31.12.1987

ACTA MINERALOGICA PAKISTANICA
VOLUME 3 (1987) pp. 140 - 158

MINERAL CHEMISTRY OF THE SAKHAKOT-QILA COMPLEX, PAKISTAN: PART 2, POLYSILICATES.

ZULFIQAR AHMED
Centre of Excellence in Mineralogy, University of Baluchistan, Post Box 43, Quetta, Pakistan.

ABSTRACT: Polysilicates contained in the SQO include enstatite, bronzite, diopside, endiopside, salite, augite, magnesio-anthophyllite and a variety of calcic amphiboles. Their compositions vary mainly with the primary rock types, and to a much less extent, with the effects of secondary metasomatic activity. Orthopyroxenes exhibit a relatively restricted range in Fe variation, except for more magnesian inclusions in chromite crystals and more Fe-rich crystals in websterite dykes. Primary Mg-Fe variations in clinopyroxenes are superimposed by the metasomatic Ca-enrichment. the primary amphiboles exhibit a less marked Fe-enrichment, Si- depletion trend with increasing SiO_2 in the rock. This is overshadowed by the secondary tremolite-actinolite formation by the interaction of fracture-controlled SiO_2-rich solutions. Minor element variations in polysilicates are not significant.

INTRODUCTION

The geological features of the Sakhakot-Qila ophiolite (abbreviated 'SQO') have been described previously by Ahmed (1982, 1984), Ahmed & Hall (1983); and in the part 1 of this 4-part series (Ahmed, 1987) in which the mineral chemistry of the monosilicates from SQO is given. Polysilicates are important components of SQO rocks and are the subject of this communication which is aimed at a systematic chemical characterization of the polysilicates from SQO and their impact on the petrology of SQO.

OCCURRENCE OF POLYSILICATES

Polysilicates present in the SQO rocks include orthopyroxenes, clinopyroxenes, calcic amphiboles and magnesio-anthophyllite. Orthopyroxenes are all primary and are the essential constituents of harzburgite which is the most abundant rock type of SQO and also of orthopyroxenite and websterite dykes. Clinopyroxenite dykes and some chromitites contain some accessory orthopyroxene. Clinopyroxenes are essential primary constituents of wehrlite, clinopyroxenite dykes, websterite dykes and metagabbro. In wehrlites, the clinopyroxenes usually form coarse disseminated crystals that are conspicuous on weathered surfaces as white specks. Some clinopyroxenite dykes show a whitish weathering colour. Some harzburgite and dunite samples contain accessory primary clinopyroxene. This is usually undetected in field outcrops and hand specimens, but is identifiable under the microscope. In metagabbro, a hydrothermal or metasomatic clinopyroxene occurs in addition to the initial magmatic one. The latter, hydrothermal or metasomatic clinopyroxene is texturally and chemically distinct from its magmatic counterpart as described in the following pages. Diopside also occurs in small amounts in the rodingitized parts of certain rocks.

Amphiboles have a widespread occurrence, and in addition to the secondary veins and

dykes of asbestose tremolite, a host of calcic amphiboles occur in the SQO rocks. Among the non-calcic amphiboles, only magnesio-anthophyllite is present in a few rocks, such as the orthopyroxenite (sample Z104). The meta-gabbros and metadolerites both contain abundant calcic amphiboles. at least a part of the serpentinite endogenous envelope of the SQO outcrop is metamorphosed to actinolite schist (sample Z384). The ultramafic rocks contain calcic amphibole in relatively smaller amounts.

MINERAL CHEMISTRY AND PETROGRAPHY

The analyses of minerals of SQO reported in this paper were performed using the electron microprobe unit at the University of Cambridge, U.K. The instrument was operated at 20kV using 80 live seconds counting time and a cobalt internal standard. The peaks were processed and measured by iterative peak stripping; the correction methods applied were after Sweatman and Long (1969). The analytical error is estimated at ± 1.5 percent for the oxides of major elements present in amounts exceeding 5%. The totals for analyses included in this study for the anhydrous minerals were between 98.5 and 101.5 percent including the minor elements as well. Oxygen was calculated by stoichiometry. The cationic ratios were calculated by a computer programme fed by numbers directly from the microprobe. The weight percentages of oxides of elements given in the tables of analyses in this paper are reduced to the second decimal. In tables 2 to 4, representative analyses of the minerals are presented; whereas more data has been utilized for construction of the diagrams and discussion. The iron contents for the pyroxenes and amphibole analyses were initially assumed to be wholly bivalent as reported in the tables 2, 4 & 6. To estimate Fe_2O_3, as given in tables 3 and 5, the analyses were run through a computer programme based on the charge balance equation and other criteria given by Papike *et al.*, (1974) and Cameron & Papike (1981). Most of the microprobe analyses fulfilled the criteria for "superior" analyses set by these authors.

ORTHOPYROXENES

The orthopyroxene analyses are selectively listed in table 2 and plotted in the pyroxene quadrilateral in figs. 1 and 2. They sometimes contain amphibole lamellae formed by alteration. Fine-grained exsolution lamellae present in orthopyroxene crystals were not analyzed by the microprobe, except when sufficiently coarse. Zoning is not observed in orthopyroxenes. An outstanding feature of the SQO orthopyroxenes is their Mg-enrichment, they are more magnesian than the compositions typical of most ophiolites. The atomic $Mg/(Mg + Fe^{2+} + Mn)$ ratios of the SQO orthopyroxenes are either identical to, or slightly higher than, those reported for the orthopyroxenes from other ophiolites such as those described by Coleman (1977).

The more Mg-rich orthopyroxenes within the SQO rocks, are found as inclusions in chromite (e.g., sample Z277). A parallel trend was observed for the olivines of SQO (Ahmed, 1987). Orthopyroxenes in harzburgites, clinopyroxene-harzburgites, orthopyroxenites and clinopyroxenites are strongly magnesian with Fs molecule varying from 9% to 10%. In the orthopyroxenes of websterite dykes, Fs varies from 10% to 15% and in those from the Fe-websterite dyke, Fs varies from 21% to 22%. Thus the overall range of variation in orthopyroxenes from the SQO rocks spans Fs_9 to Fs_{22} including enstatite and bronzite members of the orthopyroxene series, although 99% of the volume of orthopyroxenes at SQO possesses less than 10% Fs.

Minor elements in orthopyroxene consist of very small amounts of Al, Ca, Mn, Ti, Cr and Ni. The mean MnO in orthopyroxenes varies from 0.09 to 0.17% in enstatites from all the SQO ultramafic rocks except the websterites in which mainly bronzite occurs carrying enhanced FeO as well as MnO. The mean of NiO percentage for various samples ranges from nil to 0.12%. The mean Al_2O_3 values for various rock samples reach a maximum of 2.11%. CaO contents exhibit 1.3% as the highest value for the rock sample means. Ca does not exceed 0.083 atoms per formula unit (a.f.u.).

Table 1. Samples location and description. Locations are given by grid reference to the toposheets of Survey of Pakistan, under Column "GRID"; and by points plotted on geological map (Ahmed, 1987, Fig. 1) in the column "MAP". Sample numbers are given in column "Sp. No."

SP. NO.	GRID	MAP	MINERALS ANALYZED	DESCRIPTIONS
"Pseudoclastic" chromitite:				
Z277	4449-8428	C57	Chr, Chl, Tr, Edhb inclusions in Chr, Opx & Cpx inclusions in Chr.	
Disseminated-textured chromitite:				
Z31	4210-7173	C5	Chr, Fchr, Chl, Tr, Cpx.	
Z237	4454-8158	C42	Chr, Ol, Cpx, Chl, Ol inclusions in Chr.	
Massive chromitite:				
Z41A	4232-7374	C6	Chr, Cpx, Chl, Srp, Uvr, Prv, Hgrs, Chap.	
Z62	4205-7465	C8	Chr, Ol, Cpx, Cpx inclusions in Chr,	
Z235	4454-8158	C42	Chr, Di, Grs, Hgrs, Chl, Hz.	Sample partly "pseudoclastic". Rodingitic veins traverse the chromitite.
Z236	4454-8158	C42	Chr, Ol, Cpx, Chl.	Sample shows gradation to disseminated-textured chromitite.
Z260	4278-8335	C53	Chr, Ol, Srp, Chl.	
Clinopyroxene-harzburgite:				
Z16	4062-7095	C3	Opx, Ol, Cpx, Chr, Opx & Ol inclusions in Chr.	
Z222	4454-8158	C42	Opx, Ol, Cpx, Chr.	Opx is abundant and coarser; Cpx is minor.
Z323	4330-8390	–	Ol, Opx, Cpx, Chr.	
Z326	4332-8388	–	Ol, Opx, Cpx, Chr, Srp, Chl, Tr, Trhb.	
Harzburgite:				
Z324	4330-8390	–	Ol, Opx, Chr.	
Z105	4103-7452	C9	Ol, Opx, Chr, Srp.	
Z310	4543-9127	C62	Ol, Opx, Chr, Fchr.	
Z344	4484-8350	–	Ol, Opx, Chr, Srp.	
Z374	4205-7465	C8	Ol, Chr, Opx, Cpx.	Dunite rock contain a < 1 cm thick websterite band.
Z216	4459-8146	C40	Chr, Ol, Opx.	
Clinopyroxene dunite:				
Z375	4205-7465	C8	Ol, Chr, Cpx, Chl, Srp.	
Serpentinite:				
Z132	4161-7509	C11	Srp, Tr.	Vein-forming rock.
Z393	4595-8660	–*	Srp, Chl, acicular Tr, Act.	Nodular textured serpentinite.
serpentinite.				
Actinolite Schist:				
Z384	4491-7560	–	Act, Achb.	
Wehrlite:				
Z24	4060-7155	C4	Ol, Cpx, Chr, Fchr.	
Z147	4060-7640	–	Ol, Cpx, Chr, Srp.	
Z294-A	4492-8774	C60	Ol, Cpx, Chr, Srp.	
Z264	4150-8332	C55	Cpx, Ol, Srp, Chr, Mag after Chr, Aw.	
Z265	4150-8332	C55	Ol, Cpx, Srp, Chl, Chr.	
Z202	4468-4156	C39	Cpx, Ol, Chr, Fchr, Srp.	
Z183	4460-8035	C32	Ol, Cpx, Fchr, Chr, Srp.	
Z188	4396-8080	C33	Ol, Cpx, Chl, Chr.	
Z347	4480-8360	–	Ol, Cpx, Chr, Fchr, Mag, Srp, Hz.	

Mineral symbols are : Ab, albite; Achb, actinolitic hornblende; Act, actinolite; Amph, amphibole; Aw, awaruite; Chap, chlorapatite; Chl, chlorite; Chr, chromite; Cpx, clinopyroxene; Czo, clinozoisite; Di, diopside; Ed, edenite; Edhb, edinitic hornblende; Fchr, "ferritchromit", Fed, ferroedinite; Fedhb, ferroedinitic hornblende; Fprg, ferroan pargasite; Fprhb, ferroan pargasitic hornblende; Fsp, feldspar; Grs, grossular; Hgrs, hydrogrossular; Hz, heazlewoodite; Ilm, ilmenite; Math, magnesioanthophyllite; Mag, magnetite; Mhb, magnesiohornblende; Ol, olivine; Opx, orthopyroxene; Pn, pentlandite; Prgh, pargasitic hornblende; Prv, perovskite; Qtz, quartz; Spn, sphene; Srp, serpentine; Tr, tremolite; Tro, troilite; Trhb, tremolitic hornblende; Uvr, uvarovite; Zo, zoisite.

Orthopyroxenite dyke:				
Z104	4103-7452	C9	Opx, Ol, Chr, Srp, Math, Tr.	
Clinopyroxenite dykes:				
Z70	4205-7465	C8	Cpx, Ol, Chr, Chl, Srp.	Olivine-clinopyroxenite vein crosscuts orbicular chromitite.
Z123	4103-7452	C9	Cpx, Chr, Fchr, Srp, Aw, Amph.	
Z188B	4396-8080	C33	Cpx, Ol, Chl, Srp, Tr, Mhb, Chr, Aw., Hz.	
Z275A	4453-8400	C56	Cpx, Ol, Tr, Ed, Opx, Srp, Chr, Ol inclusions in Chr.	
Z33	4232-7374	C6	Cpx, Ol, Srp, Opx, Mhb, Aw.	Dyke crosscuts chromitite.
Z377B	4320-7955	–	Cpx, Tr, Act, Opx.	
Z54	4205-7465	C8	Cpx, Chr, Tr, Srp.	
Websterite:				
Z30	4210-7173	C5	Opx, Cpx, Chr.	Lacks olivine
Fe-Websterite:				
Z36	4232-7374	C6	Opx, Cpx, Ol, Chr, Edhb, Prghb, Ol inclusions in Opx, Tro, Pn.	
Gabbro:				
Z233	4510-8080	–	Cpx (tow types), Chl, Czo.	Lower stratigraphic level; lacks Qtz.
Z394	4590-8670	–	Zo, Czo, Tr, Act, Achb, Ab, Chl, Qtz, Spn.	Middle-level gabbro
Z368A	4505-8450	–	Act, Achb, Chl, Ab, Czo.	Upper-level gabbro.
Metadolerite dykes in ultramafic host rocks:				
ZB182	4478-8073	C31	Ab, Ed, Act, M hb, Achb, Czo, Cpx.	Amphibole replaces Cpx grain margins. Albite is abundant. Rock lacks Ol or Qtz.
Z219	4454-8159	–	Fprg, Fedhb, Ed, Fed, Edhb, Fprhb, Czo, Spn, Ilm, Chap.	
Z372	4510-8770	–	Fsp, Ab, Fedhb, Fprhb, Fedhb, Edhb, Ed, Fedhb, Fed, Fprg, Grs, Spn, Cpx, Hgrs.	
Rodingite dykes in ultramafic host rocks:				
Z361A	4470-8165	–	Di, Grs, Hgrs, Chl, Uvr.	

A selection of SQO orthopyroxene analyses were run through a computer programme after the procedure of Cameron & Papike (1981). These analyses have been accepted as "superior" analyses as their oxides weight percentages sum close to 100% and they passed the following crystal-chemical tests: (1) the sum of $Si + Al^{iv}$ equals 2.00 ± 0.02 a.f.u., (2) the octahedral cations sum to 0.98 a.f.u.; (3) the M2 site occupancy equals 1.00 ± 0.02; and, (4) the charge balance equation is balanced to 0.02 of a charge. In table 3, the "Quad" - "Others" proportions, and the best numbers for the "Others" components are also given. The "general" name "Mg pyroxene" is applicable to all the pyroxenes of tables 2 & 3.

For the analyses included in table 3, "Others" contents vary between 2.77 and 11.45%. The most Fe-rich orthopyroxene is from the Fe-websterite dyke mentioned above (sample Z36) showing the composition $En_{77.11}$ $Fs_{21.23}$ $Wo_{1.66}$. This composition is of the "Quad" components that make its 95.09%.

CLINOPYROXENES

Clinopyroxene analyses are presented in table 3, the sample standard deviations are calculated in case of 3 or more analyses being included from each sample. The clinopyroxenes may contain lamellae of clacic amphibole formed by alteration.

The major chemical variations of clinopyroxenes and their coexisting orthopyroxenes are in the atomic proportions of Ca: Mg: Fe; best illustrated in the compositional plots in the pyroxene quadrilateral. These are shown in figs. 2 and 3 where the coexisting olivine compositions in terms of Fo percentages are also included. It may be noticed that Fe-enrichment in olivine is parallel to similar variations in co-existing orthopyroxenes (figs. 1 and 2) and clinopyroxenes (figs. 2 and 3). The analyses mainly fall in the diopside field, a few are Ca-richer endiopsides (mostly those from wehrlites), Mg-richer salites (mostly from metadolerites), and augites (all from metadolerites). Some diopsides (mostly from inclusions in chromite or those from metagabbros) contain wollastonite molecule in excess of 50 mole percent. Mg-rich clinopyroxenes are inclusions in chromite crystals. Harzburgites show a narrow range of compositional variation in clinopyroxenes than wehrlites. Calcic amphibole occurs sometimes as alteration lamellae in clinopyroxenes.

The analyses of clinopyroxenes from individual rock samples are listed in table 3. They cover a range at whose one extreme lies the chromitite sample Z277 with the most Mg-rich clinopyroxene, and at the other extreme is the sample Z372 of metasomatized metadolerite with the most Fe-rich clinopyroxene in SQO. The Fe-enrichment and Mg- and Ca- depletion trend in clinopyroxenes follows the order: chromitite – harzburgite – wehrlite – clinopyroxenite – websterite – metagabbro –Fe websterite – Ti-poor metadolerite (sp. ZB182) – Ti-richer metadolerite (sp. Z372). Excluding metadolerites, the most Fe-rich pyroxenes of initial magmatic derivation are probably those shown by the Fe-websterite, and have the composition

Table 2. Microprobe analyses of orthopyroxenes from chromitites (1), clinopyroxene harburgites (2 - 5), harzburgites (6 - 11), orthopyroxenite (12), clinopyroxenite (13), websterite (14), and Fe-websterite (15). The sample numbers correspond to those in figs. 1 to 3. No. Anal. = Number of analyses averaged; $\bar{x}$ = mean; s = standard deviation.

	1	2	3	4	5	6	7	8
Sp. No.	Z277	Z16	Z323	Z326	Z222	Z374	Z105	Z324
No. Anal.	$\bar{x}$ (7), (s)	$\bar{x}$ (6), (s)	$\bar{x}$ (6), (s)	$\bar{x}$ (9), (s)	$\bar{x}$ (6), (s)	$\bar{x}$ (6), (s)	$\bar{x}$ (4), (s)	$\bar{x}$ (5), (s)
SiO_2	57.39(024)	56.11(0.36)	55.98(0.36)	56.30(0.82)	56.01(0.31)	56.12(0.06)	56.96(0.46)	56.30(0.30)
Al_2O_3	1.55(0.32)	1.98(0.17)	2.05(0.18)	1.27(0.21)	2.11(0.16)	1.62(0.23)	1.24(0.20)	1.47(0.27)
TiO_2	0.08(0.06)	0.03(0.04)	0.03(0.04)	0.03(0.03)	0.04(0.05)	0.09(0.01)	b.d.	0.05(0.05)
Cr_2O_3	1.03(0.12)	0.65(0.11)	0.60(0.10)	0.44(0.07)	0.63(0.07)	0.55(0.10)	0.52(0.05)	0.59(0.13)
FeO	4.20(0.29)	5.48(0.16)	5.88(0.22)	6.63(0.19)	6.02(0.08)	6.22(0.08)	5.97(0.08)	5.75(0.05)
MnO	0.14(0.05)	0.17(0.08)	0.15(0.05)	0.17(0.09)	0.14(0.06)	0.14(0.08)	0.12(0.03)	0.14(0.03)
MgO	35.30(0.46)	33.72(0.30)	32.85(0.36)	34.39(0.52)	33.39(0.36)	33.59(0.07)	33.87(0.17)	33.47(0.36)
NiO	0.08(0.04)	0.12(0.07)	0.09(0.06)	0.10(0.09)	0.08(0.05)	0.09(0.02)	0.09(0.02)	0.08(0.08)
CaO	0.42(0.45)	0.90(0.23)	1.20(0.63)	0.87(0.26)	0.89(0.20)	0.59(0.14)	1.25(0.40)	0.83(0.41)
Na_2O	0.19(0.17)	0.40(0.22)	0.03(0.03)	n.d.	0.11(0.12)	b.d.	n.d.	0.13(0.13)
Total	100.38	99.56	98.86	100.20	99.42	99.01	100.02	98.81

	9	10	11	12	13	14	15
Sp. No.	Z216	Z310	Z344	Z104	ZA275	Z30	Z36
No. Anal.	$\bar{x}$ (7), (s)	$\bar{x}$ (4), (s)	$\bar{x}$ (8), (s)	$\bar{x}$ (15), (s)	$\bar{x}$ (8), (s)	$\bar{x}$ (4), (s)	$\bar{x}$ (4), (s)
SiO_2	55.13(0.25)	56.18(0.28)	56.78(0.29)	56.84(0.30)	57.35(0.16)	56.04(0.15)	54.07(0.29)
Al_2O_3	1.78(0.16)	1.51(0.13)	1.25(0.14)	0.99(0.16)	0.00	1.40(0.20)	1.79(0.13)
TiO_2	0.17(0.07)	n.d.	0.00	0.07(0.03)	0.04(0.05)	0.07(0.03)	0.16(0.04)
Cr_2O_3	0.63(0.10)	0.61(0.06)	0.50(0.06)	0.46(0.05)	0.17(0.07)	0.34(0.09)	0.16(0.06)
FeO	6.58(0.20)	6.00(0.15)	5.27(0.21)	5.84(0.46)	5.78(0.14)	8.44(1.02)	13.90(0.17)
MnO	0.12(0.09)	n.d.	0.09(0.08)	0.13(0.05)	0.17(0.05)	0.23(0.04)	0.30(0.06)
MgO	33.11(0.35)	34.06(0.38)	34.41(0.46)	33.44(0.69)	34.23(0.27)	32.55(0.83)	28.15(0.35)
NiO	0.04(0.02)	0.00	0.00	0.09(0.06)	0.11(0.04)	0.12(0.09)	0.06(0.06)
CaO	1.30(0.42)	0.82(0.42)	0.71(0.45)	1.25(0.76)	0.80(0.27)	0.66(0.13)	0.71(0.19)
Na_2O	n.d.	n.d.	b.d.	n.d.	0.28(0.25)	n.d.	0.09(0.02)
Total	98.86	99.18	99.01	99.11	98.93	99.97	99.39

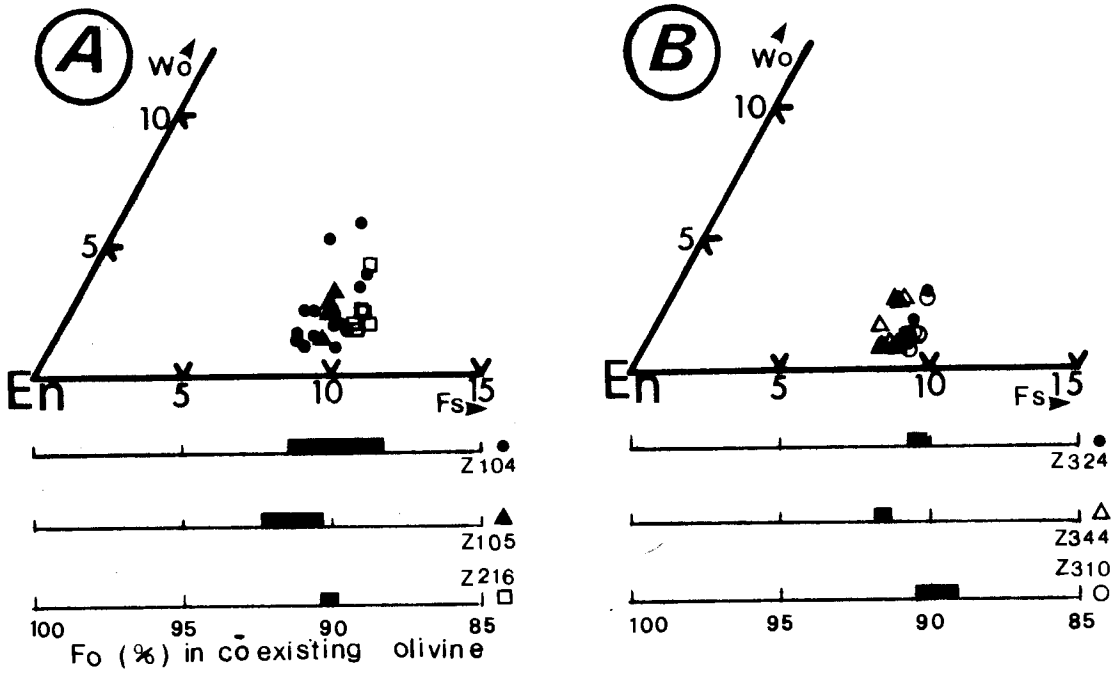

Fig. 1 (A & B). Pyroxene quadrilateral plots for orthopyroxenes for samples lacking clinopyroxenes. Fo (%) in coexisting olivines are shown as bars separately for each sample. Z104 is orthopyroxenite; the rest are harzburgites.

$Ca_{45.9}$ $Mg_{44.7}$ $Fe_{9.4}$. However, the Ca- poorer compositions of metadoleritic pyroxenes show little effect of Ca- and Al- metasomatism and probably represent products of further fractionation from the magma. The pigeonites are not present in SQO. In clinopyroxenes, Al_2O_3 content remains below 3%. Mn content tends to increase with Fe.

The replacement of Si by Al does not exceed 10% and Al_2O_3 contents are below 3% except in the type 1 grains of the metagabbro where mean Al_2O_3 is 3.81%. Cr_2O_3 is usually present in the clinopyroxenes of SQO upto a maximum of 1.77 wt %. Nickel is usually below the detection level of the microprobe. Maximum NiO observed is 0.2%. TiO_2 is also low; the maximum value found is 0.4%. The MnO content is generally low, and exhibits relative increase with increasing iron content of clinopyroxene.

Table 5 lists selected clinopyroxene analyses from various rock samples, processed by the procedure of Cameron & Papike (1981) and considered to be "superior" applying the criteria given by these authors.

Some clinopyroxenes do not appear to be magmatic. The metagabbro, in its lower level, (e.g., sample Z233) contains clinopyroxenes of two generations. Texturally the earlier- crystallized clinopyroxene, categorized here as type 1, is probably relict from initial magmatic crystallization and is chemically distinct from the later formed clinopyroxene, categorized here as type 2, which has a fresher appearance and tends to be pseudomorphous after type 1 grains, or occurs as needles, prisms, or outer margins of type 1 grains, or as subgrains within the type 1 grains. The chemistry of both types is compared in table 4. Type 1 clinopyroxene grains are

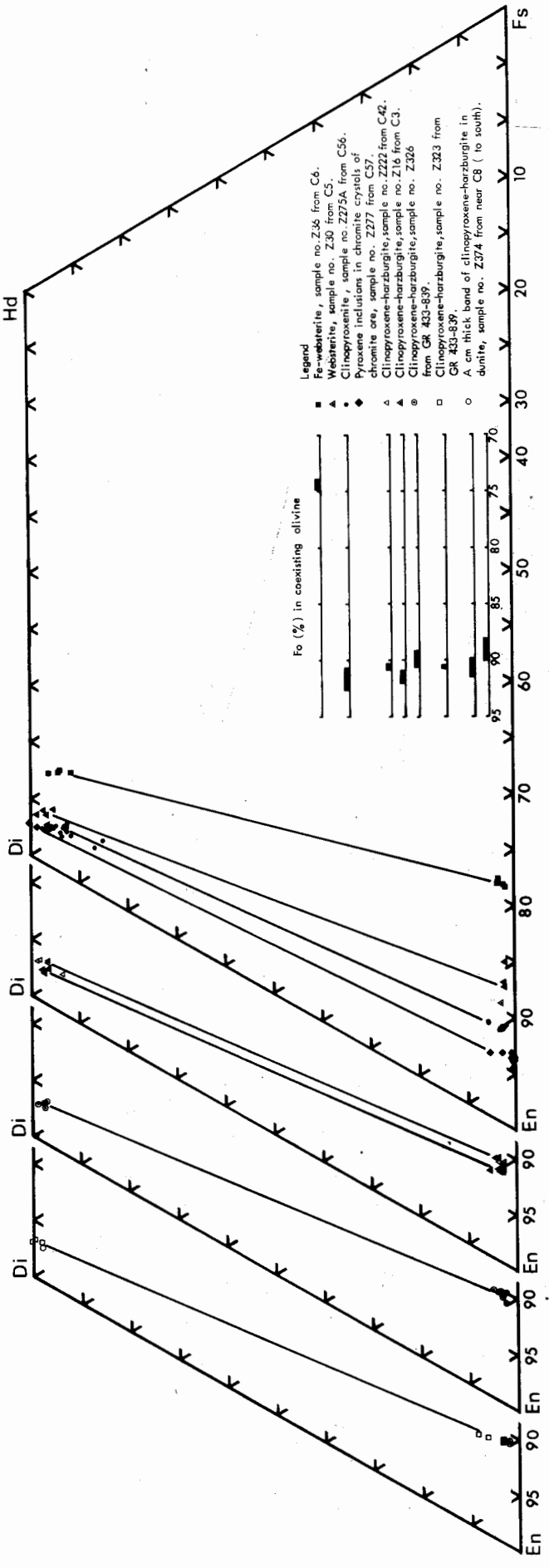

Fig. 2 Pyroxene quadrilateral plot of coexisting orthopyroxenes and clinopyroxenes from individual rock samples; joined by tie lines. Associated olivines are plotted as Fo (%).

higher in Ti, Al, Cr, Fe, and lower in Si, Ca and slightly lower (sometimes overlapping) in Mg than the type 2 clinopyroxenes. These chemical differences agree with similar differences observed by Dal Piaz *et al.*, (1980) from the rodingitized gabbro dykes of the Italian Western Alps although their Mn and Na variations are not clearly exhibited by the SQO metagabbroic clinopyroxenes. The metagabbros from the Bushveld complex of South Africa, have been shown (Schiffries & Skinner, 1987) to contain a hydrothermal clinopyroxene texturally and chemically distinct from a magmatic one. The former is enriched in Ca and depleted in Al, Ti and Cr, relative to the latter type of clinopyroxene. The above considerations lead to the conclusion that the type 2 clinopyroxenes in the SQO metagabbro may be the product of either hydrothermal activity or metasomatism (rodingitization); however, the lower Al content found in the type 2 grains does not favour rodingitization, because the SQO rodingites are exceptionally Al-eriched (Ahmed & Hall, 1983). Some rodingitized chromitites consist of chromite grains matrixed by metasomatic clinopyroxenes. Some of these clinopyroxenes show Wo content exceeding 50%.

AMPHIBOLES

The amphibole compositions are tabulated for individual rock samples in table 6. Some samples contain amphiboles of closely similar composition whereas others exhibit large within– sample variations. This is reflected in table 6, where analyses with the same sample numbers are given in separate columns if chemically different. Thus coexisting Al-poor and Al richer varieties are noticed. Following the classification scheme of I.M.A. (in Leake, 1978; Hawthorne, 1981), the amphiboles analyzed from SQO (table 4) belong mainly to the following species (fig. 5): tremolite, tremolitic hornblende, magnesio-hornblende, edenite, edinitic hornblende, ferroan pargasitic hornblende, ferroan pargasite and magnesio-anthophyllite. A few analyses also plot in each of the Mg-rich parts of the fields of the folowing species: actinolite, actinolitic hornblende, ferroedinitic hornblende, ferro-edinite, ferro-pargasitic hornblende, and anthophyllite.

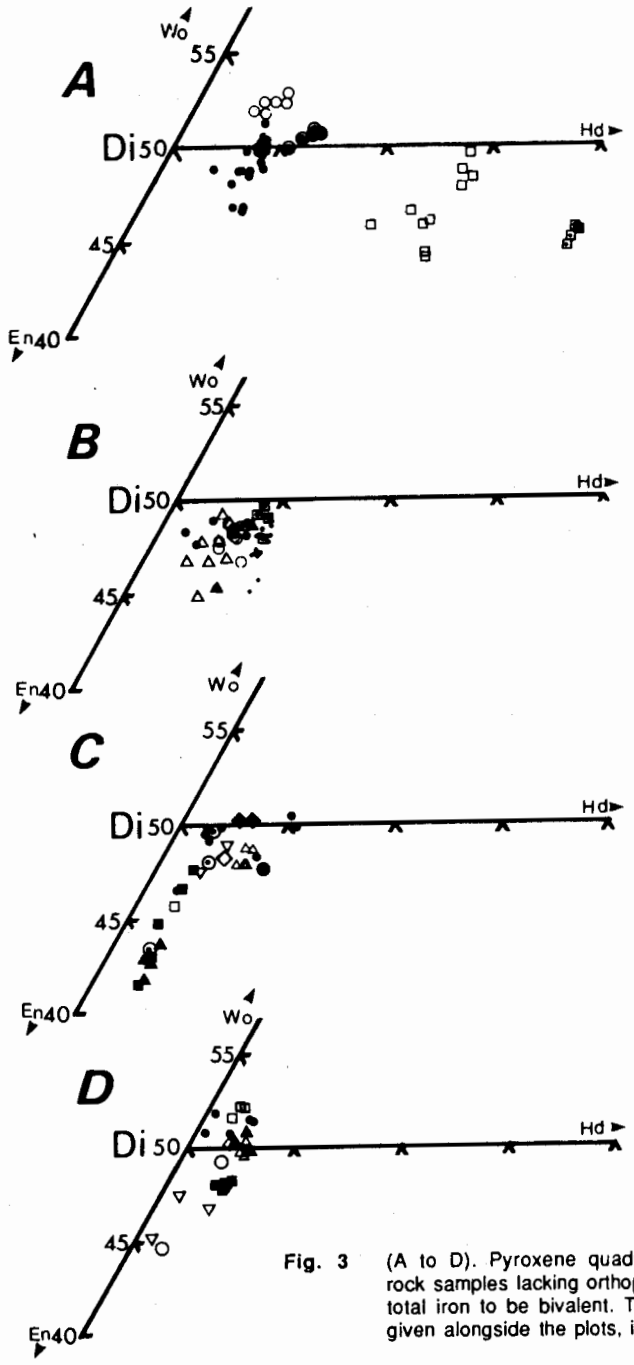

Plot 'A' : Mafic rocks

- ○ Gabbro, 'western' outcrop. Pyroxenes of type 2, sp. no. Z233 from SSW of Heru Shah.
- ◉ Gabbro, 'western' outcrop. Pyroxenes of type 1, sp.no. Z233.
- □ Metadolerite, sp.no. ZB182 from near C31.
- ⊡ Metadolerite, sp.no. Z372 from near C60 & GR 451-877.
- • Rodingite dyke, sp.no. Z361A, from GR 4470-8165.

Plot 'B' : Clinopyroxenites

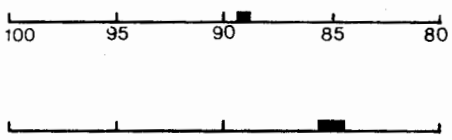

- △ Sp.no. Z123 from C9.
- ⊞ Sp.no. Z188B from C33.
- . Sp.no. Z377B from GR 4320-7955.
- • Sp.no. Z33 from C6.
- ▲ Sp.no. Z54 from C8.
- ○ Sp.no. Z70 from C8.

Plot 'C' : Wehrlites

- ▲ Sp.no. Z24 from C4.
- ■ Sp.no. Z147 from C15.
- ◇ Sp.no. Z294A from C60.
- □ Sp.no. Z265 from C55.
- ▽ Sp.no. Z264 from C55.
- ◆ Sp.no. Z202 from C39.
- △ Sp.no. Z183 from C32.
- ● Sp.no. Z188 from C33.
- • Sp.no. Z347 from GR 448-836.
- ◉ Sp.no. Z260 from C53, at in contact with chromitite.

Plot 'D' : Dunites and chromite ores

- • Sp.no. Z41A from C6. Metaso--matized massive chromite ore.
- □ Sp.no. Z62 from C8. Massive ore.
- ▽ Sp.no. Z236 from C42. Dissemi--nated ore.
- △ Sp.no. Z235 from C42. 'Pseudo--clastic' textured chromite ore.
- ▲ Sp.no. Z375 from near C8. Clinopyroxene- dunite.

Plot 'D' : Clinopyroxene inclusions in chromite crystals

- ◇ Sp.no. Z62 from C8. Massive ore.
- ○ Sp.no. Z327 from GR 431-840. Dunite.
- ⁘ Sp.no. Z34 from C8. Disseminated ore.

Fig. 3 (A to D). Pyroxene quadrilateral plots for clinopyroxenes from individual rock samples lacking orthopyroxenes; calculated in atomic percents assuming total iron to be bivalent. The legend, sample numbers and descriptions are given alongside the plots, including the Fo (%) of coexisting olivines.

Table 3. Selected analyses of orthopyroxenes from various SQO samples. The analyses are recalculated after the method of Cameron & Papike (1981) excluding the V_2O_3 and NiO contents. QUAD = Pyroxenes of the quadrilateral En-Fs-Hd-Di. NAME = Best name for the "Others" group of pyroxenes. – = not determined.

Sp. No.	Z277	Z277	Z277	Z323	Z323	Z326	Z326	Z222	Z222
SiO_2	57.29	57.62	57.58	56.40	55.57	55.71	56.21	55.64	55.73
TiO_2	0.12	0.13	0.07	0.00	0.00	0.00	0.00	0.05	0.13
Al_2O_3	1.70	1.55	1.34	1.74	2.18	1.28	1.56	2.01	1.91
Cr_2O_3	0.92	0.91	0.93	0.48	0.68	0.46	0.42	0.56	0.57
(V_2O_3)	0.00	0.00	0.00	0.04	0.04	0.00	0.03	0.07	0.00
Fe_2O_3	1.64	1.70	0.00	0.00	0.00	1.52	2.00	0.00	0.79
FeO	2.81	2.85	4.51	6.11	5.57	5.19	4.90	6.11	5.26
MnO	0.16	0.16	0.08	0.07	0.17	0.11	0.18	0.20	0.17
(NiO)	0.12	0.07	0.13	0.11	0.08	0.00	0.23	0.07	0.11
MgO	35.21	35.87	35.53	33.40	32.35	33.66	34.33	32.90	33.59
CaO	0.74	0.18	0.24	0.70	2.22	1.05	0.92	0.90	0.64
NaO	0.42	0.40	0.06	0.00	0.02	–	–	0.01	0.14
Total:	101.13	101.44	100.47	99.05	98.88	98.98	100.98	98.52	99.04
Number of ions on the basis of sixO									
Si	1.944	1.945	1.965	1.966	1.947	1.947	1.943	1.954	1.944
Al^{iv}	0.056	0.055	0.035	0.034	0.053	0.053	0.063	0.046	0.056
Al^{vi}	0.012	0.007	0.019	0.037	0.037	0.000	0.000	0.037	0.024
Ti	0.003	0.003	0.002	0.000	0.000	0.000	0.000	0.001	0.003
Cr	0.025	0.024	0.025	0.013	0.019	0.013	0.011	0.016	0.016
Fe^{3+}	0.042	0.043	0.000	0.000	0.000	0.040	0.052	0.000	0.021
Mg	1.780	1.805	1.807	1.735	1.690	1.753	1.761	1.722	1.746
Fe^{2+}	0.080	0.080	0.129	0.178	0.163	0.152	0.141	0.179	0.153
Mn	0.005	0.005	0.002	0.002	0.005	0.003	0.005	0.006	0.005
Ca	0.027	0.007	0.009	0.026	0.083	0.039	0.034	0.034	0.024
Na	0.028	0.026	0.004	0.000	0.001	–	–	0.001	0.009
SUM	4.000	4.000	3.996	3.992	3.999	4.000	4.002	3.996	4.000
En	94.35	95.41	92.93	89.47	87.26	90.17	90.96	88.89	90.79
Fs	4.22	4.25	6.62	9.18	8.43	7.80	7.28	9.27	7.97
Wo	1.43	0.34	0.45	1.35	4.31	2.02	1.75	1.75	1.24
%QUAD	91.90	92.23	95.45	94.95	94.37	94.73	93.67	94.60	93.77
%OTHERS	8.10	7.77	4.55	5.05	5.63	5.27	6.33	5.40	6.23
NAME	$MgFe^{3+}$ Cats	$MgFe^{3+}$ Cats	MgCr Cats	MgAl Cats	MgAl Cats	$MgFe^{3+}$ Cats	$MgFe^{3+}$ Cats	MgAl Cats	MgAl Cats
$M1_{Ti}$	3.51	0.34	4.37	0.00	0.00	–	–	2.74	4.93
$M2_{Na}$	31.70	95.41	9.67	0.00	2.52	–	–	1.42	13.70
iv_{Al}	64.78	4.25	85.96	100.00	97.48	–	–	95.84	81.36

Sp. No.	Z222	Z374	Z374	Z105	Z105	Z105	Z324	Z324	Z324
SiO_2	55.94	56.17	56.05	56.86	56.80	56.57	55.89	56.28	56.52
TiO_2	0.00	0.08	0.10	0.00	0.06	0.00	0.09	0.00	0.02
Al_2O_3	2.35	1.86	1.58	1.21	1.19	1.04	1.63	1.49	1.79
Cr_2O_3	0.62	0.66	0.50	0.59	0.50	0.50	0.63	0.58	0.45
(V_2O_3)	0.10	0.00	0.00	0.00	0.00	0.00	0.00	0.00	0.11
Fe_2O_3	1.93	3.38	2.35	0.22	0.00	0.00	1.27	0.19	0.00
FeO	4.33	3.20	4.01	5.78	6.07	5.91	4.60	5.57	5.77
MnO	0.19	0.04	0.19	0.11	0.15	0.11	0.16	0.18	0.14
(NiO)	0.06	0.07	0.11	0.07	0.08	0.12	0.07	0.04	0.20
MgO	33.80	33.64	33.61	33.84	34.03	33.64	33.74	33.51	33.34
CaO	0.65	0.55	0.47	1.40	0.71	1.27	0.67	0.92	0.61
Na_2O	0.28	0.72	0.52	–	0.00	–	0.25	0.14	0.29
Total	100.25	100.37	99.49	100.08	99.59	99.16	99.00	98.90	99.24
Si	1.928	1.931	1.945	1.964	1.969	1.972	1.947	1.964	1.968
Al^{iv}	0.072	0.069	0.055	0.036	0.031	0.028	0.053	0.036	0.032
Al^{vi}	0.024	0.007	0.010	0.014	0.018	0.015	0.014	0.025	0.041
Ti	0.000	0.002	0.003	0.000	0.002	0.000	0.002	0.000	0.001
Cr	0.017	0.018	0.014	0.016	0.014	0.014	0.017	0.016	0.012
Fe^{3+}	0.050	0.088	0.061	0.006	0.000	0.000	0.033	0.005	0.000
Mg	1.736	1.724	1.738	1.742	1.758	1.748	1.752	1.742	1.730
Fe^{2+}	0.125	0.092	0.116	0.167	0.176	0.172	0.134	0.163	0.168
Mn	0.006	0.001	0.006	0.003	0.004	0.003	0.005	0.005	0.004
Ca	0.024	0.020	0.017	0.052	0.026	0.047	0.025	0.034	0.023
Na	0.019	0.048	0.035	–	–	–	0.017	0.009	–
SUM	4.000	4.000	4.000	4.000	3.998	4.000	4.000	4.000	3.999
En	92.10	93.88	92.85	88.84	89.68	88.83	91.67	89.85	90.07
Fs	6.63	5.02	6.22	8.52	8.98	8.76	7.02	8.38	8.75
Wo	1.27	1.10	0.93	2.64	1.35	2.41	1.31	1.77	1.18
%QUAD	90.94	88.55	91.26	96.44	96.69	97.13	93.27	95.41	94.58
%OTHERS	9.06	11.45	8.74	3.56	3.31	2.87	6.73	4.59	5.42
NAME	$MgFe^{3+}$ Cats	$MgFe^{3+}$ Cats	$MgFe^{3+}$ Cats	MgCr Cats	MgAl Cats	MgAl Cats	$MgFe^{3+}$ Cats	MgAl Cats	MgAl Cats
$M1_{Ti}$	0.00	1.74	2.82	–	4.83	–	3.28	0.00	1.00
$M2_{Na}$	20.66	40.48	37.77	–	0.00	–	23.46	20.65	37.42
iv_{Al}	79.34	57.78	59.42	–	95.17	–	73.27	79.35	61.57

Sp. No.	Z216	Z216	Z216	Z310	Z310	Z344	Z344	Z344	Z104
SiO_2	55.31	55.34	54.89	55.97	56.53	56.44	56.42	56.92	56.35
TiO_2	0.11	0.10	0.28	0.00	0.00	0.00	0.00	0.00	0.07
Al_2O_3	1.98	1.76	1.90	1.49	1.34	1.00	1.29	1.38	1.23
Cr_2O_3	0.49	0.64	0.84	0.66	0.53	0.45	0.46	0.56	0.47
(V_2O_3)	0.02	0.00	0.00	–	–	–	–	–	0.00
Fe_2O_3	0.84	1.10	1.49	1.12	0.00	0.07	0.00	0.37	0.15
FeO	5.78	5.87	4.88	5.13	5.82	5.25	5.15	5.24	6.34
MnO	0.24	0.05	0.19	0.00	0.00	0.19	0.00	0.00	0.11
(NiO)	0.00	0.05	0.04	0.00	0.00	0.00	0.00	0.00	0.08
MgO	32.84	33.12	32.55	34.33	33.50	34.53	33.82	34.88	33.85
CaO	1.32	1.03	2.19	0.48	1.44	0.40	1.44	0.52	0.52
Total	98.93	99.06	99.25	99.18	99.16	98.33	98.58	99.87	99.17
Si	1.938	1.938	1.922	1.964	1.967	1.972	1.969	1.960	1.964
Al^{iv}	0.062	0.062	0.078	0.054	0.033	0.028	0.031	0.040	0.036
Al^{vi}	0.020	0.010	0.001	0.007	0.022	0.013	0.022	0.016	0.015
Ti	0.003	0.003	0.007	0.000	0.000	0.000	0.000	0.000	0.002
Cr	0.014	0.018	0.023	0.018	0.015	0.012	0.013	0.015	0.013
Fe^{3+}	0.022	0.029	0.039	0.029	0.000	0.002	0.000	0.010	0.004
Mg	1.715	1.728	1.699	1.779	1.738	1.798	1.759	1.790	1.759
Fe^{2+}	0.169	0.172	0.143	0.149	0.169	0.153	0.150	0.151	0.185
Mn	0.007	0.001	0.006	0.000	0.000	0.006	0.000	0.000	0.003
Ca	0.050	0.039	0.082	0.018	0.054	0.015	0.054	0.019	0.019
SUM	4.000	4.000	4.000	4.000	4.000	4.000	3.998	4.000	4.000
En	88.68	89.14	88.30	91.41	88.62	91.44	89.60	91.33	89.59
Fs	8.76	8.87	7.43	7.67	8.64	7.80	7.66	7.70	9.42
Wo	2.56	1.99	4.27	0.92	2.74	0.76	2.74	0.98	0.99
%QUAD	93.84	93.77	92.22	94.58	96.30	97.23	96.52	95.96	96.44
%OTHERS	6.16	6.23	7.78	5.42	3.70	2.77	3.48	4.04	3.56
NAME	$MgFe^{3+}$ Cats	$MgFe^{3+}$ Cats	$MgFe^{3+}$ Cats	$MgFe^{3+}$ Cats	MgAl Cats	MgAl Cats	MgAl Cats	MgAl Cats	MgAl Cats
$M1_{Ti}$	4.49	4.06	8.66	–	–	–	–	–	4.90
$M2_{Na}$	0.00	0.00	0.00	–	–	–	–	–	0.00
iv_{Al}	95.51	95.94	91.34	–	–	–	–	–	95.10

Sp. No.	Z104	Z104	Z104	Z30	Z30	Z36	Z36	Z36	Z36
SiO_2	56.53	56.73	56.63	56.27	56.22	54.47	54.05	53.78	53.99
TiO_2	0.06	0.07	0.05	0.00	0.05	0.18	0.20	0.11	0.15
Al_2O_3	0.98	0.96	1.21	1.53	1.27	1.95	1.81	1.63	1.77
Cr_2O_3	0.52	0.36	0.52	0.36	0.45	0.21	0.18	0.08	0.18
(V_2O_3)	0.00	0.00	0.00	0.00	0.00	0.03	0.01	0.11	0.02
Fe_2O_3	0.72	0.00	0.00	0.29	0.00	0.83	1.52	1.09	0.47
FeO	5.73	5.54	6.00	8.29	7.11	13.10	12.65	12.70	13.61
MnO	0.15	0.19	0.17	0.20	0.25	0.31	0.25	0.37	0.26
(NiO)	0.16	0.21	0.06	0.11	0.12	0.04	0.15	0.01	0.06
MgO	33.17	34.05	33.37	32.51	33.01	28.47	28.41	27.99	27.74
CaO	2.07	0.66	1.30	0.67	0.83	0.53	0.56	0.90	0.83
Na_2O	–	–	–	0.00	0.00	0.10	0.12	0.06	0.07
Total	100.09	98.77	99.31	100.23	99.31	100.22	99.91	98.83	99.15
Si	1.962	1.980	1.971	1.960	1.966	1.943	1.938	1.948	1.952
Al^{iv}	0.038	0.020	0.029	0.040	0.034	0.057	0.002	0.052	0.048
Al^{vi}	0.002	0.019	0.021	0.023	0.019	0.026	0.014	0.018	0.027
Ti	0.002	0.002	0.001	0.000	0.001	0.005	0.005	0.003	0.004
Cr	0.014	0.010	0.014	0.010	0.012	0.006	0.005	0.002	0.005
Fe^{3+}	0.019	0.000	0.000	0.008	0.000	0.022	0.041	0.030	0.013
Mg	1.716	1.771	1.731	1.687	1.721	1.514	1.518	1.512	1.494
Fe^{2+}	0.166	0.162	0.175	0.241	0.208	0.391	0.379	0.385	0.411
Mn	0.004	0.006	0.005	0.006	0.007	0.009	0.008	0.011	0.008
Ca	0.077	0.025	0.048	0.025	0.031	0.020	0.022	0.035	0.032
Na	–	–	–	0.000	0.000	0.007	0.008	0.004	0.005
SUM	4.000	3.994	3.996	4.000	4.000	4.000	4.000	4.000	4.000
En	87.57	90.48	88.58	86.36	87.80	78.64	79.11	78.27	77.11
Fs	8.50	8.26	8.94	12.36	10.61	20.31	19.77	19.92	21.23
Wo	3.93	1.26	2.48	1.28	1.59	1.05	1.12	1.81	1.66
%QUAD	96.19	96.91	96.36	95.98	96.64	94.14	93.46	94.71	95.09
%OTHERS	3.81	3.09	3.64	4.02	3.36	5.86	6.54	5.29	4.91
NAME	$MgFe^{3+}$ Cats	MgAl Cats	MgAl Cats	MgAl Cats	MgAl Cats	MgAl Cats	$MgFe^{3+}$ Cats	$MgFe^{3+}$ Cats	MgAl Cats
$M1_{Ti}$	3.95	8.29	4.34	0.00	3.77	7.08	7.07	5.09	7.12
$M2_{Na}$	0.00	0.00	0.00	0.00	0.00	10.14	10.94	7.16	8.56
iv_{Al}	96.05	91.71	95.66	100.00	96.23	82.79	81.98	87.75	84.32

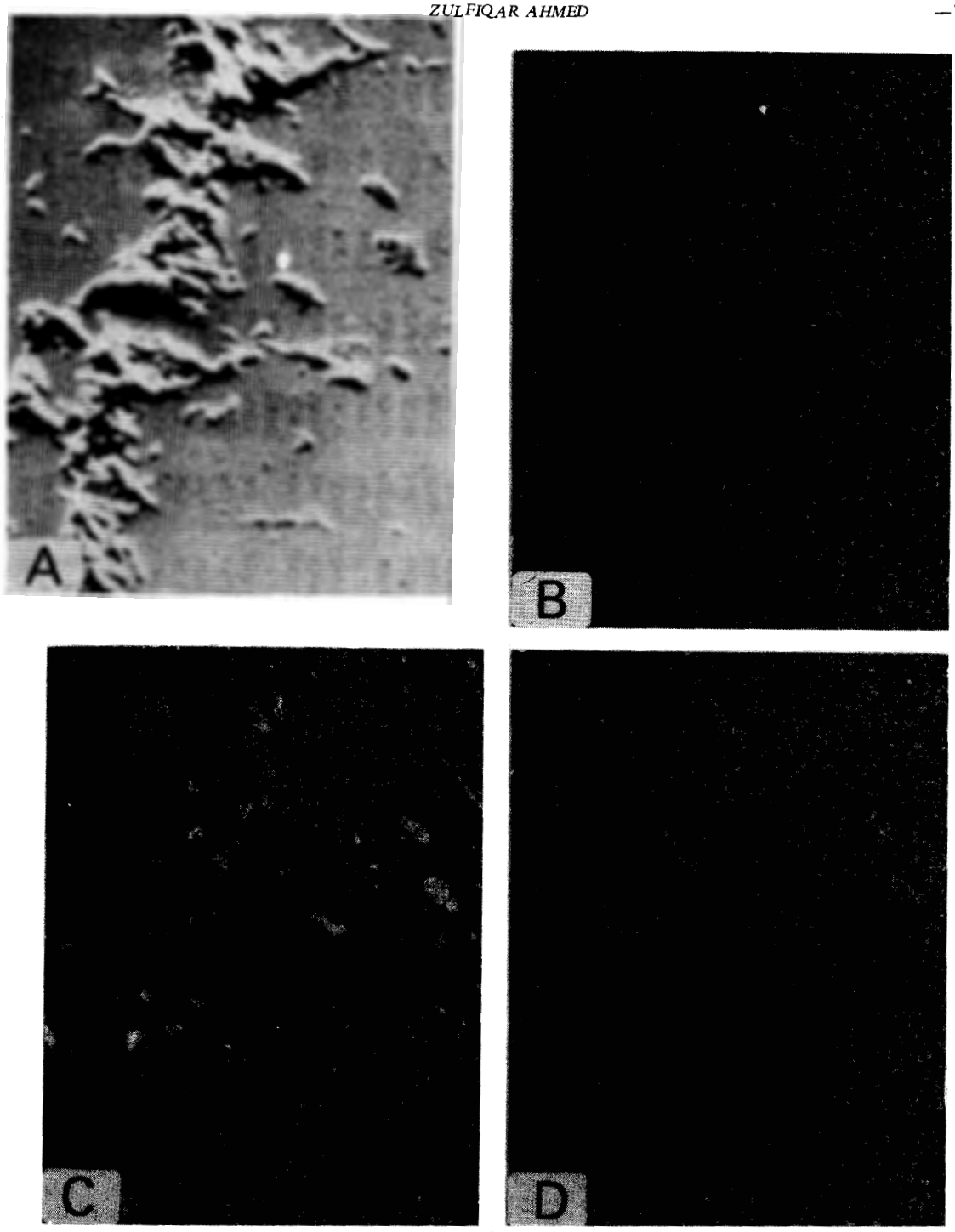

Fig.4 . Electron microprobe scanning pictures of the two types of clinopyroxene in the "western metagabbro" (sp. no. Z233). (A) Backscattered electrons image showing the boundary between the two types marked by oblique vertical fracture and chlorite-filled area developed along the margin of type 1 clinopyroxene grain to its right. Type 2 clinopyroxene is on its left. Optical distinctions are stated in text; and are supported by separate analyses in table 4 . (B) Cr distribution image. (C) Al distribution, showing also the Al-rich (chlorite) inclusions.(D) Fe distribution image.

Table 4. Microprobe analyses of clinopyroxenes. Sample nos. correspond to those in figs. 1 to
Where not given, K_2O is absent. Samples Z277, Z34 and Z62 report inclusions in chromite crystals.

Sp.No.	Z277	Z34		Z62		Z327	Z236		Z41A		Z375	Z235	
No.Anal.	X̄(2)	X̄(4) ,	s	X̄(4) ,	s	X̄(2) ,	X̄(5) ,	s	X̄(5) ,	s	X̄(2)	X̄(4) ,	s
SiO_2	53.20	53.78	(0.58)	53.79	(0.62)	52.77	53.04	(0.46)	53.96	(0.22)	53.11	53.33	(0.79)
Al_2O_3	2.28	1.43	(0.18)	1.62	(0.18)	1.83	1.69	(0.75)	1.05	(0.36)	2.13	2.22	(0.62)
TiO_2	0.36	b.d.		0.13	(0.06)	0.10	b.d.		0.37	(0.06)	0.10	0.08	(0.06)
Cr_2O_3	1.77	1.20	(0.14)	1.00	(0.45)	0.91	1.06	(0.42)	0.42	(0.32)	0.91	1.13	(0.22)
FeO	1.75	1.65	(0.12)	1.02	(0.21)	1.10	1.20	(0.64)	0.91	(0.60)	1.68	1.67	(0.10)
MnO	0.00	0.00		b.d.		0.00	b.d.		b.d.		b.d.	0.07	(0.04)
MgO	16.17	17.79	(0.33)	16.69	(0.41)	18.84	18.33	(1.20)	16.79	(0.47)	16.58	16.65	(0.09)
NiO	0.06	0.00		0.10	(0.06)	b.d.	n.d.		b.d.		b.d.	0.08	(0.03)
CaO	23.57	24.02	(0.20)	25.50	(0.42)	23.93	23.51	(0.54)	25.27	(0.23)	24.55	24.36	(0.31)
Na_2O	b.d.	n.d.		b.d.		0.00	n.d.		n.d.		n.d.	0.43	(0.20)
Total	99.16	99.87		99.85		99.48	98.83		98.77		99.06	100.04	

Sp.No.	Z24		Z16		Z222		Z374	Z260		Z147		Z294-A	Z265	
No.Anal.	X̄(4) ,	s	X̄(3) ,	s	X̄(5) ,	s	(1)	X̄(3) ,	s	X̄(4) ,	s	(1)	X̄(4) ,	s
SiO_2	52.98	(0.47)	53.50	(0.32)	53.20	(0.26)	53.36	54.25	(0.47)	53.67	(0.86)	53.73	52.62	(0.98)
Al_2O_3	1.49	(0.37)	1.93	(0.20)	2.60	(0.19)	2.33	0.17	(0.23)	0.54	(0.17)	0.37	1.48	(0.70)
TiO_2	0.00		0.05	(0.03)	0.03	(0.03)	0.03	0.00		0.00		n.d.	n.d.	
Cr_2O_3	0.54	(0.16)	0.84	(0.10)	1.06	(0.05)	0.81	0.44	(0.26)	0.56	(0.17)	0.63	0.55	(0.19)
FeO	1.42	(0.20)	1.86	(0.13)	2.24	(0.09)	1.85	1.19	(0.15)	1.32	(0.23)	1.84	1.39	(0.14)
MnO	0.00		0.02	(0.02)	0.08	(0.05)	0.13	0.00		0.06	(0.02)	n.d.	b.d.	
MgO	19.90	(1.02)	17.45	(0.15)	16.98	(0.34)	17.20	18.83	(1.39)	20.50	(0.96)	17.83	21.56	(1.68)
NiO	0.03	(0.02)	0.05	(0.04)	0.07	(0.03)	0.11	0.05	(0.07)	b.d.		0.00	0.00	
CaO	22.44	(1.16)	24.37	(0.07)	23.83	(0.53)	24.59	23.98	(0.95)	23.03	(1.13)	24.47	21.58	(1.87)
Na_2O	n.d.		0.45	(0.19)	0.18	(0.13)	1.05	n.d.		n.d.		n.d.	n.d.	
Total	98.80		100.52		100.27		101.46	98.91		99.68		98.87	99.18	

Sp.No.	Z264		Z202	Z183		Z188	Z347		Z123		ZA275	
No.Anal.	X̄(4) ,	s	X̄(2)	X̄(5) ,	s	(1)	X̄(8) ,	s	X̄(8) ,	s	X̄(14) ,	s
SiO_2	54.14	(0.13)	52.44	53.82	(0.62)	52.95	53.59	(0.64)	54.89	(0.52)	54.52	(0.29)
Al_2O_3	0.00		2.60	2.04	(0.39)	0.87	0.78	(0.56)	b.d.		0.40	(0.20)
TiO_2	0.00		0.02	0.23	(0.07)	0.19	0.04	(0.02)	b.d.		b.d.	
Cr_2O_3	0.32	(0.07)	1.07	0.98	(0.23)	0.37	0.41	(0.33)	0.40	(0.26)	1.61	(0.22)
FeO	1.78	(0.45)	1.86	2.50	(0.15)	3.24	1.85	(1.12)	1.92	(0.40)	2.34	(0.29)
MnO	0.00		0.08	b.d.		0.13	0.97	(0.04)	0.06	(0.07)	0.07	(0.06)
MgO	18.51	(0.67)	16.46	17.10	(0.41)	17.26	17.45	(1.14)	18.29	(0.57)	16.99	(0.50)
NiO	0.00		b.d.	n.d.		0.03	b.d.		0.00		b.d.	
CaO	24.57	(0.38)	24.52	23.91	(0.34)	24.05	24.71	(0.57)	24.21	(0.72)	22.11	(0.85)
Na_2O	n.d.		n.d.	n.d.		b.d.	0.14	(0.13)	n.d.		1.15	(0.21)
Total	99.32		99.05	100.58		99.09	99.94		99.77		99.19	

Sp.No.	Z33		Z70		ZB188		Z54	ZB377		ZA361		Z30	
No.Anal.	X̄(5) ,	s	X̄(7) ,	s	X̄(6) ,	s	X̄(2)	X̄(11) ,	s	X̄(23) ,	s	X̄(6) ,	s
SiO_2	53.62	(0.40)	52.97	(0.33)	53.26	(0.38)	52.98	53.43	(0.33)	51.94	(0.67)	53.44	(0.48)
Al_2O_3	0.89	(0.83)	0.85	(0.19)	1.58	(0.43)	1.26	1.35	(0.14)	2.56	(0.56)	1.45	(0.26)
TiO_2	b.d.		0.00		0.13	(0.08)	0.00	0.07	(0.04)	0.16	(0.06)	0.06	(0.03)
Cr_2O_3	0.44	(0.19)	0.50	(0.06)	0.51	(0.12)	0.76	0.53	(0.08)	1.09	(0.10)	0.63	(0.04)
FeO	1.90	(0.68)	2.31	(0.35)	2.67	(0.36)	2.68	3.29	(0.20)	2.59	(0.18)	2.65	(0.40)
MnO	0.08	(0.05)	0.17	(0.05)	0.07	(0.04)	0.09	0.12	(0.03)	0.08	(0.07)	0.09	(0.06)
MgO	17.65	(0.81)	17.72	(0.24)	16.67	(0.39)	17.52	16.78	(0.36)	15.97	(0.55)	17.01	(0.43)
NiO	0.15	(0.11)	0.10	(0.07)	0.00		0.07	b.d.		b.d.		b.d.	
CaO	24.19	(0.40)	24.26	(0.42)	24.06	(0.31)	23.43	23.41	(0.60)	23.63	(0.67)	24.24	(0.44)
Na_2O	0.34	(0.28)	n.d.		n.d.		0.11	b.d.		0.33	(0.28)	n.d.	
Total	99.26		98.88		98.95		98.93	98.98		98.35		99.57	

Sp.No.	$Z233_{TYPE-I}$		$Z233_{TYPE-II}$		Z36		ZB182		Z372	
No.Anal.	X̄(6) ,	s	X̄(6) ,	s	X̄(4)		X̄(7) ,	s	X̄(4) ,	s
SiO_2	51.24	(0.93)	54.36	(0.25)	52.20	(0.12)	53.33	(0.40)	5.17	(0.36)
Al_2O_3	3.81	(0.84)	1.37	(0.62)	2.24	(0.14)	0.38	(0.35)	1.26	(0.11)
TiO_2	0.31	(0.09)	b.d.		0.24	(0.02)	b.d.		0.21	(0.07)
Cr_2O_3	1.22	(0.16)	0.13	(0.05)	0.39	(0.12)	b.d.		b.d.	
FeO	3.69	(0.43)	2.12	(0.28)	5.49	(0.32)	9.14	(0.65)	12.83	(0.11)
MnO	0.10	(0.06)	0.14	(0.06)	0.13	(0.08)	0.30	(0.07)	0.37	(0.04)
MgO	14.95	(0.72)	15.61	(0.26)	15.47	(0.20)	14.27	(0.59)	11.63)	(0.27)
NiO	b.d.		0.06	(0.04)	b.d.		0.00		0.00	
CaO	25.55	(1.10)	25.55)	(0.51)	22.93	(0.46)	22.44	(0.84)	21.63	(0.10)
Na_2O	0.39	(0.20)	0.57	(0.40)	0.57	(0.40)	b.d.		0.21	(0.09)
Total	99.24		99.91		99.66		99.86		99.31	

Table 5. Selected microprobe analyses of clinopyroxenes from SQO rocks. Analyses are recalculated by the procedure of Cameron & Papike (1981) exclusive of the amounts of V_2O_3 and NiO. QUAD = Pyroxenes of the quadrilateral En-Fs-Hd-Di. NAME = Best name for the "Others" group of pyroxenes. – = not determined.

Sp. No.	Z277	Z277	Z34	Z375	Z235	Z327	Z326	Z326
SiO_2	52.77	53.64	53.87	53.22	53.55	53.82	53.23	53.73
TiO_2	0.46	0.26	0.00	0.03	0.07	0.05	0.02	0.00
Al_2O_3	2.59	1.96	1.38	2.44	1.98	0.95	1.21	1.45
Cr_2O_3	1.79	1.75	1.07	1.01	1.08	0.87	0.75	0.75
(V_2O_3)	0.01	0.05	0.00	–	0.06	0.05	0.03	0.05
Fe_2O_3	0.97	0.50	0.00	0.00	0.00	0.55	0.86	0.59
FeO	0.92	1.26	1.51	1.88	1.78	0.75	1.22	1.84
MnO	0.00	0.03	0.00	0.18	0.04	0.01	0.07	0.13
(NiO)	0.11	0.01	0.00	–	0.08	0.16	0.10	0.14
MgO	16.15	16.19	17.95	16.53	16.75	17.84	17.18	17.35
CaO	23.86	23.28	24.03	24.07	24.17	25.02	24.79	24.47
Na_2O	0.70	0.95	–	–	0.29	0.03	–	–
Total	100.33	99.88	99.81	99.36	99.85	100.10	99.46	100.50
Number of ions on the basis of sixO:								
Si	1.918	1.952	1.956	1.945	1.951	1.956	1.951	1.950
Al^{iv}	0.082	0.048	0.044	0.055	0.049	0.041	0.049	0.050
Al^{vi}	0.029	0.036	0.015	0.050	0.036	0.000	0.003	0.012
Ti	0.013	0.007	0.000	0.001	0.002	0.001	0.001	0.000
Cr	0.051	0.050	0.031	0.029	0.031	0.025	0.022	0.022
Fe^{3+}	0.027	0.014	0.000	0.000	0.000	0.015	0.024	0.016
Mg	0.875	0.878	0.972	0.900	0.910	0.966	0.938	0.938
Fe^{2+}	0.028	0.038	0.046	0.057	0.054	0.023	0.037	0.056
Mn	0.000	0.001	0.000	0.006	0.001	0.000	0.002	0.004
Ca	0.929	0.908	0.935	0.943	0.944	0.974	0.973	0.952
Na	0.049	0.067	–	–	0.020	0.002	–	–
SUM	4.000	4.000	3.999	3.987	4.002	4.004	4.000	4.000
En	47.75	48.14	49.76	47.38	47.68	49.21	48.14	48.22
Fs	1.52	2.10	2.35	3.02	2.84	1.17	1.92	2.88
Wo	50.73	49.76	47.89	49.60	49.47	49.62	49.94	48.90
%QUAD	88.09	89.24	95.38	91.95	93.05	95.86	95.06	95.01
%OTHERS	11.91	10.76	4.62	8.05	6.95	4.14	4.94	4.99
NAME	CaCr Cats	Ureyite	CaCr Cats	CaAl Cats	CaAl Cats	CaCr Cats	$CaFe^{3+}$ Cats	CaCr Cats
$M1_{Ti}$	8.71	5.84	–	–	2.70	3.09	–	–
$M2_{Na}$	34.19	55.02	–	–	28.85	4.78	–	–
iv_{Al}	37.10	39.14	–	–	68.45	92.12	–	–

Sp. No.	Z222	Z222	Z323	Z202	Z24	Z147	Z183	Z183
SiO_2	53.52	53.32	53.15	52.26	53.61	54.91	53.77	52.95
TiO_2	0.08	0.07	0.00	0.02	0.00	0.00	0.15	0.33
Al_2O_3	2.63	2.64	1.97	2.64	0.95	0.34	1.78	2.50
Cr_2O_3	0.98	1.03	0.95	1.12	0.34	0.36	0.95	1.11
(V_2O_3)	0.05	0.10	0.14	0.02	0.10	–	–	–
Fe_2O_3	0.11	1.40	0.00	1.96	0.89	0.15	0.00	0.00
FeO	2.28	0.99	1.85	0.00	0.34	1.11	2.74	2.50
MnO	0.07	0.07	0.02	0.05	0.00	0.09	0.00	0.00
(NiO)	0.04	0.07	0.06	0.00	0.04	0.06	–	–
MgO	16.99	16.88	16.45	16.54	18.46	19.48	17.23	17.10
CaO	23.92	24.42	24.47	24.49	24.09	24.52	23.87	23.67
Na_2O	0.17	0.30	0.08	0.38	–	–	–	–
Total	100.84	101.29	99.14	99.48	98.82	101.02	100.49	100.16
Si	1.932	1.919	1.953	1.911	1.962	1.969	1.948	1.925
Al^{iv}	0.068	0.81	0.047	0.089	0.038	0.014	0.052	0.075
Al^{vi}	0.044	0.031	0.038	0.025	0.003	0.000	0.024	0.032
Ti	0.002	0.002	0.000	0.001	0.000	0.000	0.004	0.009
Cr	0.028	0.029	0.028	0.032	0.010	0.010	0.027	0.032
Fe^{3+}	0.003	0.038	0.000	0.054	0.024	0.004	0.000	0.000
Mg	0.914	0.905	0.910	0.902	1.007	–	0.930	0.926
Fe^{2+}	0.069	0.030	0.057	0.000	0.010	0.033	0.083	0.076
Mn	0.002	0.002	0.001	0.002	0.000	0.013	0.000	0.000
Ca	0.925	0.942	0.0963	0.960	0.945	0.942	0.927	0.922
Na	0.012	0.021	0.006	0.027	–	–	–	–
SUM	4.000	4.000	3.993	4.002	4.000	4.017	3.996	3.997
En	47.90	48.24	46.89	48.44	51.32	51.63	47.96	48.14
Fs	3.61	1.59	2.96	0.00	0.53	1.65	4.28	3.95
Wo	48.49	50.17	50.15	51.56	48.15	46.72	47.77	47.91
%QUAD	92.26	89.99	93.41	88.81	96.24	98.56	94.43	92.46
%OTHERS	7.74	10.01	6.59	11.19	3.76	1.44	5.57	7.54
NAME	CaAl Cats	$CaFe^{3+}$ Cats	CaAl Cats	$CaFe^{3+}$ Cats	$CaFe^{3+}$ Cats	CaCr Cats	CaCr Cats	CaCr Cats
$M1_{Ti}$	2.66	1.82	0.00	0.47	–	–	7.33	–
$M2_{Na}$	14.57	20.15	10.81	23.19	–	–	0.00	–
iv_{Al}	82.77	78.03	89.19	76.34	–	–	92.67	–

Sp. No.	Z188	Z347	Z347	Z123	Z70	Z54	Z54	Z361A
SiO_2	52.95	53.59	53.27	55.70	52.70	53.11	52.85	50.99
TiO_2	0.19	0.02	0.05	0.00	0.00	0.00	0.00	0.10
Al_2O_3	0.87	1.09	0.85	0.24	1.11	1.33	1.19	4.35
Cr_2O_3	0.37	0.68	0.54	0.27	0.56	0.76	0.77	1.20
(V_2O_3)	–	0.00	0.15	–	0.00	0.15	0.00	0.00
Fe_2O_3	0.59	1.03	0.69	0.09	1.15	0.00	1.62	1.16
FeO	2.71	0.30	0.50	1.39	1.94	2.68	1.21	1.54
MnO	0.13	0.12	0.09	0.09	0.09	0.17	0.00	0.00
(NiO)	0.03	0.02	0.05	0.03	0.16	0.13	0.01	0.00
MgO	17.26	17.47	17.81	18.71	17.58	16.74	18.31	15.18
CaO	24.05	25.18	24.72	24.96	23.48	24.04	22.83	25.34
Na_2O	–	0.06	0.01	–	–	0.00	0.22	–
Total	100.14	99.56	98.73	101.48	98.77	99.11	99.01	99.86
Si	1.953	1.954	1.960	1.988	1.947	1.960	1.939	1.870
Al^{iv}	0.038	0.046	0.037	0.010	0.048	0.040	0.051	0.130
Al^{vi}	0.000	0.001	0.000	0.000	0.000	0.018	0.000	0.058
Ti	0.005	0.001	0.001	0.000	0.000	0.000	0.000	0.003
Cr	1.011	0.020	0.016	0.008	0.016	0.022	0.022	0.035
Fe^{3+}	0.016	0.028	0.019	0.002	0.032	0.000	0.045	0.032
Mg	0.949	0.949	0.977	0.995	0.968	0.921	1.001	0.830
Fe^{2+}	0.083	0.009	0.015	0.041	0.060	0.083	0.037	0.047
Mn	0.004	0.004	0.003	0.003	0.003	0.005	0.000	0.000
Ca	0.950	0.984	0.975	0.955	0.930	0.951	0.898	0.996
Na	–	0.004	0.001	–	–	0.000	0.016	–
SUM	4.009	4.000	4.003	4.002	4.004	4.000	4.009	4.000
En	47.85	48.87	49.66	49.98	49.45	47.12	51.72	44.30
Fs	4.21	0.48	0.78	2.08	3.07	4.23	1.92	2.53
Wo	47.94	50.65	49.56	47.94	47.48	48.65	46.36	53.17
%QUAD	96.22	95.05	96.31	98.99	95.16	95.98	93.29	86.98
%OTHERS	3.78	4.95	3.69	1.01	4.84	4.02	6.71	13.02
NAME	$CaFe^{3+}$ Cats	$CaFe^{3+}$ Cats	$CaFe^{3+}$ Cats	CaCr Cats	$CaFe^{3+}$ Cats	CaCr Cats	$CaFe^{3+}$ Cats	CaAl Cats
$M1_{Ti}$	–	1.08	3.55	–	–	0.00	0.00	-
$M2_{Na}$	–	8.39	1.83	–	–	0.00	23.32	–
iv_{Al}	–	90.53	94.62	–	–	100.00	76.68	–

Sp. No.	Z361A	Z30	Z30	Z233	Z36	Z36	Z372	Z372
SiO_2	52.56	56.04	56.22	51.30	52.29	52.28	50.91	51.55
TiO_2	0.12	0.08	0.05	0.21	0.22	0.24	0.23	0.10
Al_2O_3	2.95	1.62	1.27	3.11	2.20	2.27	1.24	1.11
Cr_2O_3	1.15	0.35	0.45	1.17	0.48	0.24	0.00	0.00
(V_2O_3)	0.08	0.00	0.00	–	0.05	0.16	0.02	0.04
Fe_2O_3	0.11	0.00	0.00	2.35	1.81	0.00	2.33	0.96
FeO	2.25	9.61	7.11	1.32	3.86	5.86	10.82	11.97
MnO	0.14	0.28	0.25	0.11	0.06	0.15	0.39	0.42
(NiO)	0.00	0.03	0.12	–	0.10	0.00	0.00	0.07
MgO	17.06	31.40	33.01	15.94	15.59	15.68	11.94	11.46
CaO	23.54	0.52	0.83	24.74	23.23	22.34	21.56	21.73
Na_2O	–	0.00	0.00	–	0.27	0.00	0.33	0.23
Total	99.96	99.93	99.31	100.25	100.16	99.22	99.77	99.64
Si	1.915	1.965	1.966	1.878	1.924	1.942	1.938	1.967
Al^{iv}	0.085	0.035	0.034	0.122	0.076	0.058	0.056	0.033
Al^{vi}	0.042	0.032	0.019	0.012	0.019	0.041	0.000	0.017
Ti	0.003	0.002	0.000	0.006	0.006	0.007	0.007	0.003
Cr	0.033	0.010	0.010	0.034	0.014	0.007	0.000	0.000
Fe^{3+}	0.003	0.000	0.008	0.065	0.050	0.000	0.067	0.028
Mg	0.926	1.641	1.721	0.870	0.855	0.868	0.678	0.652
Fe^{2+}	0.069	0.282	0.208	0.040	0.119	0.182	0.345	0.382
Mn	0.004	0.008	0.007	0.003	0.002	0.005	0.013	0.014
Ca	0.919	0.020	0.031	0.970	0.916	0.889	0.880	0.888
Na	–	0.000	0.000	–	0.019	0.000	0.024	0.017
SUM	4.000	3.994	4.000	4.000	4.000	3.998	4.006	4.000
En	48.40	84.48	87.80	46.25	45.24	44.76	35.63	33.90
Fs	3.59	14.51	10.61	2.14	6.29	9.39	18.12	19.88
Wo	48.02	1.01	1.59	51.61	48.47	45.85	46.25	46.22
%QUAD	91.53	95.61	96.64	87.78	91.67	94.16	92.66	95.27
%OTHERS	8.47	4.39	3.36	12.22	8.93	5.84	7.34	4.73
NAME	CaAl Cats	MgAl Cats	MgAl Cats	$CaFe^{3+}$ Cats	$CaFe^{3+}$ Cats	CaAl Cats	$CaFe^{3+}$ Cats	$CaFe^{3+}$ Cats
$M1_{Ti}$	–	5.70	3.77	4.52	6.00	10.30	7.60	5.41
$M2_{Na}$	–	0.00	0.00	–	18.98	0.00	28.13	32.09
iv_{Al}	–	94.30	94.48	95.48	75.03	89.70	64.27	62.50

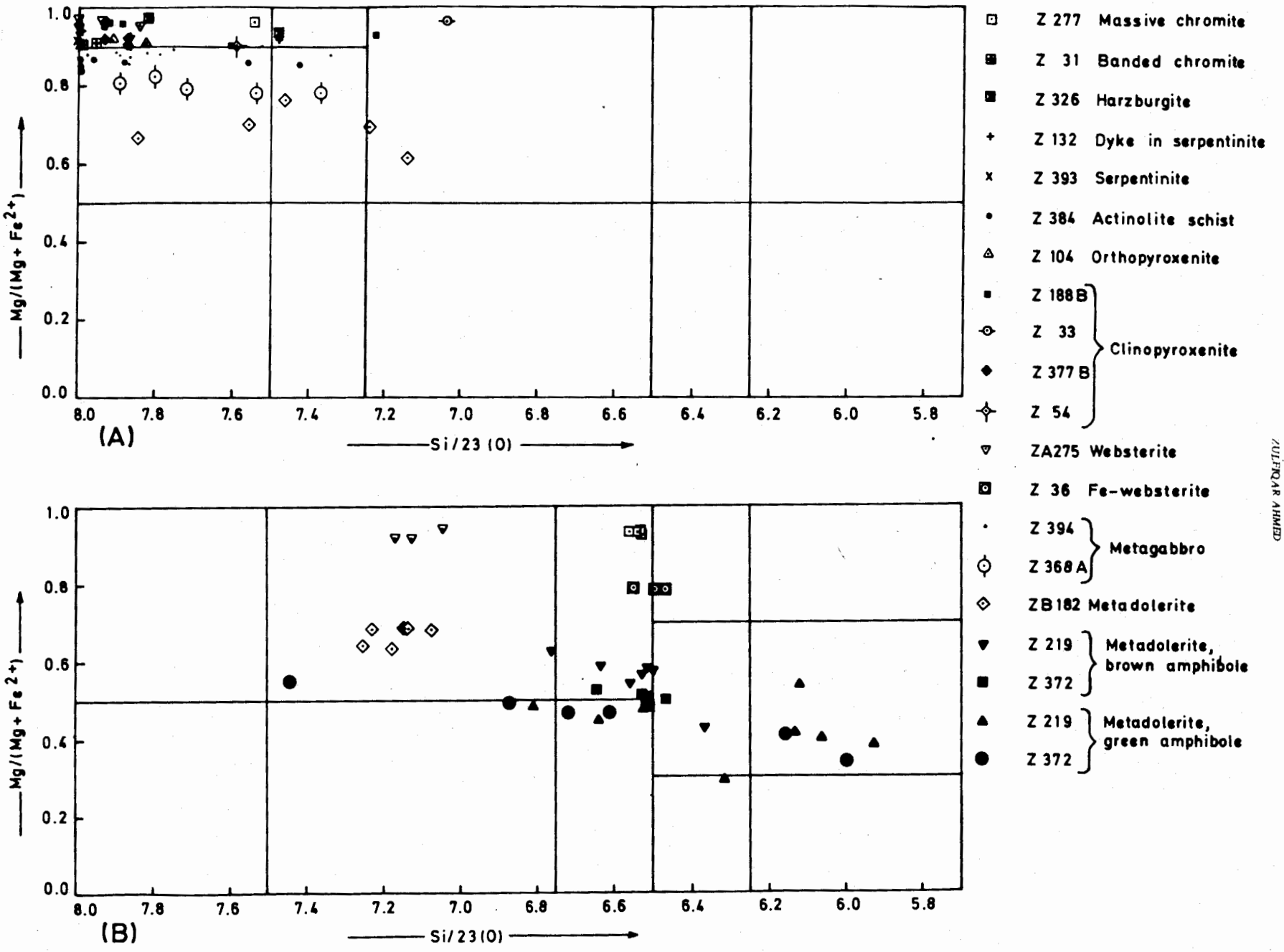

Fig.5. Plot of calcic amphiboles from different rock types of SQO.
(A) Calcic amphiboles with $(Na+K)_A < 0.50$ and $Ti < 0.50$.
(B) Calcic amphiboles with $(Na+K)_A \geq 0.50$ and $Ti < 0.50$.

Table 6. Amphibole analyses. All Fe is expressed as FeO. Where not given, K_2O values are below detection level.

Anal. No.	1	2	3	4	5	6	7	8	9	10	11	12
Sp. No.	Z277	Z277	Z31	Z326	Z326	Z132	Z393	Z393	Z104	Z104	Z104	Z123
No. Anal.	$\bar{x}$ (4), s	(1)	$\bar{x}$ (5), s	(1)	(1)	$\bar{x}$(2)	$\bar{x}$ (4), s	(1)	$\bar{x}$ (2)	$\bar{x}$ (2)	$\bar{x}$ (3), s	(1)
SiO_2	46.72 (0.36)	54.96	56.81 (0.79)	55.19	52.41	57.06	56.87 (0.72)	54.09	55.95	56.16	59.63 (1.49)	57.44
Al_2O_3	10.77 (0.50)	3.81	0.17 (0.07)	1.41	3.69	b.d.	b.d.	1.54	1.06	0.76	0.57 (0.37)	0.56
TiO_2	0.88 (0.08)	0.22	0.07 (0.03)	0.10	0.00	n.d.	b.d.	0.15	0.08	0.07	0.07 (0.03)	b.d.
Cr_2O_3	2.50 (0.18)	1.03	0.04 (0.02)	0.39	0.09	0.14	0.00	0.07	0.44	0.20	0.37 (0.11)	0.20
FeO	2.37 (0.67)	1.54	4.26 (1.19)	2.50	3.02	3.22	3.19 (0.40)	4.29	3.58	6.93	2.29 (0.12)	2.80
MnO	0.00	0.13	0.19 (0.02)	0.09	0.11	n.d.	0.12 (0.04)	0.17	0.23	0.50	0.00	0.00
MgO	19.56 (0.27)	22.14	21.29 (0.21)	21.98	23.29	22.39	21.09 (0.51)	21.75	22.33	24.03	29.08 (0.61)	23.14
NiO	0.16 (0.05)	0.16	0.00	0.16	0.30	n.d.	b.d.	0.18	0.04	0.00	0.12 (0.08)	0.16
CaO	12.37 (0.09)	13.25	13.33 (0.30)	12.94	11.39	12.50	13.44 (0.15)	11.87	11.78	7.36	0.00	14.50
Na_2O	2.43 (0.05)	0.62	b.d.	n.d.	n.d.	n.d.	b.d.	b.d.	n.d.	n.d.	n.d.	n.d.
Total	97.88	97.86	96.16	94.76	94.30	95.31	94.71	94.11	95.49	96.01	92.13	98.80

Anal. No.	13	14	15	16	17	18	19	20	21	22	23
Sp. No.	Z188	ZA275	ZA275	Z33	Z377B	Z54	Z54	Z36	Z394	Z394	Z368A
No. Anal.	$\bar{x}$ (6), s	$\bar{x}$ (4), s	$\bar{x}$ (3), s	(1)	$\bar{x}$ (3), s	(1)	(1)	$\bar{x}$ (3), s	(1)	(1)	(1)
SiO_2	56.83 (0.36)	57.18 (1.12)	49.37 (0.63)	49.81	56.28 (0.18)	54.28	57.05	45.09 (0.12)	53.24	51.46	55.16
Al_2O_3	0.54 (0.15)	b.d.	5.76 (0.40)	0.92	0.55 (0.40)	2.26	0.27	11.05(0.52)	4.04	8.31	1.59
TiO_2	b.d.	b.d.	0.15 (0.02)	0.04	0.08 (0.04)	0.00	0.00	1.08 (0.11)	0.06	0.00	0.03
Cr_2O_3	0.19 (0.10)	0.62 (0.50)	1.89 (0.29)	0.24	0.38 (0.12)	0.67	0.17	1.01 (0.15)	0.01	0.09	0.21
FeO	1.52(0.12)	1.24 (0.35)	2.90 (0.33)	2.01	3.53 (0.70)	4.52	4.09	7.93 (0.14)	3.81	3.63	7.53
MnO	b.d.	0.05 (0.02)	b.d.	0.12	0.09 (0.07)	0.23	0.11	b.d.	0.13	0.06	0.15
MgO	22.87 (0.29)	23.02 (0.42)	21.03 (1.39)	31.90	21.82 (0.07)	23.07	21.25	16.42 (0.05)	20.42	15.08	17.80
NiO	b.d.	b.d.	0.14 (0.01)	0.07	0.10 (0.06)	0.06	0.01	0.00	0.09	0.06	0.08
CaO	13.43 (0.47)	13.30 (0.38)	10.79 (0.47)	10.76	12.82 (0.76)	11.42	12.93	12.40 (0.23)	13.11	16.15	13.11
Na_2O	n.d.	0.41 (0.13)	2.69 (0.43)	0.10	0.59 (0.39)	0.22	0.34	2.26 (0.46)	1.16	0.37	0.23
K_2O	n.d.	0.00	0.20 (0.05)	0.00	0.00	0.15	0.03	0.00	0.00	0.12	0.03
Total	95.38	95.82	94.92	95.97	96.24	96.88	96.25	97.24	96.07	95.33	95.92

Anal. No.	24	25	26	27	28	29	30	31	32	33	34
Sp. No.	Z368A	Z368A	Z384	Z384	ZB182	ZB182	ZB182	Z219	Z219	Z219	Z219
No. Anal.	$\bar{x}$ (2)	$\bar{x}$ (2)	x (5), s	$\bar{x}$ (2)	$\bar{x}$ (4), s	$\bar{x}$ (8), s	(1)	$\bar{x}$ (7), s	(1)	(1)	(1)
SiO_2	55.41	52.23	55.83 (0.52)	51.40	53.79 (0.29)	50.84 (0.84)	48.05	43.14 (1.33)	44.55	43.35	43.55
Al_2O_3	2.71	4.91	0.50 (0.13)	3.65	1.78 (0.78)	4.89 (0.50)	6.37	10.13 (1.14)	9.63	10.26	11.71
TiO_2	0.10	0.28	b.d.	0.08	0.13 (0.5)	0.70 (0.16)	0.99	1.98 (0.38)	0.53	0.60	0.68
Cr_2O_3	0.12	0.31	0.21 (0.19)	0.32	b.d.	0.11 (0.06)	0.04	0.06 (0.03)	0.00	0.17	0.04
FeO	7.58	8.23	5.44 (0.44)	6.01	12.77 (1.28)	14.18 (0.53)	14.37	15.32 (1.50)	17.91	18.87	18.11
MnO	0.16	0.12	0.20 (0.06)	0.21	0.19 (0.06)	0.21 (0.07)	0.30	0.20 (0.08)	0.32	0.19	0.15
MgO	18.23	17.17	19.61 (0.36)	20.83	16.49 (0.87)	15.14 (0.39)	13.14	10.91 (1.74)	9.34	8.56	9.04
NiO	0.02	0.08	0.26 (0.08)	0.51	0.00	b.d.	0.00	0.00	0.00	0.07	0.04
CaO	13.09	12.68	13.04 (0.23)	10.58	12.03 (0.29)	10.96 (0.16)	11.49	11.36 (0.40)	11.78	12.06	12.02
Na_2O	0.67	1.15	b.d.	0.10	0.88 (0.50)	2.03 (0.27)	1.56	2.79 (0.27)	1.73	2.74	2.81
K_2O	0.04	0.08	0.00	0.00	0.08 (0.02)	0.13 (0.06)	0.17	0.11 (0.04)	0.08	0.15	0.14
Total	98.13	97.24	95.09	93.69	98.14	99.19	96.48	96.00	95.87	97.02	98.29

Anal. No.	35	36	37	38	39	40	41	42
Sp. No.	Z219	Z219	Z219	Z219	Z372	Z372	Z372	Z372
No. Anal.	(1)	(1)	$\bar{x}$ (2)	(1)	$\bar{x}$ (6), s	(1)	$\bar{x}$ (3)	$\bar{x}$ (2)
SiO_2	40.60	39.24	40.05	39.00	43.13 (0.57)	49.71	44.87	39.75
Al_2O_3	12.86	14.54	14.67	18.62	9.54	4.89	10.39	16.63
TiO_2	0.61	0.32	0.53	0.25	2.20	0.19	0.30	0.36
Cr_2O_3	0.00	0.00	0.00	0.04	0.06 (0.03)	0.00	0.10	b.d.
FeO	20.22	17.68	19.55	17.99	17.54 (0.48)	16.28	18.13	19.20
MnO	0.19	0.15	0.16	0.10	0.24 (0.06)	0.31	0.27	0.23
MgO	7.10	11.29	7.41	6.21	10.00 (0.44)	11.27	9.14	6.37
NiO	0.00	b.d.	0.00	0.00	0.00	0.00	0.00	0.00
CaO	11.71	8.51	12.09	11.37	10.88 (0.13)	10.15	11.17	10.33
Na_2O	2.83	1.92	3.47	3.46	3.79 (0.55)	3.55	3.51	4.19
K_2O	0.12	0.06	0.24	0.22	0.12 (0.02)	0.15	0.17	0.21
Total	96.24	93.71	98.17	97.26	97.50	96.50	98.05	97.27

A large majority of the analyzed amphiboles are (fig. 5) either tremolite, or actinolite that plots very close to the tremolite boundary. Such amphiboles mostly form asbestos veins in ultramafic rocks, some of which make fibres of mineable commercial grade.

The mafic rocks comprising metagabbros and metadolerites contain a high modal content of calcic amphiboles of both primary and secondary origin. Among the amphibole-bearing rocks of SQO, the latest magmatic differentiates are represented by the metadolerites (sample nos. ZB182, Z372 and Z219 in table 4). The samples of these rocks show greatest within-sample variation. They contain Ti-rich brown coloured, calcic amphiboles coexisting with Ti-poor, faintly green coloured calcic amphiboles. In textural appearance, the Ti-rich brown amphibole is differentiated from primary magma. Similar Ti-rich brown hornblende is reported from the latest differentiates of many ophiolites (Coleman, 1977).

In general, analyses in table 4 demonstrate a trend of Fe-enrichment and SiO_2- depletion in the amphiboles, from ultramafic rocks, towards metagabbros and then metadolerites. It follows the change in the bulk composition of the containing rocks.In deriving this conclusion, the amphiboles of tremolite, actinolite or tremolitic hornblende compositions are excluded as they are vein-forming and mainly secondary in origin. As portrayed in fig. 5, the Si atoms per formula unit in amphiboles of SQO decrease with the rock composition becoming SiO_2 - richer or more evolved. Support to this relationship also accrues from parallelism with the results derived by Leake's (1968) compilation of 245 better quality analyses related to rock types, projected onto the triangular plane SiO_2-(FeO + Fe_2O_3)–(Na_2O + K_2O). Using these data, it was shown by Wones & Gilbert (1982) that as the rock composition becomes SiO_2 - rich, the calcic amphiboles become more iron-rich.

At SQO, the amphiboles included in chromite crystals of the massive chromitite (sample Z277) are edenitic hornblende. The orthopyroxenite (Z104) contains magnesio-anthophyllite. The clinopyroxenites (samples Z188B, ZA275, Z33, Z54) contain edenite, edenitic hornblende and magnesio-hornblende all of which plot close together on fig. 5. Fe-websterite (Z36) contains pargasitic hornblende, and edenitic hornblende both of which plot adjacent to each other in fig. 5 However, very wide within-sample variation is noticed for the rodingitized metadolerites (samples Z219, Z372, ZB182). The brown and the light green types of amphibole coexist in the metalolerites. Brown amphibole is Ti-rich and contains 0.179 to 0.286 Ti cations per formula unit, compared to the Ti-poor, light green amphibole with nil to 0.072 Ti cations per formula unit. In sample ZB182, the distinction between brown and greenish colours is not marked; but analyses yield bimodal Ti distribution; Ti in one set ranges from 0.084 to 0.110, and in the other set from 0.008 to 0.062 catios per formula unit.

DISCUSSION AND CONCLUSIONS

At SQO, variations in orthopyroxene are not large and are mostly the result of primary processes. The orthopyroxene over most part of the SQO is Mg-rich enstatite; bronzite is present only in a few small sized dykes of websterite. Harzburgite is the most abundant rock-type; its orthopyroxene varies from Fs_9 to Fs_{10}. The enstatite with the lowest Fs molecule occurs as inclusions in chromite crystals.

In terms of Fe-enrichment of clinopyroxenes, metadolerites are the most evolved rock-type. Fe-websterite has more evolved diopside than that of the gabbro; but most gabbroic clinopyroxenes have Wo exceeding 50%.

The Ca-enrichment of some clinopyroxenes is reflected in their plots above the Di—Hd join in the pyroxene quadrilateral. Such compositions are observed mainly in the plots of fig. 3, A and D, and are dominated by metasomatic clinopyroxenes such as those of metagabbro, rodingite, and rodingitized chromitite.

Amphibole may form in basic rocks by crystallization from magmas; or by subsolidus but high temperature reaction between the cumulus minerals formed from a basic magma and a hydrous fluid (e.g., Otten, 1984), or it may form during secondary alteration processes, or by low temperature metamorphism.

Hynes (1982) compared the metabasite amphiboles from medium- and low- pressure metamorphic terrains and found that the low-pressure amphiboles generally have higher Ti/Al ratios. The amphiboles from SQO show Ti content of upto 0.286 and total Al upto 3.334 per 23 oxygens. Their Ti versus Al plot resembles that of low pressure metabasites of Hynes (1982, fig. 4).

The FeO contents of the amphiboles (table 4) is below 5% in harzburgite, chromitite and serpentinite; the pyroxenites also contain similarly low-Fe amphiboles but it sometimes coexists with another species with FeO content of 7 to 8% which is the typical amphibole of Fe-websterite, and metagabbro. Amphibole in the actionolite schist contains 5% to 6% FeO. The distinctly Fe-rich amphiboles are found in the metadolerites with FeO content of 13% to 21%.

In gabbro samples, the amphiboles are tremolite, actinolite and actinolitic hornblende; the latter two plot nearer the Mg-rich margin of their fields in fig. 6. Their TiO_2 content is very low, especially when compared to that in the amphiboles of the metadolerites. There is a slight increase in TiO_2 content upwards within the metagabbro. Thus, sample Z394 has 0.00 to 0.12% TiO_2 compared to 0.09% to 0.36% TiO_2 in the relatively upper level sample no. Z368A.

The Ti-bearing brown hornblende is described from the mafic Artfjalet rocks by Otten (1984). This is of subsolidus origin in the gabbro, formed by introduction of water when the gabbro was deformed early in the cooling period of gabbro. There is no magmatic hornblende in this gabbro; however, the asociated dolerites contain the magmatic amphiboles in two forms: a pale-green magnesio-hornblende and a brown hornblende formed by late- stage crystallization from magma. The Ti–bearing brown hornblende in the SQO is not present in the metagabbros but is found in the metadolerites (e.g., anal. 39, sample Z372, table 5) where it occurs alongside the pale green amphibole with much lower TiO_2 (anal. 40 to 42, sample Z372, table 5). The brown hornblende of SQO is not of subsolidus origin, as it does not display textural features observed by Otten (1984) in the Artfjallet gabbro.

In composition, Ti-rich brown hornblende in the metadolerites is mainly "edenitic hornblende" although a few analyses do fall in the adjoining parts of the fields of ferroan edenitic hornblende, ferro-edenitic hornblende, edenite, edenitic hornblende, ferroan-pargasitic hornblende. The associated low- Ti, pale green amphibole is ferro- edenitic hornblende, edenite, ferro-edenite, ferro-edenitic hornblende, ferroan pargasite, or ferroan pargasitic hornblende.

The largest within-sample variation in amphibole composition is displayed by the metadolerites, probably because their metamorphic amphiboles suffered subsequent metasomatism by rodingitizing fluids.

REFERENCES

AHMED, Z. (1982) Porphyritic-nodular, nodular and orbicular chrome ores from Sakhakot-Qila Complex, Pakistan, and their chemical variations. Min. Mag. **45**, "Deer, Howie & Zussman Volume", p. 167-178.

_____ (1984) Stratigraphic and textural variations in the chromite composition of the ophiolitic Sakhakot-Qila complex, Pakistan. Econ. Geol. **79**(6), pp. 1334-1359.

_____ (1987) Mineral chemistry of the Sakhakot-Qila ophiolite, Pakistan: Part 1, Monosilicates. This volume.

_____ & HALL, A. (1983) Petrology and mineralization of the Sakhakot-Qila Ophiolite, Pakistan. *In:* Gass, I.G, Lippard, S.J. & Shelton, A.W. (eds) OPHIOLITES AND OCEANIC LITHOSPHERE Geol. Soc. London Spec. Publ. **13**, pp. 241-252.

CAMERON, M. & PAPIKE, J.J. (1981) Structural and chemical variations in pyroxenes. Amer. Mineral. **66**, pp. 1-50.

COLEMAN, R.G. (1977) OPHIOLITES - Ancient Oceanic Lithosphere?, Springer-Verlag, Berlin, 229p.

DAL PIAZ, G.V., DI BATTISTANI, G., GOSS, G. & VENTURELLI, G. (1980) Rodingitic gabbro dykes and rodingitic reaction zones in the upper Valtournanche-Breuil area, Piemonte ophiolite nappe, Italian Western Alps. Archives des Sciences **33** (2-3), pp. 161-179.

DEER, W.A., HOWIE, R.A. & ZUSSMAN, J. (1987) ROCK-FORMING MINERALS: Vol. 2A, Single Chain Silicates. Longman Group Ltd. London. 668p.

HAWTHORNE, F.C. (1981) Crystal chemistry of the amphiboles. *In:* Veblen, D.R. (ed) AMPHIBOLES AND OTHER HYDROUS PYRIBOLES--MINERALOGY. Min. Soc. Amer. Rev. Min, **9A**, pp. 1-102.

HYNES, A. (1982) A comparison of amphiboles from medium- and low- pressure metabasites. Contrib. Mineral. Petrol. **81**, pp. 119-125.

LEAKE, B.E. (1968) A catalogue of analyzed calciferous and subcalciferous amphiboles together with their nomenclature and asociated minerals. Geol. Soc. Amer. Spec. Paper **98**, 210 p.

LEAKE, B.E. (1978) Nomenclature of amphiboles. Min. Mag. **42**, pp. 533-563.

OTTEN, M.T. (1984) The origin of brown hornblende in the Arfjallet gabbro and dolerites. Contrib. Mineral. Petrol. **86**, pp. 189-199.

PAPIKE, J.J., CAMERON, K.L. & BALDWIN, K. (1974) Amphiboles and pyroxenes: Characterization of other than quadrilateral components and estimates of ferric iron from microprobe data. Geol. Soc. Amer. Abstracts with Programs **6**, pp. 1053-1054.

SCHIFFRIES, G.M. & SKINNER, B.J. (1987) The Bushveld hydrothermal system: field and petrographic evidence Amer. Jour. Sci. **287**, p. 566-595.

SWEATMAN, T.R. & LONG, J.V.P. (1969) Quantitative electron probe microanalysis of rock- forming minerals. Jour. Petrology **10**, pp. 332-379.

WONES, D.R. & GILBERT, M.C. (1982) Amphiboles in the igneous environment. *In:* Veblen, D.R. & Ribbe, P.H. (eds) AMPHIBOLES: Petrology and experi-
-mental phase relations. Min.Soc.Amer. Rev. Mineral. 9b, pp. 355–90.

Orally presented on 22.10.1987
Manuscript revised on 31.12.1987

ACTA MINERALOGICA PAKISTANICA
VOLUME 3 (1987) pp. 159 - 160

SHORT COMMUNICATIONS

OCCURRENCE OF PINK ZOISITE AT NOMAL, GILGIT DISTRICT PAKISTAN

TAHSEENULLAH KHAN, IMTIAZ ALI, REHANUL HAQUE SIDDIQUI & HAIDER KAMAL
Geological Survey of Pakistan, Quetta.

An occurrence of pink zoisite has been located 2 kms northwest of Nomal along the Nomal-Naltir road which is located by longitude 74°15′ E and latitude 36° 05′ N on toposheet No. 42/L. A 27 km long NW trending dirt road connects Nomal with Gilgit on the southern flank of the Hunza river.

A 10 metre long by 1–2 metres wide milky white quartz vein traversing a granodiorite stock contains pockets of hydrothermal calc-silicate rock. The pockets range in size from 10 cms to 64 cms in diameter (fig. 1). Pink zoisite ± clinozoisite are ubiquitous mineral constituents of the calc-silicate rock. Pink zoisite imparts a pinkish color to the fresh surfaces of the calc-silicate rock whereas the weathered surfaces are brownish.

Calc-silicate rock under the microscope reveals that the earliest formed mineral of the rock is pink zoisite ± clinozoisite followed by muscovite, orthoclase and quartz. Sericite is the alteration product of the orthoclase whereas pyrophyllite and calcite occur in minor amounts. Calcite occurs as a filling material within the pink zoisite. Muscovite and orthoclase replace pink zoisite and muscovite is replaced by orthoclase.

A very small amount of the mineral is analysed using the colorimetry method for SiO_2, Al_2O_3, Fe_2O_3, MgO and Cao (table 1). Analyses of zoisite and manganese zoisite reported from Finland and Urals respectively, (Deer *et al.*, 1962) are given in table 1 for comparison.

Table 1. Partial analysis of pink zoisite from Nomal (1) compared with analyses of zoisite from Tytyri Lohja, Finland (2) and manganese- zoisite from Banzuka, Urals (3).

	1	2	3
SiO_2	34.93	39.20	37.86
TiO_2	–	0.08	–
Al_2O_3	27.69	32.01	31.78
Fe_2O_3	3.15	0.76	0.90
FeO	–	0.54	–
MnO	–	0.05	0.47
MgO	0.89	0.20	0.11
CaO	23.47	25.68	25.36
H_2O+	–	2.03	3.80
H_2O-	–	0.00	–
Total	90.13	100.55	100.28

The pale pinkish colour in the zoisite is possibly due to manganous oxide. Pinkish zoisite is easily differentiated from Piemontite. The former is orthorhombic whereas the latter is monoclinic. Manganese and iron contents are much less in pink zoisite compared to piemonitite.

Pink zoisite has been reported by Schaller and Glass (1942) to occur in quartz vein, pegmatites, metamorphosed limestone and dolomites and altered granitic rocks and gneisses. At Nomal, zoisite ± clinozoisite bearing calc-silicate rock occurs in the form of cavity fillings within a quartz vein.

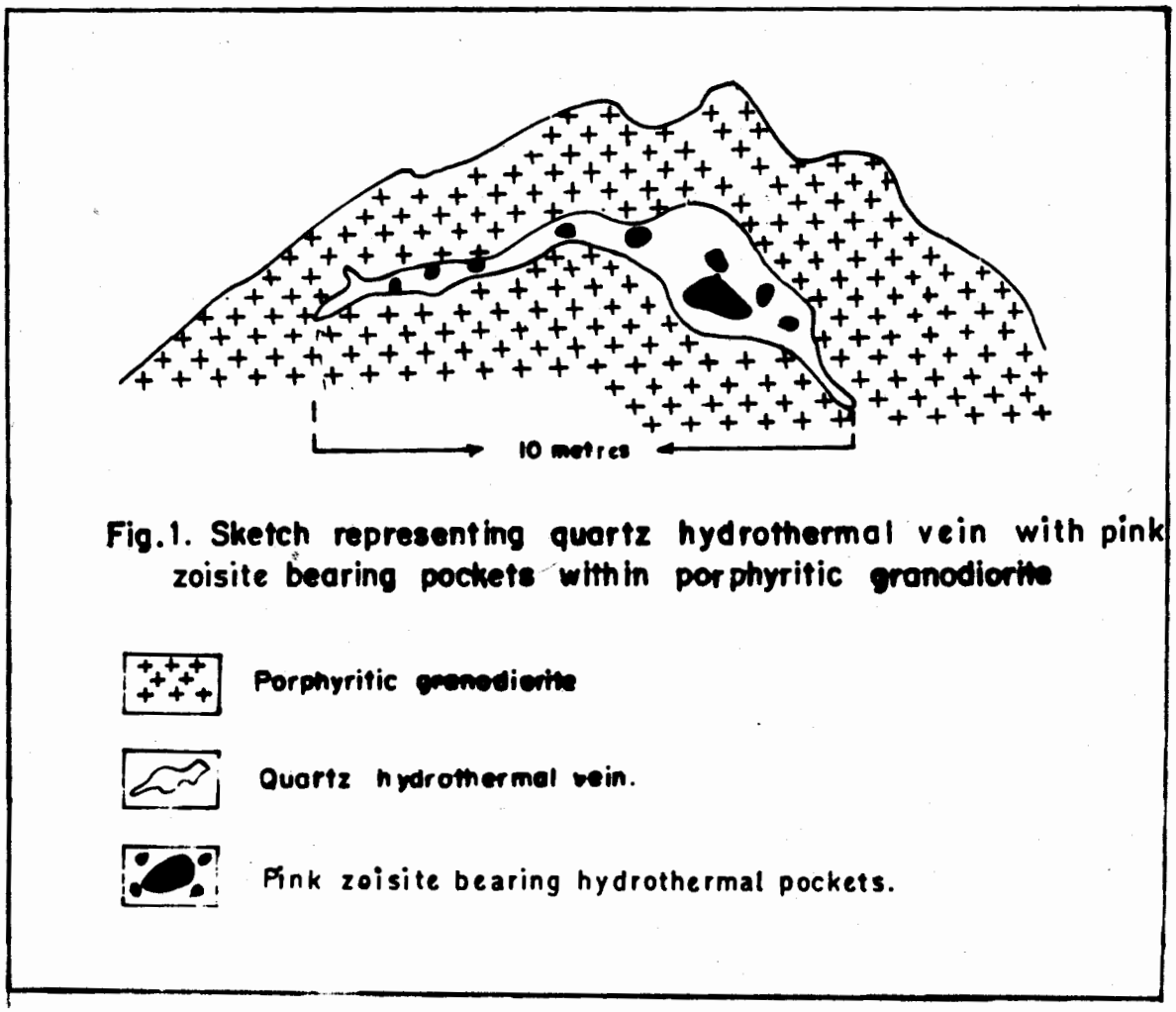

Fig.1. Sketch representing quartz hydrothermal vein with pink zoisite bearing pockets within porphyritic granodiorite

Pink zoisite is a low temperature hydrothermal mineral. The pale pink zoisite of Nomal is opaque to translucent and occurs in the form of showings, grains and crystals (minor). In hand specimen, pinkish zoisite of Nomal may be mistaken for corundum or ruby, of Hunza.

Owing to the poor quality and quantity of this pink zoisite, the usege of this mineral can be ruled out for gemstone purposes.

The authors are deeply indebted to Messrs. A.H. Kazmi and Saeed-uz-Zafar Khan under whose guidance field work was conducted in the Gilgit area. Dr. Mahmooduddin Ahmad Siddiqui, is thanked for a critical review of this report.

REFERENCES

DEER, W.A., HOWIE R.A. & ZUSSMAN, J. (1962) ROCK-FORMING MINERALS VOL. I: ORTHO – AND RING SILICATES, Longman, London.

SCHALLER, W.T. & GLASS, J.J. (1942) Occurrence of pink zoisite (Thulite) in United States. Amer. Mineral. 27, p. 519.

Orally presented on 22.10.1987
Manuscript revised on 31.12.1987

ANNUAL REPORT OF THE CENTRE OF EXCELLENCE IN MINERALOGY, QUETTA (1987)

STAFF AND STUDENTS

ACADEMIC STAFF

Date of joining C.E.M.

Professor & Director
ZULFIQAR AHMED
Ph.D. (London), P.D.M.P. (Min. Univ .Austria)
M.Sc. & B.Sc. Hons. (Punjab) 25.8.1984

Fulbright Professor
GEORGE R. McCORMICK
Ph.D. (Ohio State)

Associate Professor
MOHAMMAD MUMTAZUDDIN
M.Sc. (McGill), B.Sc. (Aligarh). 1.4.1974

Assistant Professors
MOHAMMAD MUNIR
M.Sc. (Baluchistan) 1.10.1976

JAWED AHMED
M.Sc. (Karachi) 1.4.1980

Visiting Lecturer
CHRISTOPHE MIOULLET
D.E.A. (Bordeaux, France) 15.12.1986

Part-time Lecturers
AFTAB AHMAD BUTT
Ph.D. (Utrecht, Hollad),
M.Sc. (Punjab)

ABDUL HAQUE
Dr. 3eme Cycle (France),
M.Sc. (Baluchistan)

GENERAL STAFF

Administrative Officer
S. SHAHABUDDIN
M.Sc. (Baluchistan) 21.5.1977

Accounts Officer
MIRZA MANZOOR AHMED
B.Com. (Karachi) 7.5.1980

Technician
KHUSHNOOD AHMED SIDDIQUI
Dipl. Assoc. Engr. (Hydcrabad) 1.3.1976

Photographer
HUSSAINUDDIN 16.6.1981

Assistant Librarian
ABDUL GHAFOOR
M.L.S. (Baluchistan) 2.5.1985

Draftsman
AHMED KHAN MANGI
B.A. (Sind), Cert. Drawing 1.7.1981

Steno-typist
GHALIB SHAHEEN 17.7.1985

Assistant (Office)
LAL MOHAMMAD DURRANI
12.5.1973

Store Keeper
MUSA KHAN 20.8.1977

Senior Clerk
MOHAMMAD ANWAR 18.9.1973

Junior Clerk
GHULAM QASIM 3.10.1983

Cashier-cum-clerk
JUMA KHAN 11.6.1985

Laboratory Assistant
SHER HASSAN 22.8.1977

Rock Cutter
FARID KHAN 8.4.1985

Junior Mechanic
ABDUL QADIR 21.8.1977

Driver
ALI MOHAMMAD 17.7.1984

Loader
RAWAT KHAN 2.7.1977

Laboratory Attendants

GHULAM RASOOL	20.8.1977
MEHRAB KHAN	21.8.1977

Peons (Naib Qasid)

SIKANDAR KHAN	30.4.1976
MOHAMMAD RAFIQ	12.10.1978
ATTA MOHAMMAD	25.3.1986

Cleaner

NAZIR MASIH	1.4.1977

POSTGRADUATE STUDENTS

(SESSION 1985-87)

ABDUL WAHEED TAREEN, M.Sc. (Baluchistan)
QAISER MAHMOOD, M.Sc. (Punjab)
MEHRAB KHAN, M.Sc. (Baluchistan)
KHALID MAHMOOD, M.Sc. (Baluchistan)
MORTAZA BOSTANI, M.Sc. (Baluchistan)

(SESSION 1986-88)

DIN MUHAMMAD, M.Sc. (Baluchistan)
HAMID RAZA MIRKIANI, M.Sc. (Baluchistan)
SAADAT HUSSAIN, M.Sc. (Baluchistan)
MOHAMMAD AYUB, M.Sc. (Baluchistan)
ZIAUD DIN, M.Sc. (Baluchistan)

ACADEMIC ACTIVITIES

During 1987, geoscientific field and laboratory studies on the following M.Phil. dissertations have remained in progress:

Mortaza Bostani
Geological studies of a portion of oil-bearing strata of Potwar region, Pakistan.

Khalid Mahmood
Geology of igneous rocks and their sedimentary envelope near Nal area, Khuzdar District, Pakistan.

Mehrab Khan
Geology of ophiolitic rocks from Nal area, Khuzdar District, Pakistan.

Qaiser Mahmood
Geology of Wad-Goth Haji Shakar area, Khuzdar District, Baluchistan.

Jawed Ahmad
Clay mineralogy of the Ghazij Shale Formation of Baluchistan.

Shamim Ahmad Siddiqui
Mineralization, controls and genesis of lead-zinc-iron and barite deposits near Shekran and Gunga, Khuzdar Division, Baluchistan.

Abdul Tawab
Petrology and mineralogy of ultramafic and associated rocks near Nal, Khuzdar District, Baluchistan.

Hassan Khan Kharoti
Igneous rocks south of Khuzdar-Nal section, Baluchistan.

From 12th to 25th January, 1987, a professional course in "industrial mineralogy" was organized at the Institute of Geology, Punjab University, Lahore, led by Professor A.C. Dunham of the Hull University, U.K. From CEM, Jawed Ahmed participated in the programme. Zulfiqar Ahmed delivered lecture on "fluorite and barite in industry" to the course participants on 16th January, 1987. In continuation with his previous year's work, Jawed Ahmed carried out X-ray diffraction studies on the clay minerals of the Ghazij Formation at the laboratories of Pakistan Atomic Energy Minerals Centre, Lahore, during February, 1987.

Zulfiqar Ahmed participated in the Symposium organized by the National Institute of Oceanography (NIO) at Karachi, on 9th and 10th March, 1987. Preliminarily C.E.M. agreed to work on geoscientific research projects jointly with N.I.O. Visitors from the British Council and ODA, UK, were apprised of the CEM activities and a very small scale linkage programme with the Geology Department at RHB New College, University of London, was proposed. U.S.I.S. representatives visited CEM on 15th April, and discussed cooperation in the academic programmes of C.E.M. Dr. Robert Lawrence of the Oregon State University, visited CEM on 8th July. Michel Leleu, Director CIFEG, France, visited CEM on 18.5.1987, and a collaborative programme for exchange of scientific information was chalked out.

Dr. A.A. Butt and Dr. M.M. Qureshi, both from the Punjab University, Lahore, delivered a series of special lectures on "sedimentary petrography" and "rock and mineral analysis" respectively, during the first half of October, 1987.

The first Pakistan national symposium on "Mineral Resources and Geology of Pakistan" was organized by CEM. The symposium was inaugurated by the General (Retd.) Muhammad Musa, Governor of Baluchistan, on 20th October, 1987. The session, held at the University Law College, Khojak Road, Quetta, was opened by recitation from Holy Quran and the welcome address by Mr. Muhammad Hassan Baluch, Vice Chancellor, University of Baluchistan. Dr. Zulfiqar Ahmed, delivered the keynote address. General Muhammad Musa, in his inaugural address, laid emphasis on the need to enhance mineral resources exploration activities in Pakistan.

The scientific paper reading sessions, started on the afternoon of 20th October, were actively pursued till the late evening of 22th October. The titles of papers, names of authors are reported in the "Programme with Abstracts" which was included in the bags distributed to the registered delegates. Total 68 professional geoscientists registered for the symposium. They came from all over Pakistan and represented most of the mineral- related Organizations. Each registered delegate received symposium bag with included symposium literature and stationery items. The themes of the scientific paper reading sessions were as under:

1. Geology of oil and gas in Pakistan.
2. Minerals in relation to plate tectonics.
3. Marine geology and coastal areas of Pakistan.
4. Application of mineral exploration techniques in Pakistan.
5. Minerals of acidic rocks.
6. Base metal deposits and geology of Baluchistan.
7. Sedimentary minerals and stratigraphy of Pakisan.
8. Ophiolites of Pakistan.

A total of 22 papers were presented. A poster session was also organized.

A geological field excursion attended by 25 delegates and 5 organizational staff was held from 23rd to 28th October, 1987. The excursion visited the fluorite deposits of Kohi Maran area; barite deposits of Gunga area and nearby gossans overlying the Mississippi Valley-type lead-zinc deposits; Mesozoic sedimentary rocks of Ferozabad area; barite mill at Khuzdar; ophiolitic melange, gabbro and harzburgite bodies with chromite mines near Nal with its underlying and overlying strata, especially the Eocene limestones rich in fauna. Observations were also made alongside a 200 kms long north-south road section of the gigantic and spectacular Bela Ophiolite featuring thick sequence of pillow lavas, sheeted dykes, pyroxenite horizon and dykes, plagiogranitic differentiates, rodingitic dykes and mines and deposits of chromite and magnesite. The success of the symposium strongly suggested its recurrence. Full length papers presented in the symposium after being refereed and revised are published in this volume.

Zulfiqar Ahmed presented the paper with the title "compositions of pyroxenes and pyroxenite dykes from the Sakhakot-Qila ophiolite, Malakand Agency, Pakistan".

Jawed Ahmed has further extended his work on the clay minerals of Ghazij Shale Formation and has performed the x-ray diffraction and differential thermal analyses on 20 more samples. These are found to be composed of illite, kaolinite, chlorite and mixed-layer clay minerals in various proportions.

Jawed Ahmed and Muhammad Munir have jointly carried out X-ray diffraction and differential thermal analysis on ten samples of a thin layer found at the base of Cretaceous age Parh Limestone rocks exposed in the Murree Brewery Gorge near Quetta. The layer is 2 cms thick and extends laterally for 4 miles. This layer is was found to be composed of sodium-smectite throughout its lateral extent.

ACTA MINERALOGICA PAKISTANICA
VOLUME 3 (1987) 164 - 165

1987 PAPERS OF REGIONAL INTEREST FROM OTHER JOURNALS

A. WITH COVER DATES OF 1987

1. COWARD, M.P., BUTLER, R.W.H., KHAN, M.A. & KNIPE, R.J. (MAY, 1987) The tectonic history of Kohistan and its implications for Himalayan structure. Journal of the Geological Society London, **144,** (3), pp. 377-392.

2. GARZANTI, E., BAUD, A. & MASCLE, G. Sedimentary record of the northward flight of India and its collision with Eurasia (Ladakh Himalaya, India). Geodinamica Acta **1,** (4-5), pp. 297-312.

3. KANGO, R.A., DUBEY, K.P., & ZUTSHI, D.P. Sediment chemistry of Kashmir Himalayan lakes. Chemical Geology, **64,** (1-2), pp. 121-126.

4. KOLLA, V. & COUMES, F.Morphology, internal structure, seismic stratigraphy, and sedimentation of Indus fan. American Association of Petroleum Geologists Bulletin **71,** (6), pp. 650-677.

5. LEBAS, M.J., MIAN, I. & REX, D.C. Age and nature of carbonatite emplacement in North Pakistan. Geologische Rundschau, **76,** (2), pp. 317-323.

6. MERCIER, J.L., ARMIJO, R., TAPPONNIER, P., CAREY-GAILHARDIS, E. & LIN, H.T. Change from Late Tertiary compression to Quaternary extension in southern Tibet during the India Asia collision. Tectonics **6,** (3), pp. 275-304.

7. MIAN, I. & LEBAS, M.J. The biotite-phlogopite series in fenites from the Loe Shilman carbonatite complex, NW Pakistan. Min. Mag. **51,** pp. 397-408.

8. RAI, H. Geochemical study of volcanics associated with Indus ophiolitic mélange in western Ladakh, Jammu and Kashmir, India. Ofioliti **12** (1), pp. 71-82.

9. REUBER, I., COLCHEN, M. & MEVEL, C. The geodynamic evolution of the South-Tethyan margin in Zanskar, NW-Himalaya, as revealed by the Spongtang ophiolitic melanges. Geodinamica Acta (Paris) **1,** (4-5), pp. 283-296.

10. SEARLE, M.P., WINDLEY, B.F., COWARD, M.P., COOPER, D.J.W., REX, A.J., REX, D. LI, T.D., XIAO, X.C. JAN, M.Q., THAKUR, V.C. & KUMAR, S. The closing of Tethys and the tectonics of the Himalaya. Geological Society of America Bulletin, **98,** (6), pp. 678-701.

11. SHANKAR, R.,SUBBARAO, K.V. & KOLLA, V. Geochemistry of surface sediments from the Arabian Sea. Marine Geology **76,** pp. 253-279.

12. SHANKAR, R., SUBBARAO, K.V. & REDDY, G.R. Distribution and origin of uranium in surficial sediments from the Arabian Sea. Chemical Geology **63,** pp. 217-223.

13. SRIMAL, N. & BASU, A.R. Tectonic inferences from oxygen isotopes in volcano-plutonic complexes of the India-Asia collision zone, NW India. Tectonics **6,** (3), pp. 261-273.

14. SYMES, R.F. BEVAN, J.C. & JAN, M. Q. The nature and origin of orbicular rocks from near Deshai,Swat Kohistan, Pakistan. Min.Mag. **51,** (363), pp. 635-648.

15. YEATS, R.S. & HUSSAIN, A. Timing of structural events in the Himalayan foothills of northwestern Pakistan. Geological Society of America Bulletin, **99** (2), pp. 161-176.

B. WITH COVER DATES OF 1986

1. ALIZAI, S.A.K. & MIRZA, M.I. Remote sensing applications in Pakistan: Current status and future programmes. Internat. Jour. Remote Sensing **7,** (9), pp. 1147-1151.

2. BISWAS, S. & DAS GUPTA, A. Some observations on the mechanism of earthquakes in the Himalaya and the Burmese arc. Tectonophysics **122,** (3/4), pp. 325-343.

3. COWARD, M.P. WINDLEY, B.F., BROUGHTON, R.D., LUFF, I.W., PETTERSON, M.G., PUDSEY, C.J., REX, D.C. & KHAN, M.A. Collision tectonics in the NW Himalayas, ***In:*** Coward M.P. & Ries, A.C. (eds.) COLLISION TECTONICS, Geol. Soc. London Spec. Publ. **19,** pp. 203-219.

4. LE FORT, P. Metamorphism and magmatism during the Himalayan Collision. ***In:*** Coward, M.P. & Ries, A.C. (eds.) COLLISION TECTONICS, Geol. Soc. London Spec. Publ. **19,** pp. 159-172.

5. MALINCONICO, L.L. The structure of the Kohistan- Arc terrain in northern Pakistan as inferred from gravity data. Tectonophysics 124, pp. 297-307. Discussion by C.Ebblin and Reply (1987) Tectonophysics **141,** pp. 349-353.

6. MATTAUER, J. Intracontinental subduction, crust-mantle docollement and crustal stacking wedge in the Himalayas and other collision belts. ***In:*** Coward, M.P. & Ries, A.C. (eds.) COLLISION TECTONICS, Geol. Soc. London Spec. Publ. **19,** pp. 37-50.

7. NEGI, J.G., THAKUR, N.K., & AGRAWAL, P.K. Crustal magnetisation- model of the Indian subcontinent through inversion of satellite data. Tectonophysics **122,** (1/2), pp. 123-133.

8. NEGI, J.G., THAKUR, N.K., & AGRWAL, P.K. Prominent MAGSAT anomalies over India. Tectonophysics, **122,** (3/4), pp. 345-356.

9. SHUJA, TAUQIR A. Geothermal areas in Pakistan. Geothermics **15,** (5-6), pp. 719–724.

INFORMATION FOR AUTHORS

ACTA MINERALOGICA PAKISTANICA publishes in English annually the results of original scientific research in the multifaceted field of mineral sciences, covering mineralogy, petrology, crystallography, geochemistry, economic geology, isotope mineralogy, petrography, petrogenesis, mineral chemistry and related disciplines. Review articles and short notes are also considered for publication.

In general, the manuscripts be organized in the following order: title; name(s) and institutional address(es) of the author(s); abstract; introduction; methods, techniques, material studied and area descriptions; results; conclusions; acknowledgements; references; tables; figure captions. The abstract should not exceed 300 words. All tables and figures should be referred in the text and numbered according to their sequence in the text. All references to publications are given in the text by author's name and year of publication; and are listed at the end of text alphabetically by author's names and chronologically per author.

Authors of the articles submitted for publication in ACTA MINERALOGICA PAKISTANICA should send two complete copies of the manuscript, typed double-spaced on one side of the paper only. Copies of tables should be in final format. As far as possible, tables and figures should be prepared for reduction to the single column size or to the page size (204mmX278mm). Use of mineral symbols by Kretz (The American Mineralogist, 1983, Volume 68, pp. 277-279) is recommended for superscripts, subscripts, equations, figures and tables. The Concise Oxford Dictionary is adopted for spelling. Underlining of text by a single line will mean printing in italics; that by a double line will mean printing in bold letters. The use of metric system and S.I. units is recommended. Bar scales should be used in all figures rather than numerical scales.

Only articles not previously published and not about to be published, wholly or in part, in either Pakistani or foreign journals, are considered for publication. Submission of an article is understood to imply that the article is original and unpublished and is not being considered for publication elsewhere. Publication is subject to the discretion of the Editor. All manuscripts are refereed before being accepted. Accepted papers become copyright of the Centre of Excellence in Mineralogy, Quetta. Authors alone are responsible for the accuracy of the contents and views expressed in their respective papers. Fifty off-prints of each published paper will be sent to authors free of charge. Additional copies may be ordered just after receiving the acceptance letter from the Editor. Manuscripts should be sent to: Acta Mineralogica Pakistanica C/O Centre of Excellence in Mineralogy, University of Baluchistan, G.P.O. Box 43, Quetta, Pakistan. Phone Nos. are (081) 41974 & 40500.

ACTA MINERALOGICA PAKISTANICA VOLUME 3, 1987.

CONTENTS